Solving for the Low-Voltage/Large-Angle Power-Flow Solutions by Using the Holomorphic Embedding Method

by

Yang Feng

A Dissertation Presented in Partial Fulfillment
of the Requirements for the Degree
Doctor of Philosophy

Approved July 2015 by the
Graduate Supervisory Committee:

Daniel J. Tylavsky, Chair
Dieter Armbruster
Keith E. Holbert
Lalitha Sankar

ARIZONA STATE UNIVERSITY

August 2015

ABSTRACT

For a (N+1)-bus power system, possibly 2^N solutions exists. One of these solutions is known as the high-voltage (HV) solution or operable solution. The rest of the solutions are the low-voltage (LV), or large-angle, solutions.

In this report, a recently developed non-iterative algorithm for solving the power-flow (PF) problem using the holomorphic embedding (HE) method is shown as being capable of finding the HV solution, while avoiding converging to LV solutions nearby which is a drawback to all other iterative solutions. The HE method provides a novel non-iterative procedure to solve the PF problems by eliminating the non-convergence and initial-estimate dependency issues appeared in the traditional iterative methods. The detailed implementation of the HE method is discussed in the report.

While published work focuses mainly on finding the HV PF solution, modified holomorphically embedded formulations are proposed in this report to find the LV/large-angle solutions of the PF problem. It is theoretically proven that the proposed method is guaranteed to find a total number of 2^N solutions to the PF problem and if no solution exists, the algorithm is guaranteed to indicate such by the oscillations in the maximal analytic continuation of the coefficients of the voltage power series obtained.

After presenting the derivation of the LV/large-angle formulations for both PQ and PV buses, numerical tests on the five-, seven- and 14-bus systems are conducted

to find all the solutions of the system of nonlinear PF equations for those systems using the proposed HE method.

After completing the derivation of finding all the PF solutions using the HE method, it is shown that the proposed HE method can also be used to find only the PF solutions of interest (i.e. type-1 PF solutions with one positive real-part eigenvalue in the Jacobian matrix), with a proper algorithm developed. The closet unstable equilibrium point (closest UEP), one of the type-1 UEP's, can be obtained by the proposed HE method with limited dynamic models included.

The numerical performance as well as the robustness of the proposed HE method is investigated and presented by implementing the algorithm on the problematic cases and large-scale power system.

ACKNOWLEDGEMENTS

First and foremost, I would like to express my sincere thanks to Dr. Tylavsky, my advisor for being a commendable source of knowledge and inspiration. From the beginning of my graduate career, he has inculcated a passion for the subject, guided me through several challenges in research and shaped my writing skills.

I express my sincere thanks to Muthu Kumar Subramanian, a master student graduated from ASU, Shruti Rao, a doctoral student and Yuting Li, a master student, currently at ASU. They all are hard-working team members and productive contributor in developing the algorithms. Besides, Muthu and Shruti have spent much of their valuable part time to shape my writing skills.

Dr. Antonio Trias, AIA, deserves a special mention for the valuable inputs he gave to our research group. I would like to extend to my thanks to my graduate committee Dr. Armbruster, Dr. Holbert and Dr. Sankar for their valuable feedback and suggestions to my thesis document. I am grateful to the all the faculty members of power engineering for the wonderful learning experience they provided for the last five years since I joined ASU.

I would like to express my gratitude to the School of Electrical, Computer and Energy Engineering for providing me the opportunity to work as Teaching Assistant. Finally, my heart is with my love, Fanjie Lin, my family, especially my mother, and my friends who have kept me grounded during the entire period of my study.

TABLE OF CONTENTS

Page

CHAPTER Page

CHAPTER Page

CHAPTER Page

CHAPTER Page

LIST OF FIGURES

Figure Page

Figure Page

LIST OF TABLES

Table Page

Table Page

NOMENCLATURE

Δ	Discriminant of the Difference Equation
λ	The Load Scaling Parameter Used by the Continuation Power Flow Method
λ_+, λ_-	The Roots of Characteristic Polynomial of the Difference Equations Formed by Three Term Recursion Relation
δ_i	Voltage Angle at Bus i
$\varkappa$	Condition Number of a Matrix
σ	Parameter Involved with Complex Power and Line Impedance in the Two-Bus System
σ_R	The Real Part of σ
σ_I	The Imaginary Part of σ
ω_i	Rotor Angle Velocity of the i^{th} Generator
$A_n(s)$	The n^{th} Order Numerator Term in Three Term Recursive Relation
$B_n(s)$	The n^{th} Order Denominator Term in Three Term Recursive Relation
$A^{(+)}, B^{(+)}$	Even-Order-Term of the Three Term Recursion Relation
$A^{(-)}, B^{(-)}$	Odd-Order-Term of the Three Term Recursion Relation
B_{ik}	Line Conductance Between Bus i and Bus k
C	Padé Matrix Formed by Its Corresponding Power Series

Coefficients

C_+, C_- Coefficients in the Closed Form of A

D_+, D_- Coefficients in the Closed Form of B

G_{ik} Line Susceptance Between Bus i and Bus k

$J1$ PQ Bus Set where Low-Voltage Substitution Is Not Applied

$J2$ PV Bus Set where Large-Angle Substitution Is Not Applied

$K1$ PQ Bus Set where Low-Voltage Substitution Is Applied

$K2$ PV bus Set where Large-Angle Substitution Is Applied

L_i Complex-Valued Load at Bus i for a Multi-Bus System

N Number of Buses in a Power System

N_{PQ} Total Number of PQ Buses in a Power System

N_{PV} Total Number of PV buses in a Power System

P_i Real Power Injected at Bus i

P_L Real Power Load at PQ bus for a Two-Bus System

P_{mi} Mechanical Power Input at ith Generator

Q_i Reactive Power Injected at Bus i

Q_L Reactive Power Load at PQ Bus for a Two-Bus System

R Transmission Line Resistance

Rhs_known	Calculated RHS of PV Bus PBE
S_i	Complex Power Injected at Bus *i*
U	Normalized Voltage (May Be High- or Low Voltage Variable Depending on the Context.)
U_+	High-Voltage Solution for the Two-Bus Case
U_+	Low-Voltage Solution for the Two-Bus Case
U_i	Substituted Bus *i* Voltage Variable Used in the Multi-bus Low-Voltage Formulation
V_E	Energy Function for a Dynamic System
V_P	Potential Energy for a Dynamic System
V_K	Kinetic Energy for a Dynamic System
V_i	Bus Voltage at Bus *i*
V_0	Slack Bus Voltage
$V_i(s)$	Voltage Power Series for Bus *i*
$V_i(0)$, $V_i[0]$	Voltage Series for Bus *i* Evaluated at *s*=0
$V_i(1)$	Voltage Series for Bus *i* Evaluated at *s*=1
$V_i[n]$	Voltage Series Coefficients for Bus *i* for *s* At Power of *n*
$V^{(1)}(z)$	Partial Power Series Used in Viskavatov Method
$V^{(n)}[0]$	N^{th} Term in the Continued Fraction
X	Transmission Line Reactance

X_c	Shunt Reactance for a Two-Bus System
Y_{ik}	Bus Admittance Matrix Entry Between Bus *i* and Bus *k*
$Y^{(sh)}_{ik}$	Bus Admittance Matrix Entry Between Bus *i* and Bus *k*, Including Only Shunt Elements
$Y^{(tr)}_{ik}$	Bus Admittance Matrix Entry Between Bus *i* and Bus *k*, Including Only Transmission Line Impedance
Z	Line Impedance for Two-Bus System
a_N	The Coefficient for N^{th} Order Recursion Relation
$a(s)$,$b(s)$, $c(s)$	Power Series
b	Unknown Coefficients in the Denominator Polynomial of the Padé Approximant
c	The RHS Coefficients Formed by the Power Series Coefficients when Calculating the Denominator Polynomial of the Padé Approximant
d_i	Damping Constant for the i^{th} Generator
$f(s)$	Holomorphic Function *f* with Variable *s*
i	Index Number
im	Abbreviation for Imaginary
j	Bus Number Index
k	Bus Number Index

m_i	Inertia Constant for the i^{th} Generator
n	Order Number of s in the Power Series
re	Abbreviation for Real
x	Variable
y	Variable
s	Complex Variable Used in Holomorphic Embedding

1 INTRODUCTION

1.1 Power-Flow Problems

The power-flow (PF) problem is commonly used in the power system analysis. The solution of the PF problem provides the bus voltage magnitudes and angles in the power system, given the real and reactive power injections at the load (PQ) buses and real power injection and voltage magnitude at the voltage controlled (generator/PV) buses, respectively.

For a simple two-bus system, two distinct solutions exist provided the load bus is loaded below the bifurcation-point (voltage-collapse-point) loading. The solution with the high voltage magnitude and small voltage angle is known as the high-voltage (HV) solution and the low-voltage (LV) solution is the one with the lower voltage magnitude and larger voltage angle compared to the HV solution. At the voltage collapse point, the HV and LV solutions become identical.

When the system becomes large, there usually exists more than one solution according to the nonlinear characteristic of the power-balance-equations (PBE's). The solution at the stable or operable point is the HV solution and possibly many other LV/large-angle or non-operable solutions exist in the system.

1.2 Iterative Methods

Relatively reliable iterative techniques (i.e. Gauss-Seidel (GS), Newton-Raphson (NR), and BX/XB Fast Decoupled Load Flow (FDLF)) are currently used for solving

the nonlinear PBE's that define the PF problems. Those iterative methods and many of their variants work well for operating points close to nominal [1]-[5]. However iterative methods face convergence problems when the system is in extremis, where the voltages stay far from nominal [6]. Further, the iteration trajectory is starting point dependent: depending on the initial estimate of the voltages, network specification and load/generation condition, the solution procedure can oscillate, diverge or (preferably) lead to the HV solution or possibly one of many LV/large-angle solutions, which is non-preferable in most cases. Therefore finding the HV solution is not guaranteed by any iterative algorithm known to date.

Many attempts ([7]-[17]) have been made to analyze the convergence properties of the most common PF algorithms and to improve the convergence behavior, yet convergence problems still remain [18], [19]. Perhaps the most vexing deficiency for iterative methods is that when the solution procedure does not converge, the user is left to wonder whether there is indeed no solution or whether a solution exists but the method is unable to find it.

While the convergence problems plague methods designed to find the HV solution, the methods designed to find all the solutions for the power system are notoriously unreliable. Calculation of all the solutions is important to a certain extent because the distance between the HV solution and "closest" LV solution is a crude measure of system voltage stability margin [20]-[22]. Reliably calculating all the solutions for a power system remains a hard nut to crack.

1.3 Holomorphic Embedding

The holomorphic embedding (HE) is the technique of embedding a small problem within a large problem containing newly introduced complex variables while guaranteeing that the resultant problem is analytic or, equivalently, holomorphic. The HE method can be applied to the power-balance equations (PBE's), which originally are non-holomorphic or non-analytic due to the existence of the complex conjugate operator.

1.3.1 Holomorphic Functions

A holomorphic function is a complex-valued analytic function. Functions of complex variables that are complex differentiable everywhere in a neighborhood around a point are said to be holomorphic about that point. Since the holomorphic functions are analytic, they allow the use of the powerful theorems and techniques applicable only to the analytic function. In real analysis, differentiability in a neighborhood does not guarantee the analyticity of the function; however, in complex functions, differentiability guarantees analyticity. i.e., the power series expansion of the function about a point converges to the value of the function at that point [23].

1.3.2 Holomorphic Embedding Method

The holomorphic embedding method [24], a novel non-iterative method for solving the PF problems, eliminates the convergence problems of traditional iterative methods and unequivocally signals when no solution exists. It is guaranteed to find

the HV solution for a two-bus system using a simplified version of HE, mathematically proven in [25]. This approach is generalized for the multi-bus problem in [24] and [26] but with no controlled element models (i.e. PV/generator bus, Var limiting, LTC's, SVC's etc.) included.

1.4 Objectives

The long-run objective of this research is to use the HE method to find all or a certain set of solutions in a system of arbitrary topology, which includes voltage controlled bus models (PV bus). The research work reported upon in this document is focused on the implementation of the HE method as follows:

- To propose HE formulations for both PQ and PV bus model that will allow the LV/large-angle solutions to be found.
- To theoretically prove that the proposed HE-based LV/large-angle formulations are guaranteed to find all the LV/large-angle solutions for a power system.
- To numerically test the proposed algorithm on systems for which all the solutions are known and show that all solutions are obtained for these systems, i.e. the five-, seven- and 14-bus systems.
- To propose an algorithm that only finds the type-1 PF solutions (with one real-part eigenvalue in the system Jacobian matrix) using the proposed HE method.
- To numerically test the proposed algorithm on systems for which all the

type-1 solutions are known and validate that all the type-1 solutions are obtained for the systems been tested, i.e. the three-, five-, seven-, 14-, 118-bus systems.

- To investigate the numerical issues of the HE method for the problematic cases and come up with solutions to improve the numerical performance of the HE method. Also the robustness of the HE method needs to be tested on large-scaled power systems, i.e. ERCOT system with more than 6000 buses.

1.5 Organizations

This report is organized into six chapters:

Chapter 2 contains a literature review regarding iterative methods, the HE method and the methods whose goal is to find all or a set of solutions for a PF problem.

Discussed in Chapter 3 is the theory of the HE method, its characteristics as well as the sequence of calculations used in the HE method to solve the general multi-bus PF problem.

Starting from a simple two-bus system, derived in Chapter 4 is a modified HE PBE that is guaranteed to find only the LV solution in the two-bus system. This chapter has been presented in my qualifying exam and it is included in this report as reference.

Based on the derivation discussed in Chapter 5, a generalized HE PBE's that are guaranteed to all find all the LV/large-angle solutions for a multi-bus system are pro-

posed in Chapter 5. It is theoretically proven that the proposed formulation has the capability of finding all the solutions to the PF problem. Also numerical experiments on the five-, seven- and 14-bus systems show that the proposed formulation works as predicted.

An efficient algorithm to locate the type-1 PF solutions existing for a PF system is proposed in Chapter 6. It is shown that only the type-1 solutions are obtained using the proposed HE-based method on the five-, seven-, 14-, 118-bus systems. With the dynamic models included in the system, the proposed HE-based algorithm can be used to find the type-1 unstable equilibrium points (UEPs) and to determine the closest UEP, that is, the UEP with the lowest energy function value among all type-1 UEP's.

The numerical performance of the HE method is given in Chapter 7 and the problematic cases (i.e. the heavily loaded 43-bus system) are tested. It is shown that when the system is operating near its voltage collapse point, the HE method is likely to suffer precision issue, thus higher precision arithmetic will be needed in calculating the HV solution. Further, with the special case of the 43-bus LV solution, a continuation-power-flow-liked algorithm is applied to the proposed HE method to find the existing LV solution, without encountering the precision issue. In the end, the HE method is implemented using a sparsity-based Matlab program to simulate the large-scaled power systems and the results show that the solutions obtained by the HE

method match (through three decimal places) the solutions obtained by commercial software (PowerWorld), which use traditional iterative method.

The conclusions are included in Chapter 8.

2 LITERATURE REVIEW

The objective of the PF problem is to obtain the steady-state condition of the bus voltage magnitudes and angles given the real and reactive power injection at load (PQ) buses, and to find the voltage angles and reactive power given the voltage magnitude and real power injection at voltage controlled (PV/generator) buses. The HV solution for the PF problem is of importance and frequently used as the initial condition for other power system analysis such as transient stability, fault analysis.

2.1 Iterative Methods

One may formulate the bus PBE's in different forms depending on form in which the complex bus voltages variables and branch admittance constants are expressed: While there is no industry standard, the polar form of the voltage variables and the rectangular form of the branch admittances is most widely used. The PBE's at bus *i* in an (*N*+1)-bus system can be written as shown in (2.1):

$$\begin{aligned} P_i &= |V_i| \sum_{k=0}^{N} |V_k| \left[G_{ik} \cos(\delta_i - \delta_k) + B_{ik} \sin(\delta_i - \delta_k) \right] \\ Q_i &= |V_i| \sum_{k=0}^{N} |V_k| \left[G_{ik} \sin(\delta_i - \delta_k) + B_{ik} \cos(\delta_i - \delta_k) \right] \end{aligned} \tag{2.1}$$

where P_i is the real power injection at bus *i*, Q_i is the reactive power injection at bus *i*, $|V_i|$ and δ_i are the bus voltage magnitude and voltage angle for bus *i*, respectively, and G_{ik} and B_{ik} are the line conductance and susceptance between bus *i* and bus *k*, respectively. The slack bus index is taken as 0.

With PBE's written for every bus except the slack bus, a system of nonlinear equations is formed that can be solved using a number of iterative methods given an initial estimate of voltage variables. With a reasonable initial estimate, the desired HV solution, which is the operable solution, is typically found. However for ill-conditioned systems (those that are weakly-interconnected and have high R/X ratio lines [6]) or conditions where the system operates near the voltage collapse point, divergence of the iterative methods can be observed frequently, and it is challenging to determine whether the divergence is caused by the non-existence of a solution or the lack of robustness of the iterative methods. Basically three types of problems exist when using the iterative methods on the PF problem to find the HV solution: a) No solution exists and the procedure diverges, b) An HV solution exists however the iterative method diverges or c) The iterative method converges to one of the undesired solutions (LV solutions). As shown stylized in Figure 2.1 (from [8]), using an iterative method for finding the solution for $f(x)=0$ can have the convergence problems mentioned in a), b) and c), respectively, above.

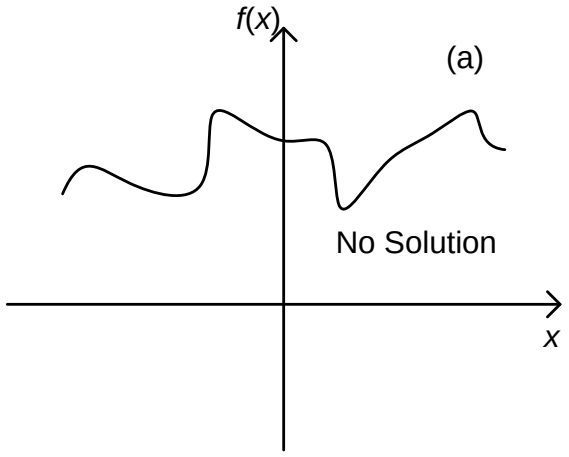

a) No Solution

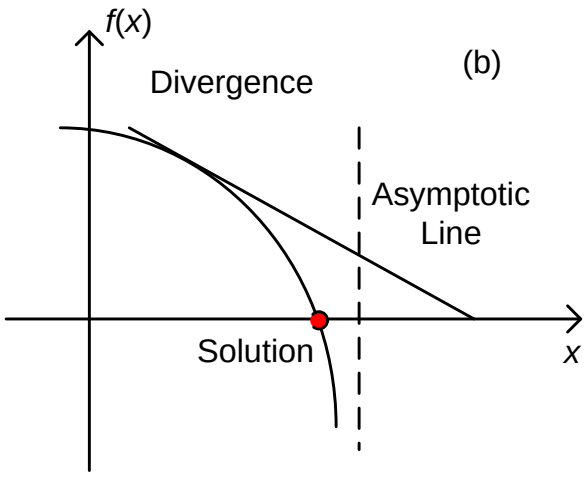

b) Divergence

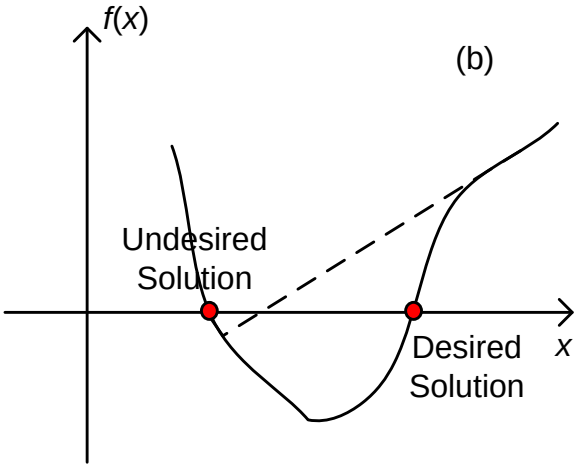

c) Undesired Solution(s)

Figure 2.1 Convergence Problems for Iterative Methods

As stated previously, it is difficult and usually impossible for the user to distinguish between cases a) and b). This is particularly true when the system is heavily loaded. With a poor initial estimate, the voltage solution can converge to (one of) the LV solution(s) as it is shown in c).

2.2 All the Solutions for a Power System

An (N+1)-bus network, characterized by the N complex nonlinear PBE's, has at most 2^N voltage solutions, not all of which may be unique. Starting from a reasonable initial estimate of the voltage profile, if the iterative methods converge, they usually, though not always, converge to the HV solution or the operable solution. While often times the HV solution is the desired solution, the LV solutions, in an appropriately reformulated but related problem, are metrics useful for assessing the system's dynamic stability margin. However finding all the solutions for a power system is usually complicated and the process heretofore has been unreliable.

2.3 Improve Convergence for Iterative Method

The GS method was the first iterative method applied for solving the PF problem, however, slow as well as unreliable convergence prevented the GS method from being widely used [27] . Consequently the NR method was developed which had better convergence behavior (for non-radial systems) as it required fewer iterations to converge compared to the GS method [27]. However despite the use of sparsity tech-

niques, the full NR method was computationally expensive as the Jacobian matrix was updated at each iteration; therefore quasi-Newton-based methods were developed for applications where the combination of complexity and computational speed were issues [27]. Newton's method and its variants relied on the function being well behaved in the region between the initial estimate and the solution. While these methods and many of their variants were ubiquitously used by the power industry and worked well for conditions close to nominal conditions, as the system moved into extremis and the voltages moved far from nominal, these methods could and did fail to converge.

The limitations and advancements in iterative methods have been a topic of research for many years and are discussed in the following sections.

2.3.1 Step-Size Adjustment Newton's Method

References [28]-[30] proposed a modified Newton's method with a step-size adjustment factor to improve the convergence behavior. Based on the traditional Newton's method, a modified correction estimate was added to the solution estimate and a cost function was introduced to determine the value of the correction. It was claimed that with the proposed method, case b) (divergence) in Figure 2.1 could be prevented and that the convergence behavior of traditional Newton's method was improved in any case.

However it was found that each of these methods converged on a subset rather than all problems with the operable solutions, the convergence improvement of the

methods proposed was not guaranteed, therefore these methods still suffered one drawback that all Newton-based methods seemed to suffer: the method did not signal if no solution existed and it was left to the users to wonder why convergence did not occur. Moreover the proposed method was more time consuming compared to the full Newton's method.

2.3.2 Decoupled Newton's Methods

By exploring the weak coupling of real power and voltage magnitude or reactive power and voltage angle, a Newton-based method, called fast decoupled load flow (FDLF) method [4], was proposed and widely used in the PF problems. The approximated Jacobian matrix needed to be calculated only once at the beginning of the iteration procedure in the FDLF method, unlike the traditional Newton's method. The less frequent evaluation of the Jacobian in the FDLF decreased its execution time compared to a full Newton method.. The convergence behavior for FDLF was discussed in [31]-[34]: Though FDLF usually took more iterations to converge, the execution time reduced considerably since the Jacobian matrix remained unchanged for each iteration. However to a greater or lesser degree, convergence problem still existed, especially when the system was heavily loaded, or when the coupling of real power and voltage magnitude (or reactive power and voltage angle) was strong, both of which made the approximation of the Jacobian matrix used inappropriate.

2.3.3 Miscellaneous Load-flow Method

Other techniques, though not in the popular category, have attracted some interest in the past. Reference [35] transformed the PF problem into a minimization problem where the objective function was constructed to minimize the sum of square of the power mismatches in PBE's. However, the method was computationally expensive and unreliable. This minimization approach did not fit into the PF problem well because of the nonlinearities in the PBE's [27]. Other approaches called hybrid Newton methods [36]-[39] used a different minimization objective to improve the computational performance for the minimization methods. The goal of the minimization was to find a 'closer' estimate to the solution of the PBE's located on the line between two consecutive iteration points. These minimization methods reduced the number of iterations needed by the traditional Newton approach; also the convergence performance was improved with the hybrid Newton's methods compared to the traditional Newton approach. However as system size and the number of PV buses increased, the algorithm was reported to needed more iterations to converge than the traditional Newton approach [27]. More critically, the minimization formulation yielded a computationally expensive solution process. Therefore, even in the cases where fewer iterations were needed, the execution time required was still large.

2.3.4 Non- Iterative Methods

A non-iterative method called the Series Load-Flow method was proposed in [40]. Though it was difficult (impossible except for textbook-size systems) to represent the PF solution in a closed form, a series approximation of the solution could be developed. However the work in [40] was essentially an analytical representation for the iteration process. Reference [41] had extended the work in [40] and the series was derived by expanding the solution function using Taylor series theory around a feasible operating point. The solution could be explicitly expressed by the Taylor series expansion thus the load sensitivity could be performed easily by checking the first-order-term coefficient of the Taylor series. Unlike other iterative methods, the voltage solution could be derived by one substitution once the series was established with non-iterative characteristics. However the solution was still initial point dependent; a reasonable feasible point that had small PBE's mismatches was required, otherwise the convergence of the Taylor series was not guaranteed. Finally, the calculation of the coefficients in the Taylor series could be computationally intensive and impractical for large system applications.

2.3.5 Continuation Power Flow Method

Another method which was widely used to improve the convergence is the continuation power flow (CPF) method (also known as the continuous Newton's method). It was proposed in [43]-[49] that for ill-conditioned systems, the CPF method could

be applied to overcome the convergence problem efficiently. The idea of CPF was to follow the characteristic curve of the power system (usually known as power-voltage (PV) or power-angle (Pδ) curve). Starting from a known solution on the curve, the load in the problem was increased until reaching the voltage collapse point, where divergence occurred for the traditional Newton's method. The CPF formulation was usually accomplished by augmenting the PF problem somewhat with one more new parameter introduced to model the load scaling and the prediction of the next solution on the curve was calculated based on a modified Jacobian matrix which allowed the user to reach the voltage collapse point, without encountering the matrix singularity issue.

The drawback for the CPF method was that the PBE's needed to be solved many times, starting from a known solution and moving incrementally toward the voltage collapse point, a process which would increase the execution time. This led to an inefficient in the algorithm, which became problematic when the system size became large. Thus the application of CPF methods had its own limitations.

2.4 Finding All the Solutions for Power-Flow Problem

There exist many algorithms proposed to find all the solutions existed for the PF problem and will be discussed in this section.

2.4.1 CPF Method

The proposed method in [50] was touted as being able to compute all the PF solutions using the CPF method. A five-bus system and a seven-bus system were numerically tested and all solutions for the system were found by the CPF method shown in [50]. While it had been conjectured that CPF method was capable of finding all solutions to the PF problems, a counterexample was published in 2013 [51] which showed that the CPF method was not 100% reliable while there existed strong voltage support in the power system. A rather simple five-bus system with all PV buses was tested which provided a counterexample that the method in [50] was not guaranteed to find all the solutions.

2.4.2 Homotopy Method

The homotopy method was another method used to solve for all the solutions existed in the power system [52], [53] reliably and the author of [54] recently developed a method called numerical polynomial homotopy continuation (NPHC) to find all the possible solutions for a set of polynomials, which could be applied to the PF problem. Before solving for the solutions of the PF problem, notated as $P(x)$, another easily solvable system of polynomials, $Q(x)$, were constructed. Requirements should be met that: all the roots for $Q(x)$ should be obtained without difficulty and the number of roots for $Q(x)$ should be identical to the number of possible roots in $P(x)$. Connected by the homotopy path, the roots of $P(x)$ could be obtained by starting from various

roots of $Q(x)$. The idea of the CPF method was somewhat similar to the homotopy method as at least one point of the analytic function had to be known. For the CPF method, the known point was on the PV curve and solved from the PF problem, where for homotopy method, the point can be obtained variously as long as the function $Q(x)$ satisfied the requirements above. The NPHC method was relatively reliable in finding all the solutions for the PF problem. It was reported in [54] that the NPHC method was computational expensive and it would produce non-physical solutions (solutions that did not satisfy the PBE's, caused by solving the real and reactive PBE's in the complex domain), resulting in more computation than required.

2.4.3 Groebner Basis

Technique using Groebner basis to find all the solutions for the PF problem was developed in [55]. The Buchberger algorithm, introduced in [55], could be used to calculate the Groebner basis in a relatively efficient way. By finding the Groebner basis for the non-linear system of equations, they could be solved in a manner similar to Gaussian elimination, which was used for solving simultaneous linear equations. The following example was given in [55] for understanding how Groebner basis technique could be used in solving a set of non-linear equations.

Two non-linear equations in (2.2) are to be solved:

$$\begin{aligned} x^3 - 2xy - 6 &= 0 \\ x^2 y - 2y^2 + x - 3.5 &= 0 \end{aligned} \tag{2.2}$$

Using Buchberger's algorithm, the Groebner basis for (2.2) can be determined as shown in (2.3):

$$\begin{aligned} 512y^3 - 196y^2 + 560y - 295 = 0 \\ -512y^2 - 588y + 407x - 392 = 0 \end{aligned} \tag{2.3}$$

Note that the first equation in (2.3) is only dependent on the variable *y*, therefore the possible solutions for *y* can obtained. Substituting the values of *y* back into the second equation in (2.3), the solution for *x* for the specific *y* value can be obtained thus all the solutions can be found for (2.2).

The system of equations for the PF problem could be solved using the Groebner basis approach to find all the possible solutions. However, the process is computationally expensive, e.g., for a five-bus system, the degree of the single-variable polynomial equation (i.e. the first equation in (2.3)) reaches 52 (given in [56]) and involves intensive calculation. Therefore the Groebner basis is impractical for large systems and it is only practical for systems of no more than five/six buses [24].

2.5 Type-1 Algebraic Solutions for Power-Flow Problem

2.5.1 Type-1 PF Solutions

For power system voltage stability assessment, only the type-1 PF solutions, where the system's Jacobian matrix has only one eigenvalue whose real-part is positive, are of interest among all the existing non-operable solutions ([57]-[59]). It had been proposed in [60]-[64] that the LV solutions for the PF problem could be determined through state-space equations (with dynamic models included) by exploring the sign

change of the eigenvalues in the system Jacobian matrix. Only one LV solution could be found by tracing the full PV curve. A simple six-bus system was tested in [60] verifying that with the known HV solution, one LV solution could be found. Moreover, [65] indicated that the search for the LV solutions could be restricted to finding the type-1 equilibrium points. These are equilibrium points whose linearized dynamic system's Jacobian matrix has a single eigenvalue with a positive real part.

In [65], an algorithm has been proposed to find the type-1 PF solutions using the NR method. The idea of the algorithm is to start with a guess at an initial estimate close to the type-1 PF solution by setting one of the bus voltage initial values close to 0.0 instead of 1.0, so that the iterative process would be expected to converge to the type-1 solution. However the drawback of this algorithm is obvious: 1) NR method is not guaranteed to find all the type-1 solutions, 2) NR method will not necessary converge to the desired solution even if the initial estimate is close to the solution [68], [69].

A more reliable algorithm based on the CPF method ([50]) was developed in [70] to find all the type-1 PF solutions in the electric power systems. It was numerically verified for the same five-/seven-bus system given in [50]. In [70], the CPF-based method traced the PV curve (for a load/PQ bus) or the Pδ curve (for a generator/PV bus) for all the buses in the system. This was achieved by:

(1) varying the loading of one PQ bus at a time or,

(2) varying the real power generation for one PV bus at a time.

The numerical continuation starts from the HV solution where all the eigenvalues of the PF Jacobian matrix were negative. Once the trace reached the bifurcation point or

a turning point, one of the eigenvalues for the system Jacobian matrix will become zero and the rest of them would remain negative. After reaching the bifurcation point, the method proposed in [70] would continue to trace the unstable branch for the PV/Pδ curve, therefore one of the eigenvalues of the Jacobian matrix would become positive, resulting a type-1 PF solution. While the theory in [70] is rigorous, the CPF-based method can fail to find all the type-1 solutions numerically, for systems with non-radial topology and weakly connected regions that have strong voltage support [51].

2.5.2 The Closest Unstable Equilibrium Point

For system with dynamic models included (i.e. a classical machine model, constant impedance load model), the system stability boundary is evaluated by the closest unstable equilibrium point (closest UEP), coming from one of the type-1 UEP's with the least-valued energy function compared to the stable equilibrium point (SEP) [71]-[76]. The author in [77] proposed a method of finding the closest UEP by redefining the problem statement such that a search of the closest UEP was replaced by the search of the SEP for a newly defined system. The newly defined system therefore could be solved by iterative algorithm (NR method) starting from a reasonable initial estimate. However it was reported in [78] that normally only two type-1 UEP's can be found by the method proposed in [77], therefore it was not guaranteed to find all the type-1 UEP's, or to find the closest UEP with the least-valued energy function among all the possible type-1 UEP's.

A homotopy-based method to find all the type-1 UEP's for the power system was developed in [78]. It was proven in [78] that if the homotopy curve passed the bifurcation point only once, the solution obtained would be a type-1 UEP. Note that a similar argument was made in [70] as a way to find all the type-1 PF solutions using the CPF-based method.. While the method proposed in [78] was reliable in finding the all the type-1 UEP's (or closest UEP), it was computational expensive to trace the homotopy curve for a large system as reported in [79] and tended to revisit of the type-1 solutions multiple times, which reduced the efficiency of the algorithm.

3 THE HIGH-VOLTAGE SOLUTION USING THE HOLOMORPHIC EMBEDDING METHOD

3.1 Embedded PBE's

As mentioned previously, the HE method is a technique of embedding a small problem within a large problem with complex variables while guaranteeing that the resultant problem is analytic or equivalently, holomorphic. In the case of the non-analytic PBE's for the PF problem, an appropriate embedding will eliminate the non-analyticity of the original PBE's caused by the complex conjugate operator.

Consider an (N+1)-bus power system: Let i be the bus number index in the (N+1)-bus system. The PBE of bus i can be expressed as:

$$\sum_{k=0}^{N} Y_{ik} V_k = \frac{S_i^*}{V_i^*} \tag{3.1}$$

Where Y_{ik} is the (i, k) entry of the bus admittance matrix, S_i is the complex power injection at bus i, and V_i is the bus voltage at bus i. The slack bus is denoted by the index 0.

Equation (3.1) may be holomorphically embedded into a larger problem with a complex variable s as shown in (3.2), giving the embedded formulation of PQ bus where N_{PQ} is the set of PQ buses in the (N+1)-bus system.

$$\sum_{k=0}^{N} Y_{ik} V_k(s) = \frac{s S_i^*}{V_i^*(s^*)}, \; i \in N_{PQ} \tag{3.2}$$

Similar formulation for the PV bus can be written in (3.3) with an additional voltage magnitude constraint, where N_{PV} is the set of PV buses and V_i^{cntr} is the controlled voltage magnitude for PV bus *i*. Note that for the PV bus, the reactive power injection/absorption is a variable to be determined after the solution is obtained, therefore Q_i is unknown in (3.3) and becomes as a function of *s*, unlike the form for PQ buses given in (3.2) where Q_i is independent of *s*. It should also be noted that the coefficients for $Q_i(s)$ is purely real.

$$\begin{aligned} &\sum_{k=0}^{N} Y_{ik} V_k(s) = \frac{sP_i - jQ_i(s)}{V_i^*(s^*)}, \; i \in m \\ &V_i(s) V_i^*(s^*) = \left| V_i^{cntr} \right|^2 \end{aligned} \tag{3.3}$$

The slack bus voltage can be written in (3.4) where V_{SLACK} is the specified slack bus voltage in the power system. The un-embedded PBE's can be recovered from (3.2) to (3.4) at *s*=1.

$$V_0 = V_{SLACK} \tag{3.4}$$

The following observations can be made regarding (3.2) to (3.4):

1) With the parameter *s* as a variable, the notation $V(s)$ is used to emphasize that the voltage has become a holomorphic function of the complex parameter *s*.
2) The complex conjugate of the voltage, V^* that appears in the PBE's is replaced by $V^*(s^*)$ instead of $V^*(s)$. The presence of s^* rather than *s* in this term retains the property of holomorphism of the function, and therefore, equivalently, analyticity.

3) At s=0, the power injection terms (S_i for the PQ bus or P_i for the PV bus) in the embedded PBE's vanish. This represents the germ case where there is no generation/no load in the system. For this case, (3.2) and (3.3) are reduced to (3.5) and (3.6), respectively

$$\sum_{k=0}^{N} Y_{ik} V_k(0) = 0,\ i \in N_{PQ} \tag{3.5}$$

$$\sum_{k=0}^{N} Y_{ik} V_k(0) = \frac{-jQ_i(0)}{V_i^*(0)},\ i \in N_{PV} \tag{3.6}$$

$$V_i(0)V_i^*(0) = \left|V_i^{cntr}\right|^2$$

The voltage solution at s=0 can be obtained by solving the set of equations given in (3.4), (3.5) and (3.6) simultaneously.

4) As stated previously, at s=1, the PBE's in (3.1) are recovered from the embedded system of equations and the solution obtained is guaranteed to be the HV solution for the PF problem. The solution at s=1 is results from the solution at s=0 by the technique of maximal analytic continuation [24].

However, solving for the solution at s=0, or the germ solution, is somewhat difficult since (3.6) is in the quadratic form. Therefore the iterative methods mentioned in Chapter 2 will have to be applied unreliably to obtain the solution at s=0 which requires a good initial estimate of the solution. A simpler way to find the germ solution is to use the modified HE PBE's given in (3.7)-(3.9). With the modified HE PBE's, the solution at s=0 can be obtained simply by observation and will be discussed in details as follows.

$$\sum_{k=0}^{N} Y_{ik}^{(tr)} V_k(s) = \frac{sS_i^*}{V_i^*(s^*)} - s\sum_{k=0}^{N} Y_{ik}^{(sh)} V_k(s)\ ,\ i \in N_{PQ} \tag{3.7}$$

$$\sum_{k=0}^{N} Y_{ik}^{(tr)} V_k(s) = \frac{sP_i - jQ_i(s)}{V_i^*(s^*)} - s\sum_{k=0}^{N} Y_{ik}^{(sh)} V_k(s)\ ,\ i \in N_{PV} \tag{3.8}$$

$$V_i(s)V_i^*(s^*) = 1 + s(\left|V_i^{cntr}\right|^2 - 1)$$

$$V_0(s) = 1 + s(V_{SLACK} - 1) \tag{3.9}$$

In (3.7) and (3.8), $Y_{ik}^{(tr)}$ is the bus admittance matrix entry between bus *i* and bus *k* considering only the non-shunt branch impedance. In other words, the shunt branches are ignored when constructing the bus admittance matrix. The variable $Y_{ik}^{(sh)}$ is a diagonal matrix containing only the shunt elements. Numerically $Y_{ik}^{(sh)} = Y_{ik} - Y_{ik}^{(tr)}$. With the embedding of *s* in front of the $\sum_{k=0}^{N} Y_{ik}^{(sh)} V_k(s)$ term in (3.7) and (3.8), the effect of shunts will vanish at *s*=0. Also the effect of slack bus and PV bus voltage being different from 1.0 per-unit vanishes at *s*=0. Therefore at *s*=0 (3.7)-(3.9) reduce to the form given in (3.10)-(3.12), respectively.

$$\sum_{k=0}^{N} Y_{ik}^{(tr)} V_k(0) = 0\ ,\ i \in N_{PQ} \tag{3.10}$$

$$\sum_{k=0}^{N} Y_{ik}^{(tr)} V_k(0) = \frac{-jQ_i(0)}{V_i^*(0)}\ ,\ i \in N_{PV} \tag{3.11}$$

$$V_i(0)V_i^*(0) = 1$$

$$V_0(0) = 1 \tag{3.12}$$

Notice that (3.10) and (3.11) can be satisfied at s=0 if all the bus voltages are 1.0 p.u. and all the reactive power injections for PV buses are zero. Therefore, with the modified HE PBE's given in (3.7)-(3.9), the solution at s=0 can be easily obtained given in (3.13) without the necessity of solving quadratic equations using the iterative methods:

$$\begin{aligned} V_i(0) &= 1,\ i = 0...N \\ Q_i(0) &= 0\ ,\ i \in N_{PV} \end{aligned} \tag{3.13}$$

The solution procedure of (3.10)-(3.12) is based on representing the voltage function as a power series and then generating the maximal analytic continuation of the power series [24].

3.2 Power Series Expansion

Assuming the PBE's are holomorphically embedded: it is guaranteed, because of analyticity, that the voltage and PV bus reactive power can be represented as power series using s as the expansion parameter. I.e. the voltage function $V(s)$ in (3.2) and reactive power function Q(s) in (3.3) can be expressed as a Maclaurin series as follows within its radius of convergence:

$$\begin{aligned} V(s) &= \sum_{n=0}^{\infty} V[n](s)^n \\ Q(s) &= \sum_{n=0}^{\infty} Q[n](s)^n \end{aligned} \tag{3.14}$$

where the $V[n]$ is the n^{th} order coefficient for the $V(s)$ function and it is complex number, $Q[n]$ is the n^{th} order coefficient for the $Q(s)$ function but it is purely real number.

The Maclaurin series expansion of the voltage function can be used to prove that the embedding in (3.2) and (3.3) is holomorphic: To be analytic, any function f must satisfy the Cauchy-Riemann equations. An equivalent condition in complex domain known as Wirtinger's ([23]) derivative requires that:

$$\partial f / \partial s^* = 0 \tag{3.15}$$

In [24], it is mentioned that the embedding can retain the holomorphicity only when V^* is embedded with variable s^* instead of s. We will prove this statement using the Wirtinger's derivative. The truncated Maclaurin series expansion of the $V^*(s)$ and $V^*(s^*)$ (if they were to exist within radius of convergence) are written below:

$$\begin{aligned} V^*(s) &\approx V[0]^* + V[1]^* s^* + \ldots + V[n]^* \left(s^*\right)^n \\ V^*(s^*) &\approx V[0]^* + V[1]^* s + \ldots + V[n]^* \left(s\right)^n \end{aligned} \tag{3.16}$$

The variable $V^*(s)$ in (3.16), is a function of s^* therefore the Wirtinger equations will not be satisfied. The expansion of $V^*(s^*)$ indeed is independent of s^* such that $\partial V^*(s^*)/\partial s^* = 0$. Thus the voltage function $V^*(s^*)$ in (3.16) is holomorphic. The power series of the voltage, (3.14), when evaluated at s=1, gives the solution to the original PBE's. However, if the power series has a radius of convergence less than 1.0, then the sum of power series terms evaluated at s=1 will not converge; however a technique known as analytic continuation [82] may be applied to extend this radius of

convergence. The maximal analytic continuation (which is unrelated to CPF) allows certain ostensibly unbounded series to converge by effectively extending the convergence region to the maximum possible value. One maximal analytic continuation, the diagonal or near-diagonal Padé Approximant [82], uses rational approximants to achieve this goal. It can be proven that the Padé Approximant is the maximal analytic continuation of the power series in [83]. In other words, if a solution of the PBE's exists, the Padé Approximant is guaranteed to converge [24]; and conversely, if the Padé Approximant does not converge, the system of PBE's does not have a solution, meaning the power system is beyond the voltage collapse point and non-operable. The idea of Padé Approximant will be discussed in Section 3.4.

3.3 Power Series Coefficients

The procedure of calculating the power series coefficients is discussed in detail given in [26] without the PV bus model. The n^{th} order coefficient for the voltage series can be calculated given the voltage series coefficients up to (n-1)-th order:

$$\sum_{k=0}^{N} Y_{ik}^{(tr)} V_k[n] = S_i^* W_i^*[n-1] - \sum_{k=0}^{N} Y_{ik}^{(sh)} V_k[n-1],\ i \in N_{PQ} \tag{3.17}$$

where $W_i(s)$ is a power series equivalent to $1/V_i(s)$ and $W_i[n]$ is the n^{th} order coefficient for $W_i(s)$.

The product of $W_i(s)$ and $V_i(s)$ is a convolution of two power series given in (3.18).

$$\left(\sum_{n=0}^{\infty} V_i[n] s^n\right)\left(\sum_{n=0}^{\infty} W_i[n] s^n\right) = 1 \tag{3.18}$$

By equating the both sides in (3.18), the convolution of $W_i(s)$ and $V_i(s)$ will be 1.0 only if its constant term (s^0) is 1.0 and other terms set equal to zero starting from s^1 term given in (3.19).

$$\sum_{m=0}^{n} V_i[m]W_i[n-m] = \delta_{n0}$$
$$\delta_{n0} = \begin{cases} 1, & n = 0 \\ 0, & otherwise \end{cases} \tag{3.19}$$

With $V_i[0]$ given in (3.13), $W_i[0]$ is 1.0 from (3.19). Then $V_i[1]$ can be calculated from (3.17), and $W_i[1]$ found using (3.19). This procedure can be repeated for calculating the remaining coefficients for the voltage series.

While determining the power series coefficients for the PQ bus is relatively straight forward, the calculation procedure for the PV bus coefficients is more involved. In the PV bus formulation given in (3.8), the reactive power injection (absorption) for the PV bus is no longer a constant but dependent on s, equivalently becoming another power series $Q_i(s)$. Therefore the $\frac{-jQ_i(s)}{V_i^*(s)}$ term in (3.8) can be written as a convolution of two power series. The n^{th} order coefficient for the voltage series can be calculated given the voltage series and reactive power coefficients up to (n-1)-th order.

$$\sum_{k=0}^{N} Y_{ik}^{(tr)} V_k[n] =$$
$$P_i W_i^*[n-1] - j\sum_{m=0}^{n} Q_i[m]W_i^*[n-m] - \sum_{k=0}^{N} Y_{ik}^{(sh)} V_k[n-1],\ i \in N_{PV} \tag{3.20}$$

where $W_i(s)$ is again the power series equivalent to $1/V_i(s)$.

Note that for the PV bus, the voltage magnitude is constant as shown in the second equation in (3.8), thus introducing the HE voltage constraint given in (3.21).

$$\sum_{m=0}^{n} V_i[m]V_i^*[n-m] = \delta_{n0} + (\left|V_i^{cntr}\right|^2 - 1)\delta_{n1}$$
$$\delta_{n0} = \begin{cases} 1, n=0 \\ 0, otherwise \end{cases}, \delta_{n1} = \begin{cases} 1, n=1 \\ 0, otherwise \end{cases} \tag{3.21}$$

Note that the real part of $V_i[n]$ can be calculated from (3.21) given the voltage series up to $V_i[n\text{-}1]$, shown in (3.21).

$$V_i[0]V_i^*[n] + V_i[n]V_i^*[0] + \sum_{m=1}^{n-1} V_i[m]V_i^*[n-m] = \delta_{n0} + (\left|V_i^{cntr}\right|^2 - 1)\delta_{n1}$$
$$\Downarrow$$
$$\mathrm{Re}(V_i[n]) = \delta_{n0} + \frac{(\left|V_i^{cntr}\right|^2 - 1)}{2}\delta_{n1} - \frac{\sum_{m=1}^{n-1} V_i[m]V_i^*[n-m]}{2} \tag{3.22}$$
$$\delta_{n0} = \begin{cases} 1, n=0 \\ 0, otherwise \end{cases}$$
$$\delta_{n1} = \begin{cases} 1, n=1 \\ 0, otherwise \end{cases}$$

With the real part of $V_i[n]$ calculated, the imaginary part of $V_i[n]$ and real-valued $Q_i[n]$ can be calculated by separating (3.20) into real and imaginary parts. Note that $Q_i[0]$=0 (3.13); consequently the first term $Q_i[0]W_i^*[n]$ in the convolution $\sum_{m=0}^{n} Q_i[m]W_i^*[n-m]$ on the RHS of (3.20) will vanish. Therefore there exist two real equations (the real and imaginary parts of (3.20)) with two real unknowns (the imaginary part of $V_i[n]$ and real-valued $Q_i[n]$). Thus the remaining coefficients for $V_i(s)$ and $Q_i(s)$ can be calculated. By massaging the PQ/PV bus formulations into one matrix

(details in [87] and given in (3.23)), it is straightforward to obtain the power series coefficients for the PQ/PV buses.

$$\begin{bmatrix} 1 & & & & & \\ & 1 & & & & \\ G_{10} & -B_{10} & 0 & -B_{11} & G_{12} & -B_{12} \\ B_{10} & G_{10} & 1 & G_{11} & B_{12} & G_{12} \\ G_{20} & -B_{20} & 0 & -B_{21} & G_{22} & -B_{22} \\ B_{20} & G_{20} & 0 & G_{21} & B_{22} & G_{22} \end{bmatrix} \begin{bmatrix} V_{0re}[n] \\ V_{0im}[n] \\ Q_1[n] \\ V_{1im}[n] \\ V_{2re}[n] \\ V_{2im}[n] \end{bmatrix} = \begin{bmatrix} \delta_{n0} + \delta_{n1}(V_{Slack} - 1) \\ 0 \\ \mathrm{Re}(Rhs\_Known\ [n-1]) \\ \mathrm{Im}(Rhs\_Known\ [n-1]) \\ \mathrm{Re}(S_2^* W_2^*[n-1] - Y_{2shunt} V_2[n-1]) \\ \mathrm{Im}(S_2^* W_2^*[n-1] - Y_{2shunt} V_2[n-1]) \end{bmatrix} - \begin{bmatrix} 0 \\ 0 \\ G_{11} \\ B_{11} \\ G_{21} \\ B_{21} \end{bmatrix} V_{1re}[n] \tag{3.23}$$

$$V_{1re}[n] = \delta_{n0} + \delta_{n1} \frac{|V_1^{cntr}|^2 - 1}{2} - \frac{1}{2} \sum_{k=1}^{n-1} V_1[k] V_1^*[n-k]$$

where the indices 0, 1, 2 are the slack bus, PV and PQ index, respectively. Subscript *re* and *im* are the abbreviation for real and imaginary, respectively. The term *Rhs_known*[*n*-1] is the calculated RHS of embedded PV bus PBE at s^{n-1}.

3.4 Maximal Analytic Continuation

While the procedure for finding the coefficients for the voltage power series is well developed and details are discussed in [26] and [87], the idea of analytic continuation is relatively unknown to engineers. Below is a simple example demonstrating the analytic continuation technique:

Consider an infinite-term power series, $f_1(s)$, given in (3.24),

$$f_1(s) = 1 + s + s^2 + \ldots = \sum_{n=0}^{\infty} s^n \tag{3.24}$$

Truncating the series at its n^{th} order and multiply the series in (3.24) by (1-*s*), the truncated series can be calculated as (3.25),

$$(1-s)(1+s+s^2+\ldots+s^n)=1-s^{n+1}$$
$$\Downarrow \tag{3.25}$$
$$1+s+s^2+\ldots+s^n=\frac{1-s^{n+1}}{1-s}$$

By taking the limit of n to infinity, $f_1(s)$ in (3.24) can be evaluated as

$$f_1(s)=1+s+s^2+\ldots=\lim_{n\to\infty}\frac{1-s^{n+1}}{1-s} \tag{3.26}$$

It can be determined that, when $|s|<1$, $f_1(s)$ is identical to $\frac{1}{1-s}$. Therefore the infinite-term series $f_1(s)$ represent an explicit function $\frac{1}{1-s}$ within the radius of converge of the series, i.e. $|s|<1$, shown in Figure 3.1.

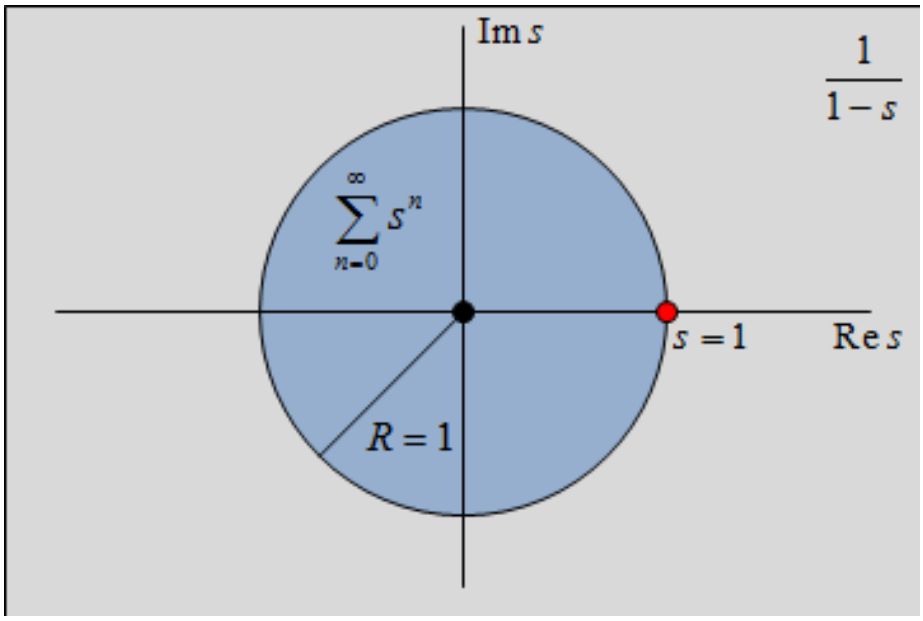

Figure 3.1 Radius of Convergence of Power Series $f_1(s)$

Consider an integral function $f_2(s)$ given in (3.27),

$$f_2(s)=\int_0^\infty e^{-(1-s)x}dx \tag{3.27}$$

The explicit form of the integral function $f_2(s)$ can be derived shown in (3.28),

$$\int_0^{\infty} e^{-(1-s)x}dx = \lim_{A\to\infty}\int_0^{A} e^{-(1-s)x}dx = \lim_{A\to\infty}\frac{1-e^{-(1-s)A}}{1-s} = \frac{1}{1-s} \qquad (3.28)$$

$IFF\ \ \mathrm{Re}(s)<1$

Note $f_1(s)$ in (3.24) and $f_2(s)$ in (3.27) can represent the explicit function $\frac{1}{1-s}$ within different regions shown in Figure 3.2. Light blue in Figure 3.2 is the region where the integral function $f_2(s)$ can represent $\frac{1}{1-s}$ and the circular dark blue region is the radius of convergence for the power series $f_1(s)$. It can be observed that the integral function can represent the explicit function $\frac{1}{1-s}$ in a larger region compared to the power series. With the above property, the integral function $f_2(s)$ is known as the analytic continuation for the power series $f_1(s)$, and the explicit function $\frac{1}{1-s}$ is the maximal analytic continuation for the power series. Note that $\frac{1}{1-s}$ is non-holomorphic only at s=1, giving the largest possible region where function is holomorphic.

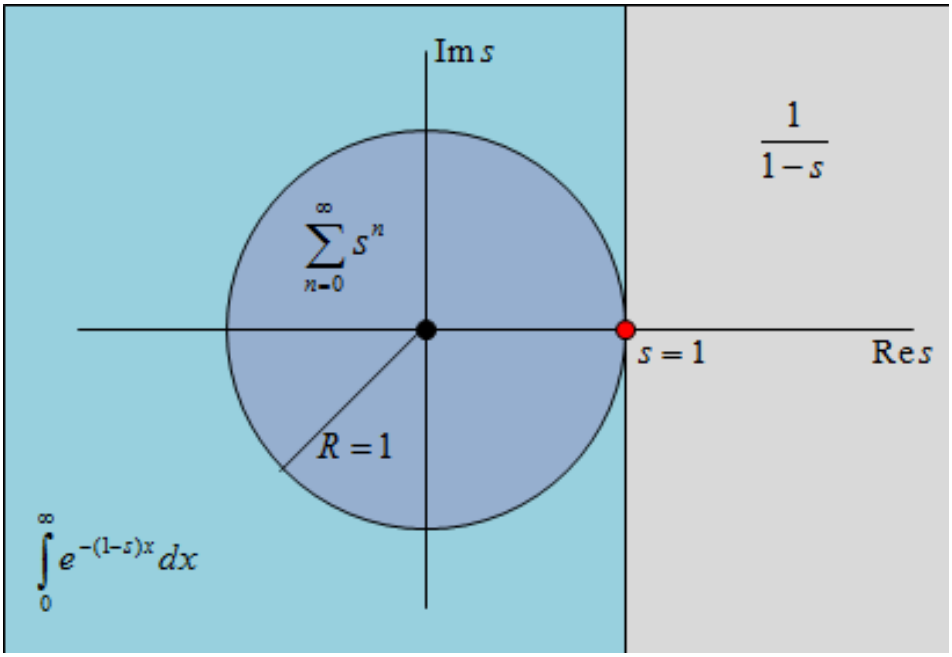

Figure 3.2 Regions for $f_1(s)$ and $f_2(s)$ Representing 1/(1-s)

As mentioned in Section 3.2, the Padé Approximant is proven to be the maximal analytic continuation (in a rational form) of a power series [83]. There exist many methods to calculate the Padé Approximant, one of which is to build the Padé Approximant from the power series coefficients by using the direct or matrix method. Another method to find the Padé Approximant is to form the continued fraction using the Viskovatov method [26]. The details for both the direct method and Viskovatov method are shown in Section 3.5 below.

3.5 Padé Approximant

3.5.1 Direct/Matrix Method

The Padé Approximant, the technique for finding a rational form representation for the power series, was developed by Henri Padé in 1890. Any general analytic function, $c(s)$, can be represented by the power series given in (3.29) within its radius of convergence:

$$c(s) = c[0] + c[1]s + c[2]s^2 + c[3]s^3 + \ldots = \sum_{n=0}^{\infty} c[n]s^n \tag{3.29}$$

where $c[n]$ is the power series coefficient for n^{th} degree term (s^n).

For the power series given by (3.29) truncated to L+M+1 terms, the Padé Approximant can be expressed as the rational form of two finite power series, $a(s)$ and $b(s)$, given in (3.30):

$$[L/M] = \frac{a[0] + a[1]s + a[2]s^2 + \ldots + a[L]s^L}{b[0] + b[1]s + b[2]s^2 + \ldots + b[M]s^M} \tag{3.30}$$

where L is the degree of the numerator polynomial $a(s)$, and M is the degree of the denominator polynomial $b(s)$.

The approximant in (3.30) is referred as an [L/M] Padé and it can be evaluated from the power series in (3.29) truncated at (L+M)-th order, given in (3.31):

$$\begin{aligned} c(s) &= c[0] + c[1]s + c[2]s^2 + \ldots c[L+M]s^{L+M} + O(s^{L+M+1}) \\ &= \frac{a[0] + a[1]s + a[2]s^2 + \ldots + a[L]s^L}{b[0] + b[1]s + b[2]s^2 + \ldots + b[M]s^M} = \frac{a(s)}{b(s)} \end{aligned} \tag{3.31}$$

where O (s^{L+M+1}) indicates the truncation error for the [L/M] Padé

In (3.31), the power series coefficients for $c(s)$ are known, giving L+M+1 known coefficients while there are L+M+2 unknowns in $a(s)$ and $b(s)$. Hence, one of the coefficients in either $a(s)$ or $b(s)$ is a free variable and for simplicity, the constant term in the denominator polynomial, $b[0]$, is chosen to be 1.0. Multiplying (3.31) by $b(s)$ on both sides:

$$\begin{aligned} &(c[0] + c[1]s + c[2]s^2 + \ldots c[L+M]s^{L+M})(b[0] + b[1]s + b[2]s^2 + \ldots + b[M]s^M \\ &= a[0] + a[1]s + a[2]s^2 + \ldots + a[L]s^L \end{aligned} \tag{3.32}$$

It can be observed that the coefficients from s^{L+1} to s^{L+M} on the LHS of

(3.32) have to be zero since there is no corresponding term on the RHS of (3.32). Hence *b[i]* coefficients are given by the set of equations in (3.33).

$$\begin{aligned} &b[M]c[L-M+1] + b[M-1]c[L-M+2] + \cdots b[0]c[L+1] = 0 \\ &b[M]c[L-M+2] + b[M-1]c[L-M+3] + \cdots b[0]c[L+2] = 0 \\ &\vdots \\ &b[M]c[L] + b[M-1]c[L-1] + \cdots b[0]c[L+M] = 0 \end{aligned} \tag{3.33}$$

The equations given in (3.33) form a system of M linear equations that can be expressed in a matrix form given in (3.34) by moving the known term to the RHS, i.e.

$b[0]c[L+1]$, $b[0]c[L+2]$, etc., where $b[0]=1$. Therefore the power series coefficients for $b(s)$ can be obtained by solving the matrix equation in (3.34) using traditional LU factorization techniques.

$$\begin{bmatrix} c[L-M+1] & c[L-M+2] & c[L-M+3] & \cdots & c[L] \\ c[L-M+2] & c[L-M+3] & c[L-M+4] & \cdots & c[L+1] \\ c[L-M+3] & c[L-M+4] & c[L-M+5] & \cdots & c[L+2] \\ \vdots & \vdots & \vdots & \ddots & \vdots \\ c[L] & c[L+1] & c[L+2] & \cdots & c[L-M] \end{bmatrix} \begin{bmatrix} b[M] \\ b[M-1] \\ b[M-2] \\ \vdots \\ b[1] \end{bmatrix} = -\begin{bmatrix} c[L+1] \\ c[L+2] \\ c[L+3] \\ \vdots \\ c[L+M] \end{bmatrix} \tag{3.34}$$

With the coefficients obtained for the denominator polynomial, the power series coefficients in $a(s)$ can be obtained by equating the coefficients from s^0 to s^L on both sides of (3.32):

$$\begin{aligned} & c[0]b[0] = a[0] \\ & b[0]c[1] + b[1]c[0] = a[1] \\ & \vdots \\ & \textit{In general}: \sum_{k=0}^{L} c[k]b[L-k] = a[L] \end{aligned} \tag{3.35}$$

Though the matrix method described above allows the calculation of a rational approximant of any arbitrary degree, Stahl's theory [83]-[85] indicates that the diagonal ($L=M$) or the near-diagonal ($|L-M|=1$) Padé Approximants yield the best accuracy when evaluating the power series outside its radius of convergence.

Using the above mentioned calculation procedure, a near-diagonal [0/1] Padé Approximant is calculated for the same series given in (3.24), where the series is truncated after the s^2 term. The Padé Approximant evaluated is found to be $\frac{1}{1-s}$, which coincides

with the explicit function in Section 3.4. This example is consistent with Stahl's proof that the Padé Approximant is indeed the maximal analytic continuation, hence giving the best rational function approximation of the power series beyond its radius of convergence.

3.5.2 Viskovatov Method

Another method to find the Padé Approximant from a given power series is to build the continued fraction using the Viskovatov method. Such continued fraction is equivalent to the diagonal (or near-diagonal for series with an even number of terms) Padé Approximant of the given power series [24]. The detailed procedure of Viskovatov method is demonstrated below for any general analytic function notated as $c(s)$:

Equation (3.29) can be written as:

$$\begin{aligned} c(s) &= c[0] + c[1]s + c[2]s^2 + \ldots + c[n]s^n + \ldots \\ &= c[0] + s(c[1] + c[2]s + \ldots + c[n]s^{n-1} + \ldots) \\ &= c[0] + \cfrac{s}{\cfrac{1}{c[1] + c[2]s + \ldots + c[n]s^{n-1} + \ldots}} \\ &= c[0] + \frac{s}{c^{(1)}(s)} \end{aligned} \tag{3.36}$$

The series $c^{(1)}(s)$ in (3.36), originally represented by the reciprocal of a power series, can be transformed into a new power series given by:

$$\begin{aligned} c^{(1)}(s) &= \frac{1}{(c[1] + c[2]s + c[3]s^2 + \ldots + c[n]s^{n-1} + \ldots)} \\ &= c^{(1)}[0] + c^{(1)}[1]s + \ldots + c^{(1)}[n-1]s^{n-1} + \ldots \end{aligned} \tag{3.37}$$

The process of calculating the coefficients of the new power series $c^{(1)}(s)$ is described below. Using the notation of (3.37), by definition,

$$\begin{aligned}&(c^{(1)}[0]+c^{(1)}[1]s+\ldots+c^{(1)}[n-1]s^{n-1}+\ldots)\\&(c[1]+c[2]s+\ldots+c[n]s^{n-1}+\ldots)=1\end{aligned} \tag{3.38}$$

Equation (3.38) is a product of two power series on the LHS. Since this product must equal one for any value of *s*, it must be the case that

$$c^{(1)}[0]=\frac{1}{c[1]} \tag{3.39}$$

Now, $c^{(1)}[n],\ \forall n=1,2,3,\cdots$ can be calculated from (3.38) as follows:

1) Assume the coefficients of $c^{(1)}[n]$ have been calculated through index k-1.

2) Multiply the appropriate terms on the LHS of the two power series, (3.38), up through the k^{th} term to find the coefficient of s raised to k. (It is shown previously in Section 3.3 that the coefficients of the product of two power series can be determined by the convolution of the two corresponding discrete sequences).

3) By equating the coefficients of the power series on the both sides of (3.38), the $c^{(1)}[k]$ term can be calculated. For example, if $c^{(1)}[1]$ is to be calculated, the coefficient for s^1 in the product of two power series in (3.38) is $(c[1]c^{(1)}[1]+c^{(1)}[0]c[2])$, which has to equal zero as the RHS of (3.38) has no term corresponding to s^1. Since $c[1]$, $c[2]$ and $c^{(1)}[0]$ are known, $c^{(1)}[1]$ can therefore be calculated as: $c^{(1)}[1]=-c^{(1)}[0]c[1]\big/c[2]$. Repetition of this procedure can be used to calculate $c^{(1)}[k]$.

Applying the technique as described above to the last equation in (3.36) recursively yields:

$$c(s) = c[0] + \cfrac{s}{c^{(1)}[0] + \cfrac{s}{\cfrac{1}{c^{(1)}[1] + \ldots + c^{(1)}[n-1]s^{n-2} + \ldots}}} \tag{3.40}$$

$$c(s) = c[0] + \cfrac{s}{c^{(1)}[0] + \cfrac{s}{c^{(2)}[0] + \cfrac{s}{c^{(3)}[0] + \ldots}}} \tag{3.41}$$

The continued fraction in (3.41) can be evaluated directly by replacing s=1. It can also be evaluated in the form $c_n(s)=a_n(s)/b_n(s)$ using the three term recursion relation (3.42) in [26] where n is the order of the recursion relation.

$$\begin{aligned} &a_0(s) = c[0], a_1(z) = c[0]c^{(1)}[0] + s \\ &a_i(s) = c^{(i)}[0]a_{i-1}(s) + sa_{i-2}(s), i = 2, 3, \ldots \\ &b_0(s) = 1, b_1(s) = c^{(1)}[0] \\ &b_i(s) = c^{(i)}[0]b_{i-1}(s) + sb_{i-2}(s), i = 2, 3, \ldots \end{aligned} \tag{3.42}$$

It should be noted that the $a(s)$ and $b(s)$ obtained by the Viskovatov method theoretically coincides with the $a(s)$ and $b(s)$ obtained from the matrix method in Section 3.5.1, while different though comparable numerical values are obtain due to the limit of machine precision. The three term recursion relation is preferred over the continued fraction since it gives flexibility in choosing the number of terms in the continued fraction and reduces the number of steps for calculation. To be more precise, when using the three term recursion relation, *a posteriori* increase in the length of the con-

tinued fraction, involves fewer calculations than direct evaluation, which requires starting the continued fraction anew. This occurs because b_i is a function of $c[i]$ and previous b_k values, $k<i$; hence if an extra term is added to the continued fraction, it can be incorporated into the rational approximant by one more evaluation of (3.42).

In the numerical implementation of the above mentioned steps, the power series of voltage function and reactive power function, (3.14), and hence the continued fraction expansion, (3.41), are evaluated only for a finite number of terms. Despite using extended precision, the power series coefficients cannot be represented accurately, after about 40-60 terms, due to the accumulation of round-off error [24].

Both methods were applied to this research and the direct method was preferred since it can better detect some numerical precision issues by simply checking the condition number of the coefficient matrix.

3.6 Curve Following in HE

As stated previously, the HE method is different from the traditional continuation methods used for solving the PF problem in so many ways that the two are mathematically unrelated. In (3.2), as the parameter s is increased from 0 to 1, the load at all the PQ buses, e.g., i, increases linearly from 0 to S_i though interest is only on the case where s=0 and s=1. Based on this observation it is tempting to conclude that the HE formulation also performs curve following similar to the continuation methods. On the contrary, (3.2) represents the PBE's accurately only at s=1. If shunt reactance exists at

bus i in the system, the $s\sum_{k=0}^{N} Y_{ik}^{(sh)} V_k(s)$ term in (3.7) will be scaled as s increases, making the solution of the HE PBE's different from the un-embedded PBE's in (3.1) for $s \neq 1$. Also the modification on PV bus voltage constraint and slack bus voltage in (3.8) and (3.9) will contribute to the differences between the HE PBE's and the original PBE's. In this section, the difference will be demonstrated for a simple two-bus system with the shunt reactance connected to the PQ/load bus as shown in Figure 3.3.

The PBE for the PQ bus in Figure 3.3 can be written as:

$$\frac{V - V_0}{Z} = \frac{S^*}{V^*} + \frac{V}{jX_C} \tag{3.43}$$

Where the variable V is the voltage at the PQ bus, V_0 is the slack-bus voltage, $Z=R+jX$ is the line impedance between the PQ bus and the slack bus, $S=-(P_L+jQ_L)$ is the complex power at the PQ bus, and X_C is the shunt reactance connected to the PQ bus, which is included to emphasize the effect of the $s\sum_{k=0}^{N} Y_{ik}^{(sh)} V_k(s)$ term.

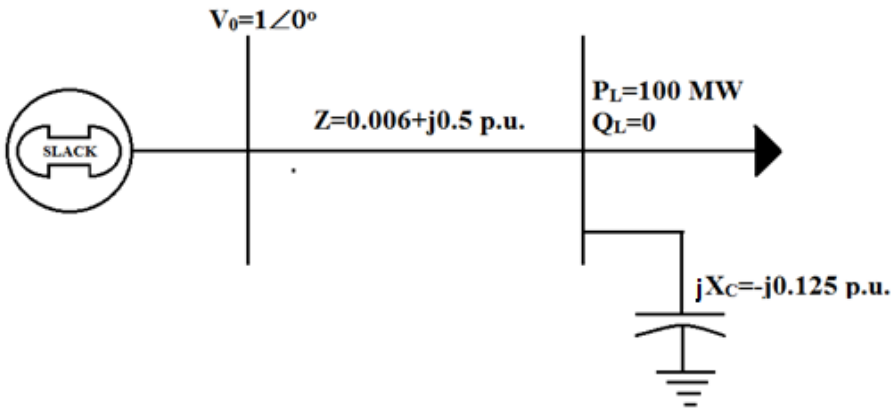

Figure 3.3 Two-Bus Example with Shunt Reactance

The system parameters for the two-bus model are specified using a 100 MVA base in Figure 3.3. In order to demonstrate the difference between the HE solution and the continuation method for solving the PBE's, a comparison is made between the power-voltage (PV) curve generated from the un-embedded PBE in (3.1) and the HE voltage function curve generated from (3.2). For the purposes of distinction, the HE voltage function curve is referred to as the sV curve to distinguish it from the traditional PV curve.

In Figure 3.4, the red dashed line represents the plot of the true PV (not sV) curve for the load bus in the two bus system that is obtained using a continuation method. The HE voltage function, $V(s)$, defined by (3.2) is plotted as a function of the parameter s, shown by the solid blue line in Figure 3.4 which is obtained using the HE formulation.

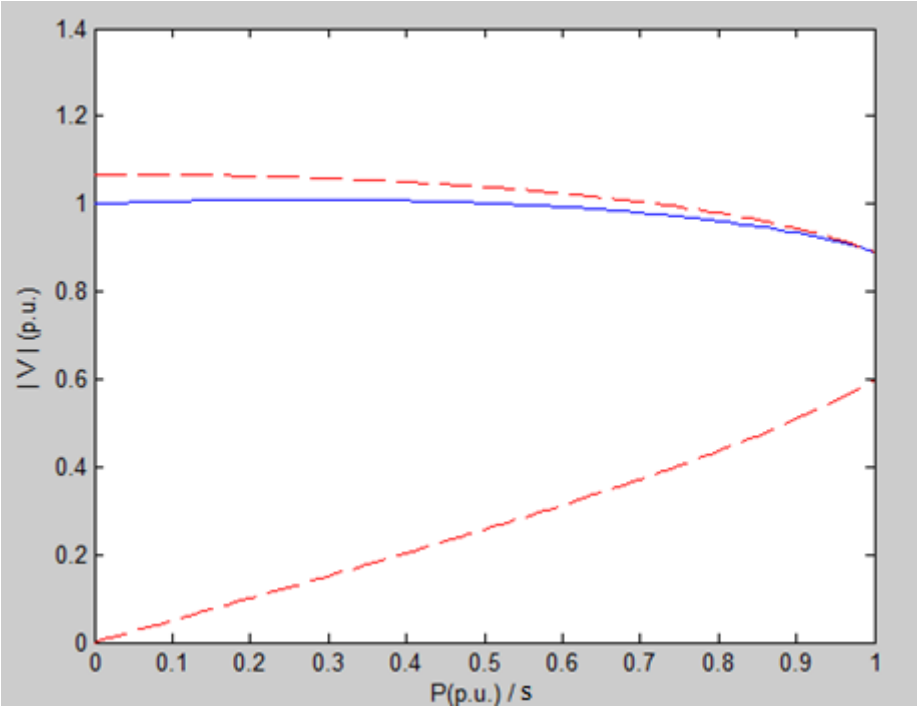

Figure 3.4 Two-Bus Model: Curve Following in HE

Observe in Figure 3.4 that a difference exists between the PV and sV curves except at the point s=1, where the original PBE for the two-bus system is recovered from the embedded equations. By modifying the embedded PBE's, the HE method can be structured to eliminate the gap between the PV and sV curves, thus providing a way of tracing the PV curve and finding the voltage collapse point. This is the ongoing work for one of our research group members.

4 TWO-BUS LOW-VOLTAGE SOLUTION

To find the LV solutions in the power system, starting from a two-bus system, a proposed two-bus HE LV formulation will be discussed in this chapter. This work was presented in my qualifying exam and it is reproduced here for reference. The traditional schematic of a two-bus system without the shunt reactance is shown in Figure 4.1 (copied from PowerWorld) where bus 1 is the slack bus.

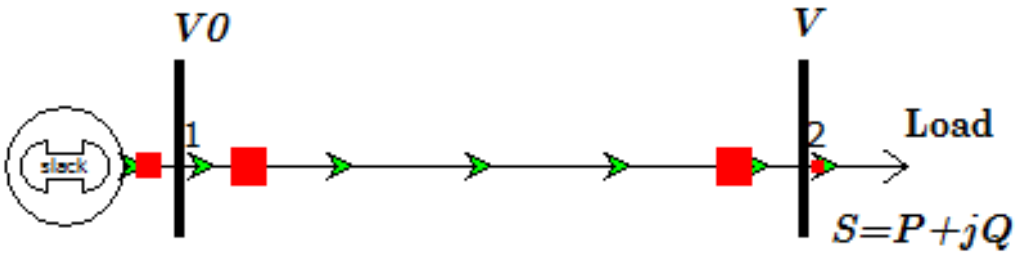

Figure 4.1 Two-Bus Example without Shunt Reactance

The PBE for the PQ bus (bus 2) may be written in several forms. For our purposes, the form below is expeditious:

$$\frac{V - V_0}{Z} = \frac{S^*}{V^*} \tag{4.1}$$

where the variable V is the voltage at the PQ bus, V_0 is the slack-bus voltage, $Z=R+\mathrm{j}X$ is the line impedance between these two buses, and $S=P+\mathrm{j}Q$ is the complex power at the PQ bus.

Equation (4.1) represents a nonlinear equation for which two solutions exist, when the load is less than the bifurcation point load.

4.1 Theoretical Derivation

It will be convenient to introduce a unitless variable *U*:

$$U = \frac{V}{V_0} \tag{4.2}$$

Equation (4.1) can be written as:

$$\frac{U-1}{Z} = \frac{S^*}{V_0 V_0^* U^*} \tag{4.3}$$

Multiply both sides by *Z* in (4.3), add 1.0 to both sides, and define $\frac{ZS^*}{|V_0|^2} = \sigma$. The PBE then becomes:

$$U = 1 + \frac{\sigma}{U^*} \tag{4.4}$$

$$\sigma = \sigma_R + j\sigma_I, \begin{cases} \sigma_R = \dfrac{XQ + RP}{|V_0|^2} \\ \sigma_I = \dfrac{XP - RQ}{|V_0|^2} \end{cases} \tag{4.5}$$

There exist two solutions for the PBE, (4.1), which can be obtained in closed form:

$$U_{\pm} = \frac{1}{2} \pm \sqrt{\frac{1}{4} + \sigma_R - \sigma_I^2} + j\sigma_I \tag{4.6}$$

These two solutions exist when:

$$\frac{1}{4} + \sigma_R - \sigma_I^2 > 0 \tag{4.7}$$

where U_+ is the HV solution and U_- is the LV solution.

Now taking the complex conjugate of (4.4) yields:

$$U^* = 1 + \frac{\sigma^*}{U} \tag{4.8}$$

Equations (4.4) and (4.8) are used in [25] to find only the HV solution for a two-bus system. The main idea in the convergence proof in [25] is to formulate a continued fraction by first substituting (4.8) into (4.4) and then continuing the substitution by alternately substituting for U and U^* using (4.4) and (4.8) respectively. The first step in this process is to substitute (4.8) into (4.4), which gives:

$$U = 1 + \frac{\sigma}{1 + \frac{\sigma^*}{U}} \tag{4.9}$$

By continuing the substitution presented in (4.9), the continued fraction in (4.10) can be easily established. The author of [25] proves that the continued fraction converges to the HV solution regardless to the starting point.

$$U = 1 + \cfrac{\sigma}{1 + \cfrac{\sigma^*}{1 + \cfrac{\sigma}{1 + \ldots}}} \tag{4.10}$$

While the formulation in (4.4) is guaranteed to find the HV solution, it is necessary to reformulate the PBE to find the LV solution: Moving 1 to the LHS in (4.4), multiplying both sides by U^* and then dividing both sides by (U-1) yields:

$$U^* = \frac{\sigma}{-1 + U} \tag{4.11}$$

Taking the complex conjugate of both sides in (4.11) yields:

$$U = \frac{\sigma^*}{-1+U^*} \tag{4.12}$$

4.1.1 Embedding

The idea of HE method is to introduce a complex parameter, *s*, and perform the embedding in (4.11) and (4.12), yielding a pair of equations, (4.13) and (4.14), respectively. Though embedding *s* into (4.13) and (4.14) is not necessary for the mathematical derivation of the formulation to find the LV solution for the two-bus system, HE is of importance in solving for the LV/large-angle solutions while applied to the multi-bus system in Chapter 5.

$$U^*(s^*) = \frac{s\sigma}{-1+U(s)} \tag{4.13}$$

$$U(s) = \frac{s\sigma^*}{-1+U^*(s^*)} \tag{4.14}$$

Equation (4.11) can be recovered from (4.13) by setting s=1. It is important to emphasize that the parameter embedded in function U^* needs to be s^* instead of s to retain the holomorphicity of the equations; otherwise the equations would not be analytic, something that is necessary in the subsequent proof.

4.1.2 Continued Fraction

Using (4.13) and (4.14) and then following the same substitution process that resulted in (4.10), a new continued fraction can be found:

$$U(s)=\cfrac{s\sigma^{*}}{-1+\cfrac{s\sigma}{-1+\cfrac{s\sigma^{*}}{-1+\ldots}}} \tag{4.15}$$

In order to put (4.15) into a form with structural regularity, it is necessary to subtract 1.0 from both sides of (4.15), which gives a continued fraction in form similar to that of (4.10):

$$U(s)-1=-1+\cfrac{s\sigma^{*}}{-1+\cfrac{s\sigma}{-1+\cfrac{s\sigma^{*}}{-1+\ldots}}} \tag{4.16}$$

4.1.3 The LV Solution

The rational-function form of $U(s)$-1 is well known to be ([25]):

$$U(s)-1=\frac{A_N(s)}{B_N(s)} \tag{4.17}$$

where

$$A_N(s)=-A_{N-1}(s)+a_N A_{N-2}(s) \tag{4.18}$$

$$A_{-1}(s)=1,\ A_0(s)=-1 \tag{4.19}$$

$$B_N(s)=-B_{N-1}(s)+a_N B_{N-2}(s) \tag{4.20}$$

$$B_{-1}(s)=0,\ B_0(s)=1 \tag{4.21}$$

$$a_N=\begin{cases} a_{2n+1}=s\sigma^{*};\ n=0,1\ldots \\ a_{2n}=s\sigma;\ n=1,2\ldots \end{cases} \tag{4.22}$$

It will be convenient to separate odd and even order index terms of A_n and B_n which may be expressed with the following notation, respectively:

$$A_{2n+1}(s) = A_n^{(-)}(s); A_{2n}(s) = A_n^{(+)}(s) \tag{4.23}$$

$$B_{2n+1}(s) = B_n^{(-)}(s); B_{2n}(s) = B_n^{(+)}(s) \tag{4.24}$$

Substituting (4.23) and (4.24) back into (4.18) and (4.20), respectively, the recursion relations obtained become:

$$A_n^{(-)}(s) = -A_n^{(+)}(s) + s\sigma^* A_{n-1}^{(-)}(s) \tag{4.25}$$

$$A_{n+1}^{(+)}(s) = -A_n^{(-)}(s) + s\sigma A_n^{(+)}(s) \tag{4.26}$$

$$B_n^{(-)}(s) = -B_n^{(+)}(s) + s\sigma^* B_{n-1}^{(-)}(s) \tag{4.27}$$

$$B_{n+1}^{(+)}(s) = -B_n^{(-)}(s) + s\sigma B_n^{(+)}(s) \tag{4.28}$$

The odd terms, $A_n^{(-)}$ and $B_n^{(-)}$, can be substituted in terms of the even parts. Substituting (4.25) into (4.26) yields:

$$A_{n+1}^{(+)}(s) = A_n^{(+)}(s) - s\sigma^* A_{n-1}^{(-)}(s) + z\sigma A_n^{(+)}(s) \tag{4.29}$$

Rearranging (4.26) by moving the odd part of A_n to LHS of the equation and even part of A_n to the RHS yields:

$$A_n^{(-)}(s) = s\sigma A_n^{(+)}(s) - A_{n+1}^{(+)}(s) \tag{4.30}$$

Substituting (4.30) into (4.29) yields:

$$\begin{aligned} A_{n+1}^{(+)}(s) &= A_n^{(+)}(s) - s\sigma^*(z\sigma A_{n-1}^{(+)}(s) - A_n^{(+)}(s)) + s\sigma A_n^{(+)}(s) \\ &= (1 + 2s\sigma_R) A_n^{(+)}(s) - s^2 |\sigma|^2 A_{n-1}^{(+)}(s) \end{aligned} \tag{4.31}$$

After rearranging (4.31), the three terms recursion relationship for $A_n^{(+)}$ is:

$$A_{n+1}^{(+)}(s) - (1 + 2s\sigma_R) A_n^{(+)}(s) + s^2 |\sigma|^2 A_{n-1}^{(+)}(s) = 0 \tag{4.32}$$

A similar derivation from (4.29) to (4.32) can be applied to the even-order terms of B_n yielding the three terms recursion relationship for $B_n^{(+)}$ is given in (4.33):

$$B_{n+1}^{(+)}(s)-(1+2s\sigma_R)B_n^{(+)}(s)+s^2\left|\sigma\right|^2 B_{n-1}^{(+)}(s)=0 \tag{4.33}$$

Recursion equations (4.32) and (4.33) may be thought of as second-order difference equations. The solutions of even-order-index terms of A_n and B_n are dependent on the roots of the characteristic polynomial of the difference equations. For a second-order difference equation, two polynomials (λ_+ and λ_-) exist.

$$\begin{aligned} A_n^{(+)}(s) &= C_+\lambda_+^n + C_-\lambda_-^n \\ B_n^{(+)}(s) &= D_+\lambda_+^n + D_-\lambda_-^n \end{aligned} \tag{4.34}$$

where

$$\lambda_\pm^2-(1+2s\sigma_R)\lambda_\pm+s^2\left|\sigma\right|^2=0 \tag{4.35}$$

$$\lambda_+=\frac{1}{2}+s\sigma_R+\Delta \tag{4.36}$$

$$\lambda_-=\frac{1}{2}+s\sigma_R-\Delta \tag{4.37}$$

$$\Delta=\sqrt{\frac{1}{4}+s\sigma_R-s^2\sigma_I^2} \tag{4.38}$$

Consider the initial conditions for A_n and B_n in (4.19) and (4.21), respectively. The odd order terms of A_n and B_n (say A_{-1} and B_{-1}) can be determined from the even order terms by (4.30) for A_n and similar formulation for B_n. For example, by setting n=-1 in (4.30), A_{-1} can be determined as:

$$A_{-1}^{(-)}(s)=s\sigma A_{-1}^{(+)}(z)-A_0^{(+)}(s) \tag{4.39}$$

where $A_{-1}^{(-)}, A_{-1}^{(+)}, A_0^{(+)}$ are the same to A_{-1}, A_{-2} and A_0, respectively.

Similarly B_{-1} can be determined as:

$$B_{-1}^{(-)}(s) = s\sigma B_{-1}^{(+)}(s) - B_0^{(+)}(s) \tag{4.40}$$

By substituting (4.40) and (4.41) into (4.19) and (4.21), respectively, the following can be derived:

$$\begin{aligned} A_0 &= C_+ + C_- = -1 \\ A_{-1} &= 1 + s\sigma(C_+\lambda_+^{-1} + C_-\lambda_-^{-1}) = 1 \\ B_0 &= D_+ + D_- = 1 \\ B_{-1} &= -1 + s\sigma(D_+\lambda_+^{-1} + D_-\lambda_-^{-1}) = 0 \end{aligned} \tag{4.41}$$

Coefficients C for A_n and D for B_n can be found using the four linear equations in (4.41) to give:

$$\begin{aligned} C_+ &= \frac{-\lambda_+}{\lambda_+ - \lambda_-}, C_- = \frac{\lambda_-}{\lambda_+ - \lambda_-} \\ D_+ &= \frac{\lambda_+ - s\sigma^*}{\lambda_+ - \lambda_-}, D_- = -\frac{\lambda_- - s\sigma^*}{\lambda_+ - \lambda_-} \end{aligned} \tag{4.42}$$

The explicit form for the even-order terms of A_n and B_n are obtained by substituting (4.42) into (4.34):

$$A_n^{(+)} = \frac{-\lambda_+^{n+1} + \lambda_-^{n+1}}{\lambda_+ - \lambda_-} \tag{4.43}$$

$$B_n^{(+)} = \frac{\lambda_+^{n+1} - \lambda_-^{n+1}}{\lambda_+ - \lambda_-} - s\sigma^* \frac{\lambda_+^n - \lambda_-^n}{\lambda_+ - \lambda_-} \tag{4.44}$$

The even-order terms of the continued fraction in (4.17) can be expressed in a rational form by substituting (4.43) and (4.44) into (4.17):

$$U_n^{(+)}(s)-1=U_{2n}(s)-1$$
$$=\frac{\dfrac{-\lambda_+^{n+1}+\lambda_-^{n+1}}{\lambda_+-\lambda_-}}{\dfrac{\lambda_+^{n+1}-\lambda_-^{n+1}}{\lambda_+-\lambda_-}-s\sigma^*\dfrac{\lambda_+^n-\lambda_-^n}{\lambda_+-\lambda_-}} \tag{4.45}$$

By cancelling the term $\lambda_+-\lambda_-$ in (4.45), it can be reduced to:

$$U_n^{(+)}(s)-1=\frac{-\lambda_+^{n+1}+\lambda_-^{n+1}}{\lambda_+^{n+1}-\lambda_-^{n+1}-s\sigma^*(\lambda_+^n-\lambda_-^n)} \tag{4.46}$$

Dividing $(\lambda_+)^n$ in both the numerator and denominator in (4.46) yields:

$$U_{2n}(s)-1=-\frac{\lambda_+-\lambda_-(\dfrac{\lambda_-}{\lambda_+})^n}{\lambda_+-s\sigma^*-(\lambda_--s\sigma^*)(\dfrac{\lambda_-}{\lambda_+})^n} \tag{4.47}$$

where $U_{2n}(s)$ is equivalent to $U_n^{(+)}(s)$.

Using the expression for λ_+ and λ_- in (4.36) and (4.37), respectively, the ratio of λ_-/λ_+ can be written:

$$\frac{\lambda_-}{\lambda_+}=\frac{\frac{1}{2}+s\sigma_R-\Delta}{\frac{1}{2}+s\sigma_R+\Delta} \tag{4.48}$$

Therefore if,

$$\frac{1}{4}+s\sigma_R-s^2\sigma_I^2>0 \tag{4.49}$$

then Δ in (4.38) is a real number. Since σ_R is real as defined, λ_+ is greater than λ_-. Therefore λ_-/λ_+ in (4.48) is less 1.0 so that:

$$\lim_{n\to\infty}\left(\frac{\lambda_-}{\lambda_+}\right)^n = 0 \tag{4.50}$$

If (4.49) is not obeyed, then no limit exists in (4.50) and the rational function of (4.47) and the rational function oscillates. Equation (4.49) then is the requirement for the continued fraction to converge. The conditions under which (4.4) has two different solutions is (4.7), which matches exactly with (4.49) at s=1 and s=1 is the solution point of interest. This verifies that if there is a solution, the lambda ratio in (4.50) goes to zero as n goes to infinity, which means, as will be shown below, that the solution of the proposed formulation to which the continued faction expansion converges is the LV solution.

Under the condition of (4.49), the limit of even-order index terms of (4.17) becomes:

$$\lim_{n\to\infty} U_n^{(+)}(s) = 1 - \frac{\lambda_+}{\lambda_+ - s\sigma^*} \tag{4.51}$$

Substituting (4.36) into (4.51):

$$\begin{aligned}\lim_{n\to\infty} U_n^{(+)}(z) &= 1 - \frac{\frac{1}{2} + s\sigma_R + \Delta}{\frac{1}{2} + s\sigma_R + \Delta - s\sigma^*} \\ &= 1 - \frac{\frac{1}{2} + s\sigma_R + \Delta}{\frac{1}{2} + \Delta + js\sigma_I}\end{aligned} \tag{4.52}$$

Simplifying (4.52) by multiplying both the numerator and denominator by $\frac{1}{2} + \Delta + js\sigma_I$ yields:

$$\begin{aligned}\lim_{n\to\infty} U_n^{(+)}(s) &= 1-\frac{\left(\frac{1}{2}+s\sigma_R+\Delta\right)\left(\frac{1}{2}+\Delta-js\sigma_I\right)}{\left(\frac{1}{2}+\Delta+js\sigma_I\right)\left(\frac{1}{2}+\Delta-js\sigma_I\right)} \\ &= 1-\frac{\left(\frac{1}{2}+s\sigma_R+\Delta\right)\left(\frac{1}{2}+\Delta-js\sigma_I\right)}{\left(\frac{1}{2}+\Delta\right)^2+s^2\sigma_I^2}\end{aligned} \tag{4.53}$$

Note that $\Delta^2=\frac{1}{4}+s\sigma_R-s^2\sigma_I^2$ (see (4.38)). By expanding $\left(\frac{1}{2}+\Delta\right)^2$, (4.53) becomes:

$$\begin{aligned}\lim_{n\to\infty} U_n^{(+)}(s) &= 1-\frac{\left(\frac{1}{2}+s\sigma_R+\Delta\right)\left(\frac{1}{2}+\Delta-js\sigma_I\right)}{\frac{1}{4}+\Delta+\frac{1}{4}+z\sigma_R-s^2\sigma_I^2+s^2\sigma_I^2} \\ &= 1-\frac{\left(\frac{1}{2}+s\sigma_R+\Delta\right)\left(\frac{1}{2}+\Delta-js\sigma_I\right)}{\frac{1}{2}+\Delta+s\sigma_R} \\ &= 1-\left(\frac{1}{2}+\Delta-js\sigma_I\right)=\frac{1}{2}-\Delta+js\sigma_I\end{aligned} \tag{4.54}$$

The limit of the (4.17) provided by (4.54) is the same as the algebraic LV solution of the quadratic PBE shown in (4.6) at s=1. This completes the first half of the proof that the proposed formulation converges to the LV solution, if one exists, for the even-order terms of the continued fraction in (4.15). It must also be shown that the same limit is obtained for the odd order terms. Indeed this is the case by the following a derivation similar to that above as follows.

From (4.30), $A_n^{(-)}(s)$ can be determined:

$$
\begin{aligned}
A_n^{(-)}(s) &= -A_{n+1}^{(+)}(s) + s\sigma A_n^{(+)}(s) \\
&= \frac{\lambda_+^{n+2} - \lambda_-^{n+2}}{\lambda_+ - \lambda_-} - s\sigma \frac{\lambda_+^{n+1} - \lambda_-^{n+1}}{\lambda_+ - \lambda_-} \\
&= \frac{\lambda_+^{n+1}(\lambda_+ - s\sigma)}{\lambda_+ - \lambda_-} - \frac{\lambda_-^{n+1}(\lambda_- - s\sigma)}{\lambda_+ - \lambda_-}
\end{aligned}
\tag{4.55}
$$

From (4.28), $B_n^{(-)}(s)$ can be determined:

$$
\begin{aligned}
B_n^{(-)}(s) &= -B_{n+1}^{(+)}(s) + s\sigma B_n^{(+)}(s) \\
&= \frac{-\lambda_+^{n+2} + \lambda_-^{n+2}}{\lambda_+ - \lambda_-} + s\sigma^* \frac{\lambda_+^{n+1} - \lambda_-^{n+1}}{\lambda_+ - \lambda_-} \\
&\quad + s\sigma \frac{\lambda_+^{n+1} - \lambda_-^{n+1}}{\lambda_+ - \lambda_-} - s^2 |\sigma|^2 \frac{\lambda_+^n - \lambda_-^n}{\lambda_+ - \lambda_-}
\end{aligned}
\tag{4.56}
$$

It is trivial to show that (4.57) is obeyed for both λ_+ and λ_-:

$$
\lambda_\pm^2 - (s\sigma + s\sigma^*)\lambda_\pm + s^2|\sigma|^2 = \lambda_\pm
\tag{4.57}
$$

Therefore $B_n^{(-)}(s)$ can be simplified as:

$$
B_n^{(-)}(s) = \frac{-\lambda_+^{n+1} + \lambda_-^{n+1}}{\lambda_+ - \lambda_-}
\tag{4.58}
$$

The odd order of the voltage can be expressed in a rational form:

$$
\begin{aligned}
\lim_{n\to\infty} U_{2n+1}(s) &= \lim_{n\to\infty} \left[1 + \frac{\dfrac{\lambda_+^{n+1}(\lambda_+ - s\sigma)}{\lambda_+ - \lambda_-} - \dfrac{\lambda_-^{n+1}(\lambda_- - s\sigma)}{\lambda_+ - \lambda_-}}{\dfrac{-\lambda_+^{n+1} + \lambda_-^{n+1}}{\lambda_+ - \lambda_-}} \right] \\
&= \lim_{n\to\infty} \left[1 + \frac{\lambda_+ - s\sigma - (\lambda_- - s\sigma)(\dfrac{\lambda_-}{\lambda_+})^{n+1}}{-1 + (\dfrac{\lambda_-}{\lambda_+})^{n+1}} \right] \\
&= 1 - \lambda_+ + s\sigma = 1 - (\frac{1}{2} + s\sigma_R + \Delta) + s\sigma_R + js\sigma_I \\
&= \frac{1}{2} - \Delta + js\sigma_I
\end{aligned}
\tag{4.59}
$$

Therefore both even and odd order index terms of the continued fraction resulting from (4.11) and (4.12) converging to the LV solution if the condition in (4.51) is satisfied. It is important to check if the solution still converges at the bifurcation point where the HV and LV solutions are identical.

If the loading condition for the two-bus system is at the bifurcation point condition, then $\lambda_+ = \lambda_-$ and $\Delta = 0$. The explicit solutions for $A_n^{(+)}$ and $B_n^{(+)}$ in (4.34), which are based on the roots of characteristic polynomials, will be changed to:

$$\begin{aligned} A_n^{(+)}(s) &= C_+ \lambda^n + C_- n\lambda^n \\ B_n^{(+)}(s) &= D_+ \lambda^n + D_- n\lambda^n \end{aligned} \tag{4.60}$$

By substituting (4.60) into the initial conditions in (4.19) for A_n and (4.21) for B_n:

$$\begin{aligned} &A_0 = C_+ = -1 \\ &A_{-1} = 1 + s\sigma(C_+\lambda^{-1} - C_-\lambda^{-1}) = 1 \\ &B_0 = D_+ = 1 \\ &B_{-1} = -1 + s\sigma(D_+\lambda^{-1} - D_-\lambda^{-1}) = 0 \end{aligned} \tag{4.61}$$

Therefore the coefficients (C_+, C_-, D_+ and D_+) can be calculated from (4.61):

$$\begin{aligned} &C_+ = -1,\ C_- = -1 \\ &D_+ = 1,\ D_- = 1 - \frac{\lambda}{s\sigma} \end{aligned} \tag{4.62}$$

Then (4.60) becomes:

$$\begin{aligned} A_n^{(+)}(s) &= -\lambda^n - n\lambda^n \\ B_n^{(+)}(s) &= \lambda^n + (1 - \frac{\lambda}{s\sigma})n\lambda^n \end{aligned} \tag{4.63}$$

By substituting (4.63) into (4.17), the limit of $U_n^{(+)}$ becomes:

$$\lim_{n\to\infty} U_n^{(+)}(s) = \lim_{n\to\infty}\left[1+\frac{-\lambda^n - n\lambda^n}{\lambda^n + (1-\frac{\lambda}{s\sigma})n\lambda^n}\right] \tag{4.64}$$

Dividing both the numerator and denominator in (4.64) by $n\lambda^n$ and simplifying the equation:

$$\lim_{n\to\infty} U_n^{(+)}(s) = \lim_{n\to\infty}\left[1+\frac{-1/n - 1}{-1/n + (1-\frac{\lambda}{s\sigma})}\right] = 1+\frac{-1}{1-\frac{\lambda}{s\sigma}} = 1-\frac{s\sigma}{s\sigma-\lambda} = \frac{\lambda}{\lambda - s\sigma} \tag{4.65}$$

Substituting the expression of λ into (4.36) (or (4.37)) with Δ=0 into (4.65) and breaking σ into real and imaginary parts:

$$\lim_{n\to\infty} U_n^{(+)}(s) = \frac{\frac{1}{2}+s\sigma_R}{\frac{1}{2}+s\sigma_R - s\sigma_R - js\sigma_I} = \frac{\frac{1}{2}+s\sigma_R}{\frac{1}{2}-js\sigma_I} \tag{4.66}$$

Since Δ in (4.38) is 0:

$$s\sigma_R = s^2\sigma_I^2 - \frac{1}{4} \tag{4.67}$$

By substituting (4.67) into (4.66), equation (4.66) becomes:

$$\lim_{n\to\infty} U_n^{(+)}(s) = \frac{\frac{1}{2} + s^2\sigma_I^2 - \frac{1}{4}}{\frac{1}{2} - js\sigma_I} = \frac{\frac{1}{4} + s^2\sigma_I^2}{\frac{1}{2} - js\sigma_I} = \frac{(\frac{1}{2} - js\sigma_I)(\frac{1}{2} + js\sigma_I)}{\frac{1}{2} - js\sigma_I} \qquad (4.68)$$

$$= \frac{1}{2} + js\sigma_I$$

Note that Δ is 0, therefore the limit of the odd-order terms of the continued fraction in (4.15) still attains the same value as when λ_-/λ_+ is less than 1.0, but now the value can be either HV or LV solutions as they are identical at the voltage collapse condition. The limit of the even-order terms of the continued fraction can be similarly derived and proven to converge to the bifurcation point.

Based on the foregoing derivations, it can be concluded that the continued fraction implied by (4.11) and (4.12) yields only the LV solution, if it exists. If the solution does not exist for a two-bus system, oscillatory behavior can be observed as the limit of (4.48) will not be zero but a complex number with magnitude of one which leads to oscillations in the evaluation of the continued fraction in (4.15).

4.2 Numerical Example for a Two-Bus System

In Section 4.1 the theoretical analysis of finding the LV solution for a two-bus system using HE is discussed. In this section, a simple numerical experiment for a two-bus system will be conducted using both NR and HE. The parameters, in per-unit, for the two-bus system are listed in Table 4.1. The HV solution and LV solution for this problem are 0.9-j0.1 and 0.1-j0.1, respectively.

Table 4.1 Parameters for the Two-Bus System of Figure 4.1

Parameter	R	X	Q	P	V_0
Value (p.u.)	0.1	0.3	-0.14	-0.38	1.0

These solutions for the two-bus system are obtained using both the NR and HE methods. The robustness of each method is tested by choosing a range of initial estimates and the observing the outcome of the algorithm. The range of the initial estimates of the voltage magnitude is chosen from 0 to 1.2 and the initial estimates of the phase angle vary between -180 to 180 degrees. Both magnitudes and voltage angles of the initial estimates are divided into 100 points, therefore the total number of initial voltage estimates used is 10,000. The tolerance of the mismatch in PBE is selected as 10^{-4} in the test. The entire range of initial estimates and the selected convergence criterion are used in both the NR and HE numerical experiments.

The results of the experiment using the NR method on the two-bus system, in Figure 4.1, are displayed in Figure 4.2. (I would like to give my gratitude to Muthu Kumar Subramanian who generated this plot and gave me permission to use it in my research). A red pixel at the coordinates of the initial voltage estimate in Figure 4.2 indicates the iterations converge to HV solution, a blue pixel indicates the iterations converge to LV solution, and a black pixel indicates the iterations failed to converge after 20 iterations. From Figure 4.2, it can be seen that the NR method does not always converge, nor, when it does, does it converge exclusively to either the HV solution or the LV solution.

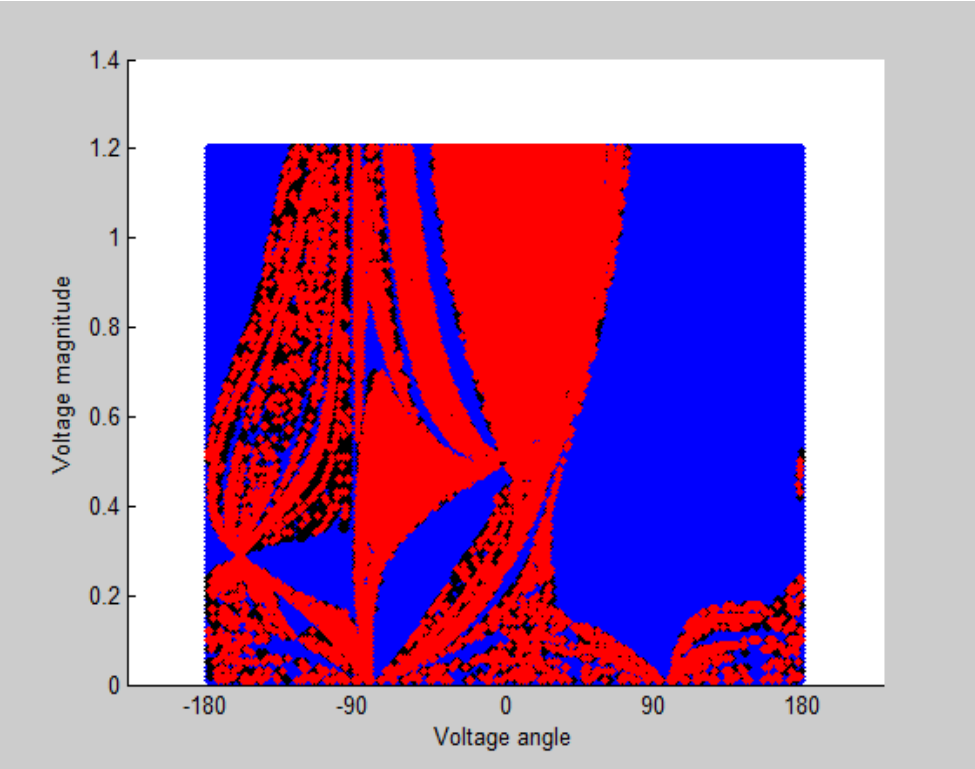

Figure 4.2 Solution of NR Method from Different Starting Points

Then multiple-initial-condition numerical experiments described above are conducted repeatedly using the proposed method LV formulation to show that it, (4.15), will obtain only the LV solution regardless of the initial estimate of *U*, as indicated by the foregoing proof. The results of this experiment confirm that the proposed method, (4.15), converges to the LV solution and (4.10) converges to the HV solution for all starting points as shown in Figure 4.3 and Figure 4.4, respectively, with the same color interpretation in Figure 4.2.

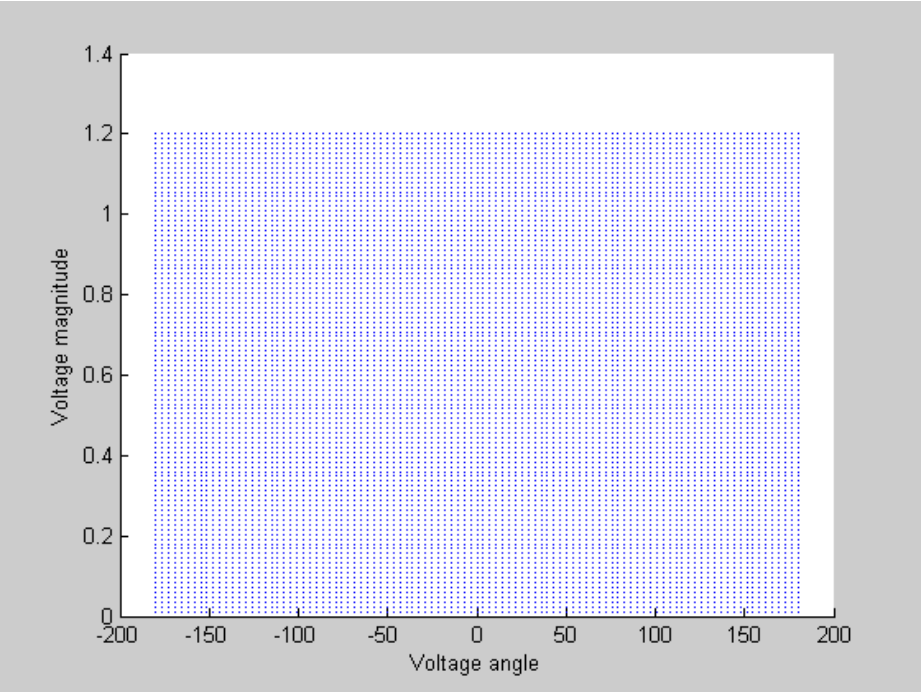

Figure 4.3 Solution of Proposed LV HE Formulation from Different Starting Points

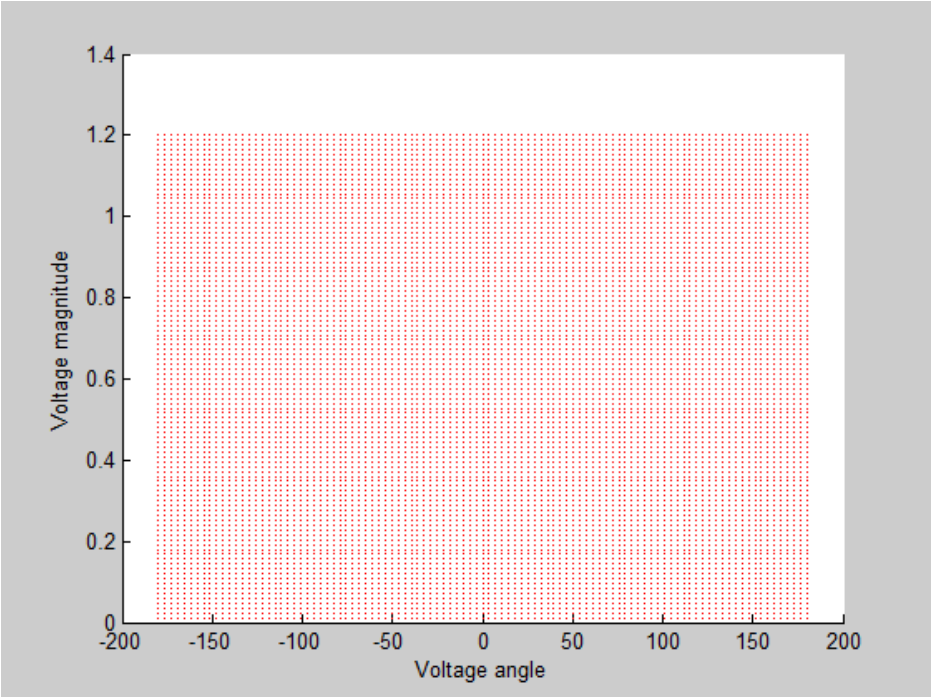

Figure 4.4 Solution of HV HE Formulation from Different Starting Points

4.3 Conclusion

The PBE LV HE formulation is proven mathematically to find and only find the LV solution for a two-bus system, if the solution exists, regardless of the starting point. A comparison between the performance of NR method and HE method shows that the former approach may or may not converge while the latter method does guarantee convergence. And, when the NR method does converge, it does not converge reliably to either the LV solution or the HV solution, indicating the NR method's performance is initial-point-dependent, something well known. In contrast, the HE formulation proposed is independent of the initial estimates and always reaches to the LV solution, if it exists.

5 MULTI-BUS LOW-VOLTAGE/LARGE-ANGLE FORMULATIONS

As has been discussed in Chapter 3, the multi-bus system PBE's can be embedded with a complex variable *s* and the solution can be obtained through a power series expansion and continued fraction conversion. A simplified HE HV formulation for the two-bus system is discussed in [25], and, in Chapter 4, by reformulating the PBE, a proposed HE method was mathematically proven to guarantee to find the LV solution for a two-bus system if it exists. The generalized multi-bus LV/large-angle formulations will be proposed in this chapter for both the PQ and PV bus model using the HE method. These three lemmas will be cited that, when combined, can be used to prove that the method proposed is capable of finding all of the solutions of the power-flow problem.

5.1 Germ

In application of analytic continuation techniques, finding a germ is necessary. The formal definition of a germ is given in [86]. Assuming $f(s)$ is a power series converging within its radius of convergence around point s_0:

$$f(s) = \sum_{n=0}^{\infty} f[n](s - s_0)^k \tag{5.1}$$

Then the vector $g=(s_0, f[0], f[1], f[2], \ldots)$ is defined as a germ of $f(s)$, where $f[n]$ is the n^{th} order coefficient for the power series.

In the HE PF method, given s_0 (which is zero), the germ is uniquely determined by the value of $f[0]$; therefore, in the HE PF method, the term "germ" can be used interchangeably with "the PF solution at s=0," or, equivalently, $f[0]$. It can be noted that the coefficients of $V(s)$ and $Q(s)$ in (3.14) with the initial conditions in (3.13) is one possible germ or solution for the specific HE PBE's, given from (3.7) to (3.9), at s_0=0. There exist other possible germs for the same set of HE PBE's ((3.7)-(3.9)) due to the quadratic characteristic of the PF problem.

5.2 Solution Existence

Lemma 1: In the HE PF method, it is guaranteed that a germ will lead to a solution of the PF problem, if the solution exists. Otherwise the oscillations of the Padé Approximants will indicate that no solution can be found by the specific germ.

With the technique of maximal analytic continuation (via Padé Approximants), the maximal region where the voltage function, $V(s)$, is holomorphic can be obtained. Within this maximal region, the voltage function can therefore be evaluated and a converged value will be obtained, given a sufficient number of power series coefficients. Therefore if the point, s=1, is within the maximal region using the domain of complex rather than quaternion numbers, the voltage solutions of the PF problem can be obtained. On the contrary, if s=1 is outside the maximal region, no solution exists over the field of complex numbers as indicated by the oscillation of the Padé Approximants [83].

5.3 Unique Germ-to-Solution Mapping

Lemma 2: In the HE PF method, each unique germ will correspond to a different solution, resulting in a unique germ-to-solution mapping if a solution corresponding to that germ exists.

In the HE PBE's, each germ will correspond to a unique solution if it exists, i.e. a unique mapping, guaranteed by the Stahl's theorem given in [83].

5.4 Finding All Possible Germs for the HE PBE's

Lemma 3: With the proposed HE LV/large-angle PBE's, given in Section 5.4.1 and Section 5.4.2, all the PF solutions at s=0 (or all the germs) for the proposed set of HE PBE's are guaranteed to be found.

For an (N+1)-bus network with one slack bus, there possibly exist (2^N+m) PF solutions, as suggested by the author of [80]. A number of 2^N possible PF solutions (out of the total (2^N+m) PF solutions) are due to the quadratic characteristics of N complex PBE's, and the so-called 'extra' m PF solutions are purely system topology and parameter dependent. The goal of this thesis is to find the 2^N PF solutions that exist for the no-load case and then "follow" these solutions as the load in the system increases toward the full load. The so-called extra PF solutions, which are excess of 2^N and system topology dependent, will not be discussed in this report. For the sake of convenience, the 2^N PF solutions are referred as "ALL" of the PF solutions of interest. A total number of 2^N unique germs must be found if all of the 2^N possible solutions

using the HE method are to be found. It should be emphasized that all the possible germs must be found using the *same* formulation of the HE PBE's since there are an infinite number of HE PBE formulations. In this study, the HE PBE formulation similar to that given in (3.7) and (3.8) is used. (The modification to (3.7) and (3.8) needed—and described below—is to move the shunt term to the RHS of (3.7) and (3.8)). The proposed method to find all possible germs for the HE PQ and PV bus models are presented as follows in Section 5.4.1 and Section 5.4.2, respectively.

5.4.1 LV Formulation for PQ Buses and Finding $2^{N_{PQ}}$ Germs

It can be observed in (3.10) that at s=0, the complex power injections at PQ buses and real power injections at PV buses vanish, which is known as the no-load/no-generation condition. The complex power (S_i) at a PQ bus, bus i, can be expressed in (5.2), where I_i is the sum of current injection at bus i.

$$S_i = V_i I_i^* \tag{5.2}$$

It can be noted that when S_i=0, two solutions exist:

(1) The sum of current injection at bus i (I_i) is zero, or

(2) The voltage at bus i (V_i) is zero.

Note that the solution obtained at s=0 in (3.13) is equivalent to the solution obtained from case (1) since there is no current flow in the system and every bus voltage are 1.0 per-unit. As mentioned before, the HV solution, if it exits, can be obtained starting from the germ given in (3.13), guaranteed by analytic continuation.

If case (2) is considered, the system will have current flow at the no-load condition, or s=0, with the bus voltage being zero. Assume the PQ bus i is considered to be in case (2), the bus voltage at s=0 therefore becomes zero, i.e. $V_i(0)=V_i[0]=0$. It can be observed that the term $\frac{sS_i^*}{V_i^*(s^*)}$ on the RHS of (3.7) becomes undefined since both the numerator and the denominator become zero at s=0. It is well known that if the indeterminate form of $\frac{0}{0}$ is encountered, one can apply the L'Hôpital's rule to evaluate the indeterminate form $\frac{0}{0}$, by using the derivatives of both the numerator and denominator. I.e.:

$$\lim_{s\to 0}\frac{sS_i^*}{V_i^*(s^*)}=\frac{\frac{d(sS_i^*)}{ds}}{\frac{dV_i^*(s^*)}{ds}}=\left.\frac{S_i^*}{\frac{d(V_i^*[0]+V_i^*[1]s+V_i^*[2]s^2+...)}{ds}}\right|_{s=0} \tag{5.3}$$

$$\left.\frac{S_i^*}{V_i^*[1]+V_i^*[2]s+...}\right|_{s=0}=\frac{S_i^*}{V_i^*[1]}$$

Since $V_i[1]$ is a non-zero term, the undefined $\frac{0}{0}$ is therefore evaluated to be $\frac{S_i^*}{V_i^*[1]}$. By starting from $V[0]$=0, instead of $V[0]$=1 in (3.13), the solution obtained is the LV solution if it exists, as guaranteed by the equation structure of (3.13) and the maximal analytic continuation provided by Padé Approximants. Note for each PQ bus in the power system, $V[0]$ can be selected to be either non-zero, which will be discussed in the following section, or zero and the resulting various germs will lead to different solutions at s=1 if they exist. Similarly, different germs can be found for formulations that include PV buses and it will be discussed in detail in Section 5.4.2.

It will be convenient to introduce a dual voltage variable in (5.4), assuming $K1$ is the set of PQ buses with $V[0]=0$.

$$V_i^{(d)}(s) = -\frac{sS_i^*}{Y_{ii}^{(tr)} V_i^*(s^*)},\ i \in K1 \tag{5.4}$$

In terms of the power series coefficients, the relationship in (5.4) can be written as:

$$\sum_{n=0}^{\infty} V_i^{(d)}[n] s^n = -\frac{S_i^*}{Y_{ii}^{(tr)} (\sum_{n=1}^{\infty} V_i^*[n] s^{n-1})},\ i \in K1 \tag{5.5}$$

It can be observed that the N^{th} power series coefficient in the dual voltage ($Vi^{(d)}[n]$) can be calculated given the coefficients in the original voltage up to the (N-1)-th term, thus resulting a "delay" in the power series coefficients between the dual voltage and original voltage.

Note that the original voltage variable, $V_i(s)$, can be recovered in (5.6).

$$V_i(s) = -\frac{sS_i}{Y_{ii}^{(tr)*} V_i^{(d)*}(s^*)},\ i \in K1 \tag{5.6}$$

With the notation used in (5.6), the HE PBE's for PQ bus in (3.7) can be separated into (5.7) and (5.8), representing the bus set $J1$ and $K1$, respectively, where $J1$ is the set of PQ buses with $V[0] \neq 0$, $K1$ is the set of PQ buses with $V[0]=0$ and 0 is the slack bus number index.

$$\sum_{j \in \{J1,\, 0\}} Y_{ij}^{(tr)} V_j(s) + \sum_{j \in K1} \frac{Y_{ij}^{(tr)}}{Y_{ij}^{(tr)*}} \frac{sS_j}{V_j^{(d)*}(s^*)} = \frac{sS_i^*}{V_i^*(s^*)} - s\sum_{k=0}^{N} Y_{ik}^{(sh)} V_k(s),\ i \in J1 \tag{5.7}$$

$$\sum_{j\in\{J1,\,0\}} Y_{ij}^{(tr)} V_j(s) - \frac{Y_{ii}^{(tr)}}{Y_{ii}^{(tr)*}} \frac{sS_i}{V_i^{(d)*}(s^*)} - \sum_{j\in K1} \frac{Y_{ij}^{(tr)}}{Y_{ij}^{(tr)*}} \frac{sS_j}{V_j^{(d)*}(s^*)} = \tag{5.8}$$

$$Y_{ii}^{(tr)} V_i^{(d)}(s) - s\sum_{k=0}^{N} Y_{ik}^{(sh)} V_k(s)\,,\ i\in K1$$

Rearranging (5.7) and (5.8) as (5.9) and (5.10), respectively:

$$\sum_{j\in\{J1,\,0\}} Y_{ij}^{(tr)} V_j(s) = \frac{sS_i^*}{V_i^*(s^*)} + \sum_{j\in K1} \frac{Y_{ij}^{(tr)}}{Y_{ij}^{(tr)*}} \frac{sS_j}{V_j^{(d)*}(s^*)} - s\sum_{k=0}^{N} Y_{ik}^{(sh)} V_k(s)\,,\ i\in J1 \tag{5.9}$$

$$Y_{ii}^{(tr)} V_i^{(d)}(s) + \sum_{j\in\{J1+0\}} Y_{ij}^{(tr)} V_j(s) = \frac{Y_{ii}^{(tr)}}{Y_{ii}^{(tr)*}} \frac{sS_i}{V_i^{(d)*}(s^*)} + \sum_{j\in K1} \frac{Y_{ij}^{(tr)}}{Y_{ij}^{(tr)*}} \frac{sS_j}{V_j^{(d)*}(s^*)} - s\sum_{k=0}^{N} Y_{ik}^{(sh)} V_k(s)\,,\ i\in K1 \tag{5.10}$$

At s=0, the germ for the LV solutions can be determined by solving for the bus voltages of set $J1$, given in (5.11). Subsequently, the dual bus voltages of set $K1$ are solved using (5.12), giving the bus voltages of set $J1$. Note that the bus voltages for set $J1$ are not necessarily 1.0 but need to be solved from (5.11), as a resultant of current flow and voltage drop in the system at s=0 mentioned previously.

$$\sum_{j\in\{J1,\,0\}} Y_{ij}^{(tr)} V_j[0] = 0,\ i\in J1 \tag{5.11}$$

$$Y_{ii}^{(tr)} V_i^{(d)}[0] + \sum_{j\in\{J1,\,0\}} Y_{ij}^{(tr)} V_j[0] = 0\,,\ i\in K1 \tag{5.12}$$

Similarly, the bus voltage power series coefficients for set $J1$ in (5.9) have to be solved prior to obtaining the coefficients for set $K1$ in (5.10). The procedure of finding the voltage power series coefficients from (5.9) and (5.10) are straightforward using the similar process given in [24] and [87].

It can be noticed that two cases, (1) and (2) in section 5.1, are the only possible cases where there is no complex power injection for each PQ bus. The first term in voltage power series, $V[0]$, can only be either zero or 1.0 (non-zero in general due to the effect of LV bus in the system as discussed above). Thus for a $(N+1)$-bus power system with only PQ buses, 2^N possible germs are to be found from (5.11) and (5.12) by varying the elements in set $J1$ or $K1$. And thus, by the maximal analytic continuation, all possible solutions existing at $s=1$ are guaranteed to be obtained guaranteed by the Stahl's theorem [24], [83].

5.4.2 Large-Angle Formulation for PV Buses and Finding $2^{N_{PV}}$ Germs

With the PQ bus LV formulation derived in Section 5.4.1, a LV/large-angle HE formulation for the PV bus will be discussed next. The goal is to find all the possible germs that exist for the PV bus formulation in (3.8), and by analytic continuation, the solutions at $s=1$ are guaranteed to be found if existed.

Equation (5.13) is the HE PV bus formulation at $s=0$ given in (3.11)[1],

[1] The specified PV bus voltage need not be 1.0 per-unit. Since the HE PV bus voltage, referred by (3.8) is given as $V=1+s(|V_{sp}|^2-1)$, the PV bus voltage will become $V_i(s)=1.0$ at $s=0$.

$$\sum_{k=0}^{N} Y_{ik}^{(tr)} V_k[0] = \frac{-jQ_i[0]}{V_i^*[0]}, \; i \in N_{PV} \tag{5.13}$$

$$V_i[0]V_i^*[0] = 1$$

In order to find all the possible germs for the PV bus formulation, all the solutions that satisfy (5.13) need to be found, of which there should be 2^N. The real power generation for the PV bus is zero at s=0, thus there is no real power flow in the system. The calculation of the germs for the PV bus formulation for the simple two-bus case (shown in Figure 5.1) is illustrated, which can be readily extended to multi-bus system.

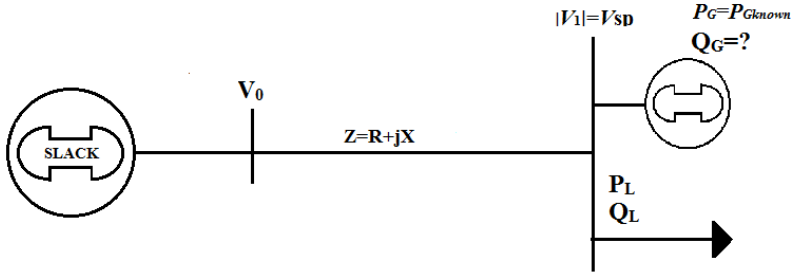

Figure 5.1 Two-Bus System with the PV Bus Model

Assuming that the transmission line is lossless (line impedance Z is purely imaginary or equivalently R=0), the real power flow on the transmission line therefore is given by:

$$P = \frac{|V_0 \| V_1| \sin(\theta_0 - \theta_1)}{X} \tag{5.14}$$

where V_0 and V_1 are the voltage magnitudes for the slack bus and the PV bus, respectively. The variables θ_0 and θ_1 are the voltage angles for the slack bus and the PV bus, respectively. And X is the line reactance.

Without loss of generality, the slack bus voltage angle is selected as 0 º, i.e. θ_0 is 0 º. Note that if θ_0-θ_1 is 0 ºor 180 º(-180 º), then V_0 and V_1 either are in the same phase or 180 ºout of phase, and the real power transferred is zero. Assuming at s=0 $|V_0|$=1 and $|V_1|$=1, V_1 therefore can be selected arbitrarily as either 1.0 or -1.0 and the real power flow will be zero or equivalently, the real power generation from the slack bus will be zero.

5.4.3 Finding 2^N Germs for a Multi-Bus Lossless System

Generally, in a multi-bus system, each PV bus voltage (at s=0) can be arbitrarily selected as either1.0 or -1.0 using the HE method, as long as the system is lossless. For PQ buses, the voltages must be selected as either zero or nonzero with the requirement that the sum of the complex power flows into the bus is zero. Two cases are considered to prove the above statements: 1) if the lossless multi-bus system has only PV buses and no PQ bus, 2) if the lossless multi-bus system has both PV and PQ buses.

Case 1: The proof for case 1) is straight forward: At s=0, if all the PV bus voltage values are either 1.0 or -1.0 as discussed above, the real power flow between any two buses therefore is calculated to be zero by (5.14), resulting in no real power flow/generation in the system. There are two options for the value of each PV bus voltage: either 1.0 or -1.0. Thus 2^N germs may be found.

Case 2: To prove for case 2), the bus voltages for the PQ buses at *s*=0 have to be examined. Note that the slack bus voltage is given as 1.0 (at angle 0 °) and assume the PV bus voltages are arbitrarily selected as either 1.0 or -1.0, giving $2^{N_{PV}}$ combinations of PV bus voltages. As discussed in Section 5.4.1, there are likewise two options for the PQ bus germ—either the PQ bus voltage is zero or the sum of PQ bus current injections is zero—giving $2^{N_{PQ}}$ combinations for PQ buses and a total of $2^N = 2^{(N_{PV}+N_{PQ})}$ germs. Note that all PQ bus voltages resulting from these constraints are feasible since each voltage is either zero or the result of the solution of a set of nonsingular linear equations. The PBE's for PQ buses at *s*=0, given in (5.11) and (5.12), can be modified as (5.15) and (5.16) by including the definition the set of PV buses:

$$\sum_{j\in\{J1,\,0,\,N_{PV}\}} Y_{ij}^{(tr)} V_j[0] = 0,\ i \in J1 \tag{5.15}$$

$$Y_{ii}^{(tr)} V_i^{(d)}[0] + \sum_{j\in\{J1,\,0,\,N_{PV}\}} Y_{ij}^{(tr)} V_j[0] = 0\ ,\ i \in K1 \tag{5.16}$$

The PQ bus voltages for *J*1 set (where the bus current injection is zero) can be calculated by solving the linear set of equations given in (5.15). Note that in (5.15), $Y_{ij}^{(tr)}$ is purely imaginary since the system is lossless. By dividing both side of (5.15) by *j*1, the set of equations becomes purely real with the slack bus voltage and PV bus voltages being purely real numbers (given the assumption that the slack bus voltage is given as 1.0 (at angle 0 °) and the PV bus voltages are either 1.0 or -1.0). Therefore the PQ bus voltages in *J*1 set are calculated to be purely real, by solving the linear set of

equations whose coefficients are real as given in (5.15). Likewise the PQ bus votlages in the $K1$ set are all real numbers since the PQ bus voltages in $K1$ set are simply selected to be zero. Thus the slack bus voltage, PQ and PV bus voltages in the system are all purely real numbers at s=0, such that the bus angle difference for any two buses is either 0 ºor 180 º. Therefore, the real power flow between any two buses is calculated to be zero by (5.14), resulting in no real power flow/generation in the system. The prove for case 2 is completed, and by summarizing case 1 and case 2, it can be concluded that there exist two options (1.0 or -1.0) for the value of each PV bus voltage, at s=0, for any multi-bus lossless system.

In general, two options exist for each PQ and PV bus germ, given the condition that the system is lossless: (1) For a PQ bus, either the bus voltage is zero or the sum of bus current injection is zero; (2) For PV bus, the bus voltage is either 1.0 or -1.0. Thus for a (N+1)-bus lossless system with both PQ and PV buses, there exist 2^N possible germs by varying the germ option for each PQ and PV bus.

5.4.4 Finding 2^N Germs for a Practical Multi-Bus System

For a practical power system, however, the resistance always exists on the transmission line. One way to eliminate the effect of the resistance in the system, so that solving for the germ of the PV bus (at s=0) becomes trivial, is to move the conductance term in the admittance matrix to the RHS of the HE PBE's, i.e.

$$\sum_{k=0}^{N} jB_{ik}^{(tr)} V_k(s) = \frac{sP_i - jQ_i(s)}{V_i^*(s^*)} - s\sum_{k=0}^{N} G_{ik}^{(tr)} V_k(s) - s\sum_{k=0}^{N} Y_{ik}^{(sh)} V_k(s)$$
$$V_i(s)V_i^*(s^*) = 1 + s(\left|V_i^{cntr}\right|^2 - 1) \tag{5.17}$$

where G_{ik} is the line conductance between bus i and k, and B_{ik} is the line susceptance. Using the same notation as in Chapter 3, i.e., $W_i(s)=1/V_i(s)$, (5.17) can be represented by the power series coefficients in (5.18).

$$\sum_{k=0}^{N} jB_{ik}^{(tr)} V_k[n] =$$
$$P_i W_i^*[n-1] - j\sum_{m=0}^{n} Q_i[m] W_i^*[n-m] - \sum_{k=0}^{N} (Y_{ik}^{(sh)} + G_{ik}^{(tr)}) V_k[n-1] \tag{5.18}$$

With (5.17), by varying the first term in the PV voltage power series to be either one or minus one, all the possible germs or solutions existing for the PV bus at s=0 can be obtained. Note that if all the PV voltage power series are set to be 1.0 at s=0 , the first term of reactive power series (Q(s)) for all the PV bus will be zero given as given in (3.13) and repeated below in (5.19).

$$V_i(0) = 1,\ i = 0...N$$
$$Q_i(0) = 0\ ,\ i \in N_{PV} \tag{5.19}$$

However, if a set (K2) of PV bus voltage series starts from -1.0, as shown in (5.20), the LHS of the first equation in (3.11) (duplicated below in (5.21)) will become non-zero, resulting in the first term of $Q_i(s)$, $Q_i[0]$ or $Q_i(0)$, becoming nonzero.

$$V_i(0) = -1,\ i \in K2$$
$$V_i(0) = 1,\ i \in \{N_{PV} \setminus K2\} \tag{5.20}$$

$$\sum_{k=0}^{N} Y_{ik}^{(tr)} V_k(0) = \frac{-jQ_i(0)}{V_i^*(0)}\ ,\ i \in N_{PV}$$
$$V_i(0)V_i^*(0) = 1 \tag{5.21}$$

Thus there will exist more unknowns (the imaginary part of $V_i[n]$, the real and imaginary part of $W_i[n]$ and the real variable $Q_i[n]$) than equations (the real and imaginary parts of (3.20)), leading to an underdetermined set of equations. This can be resolved by including a set of linear equations involving $V_i[n]$ and $W_i[n]$ shown in (5.22), which is based upon the relationship $W_i(s)=1/V_i(s)$.

$$V_i[n]W_i[0] + V_i[0]W_i[n] = -\sum_{m=1}^{n-1} V_i[m]W_i[n-m] \tag{5.22}$$

Note that for the PQ bus LV formulation, moving the conductance term to the RHS of HE PBE's is not required since the germ can be obtained by solving a set of linear equations given in (5.11) and (5.12). Considering there usually exist some PV buses in a power system, it will be convenient to extract the conductance term from the admittance matrix for the generalized form HE PBE's given in (5.23) and (5.24) for the PQ and PV, buses, respectively.

$$\sum_{j\in\{J1+0\}} jB_{ik}^{(tr)} V_j(s) =$$
$$\frac{sS_i^*}{V_i^*(s^*)} + \sum_{j\in K1} \frac{B_{ij}^{(tr)}}{B_{ij}^{(tr)*}} \frac{sS_j}{V_j^{(d)*}(s^*)} - s\sum_{k=0}^{N} (Y_{ik}^{(sh)} + G_{ik}^{(tr)}) V_k(s)\ ,\ i \in J1$$
$$jB_{ii}^{(tr)} V_i^{(d)}(s) + \sum_{j\in\{J1+0\}} jB_{ij}^{(tr)} V_j(s) = \tag{5.23}$$
$$\frac{B_{ii}^{(tr)}}{B_{ii}^{(tr)*}} \frac{sS_i}{V_i^{(d)*}(s^*)} + \sum_{j\in K1} \frac{B_{ij}^{(tr)}}{B_{ij}^{(tr)*}} \frac{sS_j}{V_j^{(d)*}(s^*)} - s\sum_{k=0}^{N} (Y_{ik}^{(sh)} + G_{ik}^{(tr)}) V_k(s)\ ,\ i \in K1$$

$$\begin{aligned}
&\sum_{k=0}^{N} jB_{ik}^{(tr)} V_k(s) = \frac{sP_i - jQ_i(s)}{V_i^*(s^*)} - s\sum_{k=0}^{N} G_{ik}^{(tr)} V_k(s) - s\sum_{k=0}^{N} Y_{ik}^{(sh)} V_k(s) \\
&V_i(s)V_i^*(s^*) = 1 + s(\left|V_i^{cntr}\right|^2 - 1) \\
&V_i(0) = -1,\ i \in K2 \\
&V_i(0) = 1,\ i \in \{N_{PV} \setminus K2\}
\end{aligned} \tag{5.24}$$

For any (N+1)-bus system with both PQ and PV buses, 2^N possible germs are to be found by varying the germ option for each PQ and PV bus. By starting from all possible germs existing at s=0, it is guaranteed through Stahl's theorem and the use of maximal analytic continuation, that all of the solutions of the PBE's at s=1 can be obtained.

5.5 The Guarantee to Find All the PF Solutions

Theorem 1: Since all 2^N possible germs for the HE PBE's can be easily found for the proposed HE PBE formulation, as given in Lemma 3, all the complex-valued solutions for the PF problem therefore are guaranteed to be obtained, using the technique of maximal analytic continuation (Lemma 1) and unique germ-to-solution mapping (Lemma 2).

The above theorem is the statement that one can find all the PF solutions using the proposed HE PBE's in (5.23) and (5.24), as a consequence of Lemma 1-3. Thus the proof that the proposed HE method is guaranteed to find all complex-valued PF solutions is completed.

5.6 Discussions

It should be noted that two sets of PQ bus PBE's are given in (5.23), providing two different PBE's for the PQ bus model. However as emphasized in Lemma 3, all the germs have to be found using the same HE PBE formulation. Does the proof in Theorem 1 still hold true while two set of HE PBE's have to be solved for the PQ bus model?

The answer is yes because the formulations are the same; they only differ due to a substitution of different variables. By looking into the details of the PQ bus LV formulation, it can be noted that a substitution of variables is made in (5.4) due to the $\frac{0}{0}$ problem. As discussed in (5.3), a form of $\frac{0}{0}$ will result in a defined/bounded number by using the L'Hôpital's rule in theory, but will result in an execution time error, not-a-number (NaN) if using Matlab. Thus, the change of variables (5.4) is necessary in implementation of the proposed algorithm in machine programming rather than in theory. Note that a variable s appears on the RHS of (5.3), resulting a delay in power series coefficients between $V_i^{(d)}(s)$ and $V_i(s)$. Therefore $V_i(s)$ has to be solved *a priori to* $V_i^{(d)}(s)$, as a resultant of change of variable in (5.3). Thus two set of HE PBE's are given in (5.23) for the PQ bus model, which theoretically represents the same HE PBE if no substitution of variable is made.

Another problem that may raise up is: what if the HE PBE's are different from (5.23) and (5.24), is it guaranteed to find all the possible solutions for the PF problem? The answer is yes, as long as all the germs can be found. However, as discussed in Lemma 3, the solutions at s=0 for the HE PBE's, in (5.23) and (5.24), can be reliably

obtained without solving a set of quadratic PBE's. If one changes the HE PBE's rather than using (5.23) and (5.24), the PBE's at s=0 again becomes the quadratic form and there will be no guarantee that all the PF solutions can be found, which in essence is the target we are trying to reach.

5.7 Numerical Tests

5.7.1 Five & Seven-Bus System

Using the LV/large-angle formulations for both PQ and PV bus derived in sections 5.4.1 and 5.4.2, numerical tests for finding all of the solutions for a five and seven-bus system will be discussed. The system topology of the five-bus system is shown in Figure 5.2 where bus 5 is the slack bus. The slack bus voltage is set to be 1.06 per-unit at angle zero and the PV bus (bus 1) voltage is controlled to be 1.0 per-unit. The system branch information is given in Table 5.1 and the bus admittance matrix is shown in Table 5.2.

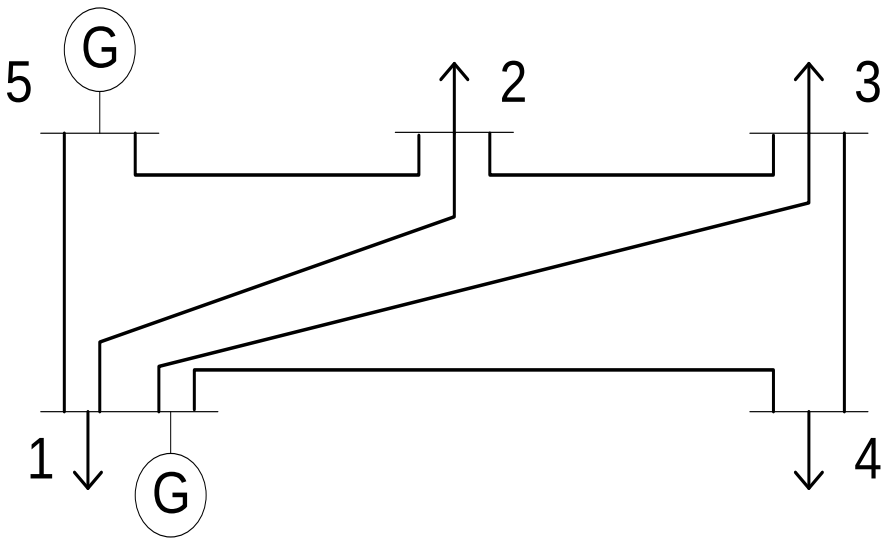

Figure 5.2 Five-Bus System

Table 5.1 Branch Data for the Five-Bus System

Branch	**Line Impedance**
1-2	0.06 + j0.18
1-3	0.06 + j0.18
1-4	0.04 + j0.12
1-5	0.02 + j0.06
2-3	0.01 + j0.03
2-5	0.08 + j0.24
3-4	0.02 + j0.24

Table 5.2 Bus Admittance Matrix for the Five-Bus System

$\boldsymbol{Y}_{\mathbf{BUS}}=$

6.25 – j18.75	-5 + j15	-1.25 + j3.75	0	0
-5 + j15	10.8334 – j32.75	-1.6667 + j5	-1.6667 + j5	-2.5 + j7.5
-1.25 + j3.75	-1.6667 + j5	12.9167 – j38.75	-10 + j30	0
0	-1.6667 + j5	-10 + j30	12.9167 – j38.75	-1.25 + j3.75
0	-2.5 + j7.5	0	-1.25 + j3.75	3.75 – j11.25

The load injections in the five-bus system are S_1, S_2, S_3 and S_4 for buses 1, 2, 3 and 4, respectively. The p.u. values of S_1 to S_4 are:

$$S_1 = -0.2 - j0.1,\ S_2 = -0.45 - j0.15,\ S_3 = -0.4 - j0.05,\ S_4 = -0.6 - j0.1$$

The solutions for the five-bus system were found by using the CPF method [50] and are given in Table 5.3.

Table 5.3 Solutions for the Five-Bus System Using Continuation Method [50]

	HV soln.	**LV soln.'s**			
Soln. NO.	1	2	3	4	5
V_1	1∠-2.067 °	1∠-138.967 °	1∠-128.586 °	1∠-12.146 °	1∠-126.625 °
V_2	0.980 ∠-4.535 °	0.501 ∠-129.851 °	0.377 ∠-116.836 °	0.793 ∠-12.679 °	0.062 ∠-159.529 °
V_3	0.977 ∠-4.853 °	0.587 ∠-134.863 °	0.410 ∠-124.173 °	0.740 ∠-13.879 °	0.215 ∠-144.796 °
V_4	0.966 ∠-5.692 °	0.831 ∠-141.660 °	0.066 ∠-185.734 °	0.057 ∠-71.501 °	0.698 ∠-133.440 °
V_5	1.06∠0 °	1.06∠0 °	1.06∠0 °	1.06∠0 °	1.06∠0 °
LV soln.'s					
Soln. NO.	6	7	8	9	10
V_1	1∠-16.504 °	1∠-18.097 °	1∠-16.908 °	1∠-22.520 °	1∠-119.882 °
V_2	0.197 ∠-26.042 °	0.056 ∠-61.126 °	0.034 ∠-69.046 °	0.196 ∠-30.681 °	0.088 ∠-141.839 °
V_3	0.030 ∠-81.865 °	0.049 ∠-80.670 °	0.184 ∠-37.786 °	0.036 ∠-85.945 °	0.165 ∠-144.756 °
V_4	0.628 ∠-23.451 °	0.632 ∠-25.443 °	0.686 ∠-23.872 °	0.081 ∠-79.418 °	0.075 ∠-178.499 °
V_5	1.06∠0 °	1.06∠0 °	1.06∠0 °	1.06∠0 °	1.06∠0 °

A total of 10 solutions are obtained and reported by [50] and, as a check, they were substituted back into the PBE's, which were satisfied for all solutions. The maximum mismatch of the PBE's is less than 10^{-4}. Therefore the 10 solutions obtained (listed in Table 5.3) for the five-bus system are used as a benchmark for comparison with the solutions obtained by the HE method.

Using the HE method, there existed 16 different germs for the five-bus system; therefore 16 possible solutions can be obtained. It will be convenient to use a binary number to represent whether the HV or LV formulation is applied to a certain bus, i.e. a 1 in position i , with the left-most position being position 1, indicates that the HV formulation is used for the PBE for bus i and a 0 in position i indicates that the LV

formulation is used for the PBE for bus *i*. A four-bit binary number will be used for the five-bus system in order to represent the HV/LV combination where the slack bus voltage is always considered to be fixed at 1.06 per-unit. For example, 1111 represents the condition where the HV PBE's are used for all buses, 1010 represents the condition where the HV PBE's are used for buses 1 and 3 and the LV PBE's are used for buses 2 and 4. Using an application developed with Matlab (16 digits of mantissa precision), 10 out of 16 solutions were obtained listed in Table 5.4, where the PBE's mismatch tolerance is set to be 10^{-5} in the program For the cases where no solution found, the oscillation of the diagonal Padé Approximant was detected indicating that no non-quaternion solution exists for this germ.

The voltage solution differences (in both magnitudes and angles) between Table 5.3 and Table 5.4 are listed in Table 5.5. It can be observed that all the 10 solutions for this five-bus system can be found using the proposed HE method.

Table 5.4 Solutions for the Five-Bus System using HE Method

Soln. NO. (Binary)	1 (1111)	2 (0111)	3 (0110)	4 (1110)	5 (0011)
V_1	1 ∠-2.0675 °	1 ∠-138.9679 °	1 ∠-128.5864 °	1 ∠-12.1469 °	1 ∠-126.6253 °
V_2	0.9805 ∠-4.5358 °	0.5012 ∠-129.8511 °	0.3770 ∠-116.8370 °	0.7933 ∠-12.6793 °	0.0626 ∠-159.5293 °
V_3	0.9771 ∠-4.8535 °	0.5879 ∠-134.8640 °	0.4108 ∠-124.1731 °	0.7403 ∠-13.8795 °	0.2160 ∠-144.7964 °
V_4	0.9662 ∠-5.6925 °	0.8317 ∠-141.6605 °	0.0666 ∠184.2660 °	0.0580 ∠-71.5017 °	0.6982 ∠-133.4401 °
V_5	1.06∠0 °	1.06∠0 °	1.06∠0 °	1.06∠0 °	1.06∠0 °
Soln. NO. (Binary)	6 (1101)	7 (1001)	8 (1011)	9 (1100)	10 (0010)
V_1	1 ∠-16.5040 °	1 ∠-18.0976 °	1 ∠-16.9089 °	1 ∠-22.5210 °	1 ∠-119.8826 °
V_2	0.1972 ∠-26.0422 °	0.0563 ∠-61.1266 °	0.0342 ∠-69.0465 °	0.1968 ∠-30.6818 °	0.0881 ∠-141.8392 °
V_3	0.0301 ∠-81.8652 °	0.0496 ∠-80.6706 °	0.1846 ∠-37.7869 °	0.0369 ∠-85.9455 °	0.1659 ∠-144.7572 °
V_4	0.6289 ∠-23.4519 °	0.6327 ∠-25.4435 °	0.6865 ∠-23.8729 °	0.0814 ∠-79.4189 °	0.0756 ∠-178.5106 °
V_5	1.06∠0 °	1.06∠0 °	1.06∠0 °	1.06∠0 °	1.06∠0 °

Table 5.5 Absolute Differences between the Solutions using Continuation Method and the HE Method

Soln. NO.		1	2	3	4	5
V_1	Mag. (p.u.)	0*	0*	0*	0*	0*
	Angle (deg.)	0.0005	0.0009	0.0004	0.0009	0.0003
V_2	Mag. (p.u.)	0.0005	0.0002	0*	0.0003	0.0006
	Angle (deg.)	0.0008	0.0009	0.0010	0.0003	0.0003
V_3	Mag. (p.u.)	0.0001	0.0009	0.0008	0.0007	0.0010
	Angle (deg.)	0.0005	0.0010	0.0001	0.0005	0.0004
V_4	Mag. (p.u.)	0.0002	0.0007	0.0006	0.0010	0.0002
	Angle (deg.)	0.0005	0.0005	1.5320	0.0007	0.0001
Soln. NO.		6	7	8	9	10
V_1	Mag. (p.u.)	0*	0*	0*	0*	0*
	Angle (deg.)	0*	0.0006	0.0009	0.0010	0.0004
V_2	Mag. (p.u.)	0.0002	0.0003	0.0002	0.0008	0.0001
	Angle (deg.)	0.0002	0.0006	0.0005	0.0008	0.0002
V_3	Mag. (p.u.)	0.0001	0.0006	0.0006	0.0009	0.0009
	Angle (deg.)	0.0002	0.0006	0.0009	0.0005	0.0012
V_4	Mag. (p.u.)	0.0009	0.0007	0.0005	0.0004	0.0006
	Angle (deg.)	0.0009	0.0005	0.0009	0.0009	0.0106

* Match up to four significant digits

The plots for the voltage magnitudes (in p.u.) and angles (in degrees) for different solutions are shown in Figure 5.3 through Figure 5.12. Observe that when the LV HE formulation is applied to one bus, the voltage solution obtained at that specific bus has a smaller magnitude or larger phase angle compared to the solution obtained with the HV HE formulation for the same bus.

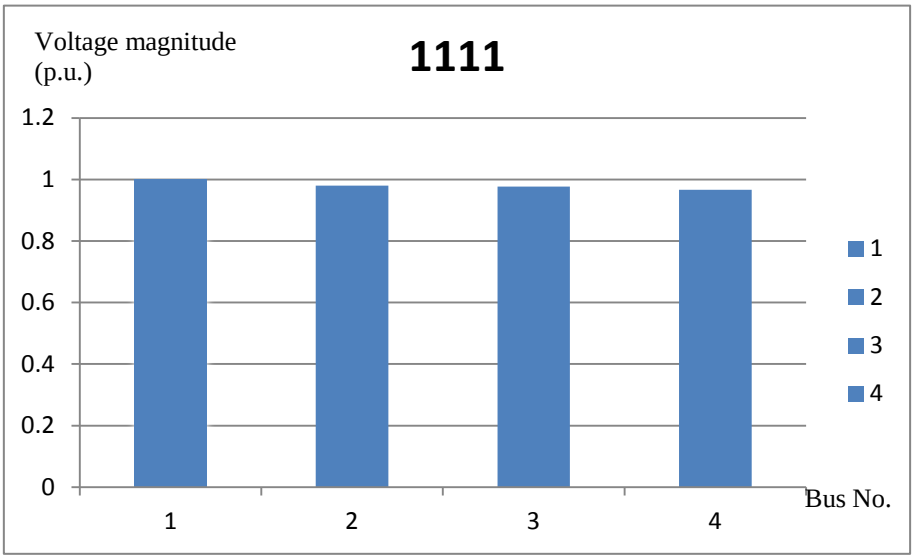

(a) Voltage Magnitudes

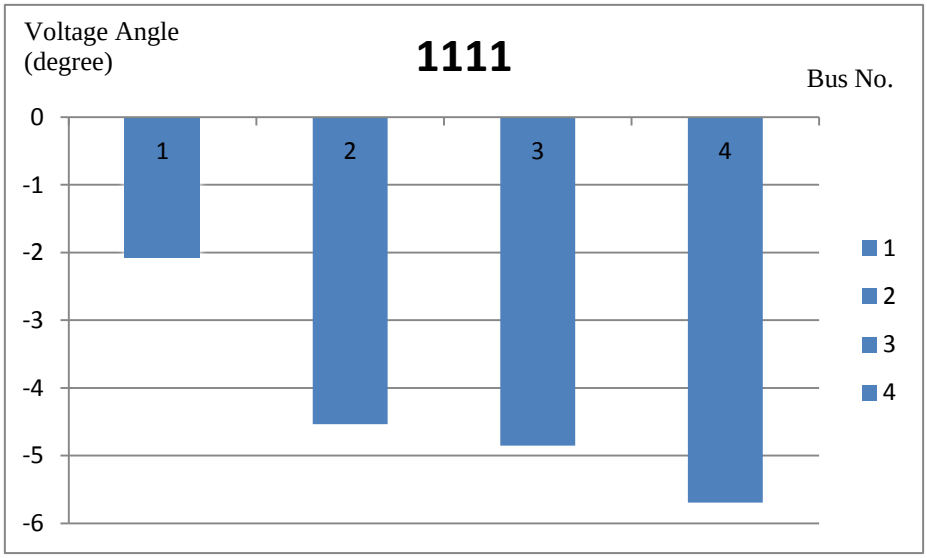

(b) Voltage Angles

Figure 5.3 HV Solution (1111)

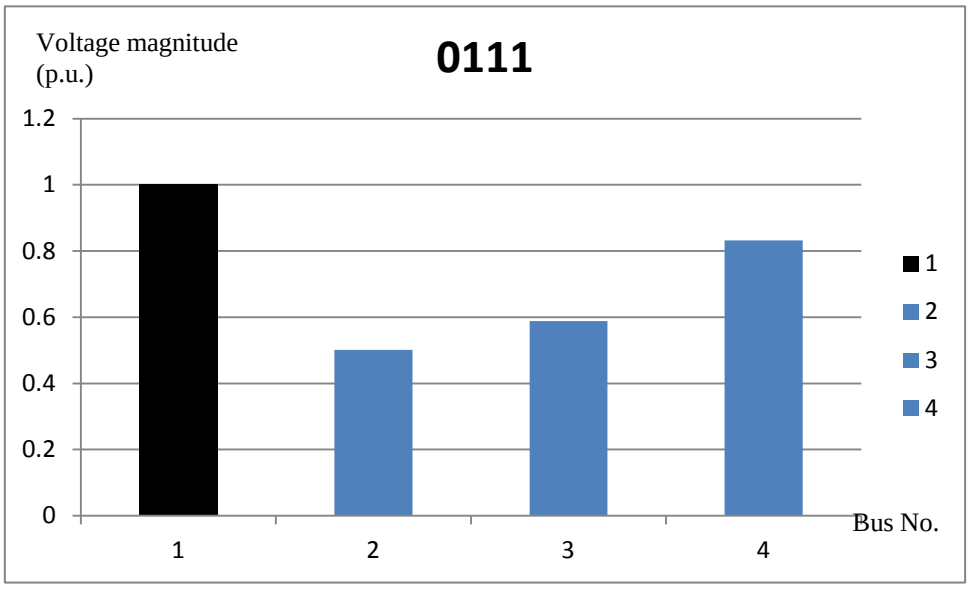

(a) Voltage Magnitudes

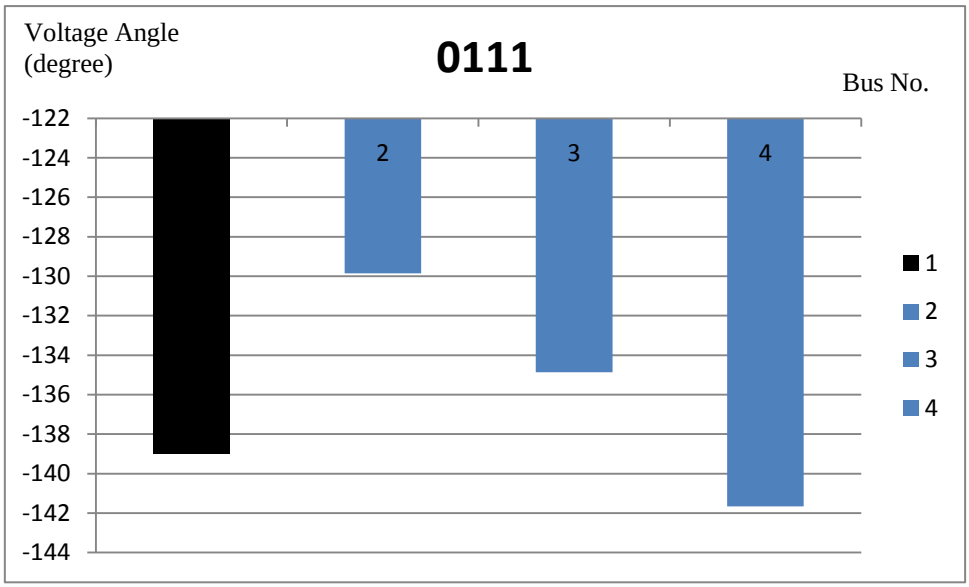

(b) Voltage Angles

Figure 5.4 LV PBE's Applied to V_1 (0111)

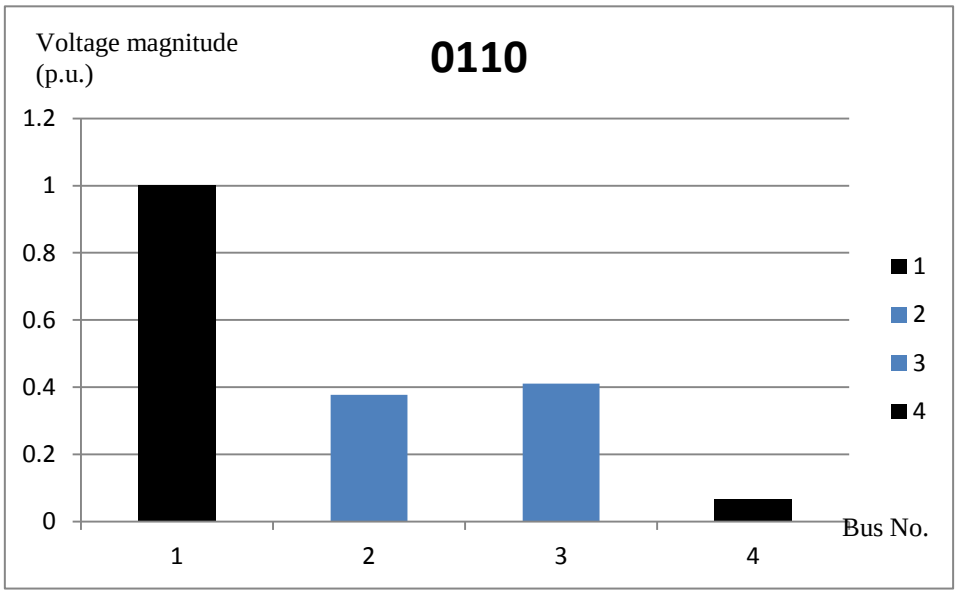

(a) Voltage Magnitudes

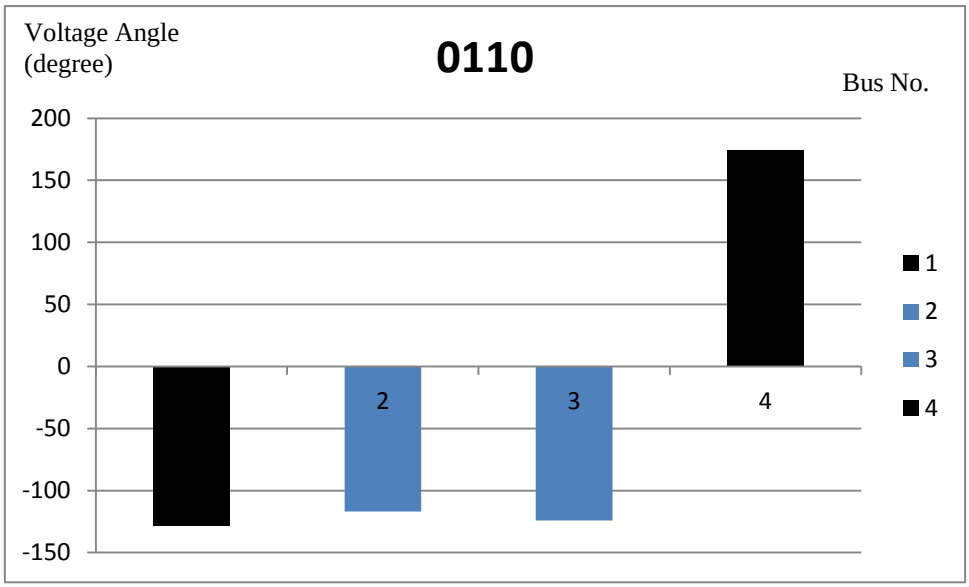

(b) Voltage Angles

Figure 5.5 LV PBE's Applied to V_1& V_4 (0110)

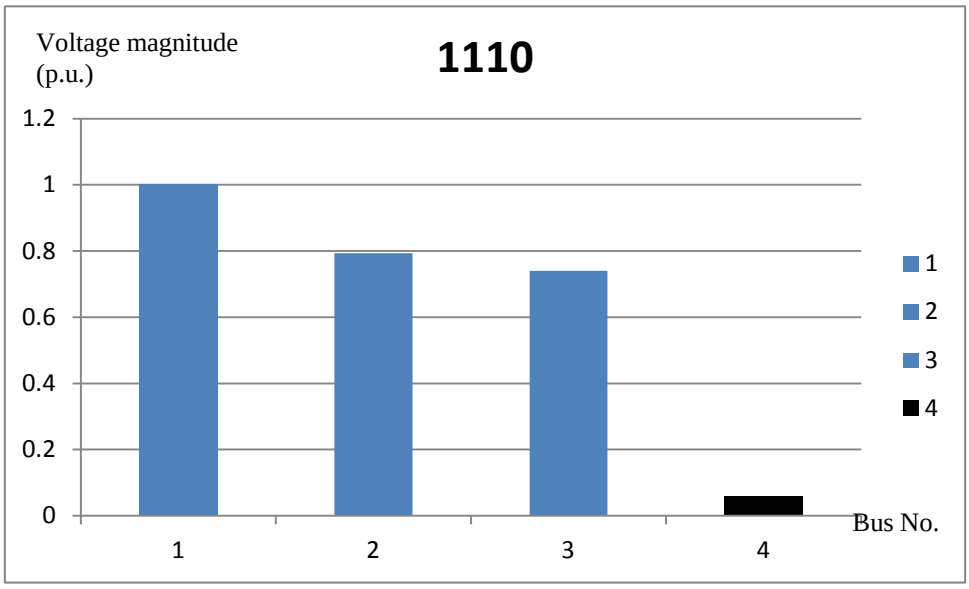

(a) Voltage Magnitudes

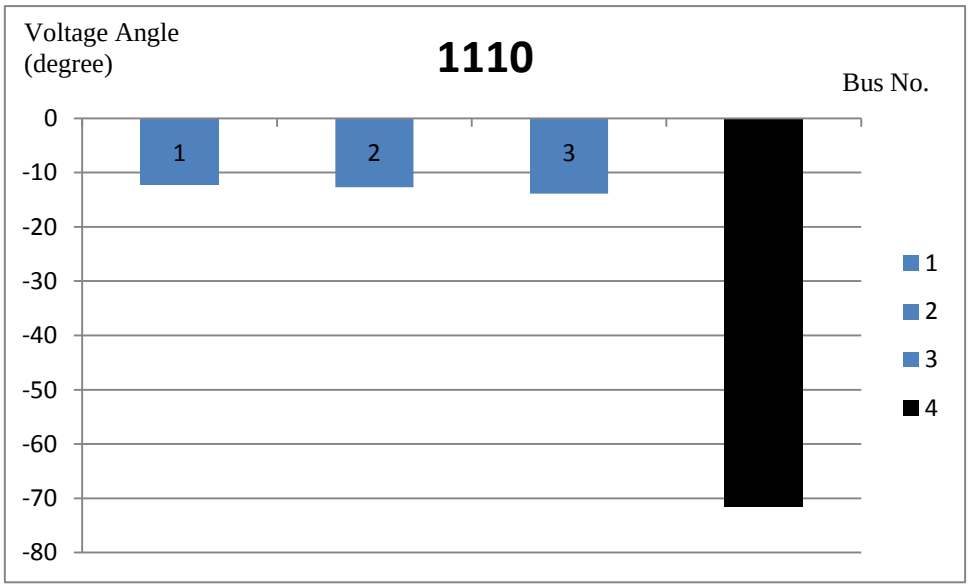

(b) Voltage Angles

Figure 5.6 LV PBE's Applied to V_4 (1110)

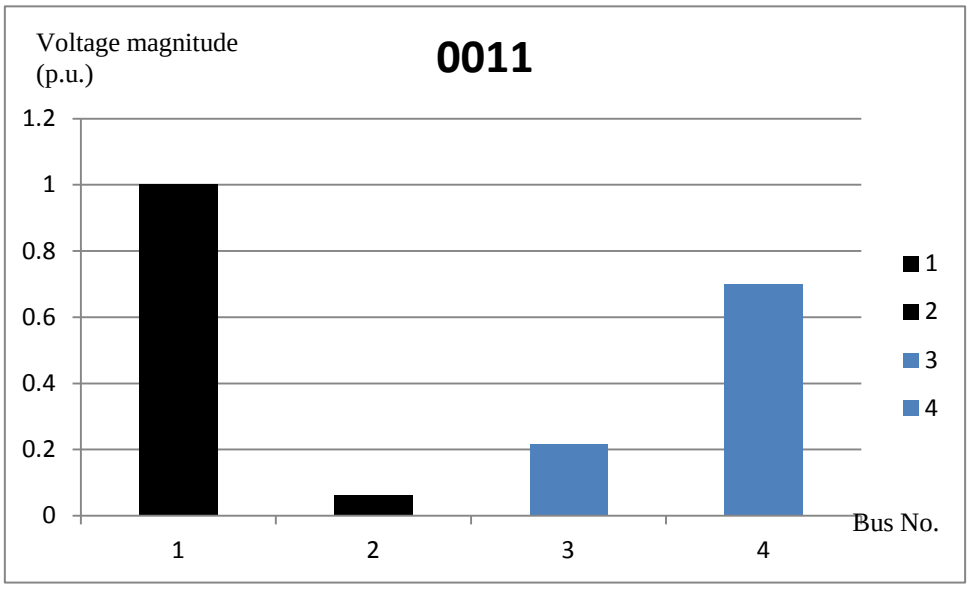

(a) Voltage Magnitudes

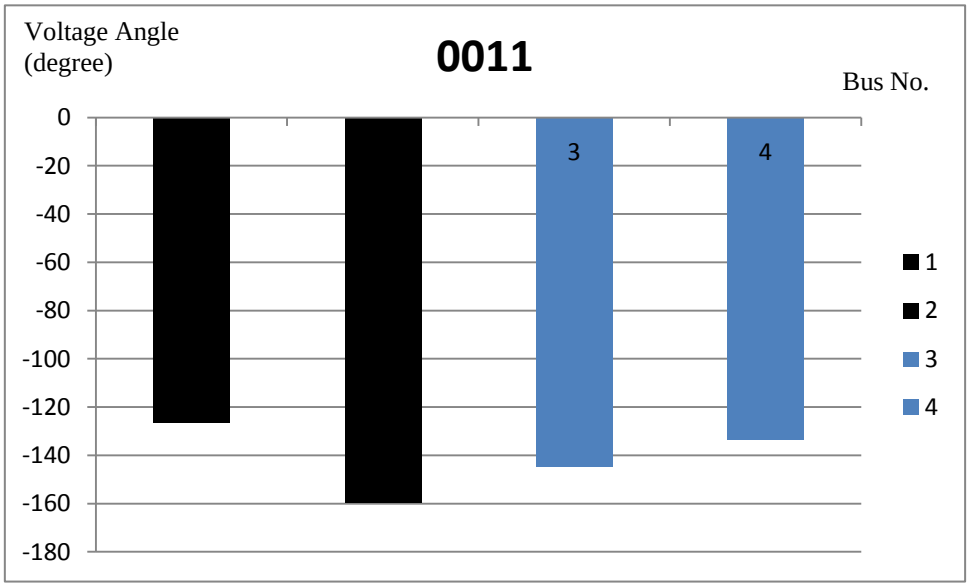

(b) Voltage Angles

Figure 5.7 LV PBE's Applied to V_1&V_2 (0011)

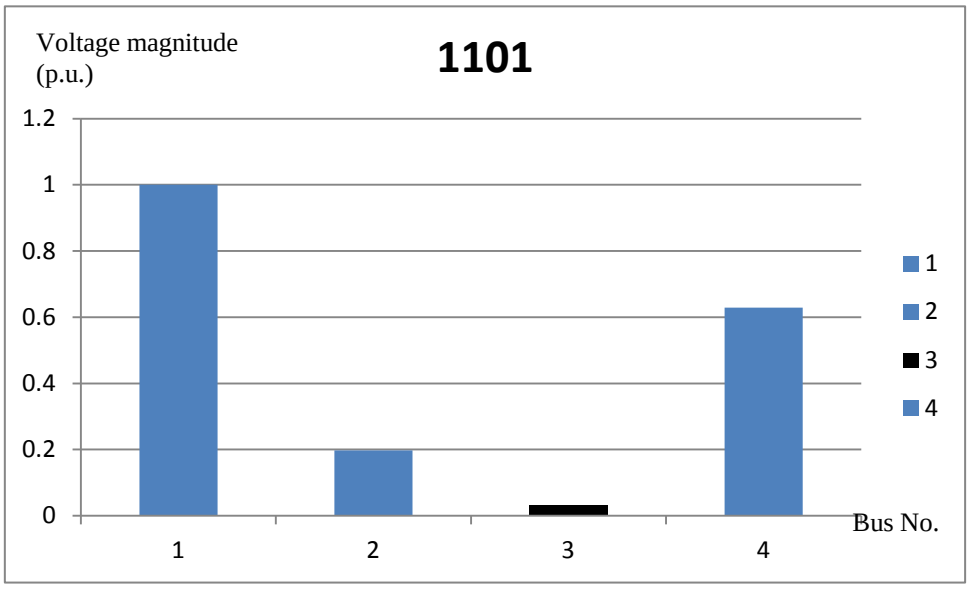

(a) Voltage Magnitudes

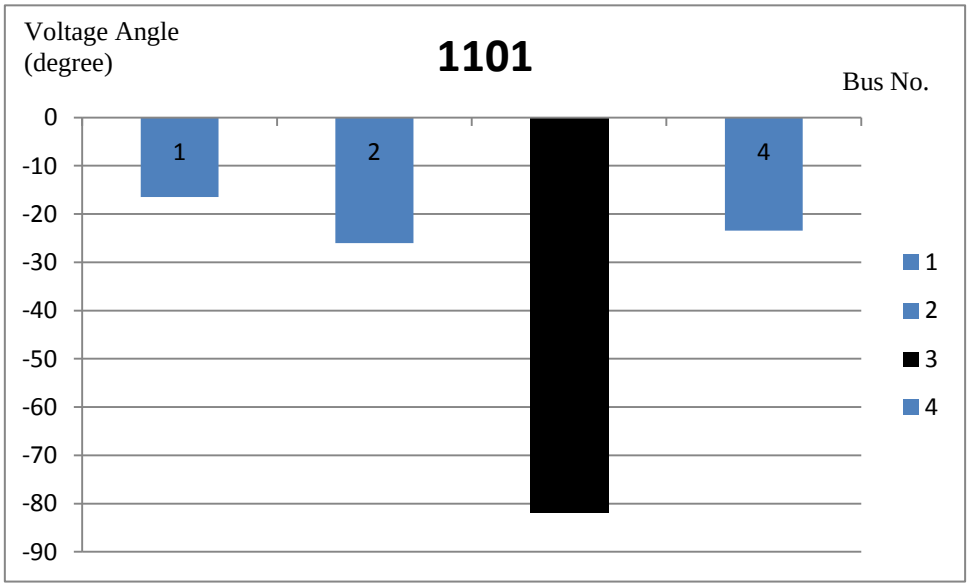

(b) Voltage Angles

Figure 5.8 LV PBE's Applied to V_3 (1101)

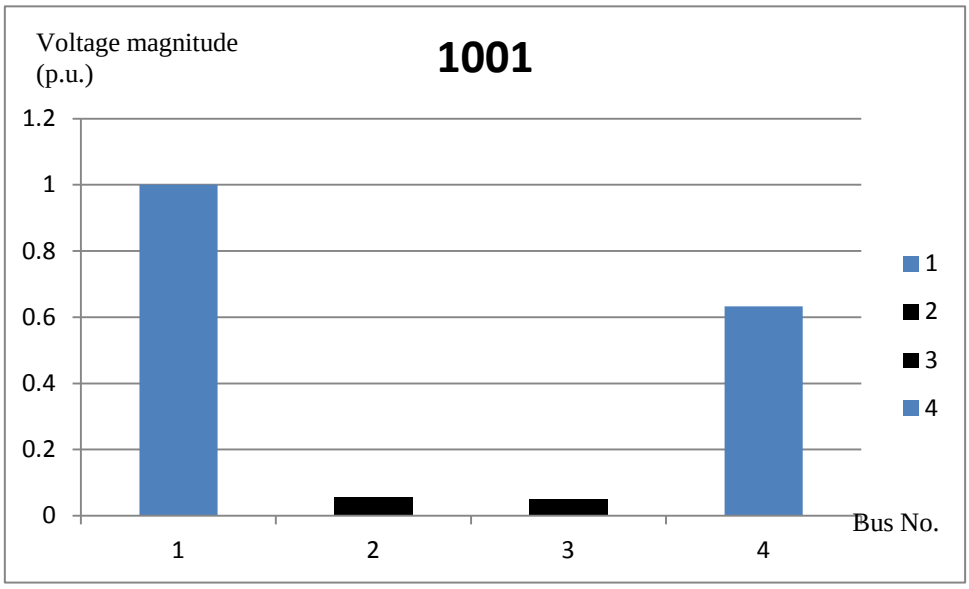

(a) Voltage Magnitudes

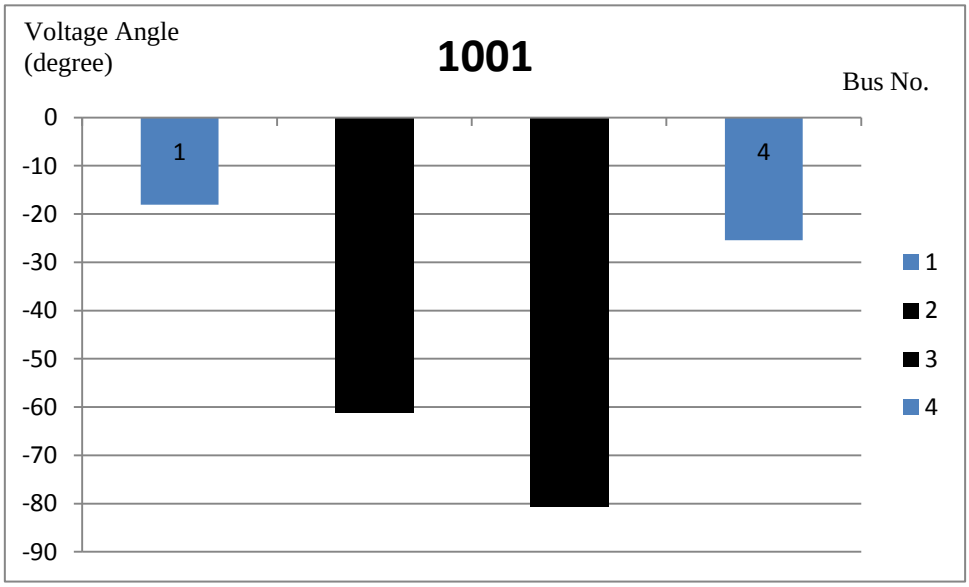

(b) Voltage Angles

Figure 5.9 LV PBE's Applied to V_2&V_3 (1001)

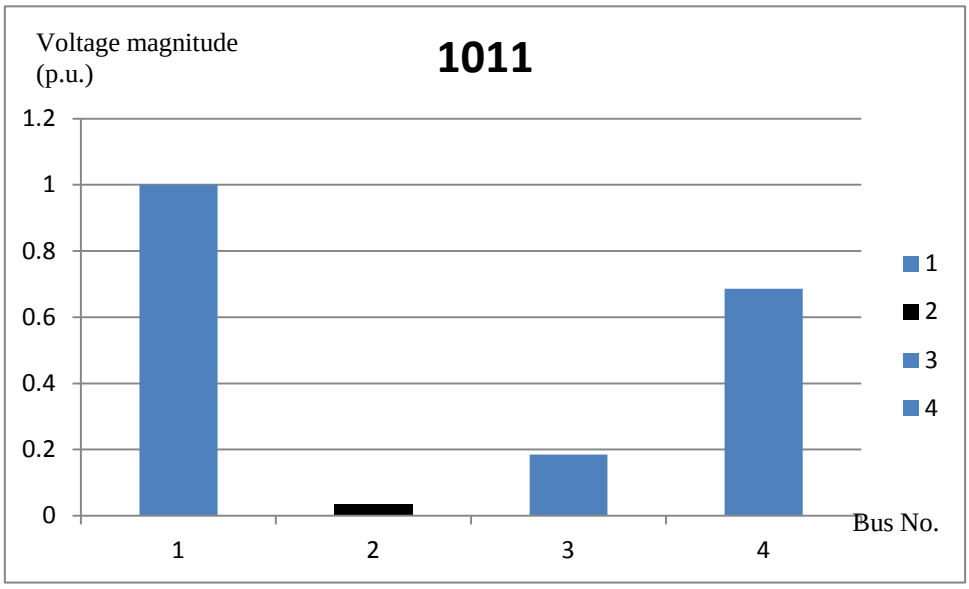

(a) Voltage Magnitudes

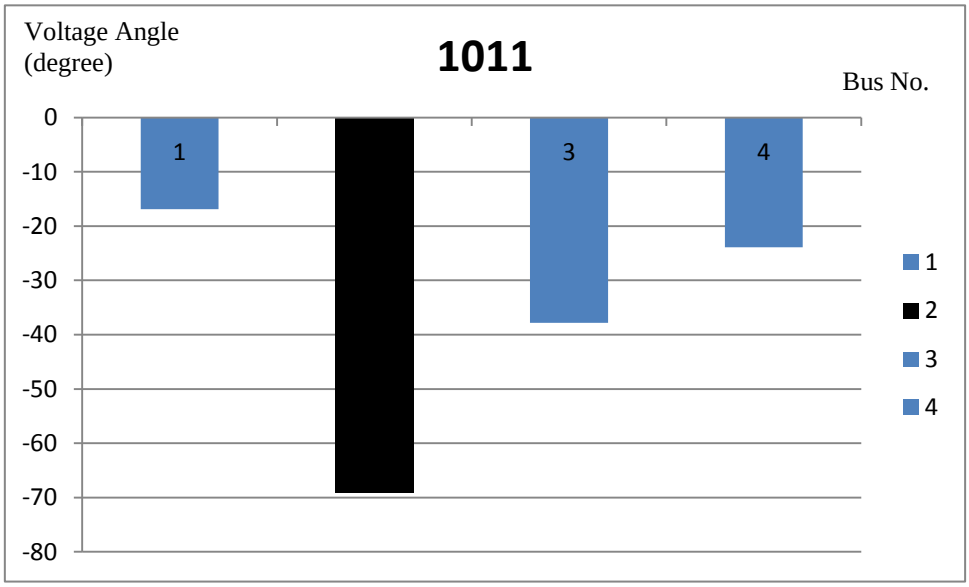

(b) Voltage Angles

Figure 5.10 LV PBE's Applied to V_2 (1011)

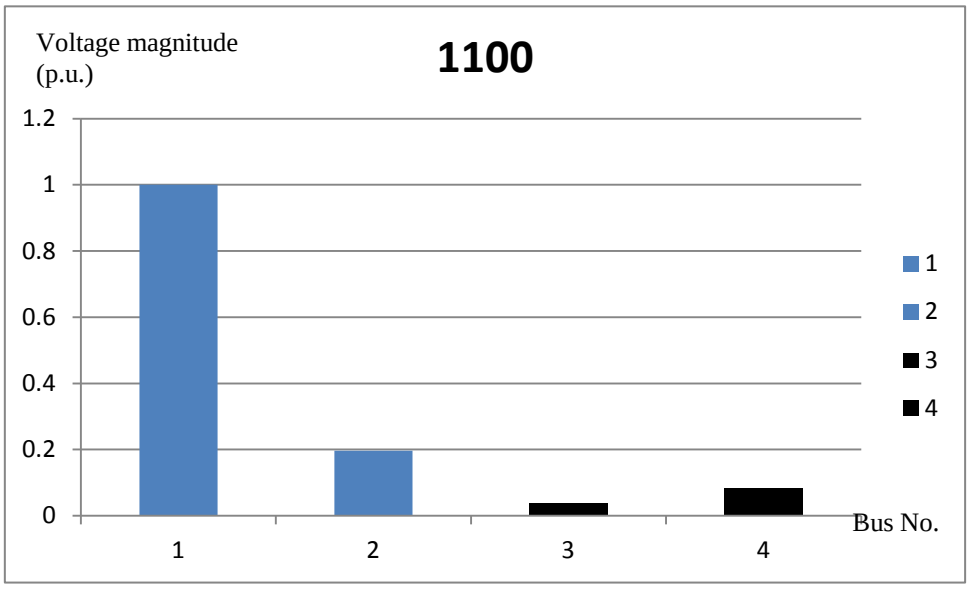

(a) Voltage Magnitudes

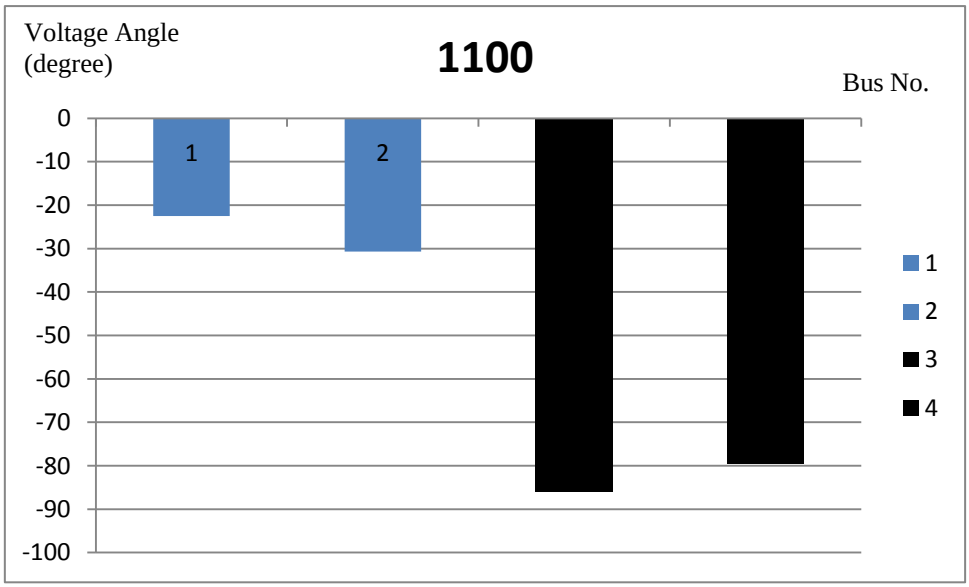

(b) Voltage Angles

Figure 5.11 LV PBE's Applied to V_3&V_4 (1100)

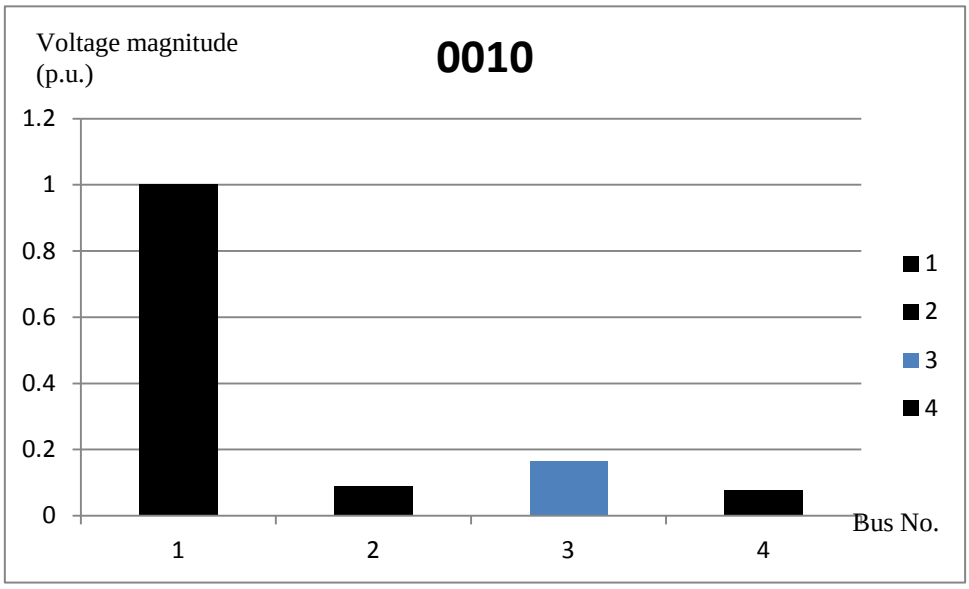

(a) Voltage Magnitudes

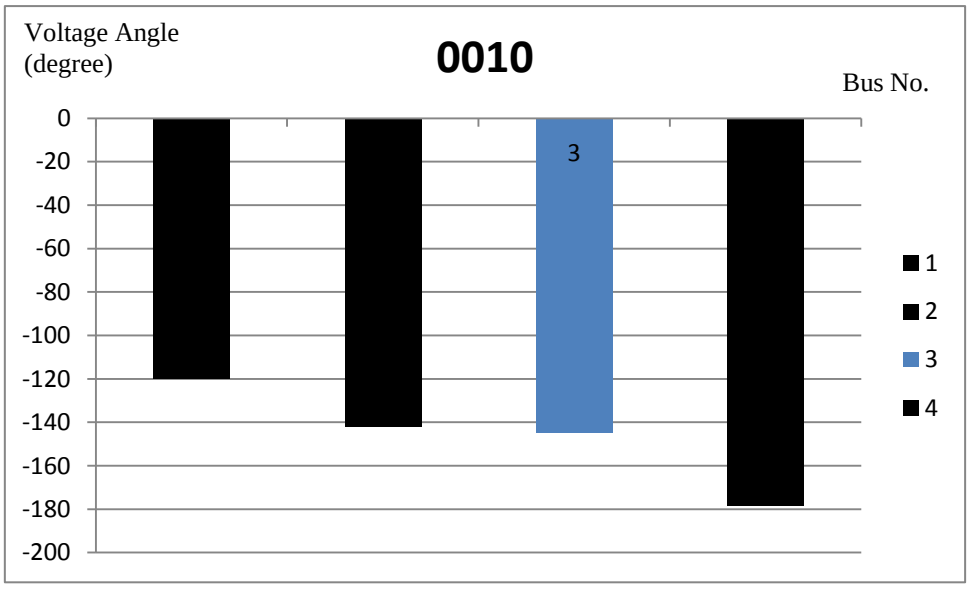

(b) Voltage Angles

Figure 5.12 LV PBE's Applied to V_1, V_2&V_4 (0010)

A seven-bus system given in [50] is also used as a numerical benchmark to verify that the proposed algorithm can find all the solutions to the PF problem. The system topology of the seven-bus system is shown in Figure 5.13 where bus 7 is the slack bus operated at 1.0 p.u. with angle 0.0. Though the large-angle HE PV bus formulation is

proposed in this report, the PV bus (bus 1) is treated as a PQ bus by specifying the real/reactive power since this bus model conversion is used in [50]. The system branch data is given in Table 5.6.

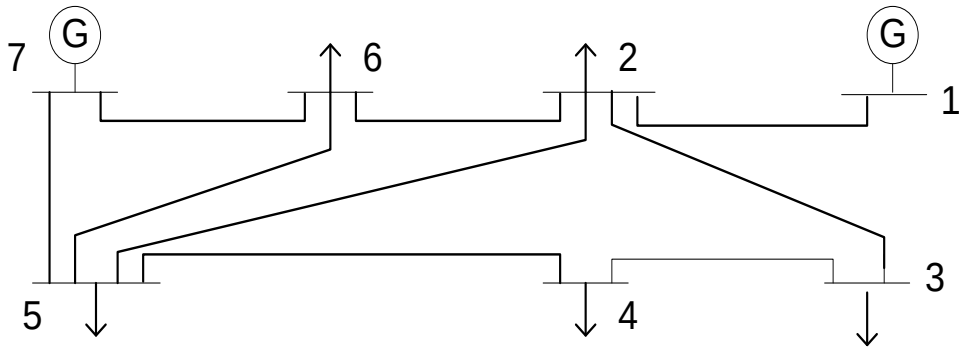

Figure 5.13 Seven-Bus System

Table 5.6 Parameters for the Seven-Bus System

Branch	**Line Impedance**	**Branch**	**Line Impedance**
1-2	0.082 + j0.192	4-5	0.024 + j0.1
2-3	0.067 + j0.171	5-6	0.057 + j0.174
2-5	0.058 + j0.176	5-7	0.019 + j0.059
2-6	0.013 + j0.042	6-7	0.054 + j0.223
3-4	0.024 + j0.1		

The load injections in the seven-bus system are S_1, S_2, S_3, S_4, S_5 and S_6 for buses 1, to 6, respectively. The p.u. values of S_1 to S_6 are:

$$S_1 = 0.9 + j0.3,\ S_2 = -0.478 - j0.039,\ S_3 = -0.942 - j0.190,$$

$$S_4 = -0.135 - j0.058,\ S_5 = -0.183 - j0.127,\ S_6 = -0.135 - j0.058$$

Note that bus 1 is injecting positive real/reactive power into the system acting as generator. The solutions for the seven-bus system taken from [50] are given in Table

5.7 and were verified by substitution into the power mismatch form yielding real and reactive mismatches of less than 10^{-5} per-unit.

Table 5.7 Solutions for the Seven-Bus System Using a Continuation Method [50]

	HV soln.	**LV soln.'s**		
Soln. NO.	1	2	3	4
V_1	1.07577 ∠-5.28593 °	0.73120 ∠14.95760 °	0.28797 ∠101.81875 °	0.34350 ∠88.33610 °
V_2	0.96352 ∠-2.93423 °	0.58756 ∠-5.22121 °	0.54147 ∠-6.29309 °	0.43321 ∠-6.83457 °
V_3	0.90411 ∠-8.44389 °	0.17451 ∠-52.67754 °	0.54303 ∠-19.80951 °	0.24973 ∠-44.27974 °
V_4	0.92780 ∠-5.74999 °	0.41217 ∠-14.20556 °	0.64577 ∠-11.24617 °	0.43590 ∠-16.13621 °
V_5	0.96382 ∠-2.44630 °	0.66377 ∠-3.20560 °	0.77500 ∠-3.86173 °	0.68791 ∠-3.91929 °
V_6	0.96747 ∠-2.59176 °	0.66377 ∠-4.30311 °	0.64015 ∠-5.01581 °	0.54957 ∠-5.31378 °
V_7	1∠0 °	1∠0 °	1∠0 °	1∠0 °

The solutions obtained from the HE method are given in Table 5.8. The binary number representation is used to represent the HV/LV formulation combination for simplicity, starting from bus 1 on the left-most bit to bus 6 on the right-most bit. I.e., solution 2, represented by 110111 in Table 5.8, is obtained by using the LV PBE for bus 3. Solution 3 is obtained by using the LV PBE for bus 1, solution 4 is obtained by using the LV PBE's for buses 1 and 3 and solution 1 is the HV solution. Otherwise no solution can be obtained, indicated by the oscillations of the diagonal Padé Approxi-mant.

Table 5.8 Solutions for the Seven-Bus System Using the HE Method

	HV soln.	**LV soln.'s**		
Soln. NO. (Bin.)	1(111111)	2(110111)	3(011111)	4(010111)
V_1	1.0758 ∠-5.2859 °	0.7312 ∠14.9587 °	0.2880 ∠101.8197 °	0.3435 ∠88.3331 °
V_2	0.9635 ∠-2.9342 °	0.5875 ∠-5.2213 °	0.5415 ∠-6.2929 °	0.4331 ∠-6.8349 °
V_3	0.9041 ∠-8.4439 °	0.1745 ∠-52.6807 °	0.5430 ∠-19.8094 °	0.2497 ∠-44.2802 °
V_4	0.9278 ∠-5.7501 °	0.4122 ∠-14.2060 °	0.6458 ∠-11.2461 °	0.4359 ∠-16.1363 °
V_5	0.9638 ∠-2.4463 °	0.7229 ∠-3.2055 °	0.7750 ∠-3.8617 °	0.6879 ∠-3.9192 °
V_6	0.9675 ∠-2.5918 °	0.6638 ∠-4.3031 °	0.6402 ∠-5.0157 °	0.5496 ∠-5.3131 °
V_7	1∠0 °	1∠0 °	1∠0 °	1∠0 °

Table 5.9 Absolute Differences between the Solutions using Continuation Method and the HE Method

Soln. NO.		1	2	3	4
V_1	Mag. (p.u)	0.00003	0*	0.00003	0*
	Angle (deg.)	0.00003	0.00110	0.00125	0.00300
V_2	Mag. (p.u)	0.00002	0.00006	0.00003	0.00011
	Angle (deg.)	0.0003	0.00011	0.00019	0.00033
V_3	Mag. (p.u)	0.00001	0.00001	0.00003	0.00003
	Angle (deg.)	0.00001	0.00346	0.00011	0.00026
V_4	Mag. (p.u)	0*	0.00003	0.00003	0*
	Angle (deg.)	0.00002	0.00044	0.00007	0.00021
V_5	Mag. (p.u)	0.00002	0.00004	0*	0.00001
	Angle (deg.)	0*	0.00010	0.00003	0.00009
V_6	Mag. (p.u)	0.00003	0.00003	0.00005	0.00003
	Angle (deg.)	0.00004	0.00001	0.00011	0.00068

* Match up to four significant digits

Observe that all four solutions for the seven-bus system can be found using the proposed HE method. The plots for the voltage magnitudes and voltage angles (in degrees) for different solutions are shown in Figure 5.14 through Figure 5.17. Similar to

the five-bus system in Figure 5.2, observe that when the LV HE formulation is applied to a bus, the voltage solution obtained at that specific bus has a smaller magnitude or a larger phase angle compared to the solutions obtained with the HV HE formulation for the same bus.

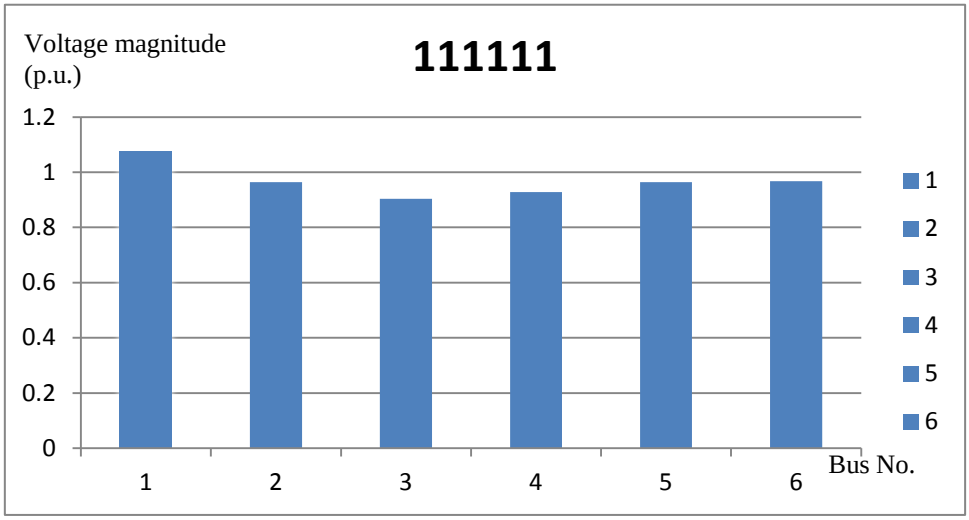

(a) Voltage Magnitudes

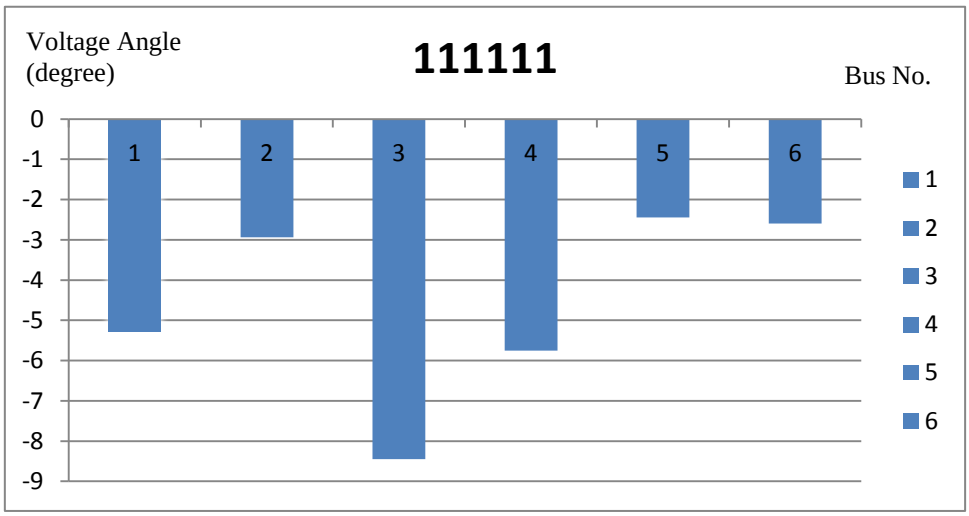

(a) Voltage Angles

Figure 5.14 HV Solution (111111)

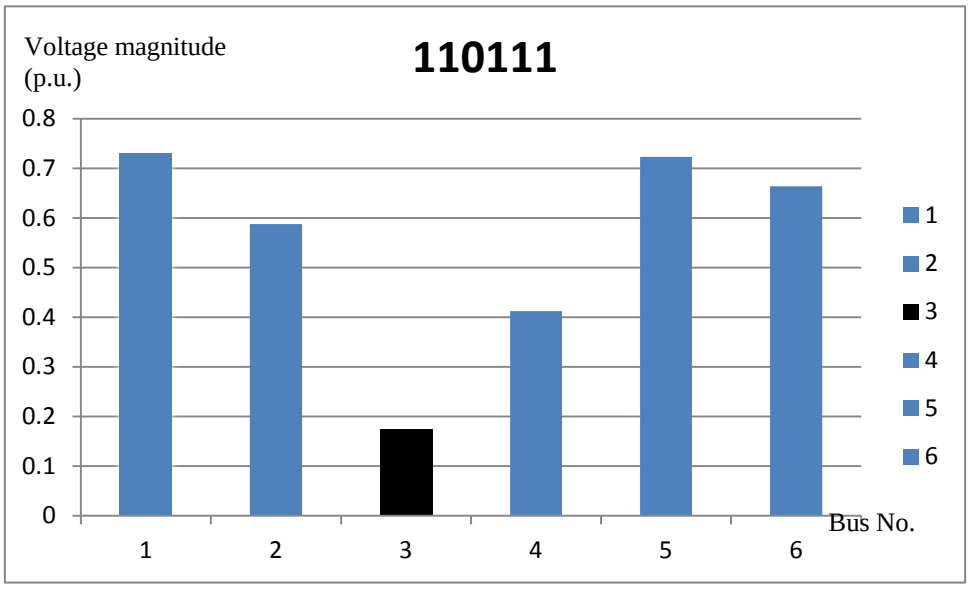

(a) Voltage Magnitudes

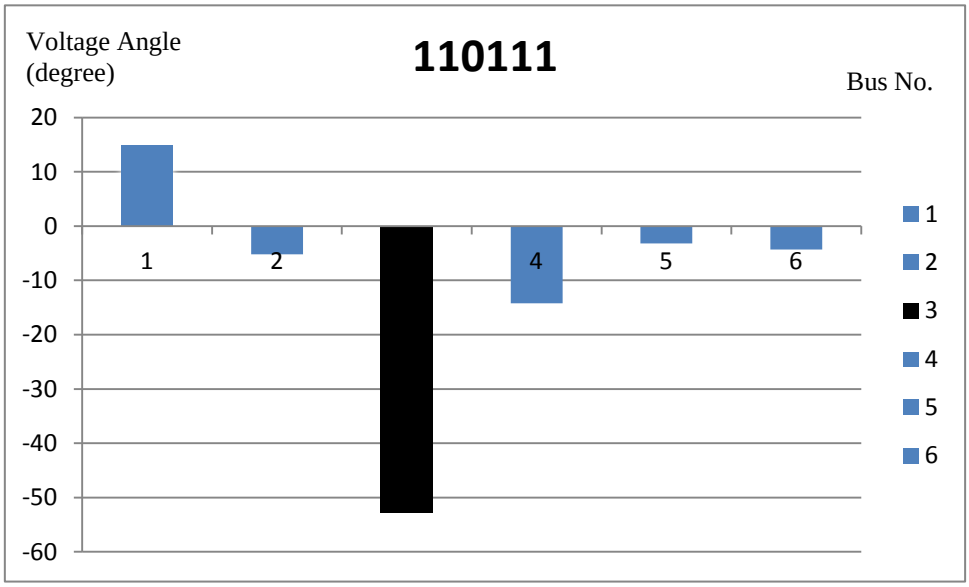

(b) Voltage Angles

Figure 5.15 LV PBE's Applied to V_3 (110111)

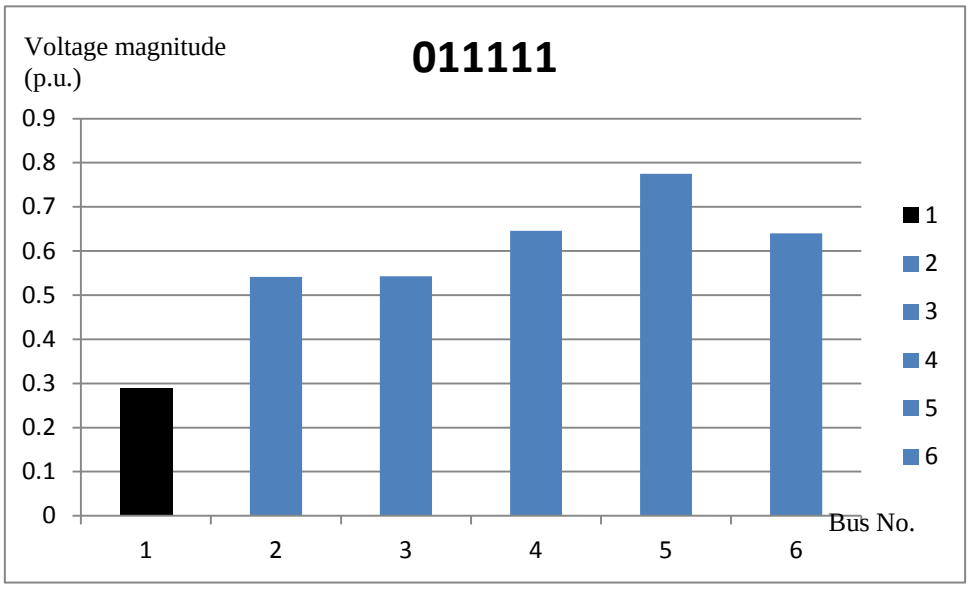

(a) Voltage Magnitudes

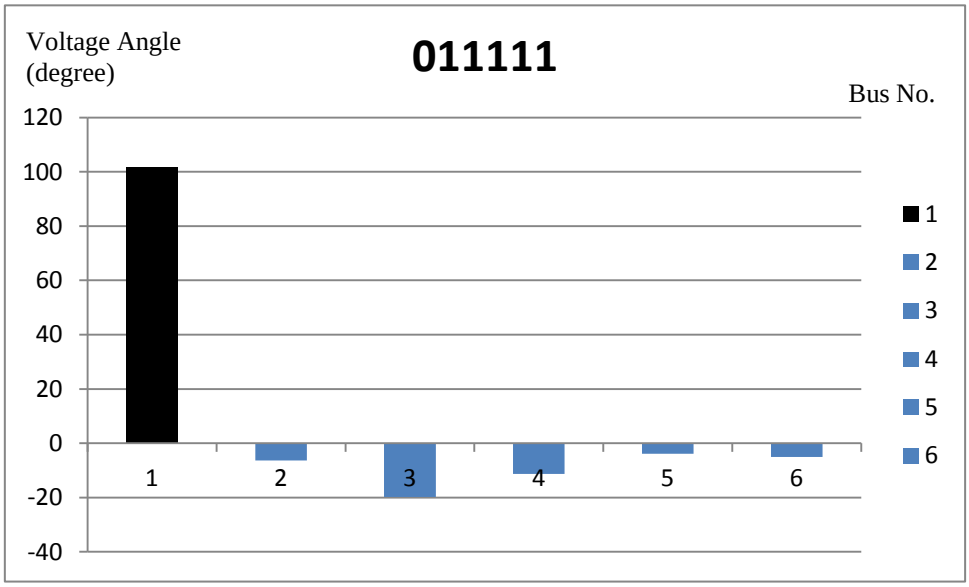

(b) Voltage Angles

Figure 5.16 LV PBE's Applied to V_1 (011111)

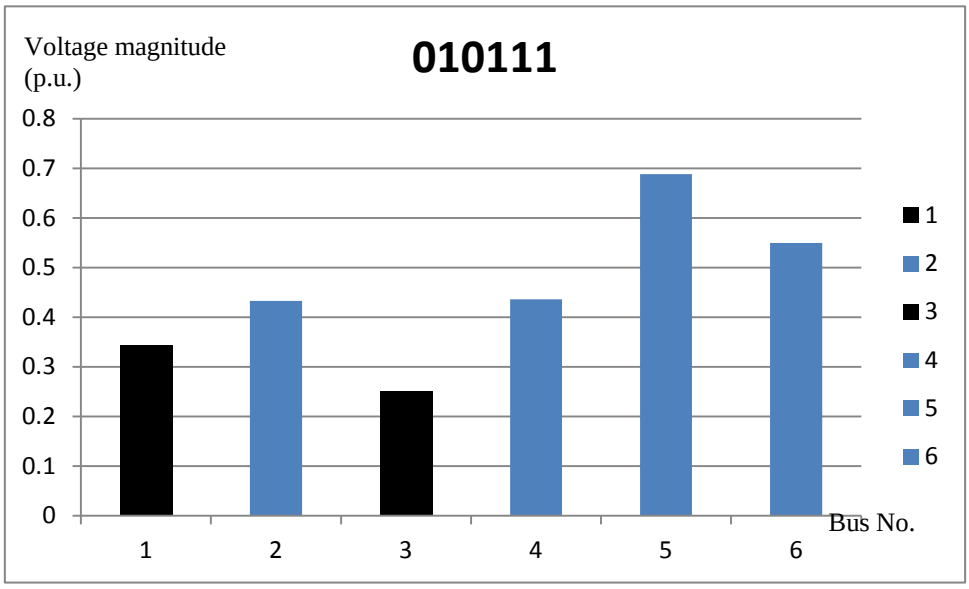

(a) Voltage Magnitudes

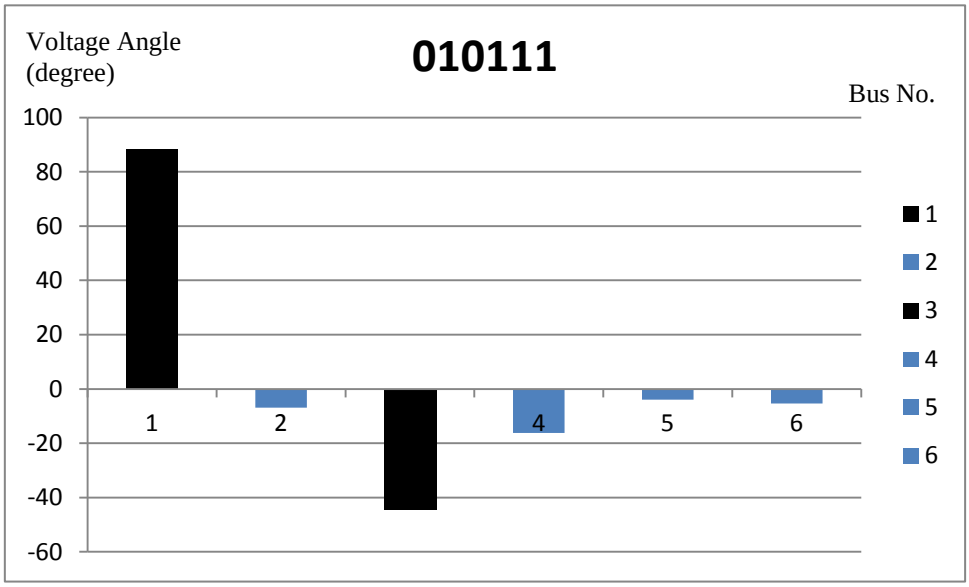

(a) Voltage Angles

Figure 5.17 LV PBE's Applied to V_1&V_3 (010111)

5.7.2 14-Bus System

After testing the five- and seven-bus systems as reported in Section 5.7.1, a more complex system, the IEEE standard 14-bus system, is tested using the proposed HE method. The topology of the 14-bus system is given in Figure 5.18, the system branch

parameters and bus data are given in per-unit in Table 5.10 and Table 5.11, respectively.. The PV buses in the system are modeled as PV buses with no Var constraints on them. The total number of solutions obtained for the 14-bus system is 90 and the solutions are given in Table 10.1. In Table 10.1, the voltage solution is split into voltage magnitude ($|V|$) and angle (θ).

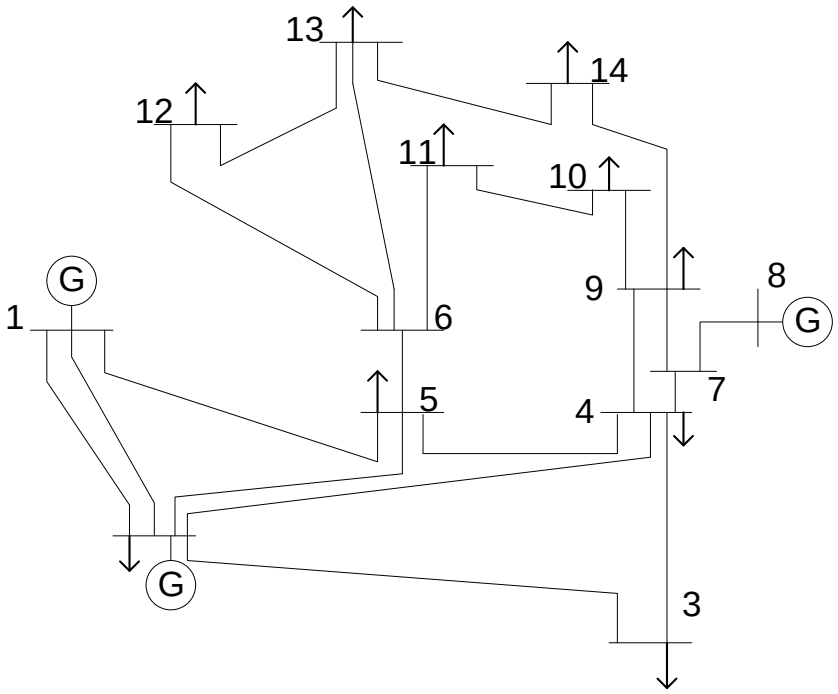

Figure 5.18 14-Bus System

Table 5.10 Branch Data for the 14-Bus System

Branch	**Line Impedance**	**Shunt (*y*)**
1-2	0.01938 + j0.05917	0.0528
1-5	0.05403 + j0.22304	0.0492
2-3	0.04699 + j0.19797	0.0438
2-4	0.05811 + j0.17632	0.034
2-5	0.05695 + j0.17388	0.0346
3-4	0.06701 + j0.17103	0.0128
4-5	0.01335 + j0.04211	0
4-7	j0.20912	0
4-9	j0.55618	0
5-6	j0.25202	0
6-11	0.09498 + j0.1989	0
6-12	0.12291 + j0.25581	0
6-13	0.06615 + j0.13028	0
7-8	j0.17615	0
7-9	j0.11001	0
9-10	0.03181 + j0.0845	0
9-14	0.12711 + j0.27038	0
10-11	0.08205 + j0.19207	0
12-13	0.22092 + j0.19988	0
13-14	0.17093 + j0.34802	0

Table 5.11 Bus Data for the 14-Bus System

Bus	Bus Type	V_{cntr}	P_{load}	Q_{load}	P_{gen}
1	3	1.06	0	0	*NA*
2	2	1.045	0.045	0.031	0.1
3	1	*NA*	0.036	0.022	0
4	1	*NA*	0.011	-0.009	0
5	1	*NA*	0.023	0.006	0
6	1	*NA*	0.024	0.017	0
7	1	*NA*	0.05	0.031	0
8	2	1.09	0.02	0.005	0
9	1	*NA*	0.052	0.036	0
10	1	*NA*	0.018	0.008	0
11	1	*NA*	0.011	0.003	0
12	1	*NA*	0.007	0.016	0
13	1	*NA*	0.012	0.009	0
14	1	*NA*	0.014	0.007	0

With the proposed method, a total of 90 solutions are found for the given IEEE standard 14-bus system under the lightly loaded condition and these solutions, generated for publications, are given in Table 10.1 in APPENDIX.A.

6 FINDING THE TYPE-1 POWER-FLOW SOLUTIONS USING THE PROPOSED HOLOMORPHIC EMBEDDING METHOD

As has been discussed in Chapter 5, of all the existing solutions, a total of 2^N solutions for the PF problem can be obtained by starting from 2^N unique germs, for a (N+1)-bus system, using the proposed HE method. For power system voltage/angle stability assessment, the type-1 PF solutions or the type-1 UEP's (where the system's Jacobian matrix has only one eigenvalue with a positive real-part) are of interest and in this section, the method of finding all the type-1 PF solutions/UPE's (out of 2^N possible solutions) using the HE method is proposed.

6.1 Type-1 PF Solutions

With the proof completed in Section 5 that a number of 2^N PF solutions can be obtained by the proposed HE method, the algorithm to find all the type-1 PF solutions, out of 2^N PF solutions, will be discussed in this section.

Theorem 2: A type-1 PF solution is found for each formulation in which one and only one bus PBE is included in its LV/large-angle form.

To prove Theorem 2 for a general power system (a (N+1)-bus power system), a two-step proof (broken into Lemma 4 and Lemma 5) will be needed.

Lemma 4: The germ, with only one bus substituted in the LV/large-angle formulation, is a type-1 PF solution at s=0 or in other words, a type-1 germ.

To complete the proof for Lemma 4, consider that the n^{th} bus, a PQ bus, in an (N+1)-bus power system is embedded with the proposed LV formulation, the embed-

ded PBE's for the system are given in (6.1) and (6.2) (derived from (5.23) and (5.24) by setting $J1=n$, $K1=\{N_{PQ}\backslash n\}$, $J2=N_{PV}$, $K2=\emptyset$), for PQ and PV buses, respectively. For convenience, the system given by (6.1) and (6.2) will be called as System A.

$$\begin{aligned}
&\sum_{j\neq n} jB_{ik}^{(tr)}V_j(s) = \\
&\frac{sS_i^*}{V_i^*(s^*)} + \frac{B_{in}^{(tr)}}{B_{in}^{(tr)*}}\frac{sS_n}{V_n^{(d)*}(s^*)} - s\sum_{k=0}^{N}(Y_{ik}^{(sh)} + G_{ik}^{(tr)})V_k(s)\ ,\ i\in\{N_{PQ}\setminus n\} \\
&\qquad jB_{nn}^{(tr)}V_i^{(d)}(s) + \sum_{j\neq n} jB_{nj}^{(tr)}V_j(s) = \\
&\qquad \frac{B_{nn}^{(tr)}}{B_{nn}^{(tr)*}}\frac{sS_n}{V_n^{(d)*}(s^*)} - s\sum_{k=0}^{N}(Y_{nk}^{(sh)} + G_{nk}^{(tr)})V_k(s)
\end{aligned} \tag{6.1}$$

$$\begin{aligned}
&\sum_{k=0}^{N} jB_{ik}^{(tr)}V_k(s) = \frac{sP_i - jQ_i(s)}{V_i^*(s^*)} - s\sum_{k=0}^{N} G_{ik}^{(tr)}V_k(s) - s\sum_{k=0}^{N} Y_{ik}^{(sh)}V_k(s) \\
&V_i(s)V_i^*(s^*) = 1 + s(\left|V_i^{cntr}\right|^2 - 1) \\
&V_i(0) = 1,\ i\in N_{PV}
\end{aligned} \tag{6.2}$$

At s=0, the PBE's in (6.1) and (6.2) represent a system with no load/real-power generation, given in (6.3) and (6.4), as given earlier. However this germ is valid for any system loading condition since s multiplies all system loads. .This is stated formally in Lemma 4.1.

$$\begin{aligned}
&\sum_{j\neq n} jB_{ik}^{(tr)}V_j(s) = 0\ ,\ i\in\{N_{PQ}\setminus n\} \\
&jB_{nn}^{(tr)}V_n^{(d)}(s) + \sum_{j\neq n} jB_{nj}^{(tr)}V_j(s) = 0
\end{aligned} \tag{6.3}$$

$$\begin{aligned}
&\sum_{k=0}^{N} jB_{ik}^{(tr)}V_k(s) = \frac{-jQ_i(s)}{V_i^*(s^*)} \\
&V_i(s)V_i^*(s^*) = 1 \\
&V_i(0) = 1,\ i\in N_{PV}
\end{aligned} \tag{6.4}$$

Lemma 4.1: The solution of (6.3) and (6.4), is the germ for any load pattern applied to the system characterized by (6.1) and (6.2).

Consider the same (N+1)-bus power system (defined by (6.5) and (6.6)) characterized by (6.1) and (6.2), but with a different load/real-power generation profile that is zero everywhere except on the n^{th} bus, where it is non-zero. For convenience, the system given by (6.5) and (6.6) will be called as System B.

$$\begin{aligned}
&\sum_{j\neq n} jB_{ik}^{(tr)}V_j(s) \\
&= \frac{sS_i^*}{V_i^*(s^*)} + \frac{B_{in}^{(tr)}}{B_{in}^{(tr)*}}\frac{sS_n}{V_n^{(d)*}(s^*)} - s\sum_{k=0}^{N}(Y_{ik}^{(sh)} + G_{ik}^{(tr)})V_k(s) \\
&\overset{S_i=0}{=} \frac{B_{in}^{(tr)}}{B_{in}^{(tr)*}}\frac{sS_n}{V_n^{(d)*}(s^*)} - s\sum_{k=0}^{N}(Y_{ik}^{(sh)} + G_{ik}^{(tr)})V_k(s),\ i \in \{N_{PQ} \setminus n\}
\end{aligned} \tag{6.5}$$

$$\begin{aligned}
&jB_{nn}^{(tr)}V_n^{(d)}(s) + \sum_{j\neq n} jB_{nj}^{(tr)}V_j(s) = \\
&\frac{B_{nn}^{(tr)}}{B_{nn}^{(tr)*}}\frac{sS_n}{V_n^{(d)*}(s^*)} - s\sum_{k=0}^{N}(Y_{ik}^{(sh)} + G_{ik}^{(tr)})V_k(s)
\end{aligned}$$

$$\begin{aligned}
&\sum_{k=0}^{N} jB_{ik}^{(tr)}V_k(s) = \frac{sP_i - jQ_i(s)}{V_i^*(s^*)} - s\sum_{k=0}^{N} G_{ik}^{(tr)}V_k(s) - s\sum_{k=0}^{N} Y_{ik}^{(sh)}V_k(s) \\
&\overset{P_i=0}{=} \frac{-jQ_i(s)}{V_i^*(s^*)} - s\sum_{k=0}^{N} G_{ik}^{(tr)}V_k(s) - s\sum_{k=0}^{N} Y_{ik}^{(sh)}V_k(s) \\
&V_i(s)V_i^*(s^*) = 1 + s(\left|V_i^{cntr}\right|^2 - 1) \\
&V_i(0) = 1,\ i \in N_{PV}
\end{aligned} \tag{6.6}$$

Since only bus n has a nonzero load, the s variable is a load scaling factor that affects only bus n for System A (unlike System B that that has many buses with non-zero loads.) Though the change in load data resulting from the change in the s parameter will be different in these two systems (System A and B), they have the same germ due to the unchanged system topology and branch data. Thus the proof of Lemma 4.1 is com-

pleted. Lemma 4.2 (given as follows) will be needed to further prove that the germ, with only bus *n* in the LV form, is a type-1 germ.

Lemma 4.2: The germ for the system, defined by (6.5) and (6.6), is a type-1 germ at s=0, using the theory developed in [70].

In [70], if only one load (on one bus) is scaled using the CPF-based method, the type-1 PF solution can be obtained by tracing the PV/Pδ curve, starting from a given HV solution. It is suggested in [70] that only one eigenvalue in the Jacobian matrix will have real-part whose sign changes as the CPF method pass the bifurcation point; thus the solutions obtained is a type-1 PF solution. Note that the HV solution of System A at the no-load condition is 1.0 per-unit for every bus in the system, which is by definition the germ. Starting from the HV solution at the no-load condition (or the HV germ), the CPF method can be used to trace the entire PV curve: Traditionally it starts by tracing the upper portion of the PV curve as the load on bus *n* increases, up to the bifurcation point, and traces the lower part of the PV curve "backward" as the load on bus *n* is scaled down to the no-load condition. Given in Figure 6.1 is the interpretation of the CPF method: it starts from the HV germ and traces the higher PV curve of bus *n* (shown as red in Figure 6.1), up to the bifurcation point (maximum loading point), while only the load at bus *n* is scaled up. After reaching the bifurcation point, the CPF method will trace the lower PV curve (shown as black in Figure 6.1), with only the load at bus *n* being scaled down. By the Ohm's law (given by (5.2) and repeated in (6.7)), at the

no-load condition, the lower PV curve of bus *n* has to start from 0.0 since it is the no-load condition (S_i=0 in (6.7)).

$$S_i = V_i I_i^* \tag{6.7}$$

Therefore the starting point of the lower PV curve is a type-1 solution guaranteed by the theory developed in [70], thus the corresponding LV germ is a type-1 germ. The proof for Lemma 4.2 is completed.

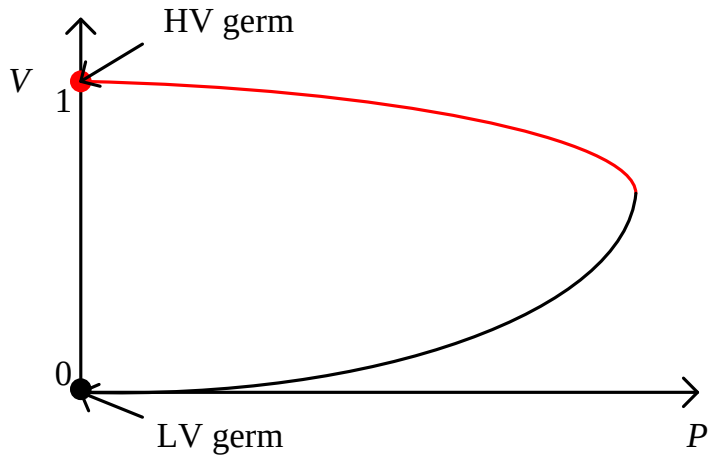

Figure 6.1 Germ Identification on a PV curve

It is shown that the germ, with only bus *n* substituted in the LV/large-angle form, is a type-1 germ for the system B, given by Lemma 4.2. As System A and B share the same LV germ given by Lemma 4.1, such LV germ (the type-1 germ for System B) is then a type-1 germ for System A, completing the proof for Lemma 4.

To prove that the PF solution corresponding to the type-1 germ is a type-1 solution, Lemma 5, must be proven.

Lemma 5: The sign of the eigenvalue in the Jacobian matrix will not change during the analytic continuation as s goes from 0.0 to 1.0, provided the base case solution exists.

It has been shown that *s* can be viewed not only as a embedding variable, but a load scaling factor that scales all loads/real-power generations in the system (given by (6.5) and (6.6)) as it goes from 0.0 to 1.0, during the analytic continuation. Therefore the analytic continuation can also be as a numerical continuation (i.e. CPF) with all the loads/real-power generations in the system scaled by *s*. By the theory given in [70], the eigenvalues of the Jacobian matrix will not change in sign unless the CPF method reaches a bifurcation point. The theory can be applied to the HE method since the analytic continuation can be viewed as a numerical continuation. Therefore it can be concluded that the eigenvalues in the Jacobian matrix for the germ (at s=0) and at the corresponding solution (at s=1), if it existing, will have the same sign. Thus the proof for Lemma 5 is completed.

Since it is proven in Lemma 4 that the germ is a type-1 germ with only one bus in the LV/large-angle form, the corresponding PF solution, if it exists, will be a type-1 PF solution, guaranteed by Lemma 5. This completes the proof for Theorem 2.

It has been theoretically proven in Chapter 5 that the proposed HE method is guaranteed to find all the PF solutions, if they exist in the PF problem, proven by Theorem 1. Therefore all the type-1 solutions are guaranteed to be found by the pro-

posed HE-based algorithm, providing a reliable algorithm to calculate all the type-1 PF solutions that exist in the power system, guaranteed by Theorem 2.

For the same 14-bus system used in Chapter 5, using the proposed algorithm, 12 type-1 solutions are obtained and it can be checked that these 12 solutions obtained in Appendix.A are all the type-1 solutions out of all the solutions obtained by the proposed HE-based method in Appendix.A. For a more generalized case, 36 type-1 solutions are obtained for the IEEE 118-bus system [88], given in Appendix.B. Numerical experiments indicate that when the proposed LV/large-angle formulation is applied to *n* buses ($n>1$), the solution obtained will usually be a type-*n* solution; while this is an empirical result, there exists cases where the above statement does not hold true.

6.2 The Closest Unstable Equilibrium Point

While the dynamic models included below are the uncomplicated classical models, the method of finding the type-1 UEP's and closest UEP using the HE-based method will be discussed as follows. For the system represented by the classical machine model and constant impedance load with purely reactance branch impedances, the dynamics of the i^{th} generator in an *n*-generator system can be expressed as:

$$\begin{aligned} \dot{\delta}_i &= \omega_i \\ m_i \dot{\omega}_i &= P_{mi} - d_i\omega_i - \sum_{j=1}^{n} V_i V_j B_{ij} \sin(\delta_i - \delta_j) \end{aligned} \tag{6.8}$$

where m_i is the inertia constant for generator i; d_i is the damping constant for generator i; P_{mi} is the constant mechanical power input for generator i; δ_i is the angle of internal voltage of the i^{th} generator; ω_i is the rotor angle velocity of the i^{th} generator with respect to the reference frequency. B_{ij} is the line susceptance between generator i and generator j.

The energy function (V_E) of (6.8) can be defined in terms of the machine angles and angular speed in (6.9):

$$V_E(\delta,\omega) = V_P(\delta) + V_K(\omega) \tag{6.9}$$

where $V_{\mathrm{P}}(\delta)$ and $V_{\mathrm{K}}(\omega)$ are the the potential energy and kinetic energy of a given state in the power system, respectively. The expression for $V_P(\delta)$ and $V_K(\omega)$ and are given by (6.10) and (6.11), respectively, for a power system bus system with N generators.

$$V_{\mathrm{P}}(\delta) = -\sum_{i=1}^{n} P_{mi}\delta_i - \sum_{i=1}^{n}\sum_{j=1}^{n} V_i V_j B_{ij} \cos(\delta_i - \delta_j) \tag{6.10}$$

$$V_{\mathrm{K}}(\omega) = \frac{1}{2}\sum_{i=1}^{n} m_i \omega_i^2 \tag{6.11}$$

To find the equilibrium condition, the derivative, with respect to time, in (6.8) is set to zero, leading to the formulation in (6.12).

$$P_{mi} - \sum_{j=1}^{n} V_i V_j B_{ij} \sin(\delta_i - \delta_j) = 0 \tag{6.12}$$

Note that the formulation in (6.12) is simply the real PBE, and it can be modeled in the complex form of the PBE and solved by the proposed HE method. Therefore all the type-1 solution(s) can be obtained using the proposed HE method in order to search for the closest UEP. Using the proposed HE method, a unique type-1 solution is obtained for each type-1 germ (unless the system is at the bifurcation point) without revisiting the same UEP for multiple times as happens with other methods. A simple three-machine system is represented by the equations given in (6.13), where the machine with index 3 is the reference machine/infinite bus which gives the reference angle at zero and the reference angular velocity.

$$\begin{aligned}
\dot{\delta}_1 &= \omega_2 \\
\dot{\omega}_1 &= 0.01 - 0.3\omega_1 - \sin(\delta_1) - 0.5\sin(\delta_1 - \delta_2) \\
\dot{\delta}_2 &= \omega_2 \\
\dot{\omega}_2 &= 0.05 - 0.3\omega_2 - 0.5\sin(\delta_2) - 0.5\sin(\delta_2 - \delta_1)
\end{aligned} \tag{6.13}$$

Note that at the equilibrium point, equation (6.13) will be reduced to (6.14) and the PBE's in (6.14) are expressed in the polar form of the voltage. It is easy to transfer the PBE's in (6.14) into the voltage rectangular form so that the HE method can be applied.

$$\begin{aligned}
\sin(\delta_1) + 0.5\sin(\delta_1 - \delta_2) &= 0.01 \\
0.5\sin(\delta_2) + 0.5\sin(\delta_2 - \delta_1) &= 0.05
\end{aligned} \tag{6.14}$$

The type-1 solutions obtained for the three-machine system using the proposed HE method are listed in Table 5.8. The results, given in Table 6.1, match those obtained in

[77] through four decimal places. By substituting the type-1 solutions into the energy function given in [77] (shown in (6.15)), solution 1 is determined to be the closest UEP in the system.

$$V_E(\delta_1,\delta_2) = -0.02\delta_1 - 0.1\delta_2 - 2\cos\delta_1 - \cos\delta_2 - \cos(\delta_1 - \delta_2) \tag{6.15}$$

Table 6.1 Type-1 Solutions for the Three-Machine System Using the HE Method

	Type-1 UEP's	
	1	**2**
δ_1 (deg.)	2.676	174.030
δ_2 (deg.)	174.030	19.143
Energy Function	-0.3133	0.3150

This three-machine system represented by (6.13) is found in the literature most frequently for validation purposes. Though the system tested for the closest UEP problem is small in size, the theory is rigorous for the HE method. The proposed HE method can be extended to find all the type-1 UEP's when the classical dynamic model is used, guaranteed by Theorem 2. After finding all the type-1 solutions, the closest UEP can be determined by evaluating the type-1 UEP with the lowest energy function value, a process that is highly parallelizable.

6.3 Conclusion

With the strategy of substituting one bus in its LV/large-angle form, the corresponding solution obtained, if it exists, is shown to be the type-1 PF solution, where the PF Jacobian has a single eigenvalue with a positive real part, among all the LV/large-angle solutions that can be possibly found by the proposed HE method. By

including an uncomplicated dynamic model for the generator and load (the classical generator model and constant impedance load), the system angle stability or transient stability margin can be evaluated using the proposed HE method by finding the closest unstable equilibrium point (UEP), which is a type-1 UEP's with the lowest value of the energy function among all the type-1 UEP's.

7 NUMERICAL PERFORMANCE OF THE HOLOMORPHIC EMBEDDING METHOD

While in theory the HE method is rigorous and guaranteed to find the solution if it exists, the limitation of the arithmetic precision affects its numerical performance as observed in different tests. In this chapter, the numerical performance of the proposed HE method will be discussed and analyzed.

7.1 Numerical Performance for Heavily Loaded System

With the idea of 'curving fitting' introduced in Chapter 3, it can be noticed that the proposed HE method will need more terms to get an accurate solution for a heavily loaded system compared to the system under lightly loaded condition. This is due to the fact that the characteristic curve (the PV curve) of the power system that the power series is trying to fit into, contains the higher order components when the system is heavily loaded, while the PV curve is more nearly linear when the system is light loaded. Given in Figure 7.1 is a conventional PV curve in a power system, the blue line indicates the system load value when it is lightly loaded and the black line indicates the load value when the system is near the voltage collapse. It can be observed that under lightly loaded conditions, the part of the PV curve (from no-load condition to the operating point) can be easily approximated by a polynomial with low order since the curve presented is almost linear. Therefore the number of terms needed for the voltage power series will be few in order to fit into the PV curve. However, at the heavily

loaded condition, the PV curve presented is more complicated and contains more higher-order components as it approaches the voltage collapse point or the saddle-node bifurcation point, leading to a higher-order polynomial/power series in the voltage function.

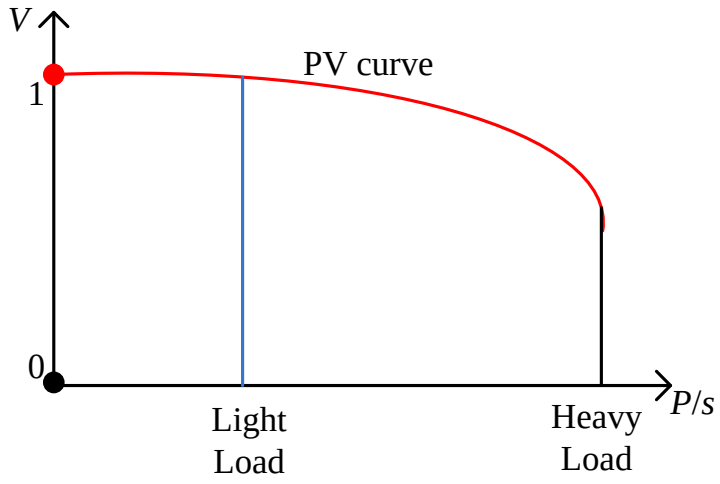

Figure 7.1 Conventional PV Curve at Different Loading Level

7.1.1 43-Bus System

An ill-conditioned 43-bus radial distribution system [6] is used to verify the numerical performance of the proposed HE method when the system is in its extremis. This system is reported as a very heavily loaded system where the traditional NR method fails to converge to the HV/operable PF solution. The system topology is given in Figure 7.2. Node 1 is the slack bus and nodes 2-43 are the PQ buses. The branch data and bus data are given in per-unit in Table 7.1 and Table 7.2, respectively.

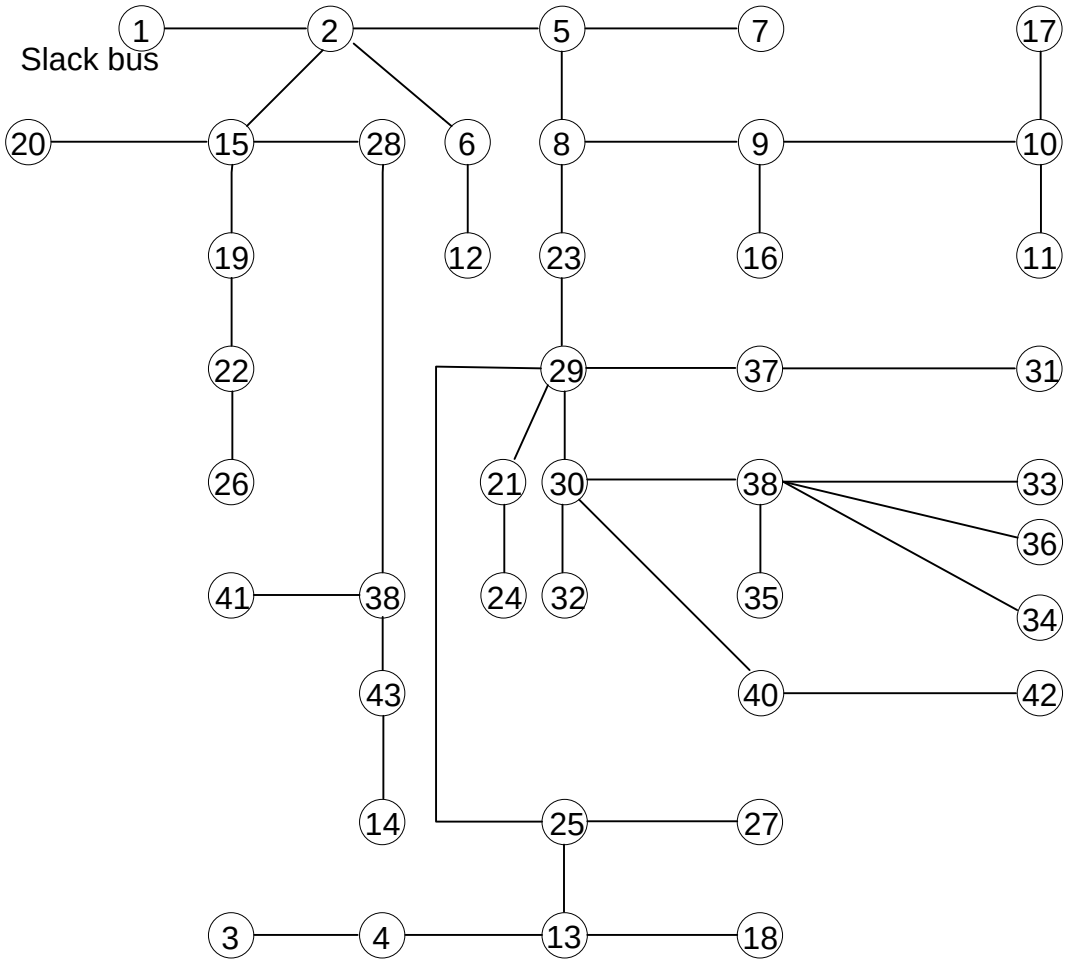

Figure 7.2 43-Bus System

Table 7.1 Non-zero *Y*matrix Entry Data for the 43-Bus System

Y(1,1)	0.0 -30.609i;	*Y*(19,19)	164.292 -280.783i;
Y(1,2)	0.0 +30.609i;	*Y*(19,22)	-164.292 +272.805i;
Y(2,2)	481.288 -1545.194i;	*Y*(20,20)	0.0 -15.002i;
Y(2,5)	-277.195 +873.583i;	*Y*(21,21)	104.312 -143.609i;
Y(2,6)	-34.368 +108.124i;	*Y*(21,24)	0.0 +9.267i;
Y(2,15)	-169.726 +534.322i;	*Y*(21,29)	-104.312 +133.623i;
Y(3,3)	0.0 -5.714i;	*Y*(22,22)	164.292 -282.281i;
Y(3,4)	0.0+ 6.015i;	*Y*(22,26)	0.0 +9.023i;
Y(4,4)	61.331 -69.160i;	*Y*(23,23)	321.579 -328.810i;
Y(4,13)	-61.331 +62.874i;	*Y*(23,29)	-157.677 +161.760i;
Y(5,5)	277.195 -916.892i;	*Y*(24,24)	0.0 -8.572i;
Y(5,7)	0.0 +21.277i;	*Y*(25,25)	87.150 -106.814i;
Y(5,8)	0.0 +20.513i;	*Y*(25,27)	0.0 +9.023i;
Y(6,6)	34.368 -118.699i;	*Y*(25,29)	-56.100 +65.824i;
Y(6,12)	0.0 +10.638i;	*Y*(26,26)	0.0 -8.572i;
Y(7,7)	0.0 -20.000i;	*Y*(27,27)	0.0 -8.572i;
Y(8,8)	452.840 -482.861i;	*Y*(28,28)	373.447 -612.837i;
Y(8,9)	-288.938 +295.777i;	*Y*(28,39)	-202.775 +256.136i;
Y(8,23)	-163.902 +167.191i;	*Y*(29,29)	318.089 -372.311i;
Y(9,9)	300.983 -317.044i;	*Y*(29,30)	0.0 +3.766i;
Y(9,10)	-12.045 +12.342i;	*Y*(29,37)	0.0 +7.895i;
Y(9,16)	0.0 +8.796i;	*Y*(30,30)	125.789 -524.464i;
Y(10,10)	12.045 -20.855i;	*Y*(30,32)	0.0 +30.769i;
Y(10,11)	0.0 +2.857i;	*Y*(30,38)	0.0 +4.131i;
Y(10,17)	0.0 +5.714i;	*Y*(30,40)	-125.789 +485.547i;
Y(11,11)	0.0 -2.857i;	*Y*(31,31)	0.0 -13.038i;
Y(12,12)	0.0 -10.000i;	*Y*(31,37)	0.0 +13.038i;
Y(13,13)	92.381 -100.709i;	*Y*(32,32)	0.0 -30.769i;
Y(13,18)	0.0 +6.015i;	*Y*(33,33)	0.0 -3.320i;
Y(13,25)	-31.050 +31.640i;	*Y*(33,38)	0.0 +3.320i;
Y(14,14)	0.0 -15.015i;	*Y*(34,34)	0.0 -7.365i;
Y(14,43)	0.0 +15.400i;	*Y*(34,38)	0.0 +6.852i;
Y(15,15)	340.398 -916.783i;	*Y*(35,35)	0.0 -6.180i;
Y(15,19)	0.0 +8.649i;	*Y*(35,38)	0.0 +6.180i;
Y(15,20)	0.0 +15.791i;	*Y*(36,36)	0.0 -2.703i;
Y(15,28)	-170.673 +357.003i;	*Y*(36,38)	0.0 +2.703i;
Y(16,16)	0.0 -8.576i;	*Y*(37,37)	0.0 -21.348i;
Y(17,17)	0.0 -5.714i;	*Y*(38,38)	0.0 -22.398i;
Y(18,18)	0.0 -5.714i;	*Y*(39,39)	512.581 -663.260i;

Y(39,41)	0.0 +15.015i;	*Y*(41,41)	0.0 -15.015i;
Y(39,43)	-309.806 +392.255i;	*Y*(42,42)	0.0 -20.000i;
Y(40,40)	125.789 -508.837i;	*Y*(43,43)	309.806 -408.029i;
Y(40,42)	0.0 +21.622i;		

Table 7.2 Bus Data for the 43-Bus System

Bus	V_{cntr}	P_{load}	Q_{load}	Bus	V_{cntr}	P_{load}	Q_{load}
1	1.06			23		0	0
2		0	0	24		0.64	0.48
3		0.16	0.12	25		0	0
4		0	0	26		0.8	0.6
5		0.53	0.4	27		0.32	0.24
6		0	0	28		0	0
7		1.6	1.2	29		0	0
8		0	0	30		0	0
9		0	0	31		-1.16	-0.52
10		0	0	32		-2.9	-0.257
11		0	0	33		-2.85	-0.3
12		0.8	0.6	34		0	0
13		0	0	35		-0.58	-0.56
14		0.8	0.6	36		0.005	0.03
15		0	0	37		0	0
16		0.64	0.48	38		1.44	1.02
17		0	0	39		0	0
18		0.24	0.18	40		0	0
19		0	0	41		0.8	0.3
20		0.88	0.66	42		2.24	1.68
21		0	0	43		0	0
22		0	0				

With the double precision arithmetic (programmed in Matlab), the proposed HE method is unable to reach the given PBE's mismatch (10^{-3}) in calculating the HV solution for the 43-bus system, with a maximum of 91 terms included in the power series. Plotted in Figure 7.3 is the maximum PBE's mismatch vs. the number of terms in the power series. It can be observed that the proposed HE method 'tends' to reach the mismatch tolerance but fails to 'converge' within the given mismatch tolerance.

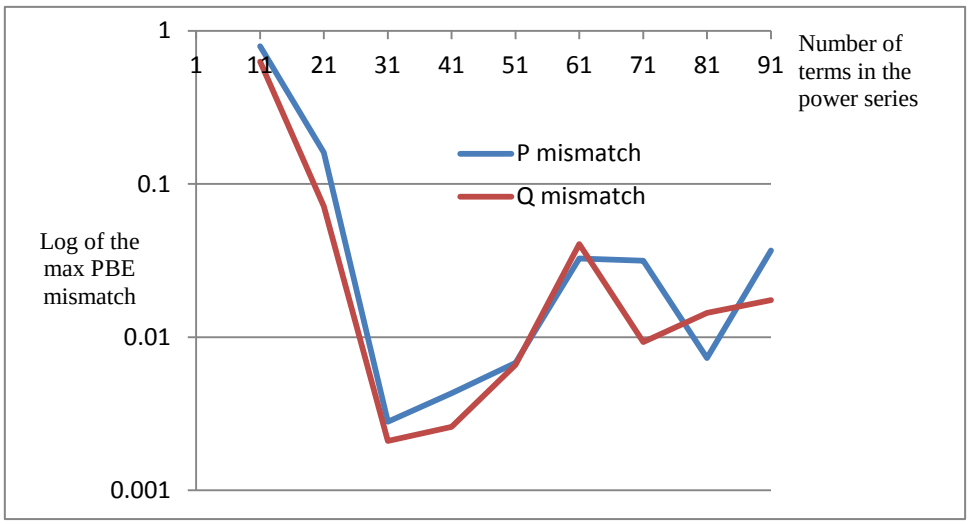

Figure 7.3 Maximum PBE's Mismatch vs. the Number of Terms in the Power Series

It is instructive to plot the condition number of the Padé coefficient matrix in the proposed HE method, as the condition number is a significant signal in determining whether precision issues occur in the matrix calculations. As a rule of thumb, if the condition number $\varkappa(C)=10^k$, then the arithmetic may lose up to k digits of accuracy due to loss of precision from LU factorization and forward/backward substitution when calculating the Padé' approximant. [89]. The maximum condition number of the Padé coefficient matrices for all buses for the voltage function is plotted in Figure 7.4 versus the number of terms included in the power series.

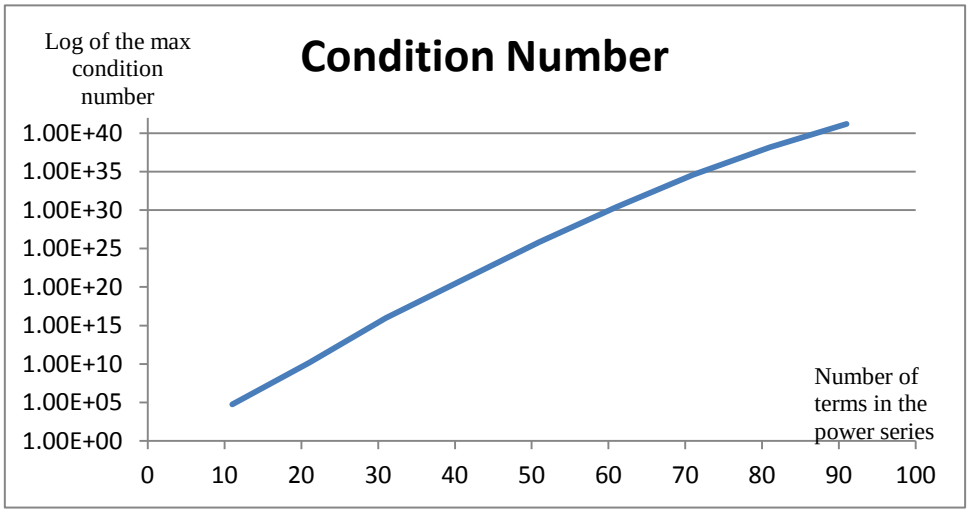

Figure 7.4 Maximum PBE's Mismatch vs. the Number of Terms in the Power Series

It can be observed that the maximum condition number of the Padématrix becomes as large as 10^{16} after 31 terms are included in the power series. Thus, in the process of calculation of the coefficients in the numerator/denominator polynomials of the Padé matrix, up to 16 digits of accuracy may be lost and it may exhaust the numerical precision of the Matlab program (double precision.)

In evaluating the rounding error in calculating the denominator polynomial of the Padéapproximant, the obtained coefficients are substituted back into the matrix form of the equations. For example, assume the matrix form of the equations are in the form of $Cb=c$ (given in (3.34) and repeated in (7.1)).

$$\begin{bmatrix} c[L-M+1] & c[L-M+2] & c[L-M+3] & \cdots & c[L] \\ c[L-M+2] & c[L-M+3] & c[L-M+4] & \cdots & c[L+1] \\ c[L-M+3] & c[L-M+4] & c[L-M+5] & \cdots & c[L+2] \\ \vdots & \vdots & \vdots & \ddots & \vdots \\ c[L] & c[L+1] & c[L+2] & \cdots & c[L-M] \end{bmatrix} \begin{bmatrix} b[M] \\ b[M-1] \\ b[M-2] \\ \vdots \\ b[1] \end{bmatrix} = -\begin{bmatrix} c[L+1] \\ c[L+2] \\ c[L+3] \\ \vdots \\ c[L+M] \end{bmatrix} \tag{7.1}$$

where C is the Padématrix on the LHS of (7.1), c is the known coefficients of the power series terms given by the vector on the RHS of (7.1) and b is the unknown coefficients of the denominator of the Padéapproximant.

The errors are calculated by $C\bar{b}$-c by substituting the calculated b values, named $\bar{b}$, into (7.1). Both the absolute value of the error and the relative percentage of the error are calculated by $|C\bar{b}-c|$ and $|C\bar{b}-c|/|c|$. The maximum value of the absolute value (in

blue) and relative value of the error (in red) are plotted in Figure 7.5 versus the number of terms included in the power series.

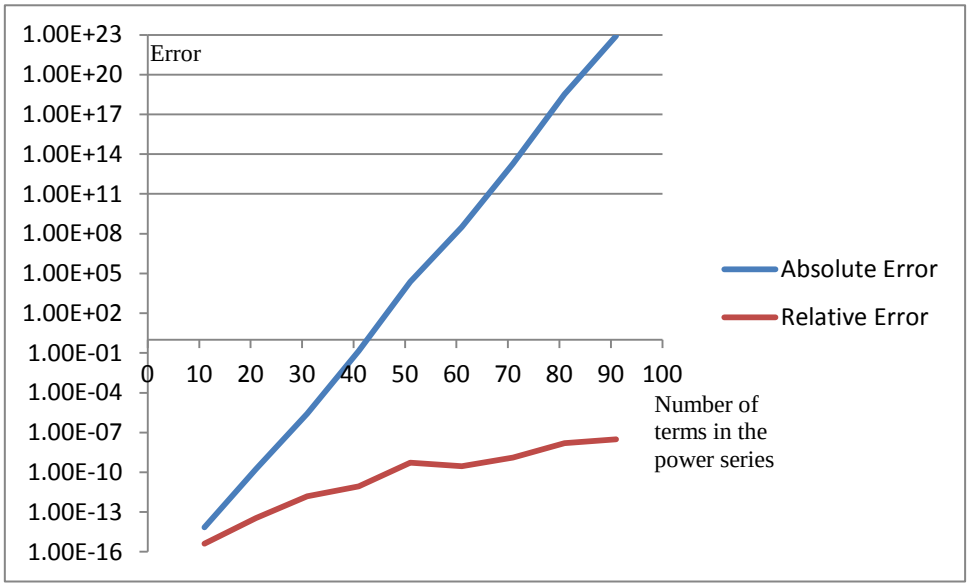

Figure 7.5 Maximum Absolute/Relative Error in *Cb-c* vs. the Number of Terms in the Power Series

7.1.2 Multi-Precision Complex (MPC) Application

Since the HV solution cannot be obtained by the Matlab program with 16 digits of arithmetic accuracy, arbitrary-precision arithmetic was used to provide adequate precision for the proposed HE method to check if an accurate solution can be obtained. There exist various software packages as well as libraries supporting arbitrary-precision real arithmetic: Maxima, Maple, Mathematica, etc. The arbitrary-precision arithmetic library used in current research is called Multi-Precision Complex (MPC). This library was selected since it supported complex arithmetic. This library is a dynamic library developed by the GNU Company [90] for performing arithmetic operations on complex numbers with arbitrarily high precision. In order to build the MPC library, Multiple Precision Floating-Point Reliably (MPFR) and

GNU Multiple Precision (GMP) libraries are needed. These libraries can be installed on most Unix-like systems. The libraries were installed on a computer running on a Windows OS with Cygwin which is a Unix-like environment in for Windows OS.

The proposed HE method is programmed in C language with the extended precision library to find the HV solution for the same 43-bus system, given in 7.1.1. The C program developed uses 200 bits precision (56 digits in the mantissa) rather than 64 bits precision (16 digits in the mantissa) in Matlab program. The proposed HE method reaches the mismatch tolerance (10^{-3}) with 37 terms in the power series and the solution obtained is given in Table 7.3. The solution obtained matches with the solution given by [10] though 3 decimal places, but with a smaller mismatch in the PBE's than that given by [10]. (The maximum PBE mismatch calculated is $5*10^{-3}$ from the solution provided in [10]).

Table 7.3 HV Solution for the 43-Bus System

Bus	*V*	Bus	*V*
1	1.1360	23	1.0839-j2.4225e-1
2	1.0704-j2.0129e-1	24	1.1018-j3.1164e-1
3	1.0985-j2.8089e-1	25	1.0762-j2.4548e-1
4	1.0664-j2.4847e-1	26	1.0192-j3.6497e-1
5	1.0677-j2.0317e-1	27	1.1008-j2.8404e-1
6	1.0687-j2.0774e-1	28	1.0628-j2.0734e-1
7	1.0650-j2.7307e-1	29	1.0834-j2.4243e-1
8	1.0840-j2.4152e-1	30	1.1289-j2.3378e-1
9	1.0825-j2.4163e-1	31	1.1256-j2.9826e-2
10	1.0845-j2.4477e-1	32	1.2073-j1.6654e-1
11	1.0845-j2.4477e-1	33	1.2205-j3.1090e-1
12	1.0658-j2.7755e-1	34	1.0551-j3.3422e-1
13	1.0682-j2.4819e-1	35	1.2219-j3.0431e-1
14	1.0346-j2.5361e-1	36	1.1425-j3.6351e-1
15	1.0659-j2.0498e-1	37	1.0881-j1.0787e-1
16	1.0415-j2.9972e-1	38	1.1341-j3.5924e-1
17	1.0845-j2.4477e-1	39	1.0578-j2.0855e-1
18	1.0878-j2.9010e-1	40	1.1243-j2.3583e-1
19	1.0567-j2.9015e-1	41	1.0274-j2.5293e-1
20	1.0706-j2.5817e-1	42	1.1194-j3.2696e-1
21	1.0791-j2.4254e-1	43	1.0559-j2.0862e-1
22	1.0537-j2.9033e-1		

In order to further investigate where the severe loss of precision occurs, different bits of precision are assigned during different steps in the proposed algorithm. There exist multiple places in the proposed HE method where round-off errors may accumulate:

1) Calculation of the LU factors of the *Y* matrix.

In (5.23) and (5.24) (repeated in (7.2) and (7.3)), the LU factors of the *Y* matrix (or the imaginary part of the *Y* matrix) has to be calculated while calculating the voltage power series coefficients. Though it is unlikely that the LU factorization of the *Y* matrix

can be of significance in the precision issues for a small system (i.e. 43-bus system), it may accumulate round-off when the system size becomes large.

$$\begin{aligned}
&\sum_{j\in\{J1+0\}} jB_{ik}^{(tr)}V_j(s) = \\
&\frac{sS_i^*}{V_i^*(s^*)} + \sum_{j\in K1}\frac{B_{ij}^{(tr)}}{B_{ij}^{(tr)*}}\frac{sS_j}{V_j^{(d)*}(s^*)} - s\sum_{k=0}^{N}(Y_{ik}^{(sh)} + G_{ik}^{(tr)})V_k(s)\ ,\ i\in J1 \\
&jB_{ii}^{(tr)}V_i^{(d)}(s) + \sum_{j\in\{J1+0\}} jB_{ij}^{(tr)}V_j(s) = \\
&\frac{B_{ii}^{(tr)}}{B_{ii}^{(tr)*}}\frac{sS_i}{V_i^{(d)*}(s^*)} + \sum_{j\in K1}\frac{B_{ij}^{(tr)}}{B_{ij}^{(tr)*}}\frac{sS_j}{V_j^{(d)*}(s^*)} - s\sum_{k=0}^{N}(Y_{ik}^{(sh)} + G_{ik}^{(tr)})V_k(s)\ ,\ i\in K1
\end{aligned} \tag{7.2}$$

$$\begin{aligned}
&\sum_{k=0}^{N} jB_{ik}^{(tr)}V_k(s) = \frac{sP_i - jQ_i(s)}{V_i^*(s^*)} - s\sum_{k=0}^{N}G_{ik}^{(tr)}V_k(s) - s\sum_{k=0}^{N}Y_{ik}^{(sh)}V_k(s) \\
&V_i(s)V_i^*(s^*) = 1 + s(\left|V_i^{cntr}\right|^2 - 1) \\
&V_i(0) = -1,\ i\in K2 \\
&V_i(0) = 1,\ i\in\{N_{PV}\setminus K2\}
\end{aligned} \tag{7.3}$$

2) Calculating the convolution of two power series

In (7.2) and (7.3), multiple convolutions exist in the procedure of calculating the power series coefficients. I.e., for the term $\frac{sS_i^*}{V_i^*(s^*)}$ in (7.2), the inverse of the voltage function has to be calculated using the convolution of two power series. For the term $V_i(s)V_i^*(s^*)$ in (7.3), the convolution occurs in the voltage magnitude constraint for the PV bus. Also, the convolution appears in the reactive power function divided by the voltage function ($\frac{-jQ_i(s)}{V_i^*(s^*)}$ in (7.3)) for the PV bus. When the nested convolutions occur in the process of obtaining the power series coefficients, roundoff error may accumulate within the procedure.

3) Calculating the numerator/denominator polynomial terms for the Padé ap-

proximant.

It has been observed in the 43-bus system, the condition number of the Padématrix increases dramatically with the increasing number of terms included in the power series. Precision lost due to the large condition number of the Padé approximant may exhaust the precision in the arithmetic.

The first 31 power series coefficients obtained, using 200 bits (56 digits) and 300 bits (86 digits) in the arithmetic using the C program, are compared against with the power series coefficients obtained from Matlab with 64 bits (16 digits), and the results are given in Table 7.4. In Table 7.4, Matlab64B/16D stands for the double precision arithmetic (in Matlab) with 64 bits/16 digits precision. MPC200B/56D stands for the extended precision arithmetic with 200 bits/56 digits precision and MPC300B/86D stands for the extended precision arithmetic with 300 bits/86 digits precision. It can be observed that the power series coefficients obtained from the Matlab program matches as few as 10 digits when compared with power-series coefficients obtained using the 56 digits extended precision MPC code. Also, the power series coefficients obtained from the Matlab program matches as few as 10 digits when compared with power-series coefficients obtained using the 86 digits extended precision MPC code. Therefore, during the process of calculating the power series coefficients, around five digits of precision are lost and 10 digits of precision can be preserved.

Table 7.4 Number of Matched-up Digits with Different Precision for the Power Series Coefficients (Worst Case)

Power Series (31 terms)	Matlab64B/16D	MPC200B/56D	MPC300B/86D
Matlab64B/16D	X	10	10
MPC200B/56D	X	X	56
MPC300B/86D	X	X	X

Further, the [15/15] Padé approximant obtained, using 200 bits (56 digits) and 300 bits (86 digits) in the arithmetic, are compared against the power series coefficients obtained from Matlab with 64 bits (16 digits), and the results are given in Table 7.5. It can be observed that the Padé approximant obtained, with 56 digits of extended precision, only matches up to at least 3 digits with the power series coefficients obtained from the Matlab program, which indicates severe loss of precision in the procedure of calculating the Padé approximant. The Padé approximant calculated with 200 bits arithmetic precision matches up to at least 49 digits when compared with the Padé approximant calculated with 300 bits precision, indicating that the precision loss occurs in calculating the Padé approximant even with 200 bits included in the computation.

Table 7.5 Number of Matched-up Digits with Different Precision for the Padé Approximant (Worst Case)

Padé([15/15])	Matlab64B/16D	MPC200B/56D	MPC300B/86D
Matlab64B/16D	X	3	3
MPC200B/56D	X	X	49
MPC300B/86D	X	X	X

The 43-bus system, in 7.1.1, is a problematic system with heavy loading, large R/X ratio branches and is a radial system. While it is uncertain if all those aspects might affect the numerical performance of the proposed HE method, it will now be shown, using the IEEE-30 bus system [91], that operation near the bifurcation point will cause severe precision issue for the proposed HE method. For the sake of validation, the load

in the IEEE-30 bus system is scaled by a factor of 2.81 to bring the system near the voltage collapse point. The Matlab program (with 64 bits precision) cannot find the HV solution within the given mismatch tolerance (10^{-3}), while the C program with extended precision (200 bits) can find the solution with 73 terms included in the power series. The number of terms needed to get the accurate HV solution using 200 bits of precision is plotted, as given in Figure 7.6, vs. the loading condition for the 30-bus system, and it can be observed that as the load increases, the number of terms needed in the power series increases.

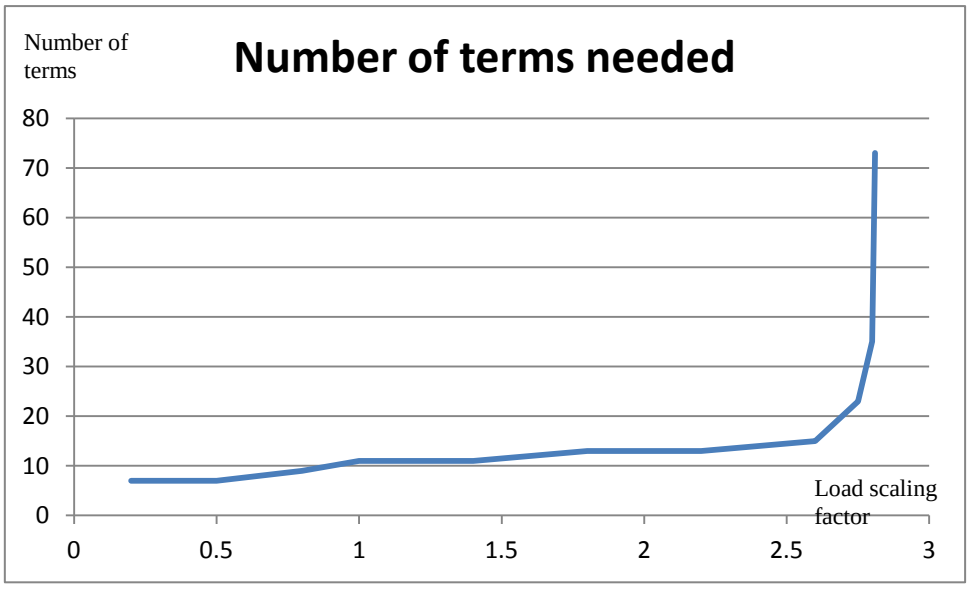

Figure 7.6 Number of Terms needed in the Power Series vs. Load using 200 bits of precision

To validate that the severe precision loss occurs in calculating the Padé approximant when the system is heavy loaded, the power series coefficients and the Padé approximant obtained for the 30-bus system under different loading conditions, using 200 bits (56 digits) and 300 bits (86 digits) representations using the C program, are compared against with the results obtained from Matlab with 64 bits (16 digits). The results

for the 30-bus system under normal condition (with scaling factor of 1.0) are given in Table 7.6 and Table 7.7 for power series coefficients and Padé approximant, respectively. The results for the 30-bus system under heavily loaded condition (with scaling factor of 2.81) are given in Table 7.8 and Table 7.9.

Table 7.6 Number of Matching Digits with Different Precision for the Power Series Coefficients (Worst Case) for Normal Loading

Power Series (31 terms)	Matlab64B/16D	MPC200B/56D	MPC300B/86D
Matlab64B/16D	X	14	14
MPC200B/56D	X	X	56
MPC300B/86D	X	X	X

Table 7.7 Number of Matching Digits with Different Precision for the Padé Approximant (Worst Case) for Normal Loading

Padé([15/15])	Matlab64B/16D	MPC200B/56D	MPC300B/86D
Matlab64B/16D	X	10	10
MPC200B/56D	X	X	56
MPC300B/86D	X	X	X

Table 7.8 Number of Matching Digits with Different Precision for the Power Series Coefficients (Worst Case) for Heavy Loading

Power Series (31 terms)	Matlab64B/16D	MPC200B/56D	MPC300B/86D
Matlab64B/16D	X	10	10
MPC200B/56D	X	X	56
MPC300B/86D	X	X	X

Table 7.9 Number of Matching Digits with Different Precision for the Padé Approximant (Worst Case) for Heavy Loading

Padé([15/15])	Matlab64B/16D	MPC200B/56D	MPC300B/86D
Matlab64B/16D	X	3	3
MPC200B/56D	X	X	46
MPC300B/86D	X	X	X

7.2 Precision Issue for the LV Solution of the 43-bus System

While the precision issues in finding the HV PF solution of the 43-bus system, using the proposed HE method, can be resolved by using extended precision arithmetic, the numerical issue for the LV solution of the 43-bus system is different and will be discussed in this section.

For a conventional lower part of the PV curve, the voltage magnitude goes up monotonically as the load increases (as shown in Figure 6.1). However, the curve presented in the 43-bus system behaves differently, as shown in Figure 7.7, when all the loads in the system are scaled up (the PV curve of bus 42 is generated by PSAT [92] where λ is the load scaling parameter used in the CPF method.)

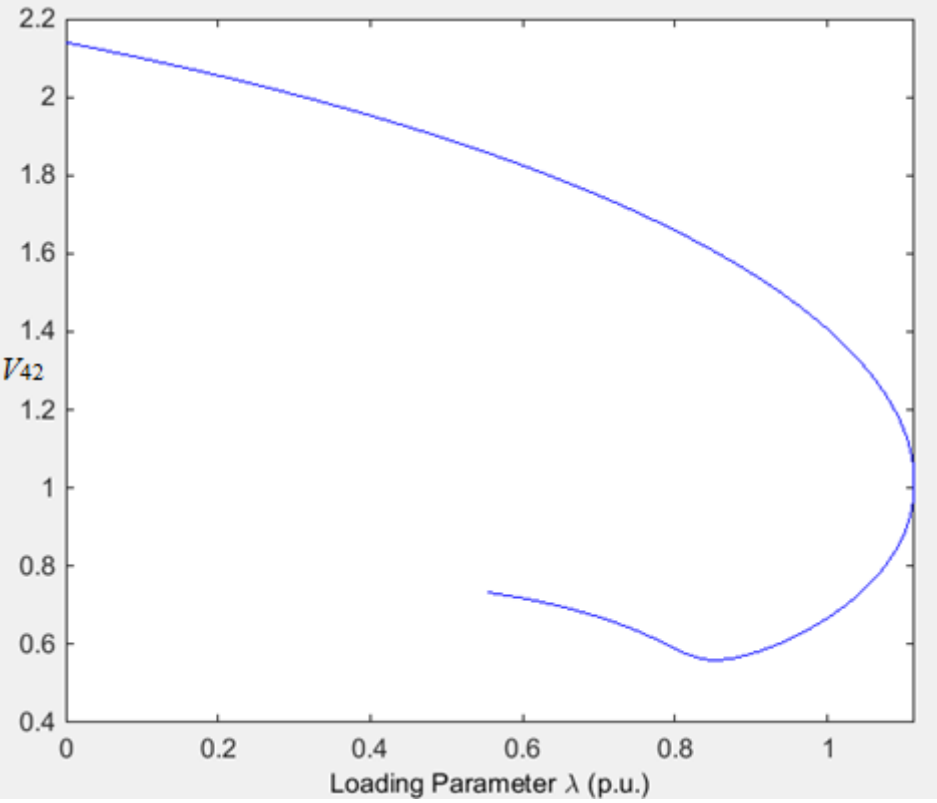

Figure 7.7 The PV curve for Bus 42 obtained using PSAT

It can be observed that the lower PV curve first goes down when the load increases and it reaches to a 'minimum', then it turns up after the 'minimum' point. The numerical tests conducted show that the proposed LV/large-angle PBE's have precision issues in convergence right before the 'minimum' point and no LV solution can be found after that 'turning point' even with the higher precision and adequate number of terms, i.e. including 56 digits precision and 99 terms in the power series. With the discussion of curve fitting and numerical tests given in Section 7.1 that the proposed HE method suffers precision issue near the voltage collapse point, it is likely that the HE method will suffer the numerical issue at the 'minimum' point of the lower PV curve, shown in Figure 7.7.

One way of overcoming the precision issue at the local minima on the PV curve is to use a process similar to the continuation-power-flow method: the load in the system is scaled by a small increment and the solution from the previous loading condition is used as the new germ for the next loading level. While the current form of the proposed HE method does not allow the algorithm to start from the previous solution, modifications can be made by adding an extra term on the RHS of the embedded PBE's to realize it, as given in (7.4) to (7.6).

$$\sum_{k=0}^{N} Y_{ik} V_k(s) = \frac{sS_i^*}{V_i^*(s^*)} + (1-s)\sum_{k=0}^{N} Y_{ik} V_k^{Last}, \; i \in N_{PQ} \tag{7.4}$$

$$\sum_{k=0}^{N} Y_{ik} V_k(s) = \frac{sP_i - jQ_i(s)}{V_i^*(s^*)} + (1-s)\sum_{k=0}^{N} Y_{ik} V_k^{Last} \ , \ i \in N_{PV} \qquad (7.5)$$

$$V_i(s)V_i^*(s^*) = \left|V_i^{Last}\right|^2 + s(\left|V_i^{cntr}\right|^2 - \left|V_i^{Last}\right|^2)$$

$$V_0(s) = 1 + s(V_{SLACK} - 1) \qquad (7.6)$$

where V_i^{Last} is the solution obtained from the last loading level.

The proposed LV/large-angle PBE's, given by (7.2) and (7.3), will be needed in calculating the first voltage solution at the first loading level which is one step away from the zero load condition. Once the solution at the first loading level is obtained, one can use the proposed HE method in (7.4) to (7.6) to calculate the next solution without the necessity of introducing the dual voltage in (7.2) and (7.3). The procedure to calculate the power series coefficients is straightforward and has been discussed in Chapter 3.

With the CPF-based computation process applied to the HE formulations, one LV solution for the 43-bus system can be obtained by substituting bus 37 in its LV form, using a PBE's mismatch tolerance of 10^{-3}. The obtained LV solution is listed in Table 7.10.

Table 7.10 LV Solution for the 43-Bus System

Bus	*V*	Bus	*V*
1	1.1360	23	1.0111 -j2.3476e-1
2	1.0346 -j2.0153e-1	24	1.0150 -j3.0396e-1
3	1.0160 -j2.7097e-1	25	1.0010 -j2.3541e-1
4	9.8998e-1 -j2.3786e-1	26	9.6550e-1 -j3.6733e-1
5	1.0311 -j2.0307e-1	27	1.0188 -j2.7503e-1
6	1.0323 -j2.0792e-1	28	1.0264 -j2.0758e-1
7	1.0226 -j2.7433e-1	29	1.0091 -j2.3272e-1
8	1.0127 -j2.3621e-1	30	9.3614e-1 -j1.9618e-1
9	1.0110 -j2.3625e-1	31	1.0568 -j5.3029e-3
10	1.0128 -j2.3920e-1	32	1.0266 -j1.1446e-1
11	1.0128 -j2.3920e-1	33	9.9023e-1 -j2.7848e-1
12	1.0238 -j2.7906e-1	34	8.2156e-1 -j3.1170e-1
13	9.9197e-1 -j2.3765e-1	35	9.9208e-1 -j2.7012e-1
14	9.9480e-1-j2.5475e-1	36	8.9322e-1 -j3.4099e-1
15	1.0297 -j2.0522e-1	37	1.0186 -j8.9303e-2
16	9.6190e-1 -j2.9676e-1	38	8.8307e-1 -j3.3504e-1
17	1.0128 -j2.3920e-1	39	1.0212 -j2.0874e-1
18	1.0043 -j2.8083e-1	40	9.3019e-1 -j1.9845e-1
19	1.0111 -j2.9152e-1	41	9.8927e-1 -j2.5439e-1
20	1.0302 -j2.5944e-1	42	8.8149e-1 -j2.9944e-1
21	1.0044 -j2.3274e-1	43	1.0192 -j2.0879e-1
22	1.0079 -j2.9164e-1		

7.3 Large Systems

While the system tested by the HE method is small in size, a sparsity-based program is being developed by our research group in order to simulate the large-scaled systems. The Electric Reliability Council of Texas (ERCOT) power system with more than 6000 buses (a total of 6057 buses without islanding) has been simulated by the proposed HE method without considering discrete controls (i.e. no remote regulation, no bus-type switching) in the system to validate the algorithm. The maximum voltage magnitude difference between the solution obtained by the proposed HE method and the solution

obtained from PowerWorld is $2.56*10^{-4}$ and the maximum angle difference is 0.71 degree, which numerically verifies that the proposed HE method can find the HV solution for a large scaled power system. The first 100 buses' voltage magnitudes (in p.u.) and angles (in degrees) are given in Table 7.11.

Table 7.11 HV Solution for ERCOT System from HE Method and PowerWorld

Bus Number	Mag. (HE)	Mag. (Power World)	Abs. Mag. Error	Angle (HE)	Angle (Power World)	Abs. Angle Error
1	1.03711	1.03717	5.94E-05	27.06	26.64	0.42
2	1.03637	1.03644	6.98E-05	27.09	26.67	0.42
3	1.03472	1.03479	6.63E-05	26.81	26.38	0.43
4	1.03112	1.03118	6.46E-05	26.35	25.92	0.43
5	1.03589	1.03595	6.37E-05	26.99	26.57	0.42
6	1.03240	1.03247	6.78E-05	26.34	25.91	0.43
7	1.03212	1.03218	6.19E-05	26.31	25.89	0.42
8	1.02461	1.02468	6.64E-05	25.76	25.31	0.45
9	1.00299	1.00308	8.56E-05	22.40	21.93	0.47
10	1.01745	1.0176	1.49E-04	25.94	25.44	0.50
11	1.01883	1.0189	7.23E-05	25.70	25.23	0.47
12	1.01774	1.01789	1.50E-04	25.80	25.3	0.50
13	1.01763	1.01777	1.38E-04	25.34	24.85	0.49
14	1.00335	1.00345	1.00E-04	22.54	22.06	0.48
15	1.01865	1.01873	8.09E-05	25.69	25.22	0.47
16	1.00457	1.00465	7.87E-05	22.77	22.31	0.46
17	1.01669	1.0167	1.32E-05	26.42	25.97	0.45
18	1.00415	1.00424	9.07E-05	20.80	20.33	0.47
19	1.00626	1.00627	6.42E-06	22.72	22.25	0.47
20	1.01055	1.01056	1.03E-05	24.28	23.83	0.45
21	1.01942	1.01949	6.82E-05	25.54	25.08	0.46
22	1.01009	1.01017	7.81E-05	23.01	22.55	0.46
23	1.00290	1.00299	9.29E-05	21.77	21.3	0.47
24	1.00372	1.00381	9.17E-05	20.82	20.35	0.47
25	1.00160	1.0017	1.01E-04	20.95	20.47	0.48
26	1.00957	1.00981	2.42E-04	28.58	27.99	0.59
27	1.00149	1.0016	1.12E-04	19.58	19.09	0.49
28	1.00714	1.0072	6.46E-05	18.99	18.48	0.51

29	0.99707	0.99718	1.09E-04	19.04	18.54	0.50
30	0.95049	0.95074	2.50E-04	24.53	23.91	0.62
31	0.99408	0.99419	1.06E-04	18.84	18.35	0.49
32	0.99536	0.99545	8.85E-05	18.67	18.18	0.49
33	1.00502	1.00509	6.63E-05	17.96	17.48	0.48
34	1.01330	1.01331	1.50E-05	24.55	24.09	0.46
35	1.00281	1.00288	6.71E-05	17.77	17.29	0.48
36	1.00909	1.00913	4.29E-05	19.84	19.35	0.49
37	1.00551	1.00556	5.43E-05	18.53	18.05	0.48
38	1.00759	1.00768	8.83E-05	19.52	19.05	0.47
39	1.01272	1.01276	4.47E-05	20.11	19.62	0.49
40	1.00654	1.00658	4.16E-05	16.32	15.83	0.49
41	0.99879	0.99883	4.18E-05	15.88	15.4	0.48
42	1.01114	1.01115	8.85E-06	24.06	23.6	0.46
43	1.00834	1.00838	3.65E-05	13.98	13.5	0.48
44	0.99094	0.99106	1.22E-04	18.93	18.44	0.49
45	1.01725	1.01735	1.04E-04	16.91	16.38	0.53
46	1.01230	1.01238	8.44E-05	15.72	15.2	0.52
47	1.00524	1.00543	1.90E-04	31.53	30.86	0.67
48	1.00951	1.00961	9.67E-05	17.50	16.98	0.52
49	1.01416	1.01426	1.00E-04	16.82	16.3	0.52
50	1.00630	1.00653	2.29E-04	30.28	29.64	0.64
51	1.00018	1.00027	9.17E-05	17.93	17.41	0.52
52	1.01636	1.01646	9.69E-05	16.79	16.26	0.53
53	1.01700	1.01709	9.21E-05	16.88	16.35	0.53
54	1.00181	1.00192	1.13E-04	18.91	18.38	0.53
55	1.02181	1.02192	1.14E-04	17.15	16.63	0.52
56	1.00457	1.0048	2.25E-04	29.73	29.09	0.64
57	1.00985	1.00999	1.36E-04	21.25	20.72	0.53
58	1.01385	1.01395	1.05E-04	19.31	18.79	0.52
59	1.00492	1.00504	1.24E-04	19.86	19.33	0.53
60	1.02326	1.02338	1.18E-04	17.78	17.25	0.53
61	1.00841	1.0085	9.36E-05	18.90	18.38	0.52
62	1.00876	1.00885	8.99E-05	19.01	18.5	0.51
63	1.00481	1.00492	1.11E-04	19.22	18.7	0.52
64	1.02725	1.02725	4.69E-06	14.50	14.03	0.47
65	1.00624	1.00634	1.01E-04	19.09	18.57	0.52
66	1.01037	1.01046	8.82E-05	11.45	10.95	0.50
67	1.01086	1.01095	9.21E-05	12.00	11.5	0.50
68	1.00199	1.00209	9.96E-05	17.46	16.96	0.50
69	0.95610	0.95624	1.43E-04	15.22	14.71	0.51

70	1.01033	1.01042	8.52E-05	11.34	10.84	0.50
71	1.01496	1.01505	8.79E-05	11.05	10.54	0.51
72	1.00169	1.00175	5.89E-05	10.34	9.85	0.49
73	1.00027	1.00032	5.19E-05	10.37	9.88	0.49
74	1.01382	1.01389	7.19E-05	18.97	18.47	0.50
75	1.01566	1.01573	6.55E-05	19.01	18.5	0.51
76	1.01440	1.01446	6.26E-05	18.87	18.36	0.51
77	1.00186	1.00195	8.64E-05	17.24	16.74	0.50
78	1.01716	1.01722	5.91E-05	19.08	18.58	0.50
79	1.02159	1.02164	4.54E-05	19.35	18.85	0.50
80	1.02355	1.02359	3.72E-05	19.57	19.07	0.50
81	1.03152	1.03154	2.45E-05	20.50	20.01	0.49
82	0.99811	0.99818	7.39E-05	18.43	17.94	0.49
83	1.00913	1.00915	2.19E-05	10.69	10.21	0.48
84	1.00932	1.00934	2.12E-05	10.55	10.07	0.48
85	1.03171	1.0317	6.15E-06	13.93	13.47	0.46
86	1.00698	1.00699	1.30E-05	9.33	8.86	0.47
87	1.01013	1.01015	1.84E-05	10.25	9.77	0.48
88	0.97928	0.9793	1.97E-05	22.68	22.23	0.45
89	1.01178	1.01178	2.31E-06	18.87	18.41	0.46
90	1.01868	1.0187	2.02E-05	23.85	23.4	0.45
91	1.00438	1.0044	1.60E-05	9.87	9.39	0.48
92	1.02250	1.0225	1.08E-06	13.96	13.49	0.47
93	1.00457	1.00458	9.48E-06	9.91	9.44	0.47
94	1.01655	1.01655	3.73E-06	10.47	10	0.47
95	1.00210	1.00212	2.09E-05	8.78	8.31	0.47
96	0.95749	0.95749	1.23E-06	13.45	12.99	0.46
97	0.99543	0.99544	1.35E-05	21.63	21.18	0.45
98	1.02604	1.02604	4.97E-06	15.60	15.14	0.46
99	1.00256	1.00258	1.66E-05	8.98	8.51	0.47
100	1.02246	1.02247	5.14E-06	15.91	15.44	0.47

The voltage magnitude/angle error between the solution obtained from the proposed HE method and the solution obtained from PowerWorld, for each bus in the ERCOT system, are plotted in Figure 7.8 and Figure 7.9, respectively.

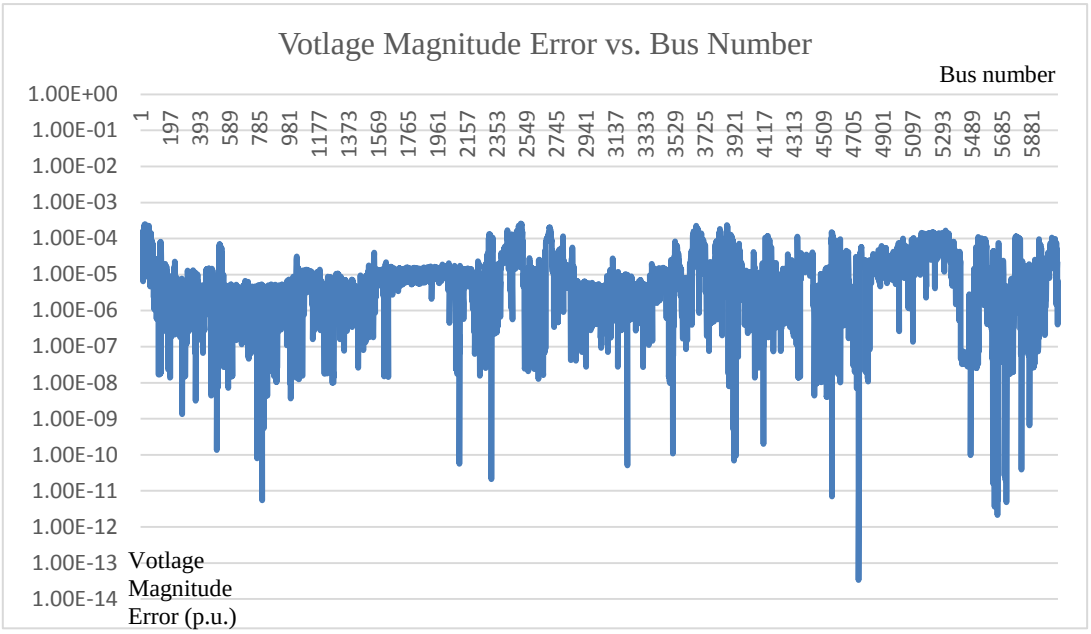

Figure 7.8 The Magnitude Error in the ERCOT system vs. Bus Number

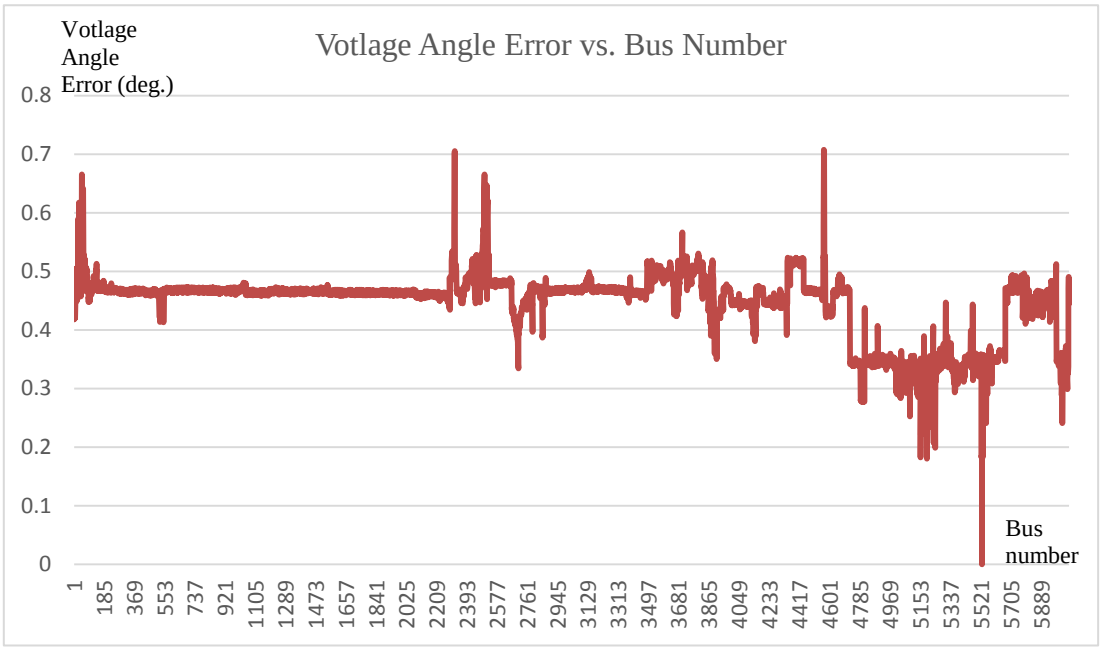

Figure 7.9 The Angle Error in the ERCOT system vs. Bus Number

7.4 Conclusion

The numerical performance of the proposed HE method has been tested on an ill-conditioned power system (i.e. 43-bus system, load scaled 30-bus system) operat-

ing near the voltage collapse point, showing that extended precision may be needed as the system approaches to the voltage collapse point or the bifurcation point. The special case of the 43-bus bus system is tested to validate the numerical performance of the proposed LV/large-angle formulation and a continuation-power-flow-liked process is proposed in order to overcome the precision issue in obtaining the LV solution of the 43-bus system. To validate the numerical performance of the HE method on a large power system, the ERCOT system, with more than 6000 buses, has been tested. The HE numerical results compared with results obtained from the commercial software (i.e. PowerWorld) shows that the HE method is capable of finding the HV PF solution when the system size is large in scale.

8 CONCLUSION

8.1 Summary

The HE method was introduced for solving the PF problem by using an HE formulation which relied on expanding the voltage as a power series in the embedding parameter, *s*. The primary advantage of the method was that it was guaranteed to converge to the HV solution for the PF problem and would signal if no solution existed.

By reformulating the PBE for a PQ bus, a PBE LV HE formulation for the two-bus system was mathematically proven to converge to only the LV solution, if the solution exists. The generalized formulation for the multi-bus system was derived and numerical experiments showed that all LV/large-angle solutions for the five- and seven-bus systems could be found and matched with the LV solutions found by other algorithms. It was observed that if one bus PBE was represented using the LV HE formulation, the voltage solution obtained (if it converged) for that specific bus would have a relatively lower voltage magnitude and larger phase angle for the system tested than the HV solution obtained for the same bus.

The proposed HE method is further developed to find only the type-1 PF solutions (where the PF Jacobian has a single eigenvalue with a positive real part), among all the LV/large-angle solutions. By including a proper dynamic model for the generator and load, the system angle stability or transient stability margin can be evaluated by

finding the closest unstable equilibrium point (UEP), which is a type-1 UEP's with the lowest value of the energy function among all the type-1 UEP's.

The numerical performance of the proposed HE method has been investigated by the system operating near the voltage collapse (i.e. 43-bus system, load scaled 30-bus system), showing that extended precision may be needed as the system approaches to the voltage collapse point or the bifurcation point. The numerical issues in finding the LV solution of the 43-bus system are tackled by a continuation-power-flow-liked process applied to the proposed HE method and it can be applied to other case where precision is a problem. To validate the numerical performance of the HE method on large power system, the ERCOT system, with more than 6000 buses, has been tested. The numerical results shows that the HE method is capable of finding the HV PF solution when the system size is large in scale, by comparing the result obtained from the commercial software (i.e. PowerWorld.)

REFERENCES

[1] J. B. Ward and H. W. Hale, “Digital computer solution of power-flow problems,” Power Apparatus and Systems, Part Ⅲ, Transactions of the American Institute of Electrical Engineers, vol. 75, no.3, pp. 398-404, Jan. 1956.

[2] W. Tinney and C. Hart, “Power flow solution by Newton’s method,” IEEE Trans. Power App. Syst., vol. PAS-86, no. 11, pp. 1449-1460, Nov. 1967.

[3] W. Tinney and J. Walker, “Direct solution of sparse network equations by optimally ordered triangular factorization,” Proc. IEEE, vol. 55, no.11, pp.1801-1809, Nov. 1967.

[4] B. Stott and O. Alsac, “Fast decoupled load flow,” IEEE Trans Power App. Syst., vol. PAS-93, no. 3, pp. 859-869, May 1974.

[5] B. Stott, “Decoupled Newton load flow,” IEEE Trans. Power App. Syst., vol. PAS-91, no. 5, pp. 1955-1959, 1972.

[6] S. C. Tripathy, G. D. Prasad, O. P. Malik, G. S. Hope, “Load-Flow Solutions for Ill-Conditioned Power Systems by a Newton-Like Method”, IEEE Trans. Power App. Syst., pp. 3648-3657, Oct 1982.

[7] B. Stott, “Effective Starting Process for Newton-Raphson Load Flows,” IEEE Trans. Power App Proc. Inst. Elect. Eng., pp. 983-987, Nov 1971.

[8] G. W. Stagg and A. G. Phadke, “Real-time evaluation of power system contingencies-detection of steady state overloads,” IEEE Summer Power Meet., Paper 70 CP 692-PWR., July 1970.

[9] R. Klump and T. Overbye, “Techniques for improving power flow convergence,” in Power Engineering Society Summer Meeting, 2000. IEEE, vol. 1, 2000, pp. 598-603.

[10] S. Iwamoto and T. Tamura, “A load flow method for ill-conditioned power systems,” IEEE Transactions on Power Apparatus and Systems, vol. PAS-100, pp. 1736-1743, Apr. 1981.

[11] M. D. Schaffer and D. J. Tylavsky, “A nondiverging polar-form Newton-based power flow,” IEEE Transactions on Industry Applications, vol. 24, No.5 ,pp. 870-877, Oct. 1988.

[12] D.J. Tylavsky, P.E. Crouch, L.F. Jarriel, and R. Adapa, "Improved Power Flow Robustness for Personal Computers," IEEE Trans. on Industry Applications, Vol. 28, No. 5, (High voltage/Oct 1993), pp. 1219-1225.

[13] D.J. Tylavsky, P.E. Crouch, L.F. Jarriel, and H. Chen, "Advances in Fast Power Flow Algorithms," in Advances in Theory and Applications, Control and Dynamics, Volume 42, Part 4 of 4, pp. 295-344, Academic Press, 1991.

[14] P. Crouch, D. Tylavsky, L. Jarriel, H. Chen, "Critically Coupled Algorithms for Solving the Power Flow Equation," PICA Conf. Record, pp. 141-148, Baltimore Md., March, 1991, and IEEE Trans. of Power Systems , Vol. 7, No. 1, (Feb. 1992), pp. 451-457.

[15] D.J. Tylavsky, P.E. Crouch, L.F. Jarriel, J. Singh, and R. Adapa, "The Effects of Precision and Small Impedance Branches on Power Flow Robustness," IEEE/PES Winter Meeting, New York, February, 1992, IEEE Trans. on Power Systems, Vol. 9, No. 1, (Feb 1994), pp. 6-14.

[16] M. D. Schaffer, D. J. Tylavsky, "A Polar Form Newton-Based Power Flow with Convergence Control, Proc. IASTED 1988 International Symposium, High Technology in the Power Industry, (Mar. 1982), pp. 143-147

[17] D. J. Tylavsky and M. D. Schaffer, "Non-Diverging Power Flow Using a Least-Power Type Theorem," IEEE Trans. on Industry Applications, (High voltage./Oct. 1987), pp. 944-951.

[18] J. Thorp and S. Naqavi, “Load-flow fractals draw clues to erratic behavior,” IEEE Comput. Appl. Power, vol. 10, no. 1, pp. 59-62, Jan 1997.

[19] F. Wu, “Theoretical study of the convergence of the fast decoupled load flow,” IEEE Trans. Power App. Syst., vol. 96, no. 1, pp. 268-275, Jan. 1977.

[20] H. Chiang, Direct Methods for Stability Analysis of Electric Power Systems: Theoretical Foundation, BCU Methodologies and Applications, Wiley IEEE Press, 2011.

[21] J. Hubbard, D. Schleicher, and S. Sutherland, “How to find all roots of complex polynomials by Newton’s method,” Inventiones Mathematicae, vol. 146, pp. 1-33, 2001.

[22] R. Klump and T. Overbye, “A new method for finding low-voltage power flow solutions,” in Power Engineering Society Summer Meeting, 2000. IEEE, vol. 1, 2000, pp. 593-597.

[23] Notes on “Functions of a complex variable,” Andrew.C.Yang Available: http://www.math.dartmouth.edu/~m43s12/

[24] Trias, “The Holomorphic Embedding Load Flow Method,” IEEE PES General Meeting, San Diego, CA, July 2012, paper #PESGM2012-000484.

[25] Trias, “Two Bus Model Detail,” Available: http://www.gridquant.com/assets/two-bus-model-detail.pdf

[26] Trias, “System and method for monitoring and managing electrical power transmission and distribution networks,” US Patents 7 519 506 and 7 979 239, 2009-2011.

[27] B. Stott, “Review of Load-Flow Calculation Methods,” Proceeding of IEEE, vol. 62, pp. 916-929, June 1974.

[28] R. Bijwe and S.M. Kelapure. “Nondivergent fast power flow methods,” Power Systems, IEEE Transactions on, pp.633-638, may 2003.

[29] L.M.C. Braz, C.A. Castro, and C.A.F. Murati. “A critical evaluation of step size optimization based load flow methods,” Power Systems, IEEE Transactions on, vol. 15, pp.:202-207, feb 2000.

[30] J. Scudder and F.L. Alvarado. “Step Size Optimization in a Polar Newton Power Flow,” University of Wisconsin, Engineering Experiment Station, 1981.

[31] R.A.M. van Amerongen, "A General-Purpose Version of the Fast Decoupled Load Flow", *IEEE PES Summer Meeting*, 1988.

[32] D. Rajicic and A. Bose, "A Modification to the Fast Decoupled Power Flow for Network with High R/X Ratios", *Proceedings of PICA Conference*, pp.360 -363 1987.

[33] F. F. Wu, "Theoretical Study of the Convergence of the Fast Decoupled Loadflow", *IEEE Transactions PAS*, vol. 96, pp.268 -275 1977.

[34] J. L. Carpentier, "CRIC: A New Active Reactive Decoupling Process in Load Flows, Optimal power Flows and System Control", *IFAC Symposium on Power Systems and Power Plant Control*, 1986.

[35] Y. Wallach, ‘Gradient methods for load flow-problems,” IEEE Trans. Power App. Syst., vol. PAS-87, pp. 1314-1318, May 1968.

[36] A. M. Sasson, “Nonlinear programming solutions for the load-flow, minimum-loss, and economic dispatching problems,” IEEE Trans. Power App. Syst., vol. PAS-88, pp. 399-409, Apr. 1969.

[37] A. M. Sasson, C. Trevino, and F. Aboytes, “Improved Newton’s load flow through a minimization technique,” IEEE PICA Conf., 1971.

[38] Y. P. Dusonchet, S. N. Talukdar, H. E. Sinnott, and A. H. El-Abiad, “Load flows using a combination of point Jacobi and Newton’s methods,” IEEE Trans. Power

App. Syst., vol. PAS-90, pp. 941-949, May/June 1971.

[39] R. H. Galloway, J. Taylor, W. D. Hogg, and M. Scott, “New approach to power-system load-flow analysis in a digital computer,” Proc. Inst. Elec. Eng., vol. 117, pp. 165-169, Jan. 1970.

[40] P. M. Sauer, “Explicit load flow series and function,” IEEE Trans. Power Systems, vol. PAS-100, pp. 3754-3763, 1981.

[41] W. Xu, Y. Liu, J. C. Salmon, T. Le, G. W. K. Chang, “Series load flow: A novel non-iterative load flow method,” IEEE Proceeding Generation, Transmission and Distribution, vol. 145, pp. 251-256, 2002.

[42] B. Sturmfels, “Solving systems of polynomial equations,” Regional conference series in Mathematics. AMS, 2002.

[43] F. Milano, “Continuous Newton’s Method for Power Flow Analysis,” IEEE Trans. Power Systems, v. 24, no. 1, pp. 50-57, Feb 2009.

[44] V. Ajjarapu and C. Christy, 'The continuation power flow: A tool for steady state voltage stability analysis," IEEE Trans. Power Syst., vol. 7, no. I, pp. 416--423, Feb. 1992.

[45] R. J. Avalos, C. A. Cafiizares, F. Milano, and A. Conejo, ""Equivalency of Continuation and Optimization Methods to Determine Saddle-node and Limit-induced Bifurcations in Power Systems," IEEE Trans. Power Syst., vol. 56, no. I, pp. 210-223, Jan. 2009.

[46] A. Z. de Souza, C. A Cafiizares, and V. H. Quintana, "New Techniques to Speed Up Voltage Collapse Computations Using Tangent Vectors," ," IEEE Trans. Power Syst., vol. 12, pp, 1380-1387., August 1997.

[47] Shao-Hua Li and Hsiao-Dong Chiang, "Continuation Power Flow With Nonlinear Power Injection Variations: A Piecewise Linear Approximation," IEEE Trans. Power Syst., Vol. 23, no. 4, Nov. 2008.

[48] Dobson, “Observations on the geometry of saddle node bifurcation and voltage collapse in electrical power systems,” IEEE Tran. Circuits Syst. I, vol. 39, no. 3, pp. 240-243, Mar 1992.

[49] C. Cañizares, “On bifurcations, voltage collapse and load modeling,” IEEE Trans. Power Syst., vol. 10, no. 1, pp. 512-522, Feb. 1995.

[50] W. Ma and S. Thorp, “An efficient algorithm to locate all the load flow solutions,” IEEE Trans. Power Syst., vol. 8, no. 3, pp. 1077–1083, Aug. 1993.

[51] D. K. Molzahn, B. C. Lesieutre and H. Chen, “Counterexample to a Continuation-Based Algorithm for Finding All Power Flow Solutions,” IEEE Transactions on Power Systems, vol. 28, pp. 564-565, Feb. 2013.

[52] S.N. Chow, J. Mallet-Paret and J.A. Yorke, “Finding zeros of maps: homotopy methods that are constructive with probability one,” Math. Comp. (32), pp. 887-899, 1978.

[53] S.N. Chow, J. Mallet-Paret and J.A. Yorke, “A homotopy method for locating all zeros of a system of polynomials,” Functional Differential Equations and Approximation of Fixed Points, H.-0. Peitgen and H.O. Walther, eds. Springer-Verlag Lecture Notes in Math. 730, PP.77-88, 1979.

[54] D. Mehta, H. D. Nguyen, K. Turitsyn, “Numerical Polynomial Homotopy Continuation Method to Locate All The Power Flow Solutions,” IEEE Tran. on Power Systems, August 2014.

[55] B. Buchberger, “Groebner Bases: A Short Introduction for Systems Theorists,” Computer Aided Systems Theory - EUROCAST 2001, pp. 1-19.

[56] J. Ning, W. Gao, G. Radman, and J. Liu, “The application of the Groebner basis technique in power flow study,” in North American Power Symposium (NAPS), 2009, oct. 2009, pp. 1-7.

[57] P.W. Sauer and M.A. Pai, “Power system steady-state stability and the load-flow Jacobian,” IEEE Trans. on Power Sys**.,** vol. 5, pp**.** 1374-1383, NOV. 1990.

[58] H. D. Chiang, I. Dobson, R. J. Thomas, J. S. Thorp, and F.-A. Lazhar, “On voltage collapse in electric power systems,” *IEEE Trans. Power Syst.*, vol. 5, no. 2, pp. 601–611, May 1990.

[59] I. Dobson and H. Chiang, "Towards a Theory of Voltage Collapse in Electric Power Systems", Systems & Control Letters, pp.253 -262 1989.

[60] Y. Tamura, H. Mori, and S. Iwamoto, “Relationship between voltage instability and multiple load flow solutions in electric power systems,” *IEEE Trans. on Power App. and Sys.,*vol. PAS-102, pp. 1115-1123, May 1983.

[61] Y. Tamura, H. Mori and S. Iwamoto, “Voltage instability proximity index (VIPI) based on multiple load flow solutions in ill-conditioned power systems,” *Proc. 27th Con$ Decision and Control,* Austin, TX, Dec. 1988.

[62] N. Yorino, S. Harada, H. Sasaki and M. Kitagawa, “Use of multiple load flow solutions to approximate closest loadability limit,” Bulk Power System Voltage Phenomena III Conference, Davos, Switzerland, Aug. 1994.

[63] Y. Tamura , K. Iba and S. Iwamoto "A method for finding multiple load flow solutions for general power systems", *IEEE PES Winter Meeting*, 1980

[64] K. Iba, H. Suzuki, M. Egawa, and T. Watanabe, "A method for finding a pair of multiple load flow solutions in bulk power systems," IEEE Trans. on Power Sys., vol. PWRS-5, pp. 582-591, May 1990.

[65] T.J. Overbye and C.L. DeMarco, "Improved techniques for power system voltage stability assessment using energy methods," IEEE Trans. on Power Sys., vol. PWRS-6, pp. 1446- 1452, Nov. 1991.

[66] A. Tiranuchit and R.J. Thomas, "A posturing strategy against voltage instabilities in electrical power systems," IEEE Tram. on Power Sys., vol. 3, pp. 87-93, Feb. 1988.

[67] T.J. Overbye, "Effects of load modeling on analysis of power system voltage stability," to appear, International Journal of Electric Power and Energy Systems.

[68] J. S. Thorp and S. A. Naqavi, "Load flow fractals", *Proc. 28th Circuits Devices Conf.*, pp.1822 -1827 1989

[69] J. J. Deng, H. D. Chiang, "Convergence Region of Newton Iterative Power Flow Method: Numerical Studies," Journal of Applied Mathematics, Volume 2013, Article ID 509496, 2013

[70] C. W. Liu, C. S. Chang, J. A. Jiang, and G. H. Yeh, "Toward a CPFLOW-based algorithm to compute all the type-1 load-flow solutions in electric power systems," IEEE Trans. Circuits Syst. I: Reg. Papers, vol. 52, no. 3, pp. 625–630, Mar. 2005.

[71] M. A. Pai, *Energy Function Analysis for Power System Stability.*, 1989: Kluwer

[72] H. D. Chiang, *Direct Methods for Stability Analysis of Electric Power Systems: Theoretical Foundation, BCU Methodologies, and Applications,* 2011: Wiley-IEEE Press

[73] H. D. Chiang and J. S. Thorp, "Stability regions of nonlinear dynamical systems: a constructive methodology", *IEEE Trans. Automat. Contr.*, vol. 34, pp.1229 -1241 1989

[74] A. H. El-Abiad and K. Nagappan, "Transient stability region of multi-machine power system", *IEEE Trans. Power App. Syst.*, vol. PAS-85, pp.169 -178 1966

[75] M. Ribben-Pavella and F. J. Evans, "Direct methods for studying dynamics of large scale power systems&mdash,A survey", *Automatica*, vol. 32, pp.1 -21 1985

[76] H.-D. Chiang and J. S. Thorp, "The closest unstable equilibrium point method for power system dynamic security assessment", *IEEE Trans. Circuits Syst*, vol. 36, pp.1187-1199, 1989

[77] C.-W. Liu and S. Thorp, "A novel method to compute the closest unstable equilibrium point for transient stability region estimate in power systems," *IEEE Trans. Circuits Syst. I*, vol. 44, no. 7, pp.630 -635, 1997

[78] J. Lee and H.-D. Chiang, "A singular fixed-point homotopy method to locate the closest unstable equilibrium point for transient stability region estimate", *IEEE Trans. Circuits Syst. II*, vol. 51, no. 4, pp.185 -189, 2004

[79] D. Mehta, H. D. Nguyen, K. Turitsyn, "Numerical Polynomial Homotopy Continuation Method to Locate All The Power Flow Solutions," IEEE Tran. on Power Systems, August 2014

[80] Klos, A., and J. Wojcicka. "Physical aspects of the nonuniqueness of load flow solutions."International Journal of Electrical Power & Energy Systems 13.5 (1991): 268-276.

[81] B.M Weedy, Electric Power Systems (3rd edition), John Wiley & Sons Ltd, Winterstoke Road, Bristol, BS, 1979.

[82] Bulthell, "Division Algorithms for Continued Fractions and the Pade Table," J. Comp. Appl. Math. No. 6, 1980.

[83] H. Stahl, "Extremal domains associated with an analytic function I, II," Complex Variables, Theory and Application: An International Journal, vol. 4, no. 4, pp. 311-324, 325-338, 1985.

[84] H. Stahl, "On the convergence of generalized Padé approximants," Constructive Approximation, vol. 5, pp. 221–240, 1989.

[85] H. Stahl, "The convergence of Padé approximants to functions with branch points," Journal of Approximation Theory, vol. 91, no. 2, pp. 139–204, 1997.

[86] "Analytic Continuation," available at: http://en.wikipedia.org/wiki/Analytic_continuation#Formal_definition_of_a_germ

[87] M. K. Subramanian, "Application of Holomorphic Embedding to the Power-Flow Problem," July 2014, Master Thesis, School of Electrical, Computer and Energy Engineering, Arizona State University, pp. 50-67.

[88] R. Christie, "IEEE 118-Bus Power Flow Test Case," May 1993, available at: http://www.ee.washington.edu/research/pstca/pf118/pg_tca118bus.htm

[89] E. W. Cheney, D. R. Kincaid, Numerical Mathematics and Computing, 5th edition, Monterey: Books Cole, 2003.

[90] "The GNU Multiple Precision Complex Library", Edition 1.0.1, Sept 2012.

[91] R. Christie, "IEEE 30-Bus Power Flow Test Case," May 1993, available at: https://www.ee.washington.edu/research/pstca/pf30/ieee30cdf.txt

[92] F. Milano "An open source power system analysis toolbox", *IEEE Trans. Power Syst.*, vol. 20, no. 3, pp.1199 -1206 2005

APPENDIX A

ALL SOLUTIONS FOR IEEE-14 BUS SYSTEM

Table 10.1 Solutions for the 14-Bus System using HE Method

Soln. NO.	**1**		**2**		**3**		**4**	
Voltage	$\|V\|$	θ	$\|V\|$	θ	$\|V\|$	θ	$\|V\|$	θ
V_1	1.060	0.000	1.060	0.000	1.060	0.000	1.060	0.000
V_2	1.045	-0.201	1.045	-2.614	1.045	-2.635	1.045	-2.868
V_3	1.048	-0.834	0.977	-3.973	0.965	-3.857	0.951	-4.073
V_4	1.051	-1.068	0.915	-4.410	0.893	-4.064	0.866	-4.144
V_5	1.051	-0.936	0.918	-3.691	0.873	-2.821	0.854	-2.899
V_6	1.047	-1.853	0.625	-14.401	0.334	-20.944	0.312	-22.440
V_7	1.061	-2.109	0.839	-12.160	0.860	-11.663	0.795	-13.442
V_8	1.090	-2.284	1.090	-12.381	1.090	-11.878	1.090	-13.675
V_9	1.053	-2.262	0.652	-17.065	0.710	-15.962	0.586	-19.706
V_{10}	1.050	-2.266	0.645	-16.833	0.642	-16.927	0.536	-20.544
V_{11}	1.048	-2.116	0.634	-15.822	0.491	-18.851	0.425	-21.829
V_{12}	1.044	-1.891	0.548	-15.618	0.160	-30.617	0.149	-31.958
V_{13}	1.045	-1.973	0.477	-13.989	0.004	-44.490	0.006	-46.201
V_{14}	1.047	-2.223	0.005	-53.577	0.397	-17.082	0.008	-57.297

Soln. NO.	**5**		**6**		**7**		**8**	
Voltage	$\|V\|$	θ	$\|V\|$	θ	$\|V\|$	θ	$\|V\|$	θ
V_1	1.060	0.000	1.060	0.000	1.060	0.000	1.060	0.000
V_2	1.045	-2.648	1.045	-2.897	1.045	-2.560	1.045	-2.795
V_3	0.985	-4.107	0.955	-4.173	0.963	-3.705	0.949	-3.928
V_4	0.929	-4.697	0.874	-4.356	0.889	-3.810	0.862	-3.904
V_5	0.911	-3.693	0.865	-3.227	0.868	-2.492	0.849	-2.590
V_6	0.488	-19.044	0.369	-21.435	0.300	-20.259	0.282	-21.814
V_7	0.918	-11.270	0.802	-13.439	0.855	-11.465	0.791	-13.240
V_8	1.090	-11.472	1.090	-13.670	1.090	-11.681	1.090	-13.474
V_9	0.813	-14.626	0.598	-19.490	0.701	-15.823	0.580	-19.565
V_{10}	0.755	-15.497	0.556	-20.200	0.629	-16.744	0.525	-20.381
V_{11}	0.624	-17.238	0.463	-21.169	0.467	-18.504	0.405	-21.549
V_{12}	0.006	-9.797	0.009	-14.286	0.018	-19.736	0.020	-21.504
V_{13}	0.391	-24.169	0.198	-27.238	0.005	-44.836	0.008	-46.692
V_{14}	0.624	-17.604	0.006	-58.595	0.393	-16.987	0.008	-57.214
Soln. NO.	**9**		**10**		**11**		**12**	
Voltage	$\|V\|$	θ	$\|V\|$	θ	$\|V\|$	θ	$\|V\|$	θ
V_1	1.060	0.000	1.060	0.000	1.060	0.000	1.060	0.000
V_2	1.045	-2.609	1.045	-2.801	1.045	-2.714	1.045	-2.762
V_3	0.963	-3.777	0.940	-3.807	0.932	-3.565	0.948	-3.851
V_4	0.889	-3.908	0.846	-3.563	0.832	-3.074	0.861	-3.770
V_5	0.882	-2.946	0.842	-2.473	0.820	-1.704	0.846	-2.470
V_6	0.436	-17.127	0.312	-20.563	0.184	-24.724	0.262	-23.809
V_7	0.817	-11.905	0.734	-13.585	0.729	-13.256	0.791	-12.798
V_8	1.090	-12.131	1.090	-13.837	1.090	-13.511	1.090	-13.032
V_9	0.620	-17.051	0.470	-21.778	0.466	-21.493	0.581	-18.857
V_{10}	0.432	-18.157	0.326	-23.150	0.324	-22.917	0.404	-20.037
V_{11}	0.003	-67.808	0.004	-71.860	0.005	-73.492	0.004	-71.690
V_{12}	0.441	-16.914	0.264	-21.835	0.056	-29.783	0.011	-14.578
V_{13}	0.457	-17.561	0.233	-20.820	0.011	-47.503	0.226	-28.769
V_{14}	0.545	-17.617	0.007	-58.798	0.010	-58.860	0.421	-21.856

Soln. NO.	**13**		**14**		**15**		**16**	
Voltage	$\|V\|$	θ	$\|V\|$	θ	$\|V\|$	θ	$\|V\|$	θ
V_1	1.060	0.000	1.060	0.000	1.060	0.000	1.060	0.000
V_2	1.045	-2.760	1.045	-2.711	1.045	-2.472	1.045	-2.542
V_3	0.934	-3.662	0.932	-3.560	0.943	-3.244	0.929	-3.164
V_4	0.835	-3.246	0.832	-3.065	0.853	-2.773	0.827	-2.383
V_5	0.825	-1.961	0.820	-1.692	0.867	-2.400	0.839	-1.922
V_6	0.216	-24.229	0.182	-24.680	0.513	-14.772	0.397	-17.287
V_7	0.730	-13.385	0.729	-13.248	0.686	-11.541	0.646	-11.939
V_8	1.090	-13.638	1.090	-13.502	1.090	-11.810	1.090	-12.225
V_9	0.467	-21.609	0.466	-21.485	0.361	-20.639	0.292	-23.859
V_{10}	0.324	-23.019	0.324	-22.908	0.004	-63.662	0.005	-66.704
V_{11}	0.005	-73.434	0.005	-73.470	0.248	-14.763	0.191	-18.086
V_{12}	0.017	-18.330	0.050	-28.983	0.495	-15.327	0.343	-18.565
V_{13}	0.113	-30.817	0.012	-47.498	0.485	-15.550	0.301	-17.297
V_{14}	0.009	-60.182	0.010	-58.864	0.409	-18.528	0.009	-57.686
Soln. NO.	**17**		**18**		**19**		**20**	
Voltage	$\|V\|$	θ	$\|V\|$	θ	$\|V\|$	θ	$\|V\|$	θ
V_1	1.060	0.000	1.060	0.000	1.060	0.000	1.060	0.000
V_2	1.045	-2.531	1.045	-2.517	1.045	-2.652	1.045	-2.557
V_3	0.920	-3.030	0.918	-2.966	0.926	-3.308	0.920	-3.060
V_4	0.810	-2.008	0.806	-1.858	0.820	-2.529	0.810	-2.039
V_5	0.809	-1.113	0.806	-1.024	0.822	-1.775	0.812	-1.307
V_6	0.207	-23.884	0.208	-23.877	0.281	-23.170	0.248	-23.010
V_7	0.653	-11.791	0.640	-11.694	0.664	-12.244	0.641	-11.797
V_8	1.090	-12.074	1.090	-11.983	1.090	-12.523	1.090	-12.086
V_9	0.315	-22.887	0.289	-23.747	0.333	-22.826	0.289	-23.812
V_{10}	0.005	-67.920	0.005	-68.580	0.005	-67.595	0.005	-68.348
V_{11}	0.094	-29.316	0.094	-29.352	0.132	-25.608	0.115	-26.552
V_{12}	0.080	-31.105	0.082	-31.211	0.011	-15.296	0.014	-16.698
V_{13}	0.007	-48.211	0.009	-47.412	0.205	-29.695	0.131	-29.575
V_{14}	0.168	-26.787	0.017	-58.901	0.269	-26.387	0.013	-61.305

Soln. NO.	**21**		**22**		**23**		**24**	
Voltage	$\|V\|$	θ	$\|V\|$	θ	$\|V\|$	θ	$\|V\|$	θ
V_1	1.060	0.000	1.060	0.000	1.060	0.000	1.060	0.000
V_2	1.045	-2.510	1.045	-2.495	1.045	-2.564	1.045	-2.552
V_3	0.920	-2.989	0.917	-2.923	0.934	-3.274	0.924	-3.104
V_4	0.809	-1.938	0.805	-1.784	0.836	-2.643	0.816	-2.182
V_5	0.807	-1.014	0.804	-0.920	0.843	-2.064	0.823	-1.554
V_6	0.197	-23.681	0.197	-23.681	0.384	-18.159	0.306	-19.979
V_7	0.653	-11.732	0.639	-11.629	0.676	-11.860	0.643	-11.893
V_8	1.090	-12.016	1.090	-11.919	1.090	-12.134	1.090	-12.181
V_9	0.315	-22.832	0.289	-23.687	0.350	-21.572	0.290	-23.908
V_{10}	0.005	-67.891	0.006	-68.554	0.005	-66.455	0.006	-68.565
V_{11}	0.088	-29.821	0.089	-29.895	0.007	-66.445	0.008	-67.679
V_{12}	0.036	-26.051	0.035	-25.826	0.372	-18.534	0.259	-21.289
V_{13}	0.008	-48.477	0.011	-47.561	0.372	-19.034	0.229	-20.382
V_{14}	0.168	-26.780	0.017	-58.969	0.353	-21.147	0.010	-59.082
Soln. NO.	**25**		**26**		**27**		**28**	
Voltage	$\|V\|$	θ	$\|V\|$	θ	$\|V\|$	θ	$\|V\|$	θ
V_1	1.060	0.000	1.060	0.000	1.060	0.000	1.060	0.000
V_2	1.045	-2.609	1.045	-2.526	1.045	-1.628	1.045	-1.671
V_3	0.923	-3.204	0.918	-2.983	0.909	-1.152	0.907	-1.184
V_4	0.815	-2.327	0.806	-1.887	0.792	1.145	0.788	1.163
V_5	0.815	-1.476	0.807	-1.069	0.821	0.327	0.814	0.409
V_6	0.239	-24.000	0.213	-23.861	0.443	-13.815	0.402	-15.185
V_7	0.662	-12.125	0.640	-11.717	0.509	-1.919	0.508	-2.029
V_8	1.090	-12.405	1.090	-12.007	1.090	-2.282	1.090	-2.393
V_9	0.331	-22.822	0.289	-23.781	0.009	-55.260	0.010	-56.368
V_{10}	0.005	-67.871	0.006	-68.688	0.063	-27.010	0.052	-33.198
V_{11}	0.011	-70.077	0.013	-69.110	0.244	-15.503	0.217	-17.484
V_{12}	0.013	-16.212	0.017	-18.074	0.401	-14.755	0.349	-16.534
V_{13}	0.179	-30.467	0.112	-30.744	0.370	-14.121	0.307	-15.461
V_{14}	0.256	-26.581	0.013	-61.231	0.151	-18.487	0.022	-48.634

Soln. NO.	**29**		**30**		**31**		**32**	
Voltage	$\|V\|$	θ	$\|V\|$	θ	$\|V\|$	θ	$\|V\|$	θ
V_1	1.060	0.000	1.060	0.000	1.060	0.000	1.060	0.000
V_2	1.045	-1.646	1.045	-1.678	1.045	-14.707	1.045	-7.304
V_3	0.908	-1.169	0.906	-1.190	0.654	-19.971	0.005	-49.573
V_4	0.791	1.144	0.787	1.166	0.304	-25.344	0.771	-9.210
V_5	0.819	0.354	0.813	0.428	0.001	-74.950	0.856	-7.681
V_6	0.428	-14.258	0.394	-15.395	0.157	-41.502	0.860	-9.438
V_7	0.509	-2.006	0.508	-2.079	0.594	-41.527	0.910	-10.674
V_8	1.090	-2.370	1.090	-2.444	1.090	-41.839	1.090	-10.877
V_9	0.010	-55.730	0.010	-56.561	0.451	-45.551	0.875	-10.798
V_{10}	0.025	-48.353	0.030	-46.247	0.396	-46.225	0.871	-10.680
V_{11}	0.215	-16.161	0.201	-17.835	0.276	-46.153	0.865	-10.159
V_{12}	0.387	-15.219	0.342	-16.750	0.155	-41.205	0.857	-9.544
V_{13}	0.357	-14.624	0.301	-15.708	0.184	-45.023	0.859	-9.731
V_{14}	0.144	-19.413	0.023	-48.731	0.328	-46.460	0.866	-10.467
Soln. NO.	**33**		**34**		**35**		**36**	
Voltage	$\|V\|$	θ	$\|V\|$	θ	$\|V\|$	θ	$\|V\|$	θ
V_1	1.060	0.000	1.060	0.000	1.060	0.000	1.060	0.000
V_2	1.045	-8.920	1.045	-8.933	1.045	-9.070	1.045	-8.965
V_3	0.005	-51.902	0.005	-51.818	0.005	-51.931	0.005	-52.054
V_4	0.670	-12.089	0.654	-11.807	0.633	-11.801	0.680	-12.430
V_5	0.751	-9.668	0.717	-8.794	0.702	-8.767	0.746	-9.703
V_6	0.511	-21.594	0.273	-28.217	0.256	-29.671	0.403	-26.408
V_7	0.729	-21.485	0.749	-21.171	0.694	-23.200	0.796	-20.384
V_8	1.090	-21.739	1.090	-21.419	1.090	-23.466	1.090	-20.616
V_9	0.547	-26.411	0.597	-25.559	0.494	-29.562	0.682	-23.735
V_{10}	0.538	-25.933	0.538	-26.405	0.450	-30.270	0.631	-24.474
V_{11}	0.522	-24.104	0.407	-27.705	0.353	-30.818	0.519	-25.666
V_{12}	0.446	-22.827	0.125	-37.249	0.115	-38.439	0.007	-17.452
V_{13}	0.389	-21.305	0.005	-52.315	0.007	-53.241	0.323	-32.038
V_{14}	0.006	-62.101	0.333	-26.962	0.010	-66.867	0.521	-26.459

Soln. NO.	**37**		**38**		**39**		**40**	
Voltage	$\|V\|$	θ	$\|V\|$	θ	$\|V\|$	θ	$\|V\|$	θ
V_1	1.060	0.000	1.060	0.000	1.060	0.000	1.060	0.000
V_2	1.045	-9.096	1.045	-8.887	1.045	-9.027	1.045	-8.906
V_3	0.005	-52.020	0.005	-51.715	0.005	-51.837	0.005	-51.727
V_4	0.640	-12.007	0.651	-11.609	0.631	-11.619	0.650	-11.608
V_5	0.710	-9.103	0.713	-8.533	0.699	-8.531	0.723	-8.900
V_6	0.303	-28.649	0.249	-27.699	0.235	-29.227	0.355	-24.253
V_7	0.701	-23.099	0.746	-21.058	0.692	-23.082	0.712	-21.514
V_8	1.090	-23.363	1.090	-21.307	1.090	-23.350	1.090	-21.774
V_9	0.504	-29.222	0.591	-25.510	0.490	-29.511	0.521	-26.799
V_{10}	0.466	-29.768	0.529	-26.337	0.442	-30.223	0.362	-28.051
V_{11}	0.385	-29.956	0.391	-27.535	0.339	-30.720	0.003	-76.260
V_{12}	0.011	-21.812	0.024	-27.990	0.025	-29.803	0.357	-24.298
V_{13}	0.162	-34.696	0.006	-52.735	0.009	-53.545	0.372	-25.366
V_{14}	0.008	-67.618	0.330	-26.964	0.010	-66.880	0.452	-26.820
Soln. NO.	**41**		**42**		**43**		**44**	
Voltage	$\|V\|$	θ	$\|V\|$	θ	$\|V\|$	θ	$\|V\|$	θ
V_1	1.060	0.000	1.060	0.000	1.060	0.000	1.060	0.000
V_2	1.045	-9.001	1.045	-8.996	1.045	-8.968	1.045	-8.745
V_3	0.005	-51.669	0.005	-51.757	0.005	-51.552	0.005	-51.141
V_4	0.618	-11.173	0.630	-11.460	0.611	-10.891	0.624	-10.265
V_5	0.693	-8.288	0.696	-8.366	0.681	-7.819	0.714	-8.265
V_6	0.250	-27.397	0.214	-30.763	0.177	-30.910	0.418	-21.792
V_7	0.644	-23.695	0.692	-22.675	0.642	-23.571	0.603	-21.180
V_8	1.090	-23.982	1.090	-22.943	1.090	-23.860	1.090	-21.487
V_9	0.398	-32.160	0.490	-28.914	0.396	-32.076	0.304	-30.528
V_{10}	0.275	-33.777	0.341	-30.265	0.274	-33.741	0.005	-72.901
V_{11}	0.005	-80.540	0.004	-80.471	0.005	-82.305	0.201	-22.412
V_{12}	0.205	-28.709	0.014	-22.316	0.023	-26.093	0.400	-22.522
V_{13}	0.183	-28.197	0.185	-36.831	0.091	-38.111	0.393	-23.047
V_{14}	0.009	-68.094	0.351	-31.643	0.010	-69.701	0.336	-27.542

Soln. NO.	**45**		**46**		**47**		**48**	
Voltage	$\|V\|$	θ	$\|V\|$	θ	$\|V\|$	θ	$\|V\|$	θ
V_1	1.060	0.000	1.060	0.000	1.060	0.000	1.060	0.000
V_2	1.045	-8.770	1.045	-8.846	1.045	-8.770	1.045	-8.800
V_3	0.005	-51.027	0.005	-51.144	0.005	-50.926	0.005	-51.146
V_4	0.605	-9.823	0.600	-9.976	0.593	-9.484	0.611	-10.121
V_5	0.692	-7.716	0.679	-7.555	0.672	-7.106	0.695	-7.893
V_6	0.321	-24.142	0.229	-30.117	0.202	-29.875	0.313	-25.232
V_7	0.571	-21.863	0.586	-22.144	0.567	-21.817	0.595	-21.649
V_8	1.090	-22.187	1.090	-22.460	1.090	-22.143	1.090	-21.960
V_9	0.248	-34.192	0.282	-33.073	0.246	-34.271	0.295	-31.672
V_{10}	0.006	-76.294	0.006	-77.358	0.006	-78.281	0.006	-76.328
V_{11}	0.153	-26.036	0.106	-34.504	0.091	-35.991	0.008	-73.029
V_{12}	0.273	-25.469	0.014	-22.939	0.019	-24.373	0.299	-25.838
V_{13}	0.241	-24.521	0.166	-37.537	0.106	-37.070	0.300	-26.775
V_{14}	0.011	-66.264	0.222	-36.399	0.015	-70.071	0.290	-30.595
Soln. NO.	**49**		**50**		**51**		**52**	
Voltage	$\|V\|$	θ	$\|V\|$	θ	$\|V\|$	θ	$\|V\|$	θ
V_1	1.060	0.000	1.060	0.000	1.060	0.000	1.060	0.000
V_2	1.045	-8.772	1.045	-8.817	1.045	-8.749	1.045	-144.794
V_3	0.005	-50.971	0.005	-51.067	0.005	-50.872	0.874	-141.787
V_4	0.597	-9.628	0.597	-9.802	0.590	-9.360	0.736	-135.744
V_5	0.680	-7.348	0.674	-7.290	0.668	-6.902	0.606	-128.508
V_6	0.247	-26.920	0.197	-30.962	0.176	-30.713	0.691	-132.184
V_7	0.569	-21.898	0.584	-22.097	0.566	-21.793	0.867	-137.430
V_8	1.090	-22.223	1.090	-22.414	1.090	-22.120	1.090	-137.644
V_9	0.247	-34.353	0.280	-33.164	0.246	-34.309	0.802	-137.610
V_{10}	0.007	-78.704	0.006	-78.042	0.007	-78.983	0.780	-136.989
V_{11}	0.011	-73.748	0.014	-75.402	0.016	-73.858	0.734	-134.968
V_{12}	0.203	-28.288	0.016	-24.043	0.023	-25.985	0.694	-132.556
V_{13}	0.182	-27.924	0.146	-38.443	0.091	-38.306	0.702	-133.262
V_{14}	0.013	-67.881	0.211	-36.808	0.016	-70.095	0.755	-136.052

Soln. NO.	**53**		**54**		**55**		**56**	
Voltage	$\|V\|$	θ	$\|V\|$	θ	$\|V\|$	θ	$\|V\|$	θ
V_1	1.060	0.000	1.060	0.000	1.060	0.000	1.060	0.000
V_2	1.045	-141.926	1.045	-141.701	1.045	-141.995	1.045	-141.414
V_3	0.824	-140.340	0.820	-140.169	0.834	-140.475	0.811	-139.989
V_4	0.637	-134.853	0.629	-134.631	0.655	-135.351	0.613	-134.366
V_5	0.512	-125.732	0.490	-124.533	0.516	-126.234	0.482	-124.259
V_6	0.375	-140.543	0.201	-146.773	0.317	-145.682	0.224	-146.913
V_7	0.705	-144.702	0.731	-144.240	0.773	-143.384	0.683	-145.756
V_8	1.090	-144.965	1.090	-144.493	1.090	-143.624	1.090	-146.027
V_9	0.512	-149.905	0.572	-148.719	0.645	-146.781	0.480	-152.016
V_{10}	0.484	-149.167	0.505	-149.318	0.586	-147.224	0.432	-152.334
V_{11}	0.427	-145.968	0.354	-149.558	0.453	-147.316	0.328	-151.430
V_{12}	0.322	-141.807	0.073	-153.533	0.009	-137.168	0.016	-140.910
V_{13}	0.282	-140.550	0.006	-172.312	0.267	-152.441	0.117	-153.493
V_{14}	0.007	175.473	0.319	-150.226	0.476	-148.746	0.008	170.563
Soln. NO.	**57**		**58**		**59**		**60**	
Voltage	$\|V\|$	θ	$\|V\|$	θ	$\|V\|$	θ	$\|V\|$	θ
V_1	1.060	0.000	1.060	0.000	1.060	0.000	1.060	0.000
V_2	1.045	-141.701	1.045	-141.710	1.045	-141.393	1.045	-141.708
V_3	0.819	-140.157	0.815	-140.112	0.806	-139.888	0.796	-139.745
V_4	0.627	-134.584	0.621	-134.351	0.604	-134.002	0.588	-132.834
V_5	0.488	-124.414	0.490	-124.423	0.470	-123.313	0.474	-122.985
V_6	0.193	-146.603	0.249	-142.576	0.149	-148.590	0.275	-140.121
V_7	0.730	-144.238	0.694	-144.747	0.679	-145.532	0.586	-144.432
V_8	1.090	-144.492	1.090	-145.014	1.090	-145.805	1.090	-144.748
V_9	0.570	-148.748	0.498	-150.262	0.475	-151.832	0.286	-154.300
V_{10}	0.501	-149.353	0.346	-151.578	0.330	-153.238	0.005	163.434
V_{11}	0.349	-149.585	0.004	162.046	0.005	158.194	0.129	-142.984
V_{12}	0.040	-149.598	0.253	-143.093	0.020	-141.531	0.261	-141.290
V_{13}	0.007	-172.590	0.275	-145.614	0.144	-156.688	0.264	-143.080
V_{14}	0.318	-150.278	0.395	-149.598	0.325	-153.855	0.267	-150.921

Soln. NO.	**61**		**62**		**63**		**64**	
Voltage	$\|V\|$	θ	$\|V\|$	θ	$\|V\|$	θ	$\|V\|$	θ
V_1	1.060	0.000	1.060	0.000	1.060	0.000	1.060	0.000
V_2	1.045	-141.458	1.045	-141.358	1.045	-141.358	1.045	-141.514
V_3	0.786	-139.490	0.787	-139.477	0.783	-139.396	0.791	-139.601
V_4	0.569	-132.202	0.569	-132.351	0.562	-131.991	0.578	-132.589
V_5	0.454	-121.654	0.451	-121.592	0.445	-121.047	0.461	-122.266
V_6	0.183	-143.252	0.148	-148.173	0.130	-147.648	0.205	-143.520
V_7	0.559	-144.922	0.573	-145.012	0.557	-144.900	0.580	-144.722
V_8	1.090	-145.253	1.090	-145.335	1.090	-145.232	1.090	-145.042
V_9	0.241	-157.402	0.271	-156.136	0.240	-157.468	0.279	-155.159
V_{10}	0.007	159.652	0.006	159.405	0.007	158.079	0.006	160.140
V_{11}	0.080	-151.331	0.059	-161.503	0.044	-168.535	0.013	171.430
V_{12}	0.138	-144.690	0.023	-142.947	0.050	-147.087	0.191	-144.572
V_{13}	0.127	-145.715	0.115	-157.563	0.069	-155.529	0.201	-147.220
V_{14}	0.015	170.725	0.192	-159.062	0.017	168.506	0.236	-154.018
Soln. NO.	**65**		**66**		**67**		**68**	
Voltage	$\|V\|$	θ	$\|V\|$	θ	$\|V\|$	θ	$\|V\|$	θ
V_1	1.060	0.000	1.060	0.000	1.060	0.000	1.060	0.000
V_2	1.045	-141.368	1.045	-141.345	1.045	-141.360	1.045	-129.020
V_3	0.783	-139.405	0.786	-139.458	0.783	-139.397	0.655	-134.288
V_4	0.563	-132.014	0.568	-132.290	0.562	-131.988	0.305	-139.672
V_5	0.446	-121.107	0.449	-121.421	0.445	-121.032	0.002	-174.765
V_6	0.135	-146.975	0.135	-148.791	0.130	-147.457	0.158	-155.667
V_7	0.557	-144.917	0.572	-145.020	0.557	-144.910	0.595	-155.770
V_8	1.090	-145.249	1.090	-145.343	1.090	-145.242	1.090	-156.082
V_9	0.240	-157.490	0.270	-156.213	0.240	-157.488	0.452	-159.774
V_{10}	0.007	157.850	0.007	158.786	0.007	157.813	0.397	-160.438
V_{11}	0.025	177.636	0.025	176.070	0.028	179.597	0.277	-160.338
V_{12}	0.076	-147.872	0.027	-144.027	0.064	-147.946	0.156	-155.388
V_{13}	0.081	-152.733	0.107	-158.200	0.074	-154.515	0.186	-159.172
V_{14}	0.017	168.896	0.188	-159.361	0.017	168.678	0.330	-160.658

Soln. NO.	**69**		**70**		**71**		**72**	
Voltage	$\|V\|$	θ	$\|V\|$	θ	$\|V\|$	θ	$\|V\|$	θ
V_1	1.060	0.000	1.060	0.000	1.060	0.000	1.060	0.000
V_2	1.045	-128.856	1.045	-137.743	1.045	-135.570	1.045	-135.647
V_3	0.651	-134.314	0.005	-176.166	0.006	-175.594	0.006	-175.695
V_4	0.298	-140.340	0.519	-127.317	0.441	-128.174	0.456	-128.674
V_5	0.002	-173.720	0.472	-117.251	0.395	-115.309	0.400	-115.922
V_6	0.092	-170.330	0.554	-123.212	0.286	-134.045	0.252	-139.003
V_7	0.579	-159.718	0.751	-130.131	0.616	-141.432	0.674	-139.368
V_8	1.090	-160.037	1.090	-130.378	1.090	-141.732	1.090	-139.642
V_9	0.424	-164.960	0.666	-130.401	0.427	-146.897	0.540	-142.886
V_{10}	0.362	-166.358	0.643	-129.625	0.397	-146.045	0.487	-143.215
V_{11}	0.227	-168.854	0.597	-126.983	0.338	-141.852	0.370	-142.601
V_{12}	0.054	-164.988	0.556	-123.734	0.239	-135.357	0.012	-131.131
V_{13}	0.110	-173.630	0.564	-124.694	0.212	-134.540	0.214	-146.756
V_{14}	0.279	-167.823	0.617	-128.429	0.008	179.387	0.393	-144.583
Soln. NO.	**73**		**74**		**75**		**76**	
Voltage	$\|V\|$	θ	$\|V\|$	θ	$\|V\|$	θ	$\|V\|$	θ
V_1	1.060	0.000	1.060	0.000	1.060	0.000	1.060	0.000
V_2	1.045	-135.212	1.045	-135.393	1.045	-135.190	1.045	-135.430
V_3	0.006	-175.427	0.006	-175.456	0.006	-175.357	0.006	-175.110
V_4	0.423	-128.025	0.428	-127.826	0.417	-127.697	0.403	-125.932
V_5	0.373	-113.983	0.378	-113.931	0.365	-112.975	0.366	-112.196
V_6	0.174	-140.700	0.183	-136.237	0.114	-141.837	0.192	-134.588
V_7	0.600	-143.283	0.608	-142.103	0.597	-143.323	0.517	-142.094
V_8	1.090	-143.591	1.090	-142.408	1.090	-143.633	1.090	-142.453
V_9	0.404	-149.790	0.416	-148.015	0.401	-149.943	0.238	-152.781
V_{10}	0.359	-150.047	0.289	-149.581	0.278	-151.617	0.007	164.997
V_{11}	0.265	-148.292	0.005	165.694	0.006	161.586	0.085	-141.901
V_{12}	0.023	-136.048	0.180	-137.317	0.030	-137.309	0.173	-136.206
V_{13}	0.089	-148.050	0.202	-141.269	0.113	-152.025	0.181	-139.467
V_{14}	0.010	173.695	0.316	-147.251	0.268	-151.823	0.201	-150.119

Soln. NO.	**77**		**78**		**79**		**80**	
Voltage	$\|V\|$	θ	$\|V\|$	θ	$\|V\|$	θ	$\|V\|$	θ
V_1	1.060	0.000	1.060	0.000	1.060	0.000	1.060	0.000
V_2	1.045	-135.306	1.045	-141.359	1.045	-129.020	1.045	-128.856
V_3	0.006	-175.039	0.783	-139.397	0.655	-134.288	0.651	-134.314
V_4	0.397	-125.801	0.563	-131.991	0.305	-139.672	0.298	-140.329
V_5	0.357	-111.544	0.445	-121.046	0.002	-174.765	0.002	-173.719
V_6	0.143	-138.384	0.131	-147.302	0.158	-155.667	0.092	-170.320
V_7	0.513	-142.673	0.557	-144.910	0.595	-155.771	0.579	-159.717
V_8	1.090	-143.035	1.090	-145.243	1.090	-156.082	1.090	-160.037
V_9	0.233	-153.940	0.240	-157.488	0.452	-159.774	0.424	-164.960
V_{10}	0.008	161.683	0.007	157.819	0.397	-160.439	0.362	-166.356
V_{11}	0.022	-176.642	0.028	179.620	0.277	-160.338	0.227	-168.856
V_{12}	0.119	-139.811	0.064	-147.795	0.156	-155.388	0.054	-164.989
V_{13}	0.134	-144.842	0.074	-154.457	0.186	-159.172	0.110	-173.625
V_{14}	0.177	-154.045	0.017	168.641	0.330	-160.658	0.279	-167.821
Soln. NO.	**81**		**82**		**83**		**84**	
Voltage	$\|V\|$	θ	$\|V\|$	θ	$\|V\|$	θ	$\|V\|$	θ
V_1	1.060	0.000	1.060	0.000	1.060	0.000	1.060	0.000
V_2	1.045	-137.743	1.045	-135.570	1.045	-135.160	1.045	-135.647
V_3	0.005	-176.167	0.006	-175.594	0.006	-175.415	0.006	-175.696
V_4	0.519	-127.317	0.441	-128.174	0.419	-127.972	0.456	-128.674
V_5	0.472	-117.251	0.395	-115.309	0.368	-113.617	0.400	-115.922
V_6	0.554	-123.212	0.286	-134.045	0.143	-142.956	0.252	-139.003
V_7	0.751	-130.131	0.616	-141.432	0.597	-143.643	0.674	-139.368
V_8	1.090	-130.378	1.090	-141.732	1.090	-143.956	1.090	-139.643
V_9	0.666	-130.401	0.427	-146.898	0.399	-150.490	0.540	-142.886
V_{10}	0.643	-129.625	0.397	-146.045	0.351	-151.162	0.487	-143.215
V_{11}	0.597	-126.983	0.338	-141.852	0.246	-150.301	0.370	-142.601
V_{12}	0.556	-123.734	0.240	-135.357	0.047	-145.210	0.012	-131.131
V_{13}	0.564	-124.694	0.212	-134.540	0.015	-162.239	0.214	-146.756
V_{14}	0.617	-128.429	0.008	179.387	0.012	172.822	0.393	-144.583

Soln. NO.	**85**		**86**		**87**		**88**	
Voltage	$\|V\|$	θ	$\|V\|$	θ	$\|V\|$	θ	$\|V\|$	θ
V_1	1.060	0.000	1.060	0.000	1.060	0.000	1.060	0.000
V_2	1.045	-135.212	1.045	-135.393	1.045	-135.190	1.045	-135.430
V_3	0.006	-175.427	0.006	-175.456	0.006	-175.357	0.006	-175.110
V_4	0.423	-128.025	0.428	-127.826	0.417	-127.697	0.403	-125.932
V_5	0.373	-113.983	0.378	-113.931	0.365	-112.975	0.366	-112.196
V_6	0.174	-140.700	0.183	-136.237	0.114	-141.837	0.192	-134.588
V_7	0.600	-143.283	0.608	-142.103	0.597	-143.323	0.517	-142.094
V_8	1.090	-143.591	1.090	-142.408	1.090	-143.633	1.090	-142.453
V_9	0.404	-149.790	0.416	-148.015	0.401	-149.943	0.238	-152.781
V_{10}	0.359	-150.047	0.289	-149.581	0.278	-151.617	0.007	164.997
V_{11}	0.265	-148.292	0.005	165.694	0.006	161.586	0.085	-141.901
V_{12}	0.023	-136.048	0.180	-137.317	0.030	-137.309	0.173	-136.206
V_{13}	0.089	-148.050	0.202	-141.269	0.113	-152.025	0.181	-139.467
V_{14}	0.010	173.695	0.316	-147.251	0.268	-151.823	0.201	-150.119

Soln. NO.	**89**		**90**	
Voltage	$\|V\|$	θ	$\|V\|$	θ
V_1	1.060	0.000	1.060	0.000
V_2	1.045	-135.306	1.045	-135.239
V_3	0.006	-175.039	0.006	-174.990
V_4	0.397	-125.801	0.392	-125.682
V_5	0.357	-111.544	0.352	-111.074
V_6	0.143	-138.384	0.112	-142.075
V_7	0.513	-142.673	0.509	-143.028
V_8	1.090	-143.034	1.090	-143.409
V_9	0.233	-153.940	0.228	-154.774
V_{10}	0.008	161.683	0.008	160.684
V_{11}	0.022	-176.642	0.031	-150.521
V_{12}	0.119	-139.811	0.044	-138.537
V_{13}	0.134	-144.842	0.089	-152.639
V_{14}	0.177	-154.045	0.154	-158.109

APPENDIX B

TYPE-1 SOLUTIONS FOR IEEE-118 BUS SYSTEM

Table 11.1 Type-1 Solutions for the 118-Bus System using HE Method

Solution NO.		**1**		**2**		**3**	
Bus NO.	Bus Type	V (p.u.)	Angle (deg.)	V (p.u.)	Angle (deg.)	V (p.u.)	Angle (deg.)
1	2	0.9550	-125.4280	0.9550	-68.7545	0.9550	-60.9903
2	0	0.0091	-161.8933	0.9713	-67.6892	0.9715	-60.9553
3	0	0.9496	-116.0593	0.9672	-68.0841	0.9651	-59.8421
4	2	0.9980	-98.1969	0.9980	-65.4053	0.9980	-55.2501
5	0	0.9991	-97.4356	1.0002	-65.1147	0.9918	-54.3202
6	2	0.9900	-102.8418	0.9900	-66.7473	0.9900	-58.3383
7	0	0.9893	-104.2881	0.9892	-66.7573	0.9894	-59.2127
8	2	1.0150	-85.8953	1.0150	-62.0051	1.0150	-46.1028
9	0	1.0429	-78.6408	0.0547	13.7151	1.0429	-38.8487
10	2	1.0501	-71.0565	1.0500	112.1399	1.0500	-31.2678
11	0	0.9812	-103.2019	0.9850	-66.3630	0.8438	-59.0108
12	2	0.9900	-106.2960	0.9900	-66.4001	0.9900	-60.2792
13	0	0.9576	-100.4058	0.9670	-65.8426	0.0259	-104.1241
14	0	0.9724	-101.5510	0.9828	-65.0660	0.9826	-58.8741
15	2	0.9700	-86.2466	0.9700	-59.5413	0.9700	-53.1484
16	0	0.9601	-99.6093	0.9779	-64.2094	0.9776	-57.5051
17	0	0.9789	-82.2311	0.9852	-56.9473	0.9879	-48.9895
18	2	0.9730	-84.0818	0.9730	-58.6851	0.9730	-51.2627
19	2	0.9620	-83.9288	0.9620	-58.5222	0.9620	-51.6704
20	0	0.9433	-79.9834	0.9507	-55.9237	0.9508	-49.0299
21	0	0.9376	-76.0635	0.9485	-53.0476	0.9487	-46.1235
22	0	0.9470	-70.8033	0.9589	-49.0100	0.9593	-42.0533
23	0	0.9885	-61.6672	0.9945	-41.7701	0.9954	-34.7674
24	2	0.9920	-54.6085	0.9920	-37.2550	0.9920	-31.2067
25	2	1.0500	-59.6495	1.0500	-38.3364	1.0500	-30.2727
26	2	1.0150	-59.6379	1.0150	-37.9391	1.0150	-29.3256
27	2	0.9680	-73.8919	0.9680	-51.5099	0.9680	-43.7609
28	0	0.9613	-76.4816	0.9615	-53.7095	0.9615	-45.9494
29	0	0.9633	-78.4382	0.9633	-55.2314	0.9633	-47.4589
30	0	0.9682	-75.2351	0.9888	-52.3736	0.9964	-42.3658
31	2	0.9670	-78.6647	0.9670	-55.3031	0.9670	-47.5262
32	2	0.9630	-74.4477	0.9630	-51.9611	0.9630	-44.3196
33	0	0.9536	-79.4088	0.9638	-56.1401	0.9648	-49.6085
34	2	0.9840	-70.5774	0.9840	-51.0791	0.9840	-44.4099
35	0	0.9775	-70.9516	0.9788	-51.5101	0.9792	-44.8298

36	2	0.9800	-71.0007	0.9800	-51.5317	0.9800	-44.8505
37	0	0.9736	-69.7768	0.9812	-50.4804	0.9836	-43.8070
38	0	0.9156	-62.5898	0.9601	-44.2307	0.9734	-37.1625
39	0	0.9642	-71.6990	0.9667	-53.4405	0.9674	-47.1483
40	2	0.9700	-71.9011	0.9700	-54.2522	0.9700	-48.1849
41	0	0.9663	-71.5592	0.9667	-54.4324	0.9668	-48.5530
42	2	0.9850	-67.8042	0.9850	-52.1091	0.9850	-46.7441
43	0	0.9230	-61.6862	0.9489	-45.5148	0.9553	-39.9797
44	0	0.9109	-44.5496	0.9405	-34.2034	0.9481	-30.5174
45	0	0.9371	-37.5269	0.9558	-29.2435	0.9608	-26.2277
46	2	1.0050	-31.3774	1.0050	-24.3627	1.0050	-21.7981
47	0	1.0037	-25.8588	1.0098	-20.0533	1.0117	-17.9144
48	0	1.0142	-28.7891	1.0143	-22.2360	1.0144	-19.8083
49	2	1.0250	-27.6296	1.0250	-21.1996	1.0250	-18.8081
50	0	1.0011	-29.6736	1.0009	-23.3646	1.0008	-21.0000
51	0	0.9668	-32.3077	0.9665	-26.1558	0.9664	-23.8258
52	0	0.9568	-33.2705	0.9564	-27.1612	0.9563	-24.8406
53	0	0.9460	-34.2713	0.9458	-28.2781	0.9457	-25.9832
54	2	0.9550	-33.3786	0.9550	-27.4708	0.9550	-25.1946
55	2	0.9520	-33.4335	0.9520	-27.5519	0.9520	-25.2815
56	2	0.9540	-33.4256	0.9540	-27.5198	0.9540	-25.2441
57	0	0.9706	-32.2152	0.9704	-26.1361	0.9703	-23.8222
58	0	0.9590	-33.0788	0.9588	-27.0314	0.9587	-24.7244
59	2	0.9850	-25.9198	0.9850	-20.4470	0.9850	-18.2660
60	0	0.9931	-21.4086	0.9931	-16.0602	0.9931	-13.9066
61	2	0.9950	-20.4948	0.9950	-15.1607	0.9950	-13.0102
62	2	0.9980	-20.9472	0.9980	-15.5885	0.9980	-13.4324
63	0	0.9916	-21.9700	0.9919	-16.6328	0.9919	-14.4817
64	0	0.9977	-19.9624	0.9979	-14.6958	0.9980	-12.5601
65	2	1.0050	-16.3464	1.0050	-11.2610	1.0050	-9.1652
66	2	1.0500	-16.0790	1.0500	-10.6319	1.0500	-8.4558
67	0	1.0194	-19.0895	1.0194	-13.6800	1.0194	-11.5130
68	0	1.0113	-11.7290	1.0121	-8.3431	1.0122	-6.9565
69	3	1.0350	0	1.0350	0	1.0350	0
70	2	0.9840	-20.5764	0.9840	-15.5910	0.9840	-13.8510
71	0	0.9823	-23.9119	0.9850	-17.7919	0.9856	-15.6626
72	2	0.9800	-39.8231	0.9800	-27.9418	0.9800	-23.8450
73	2	0.9910	-24.1753	0.9910	-18.0246	0.9910	-15.8879
74	2	0.9580	-17.4788	0.9580	-14.1007	0.9580	-12.9120
75	0	0.9617	-14.8157	0.9643	-12.0081	0.9651	-11.0106
76	2	0.9430	-15.6305	0.9430	-13.0797	0.9430	-12.1486

77	2	1.0060	-10.0741	1.0060	-7.9588	1.0060	-7.1428
78	0	1.0017	-10.3746	1.0018	-8.1918	1.0018	-7.3454
79	0	1.0043	-10.0799	1.0043	-7.7665	1.0042	-6.8615
80	2	1.0400	-8.0121	1.0400	-5.3402	1.0400	-4.2719
81	0	1.0277	-10.4409	1.0281	-7.3099	1.0282	-6.0377
82	0	0.9773	-8.7818	0.9773	-6.4111	0.9773	-5.4804
83	0	0.9717	-6.4803	0.9717	-4.0923	0.9717	-3.1537
84	0	0.9747	-2.3019	0.9747	0.1141	0.9747	1.0653
85	2	0.9850	0.0243	0.9850	2.4537	0.9850	3.4109
86	0	0.9867	-1.3453	0.9867	1.0843	0.9867	2.0414
87	2	1.0150	-1.0852	1.0150	1.3434	1.0150	2.3007
88	0	0.9859	4.6473	0.9859	7.1004	0.9859	8.0684
89	2	1.0050	9.7266	1.0050	12.1966	1.0050	13.1720
90	2	0.9850	-2.5454	0.9850	-0.0599	0.9850	0.9228
91	2	0.9800	-4.4007	0.9800	-1.9012	0.9800	-0.9126
92	2	0.9900	-6.6706	0.9900	-4.1515	0.9900	-3.1541
93	0	0.9854	-8.6266	0.9854	-6.1031	0.9854	-5.1035
94	0	0.9886	-9.8670	0.9886	-7.3392	0.9886	-6.3378
95	0	0.9776	-10.2955	0.9777	-7.7773	0.9777	-6.7802
96	0	0.9877	-9.7693	0.9878	-7.2639	0.9879	-6.2725
97	0	1.0088	-9.2429	1.0088	-6.6528	1.0088	-5.6231
98	0	1.0233	-10.1762	1.0233	-7.5423	1.0233	-6.4936
99	2	1.0100	-11.0996	1.0100	-8.5052	1.0100	-7.4739
100	2	1.0170	-10.5703	1.0170	-8.0091	1.0170	-6.9939
101	0	0.9921	-9.7948	0.9921	-7.2501	0.9921	-6.2416
102	0	0.9896	-7.8164	0.9896	-5.2895	0.9897	-4.2884
103	2	1.0100	-14.3129	1.0100	-11.7517	1.0100	-10.7350
104	2	0.9710	-16.8834	0.9710	-14.3217	0.9710	-13.3050
105	2	0.9650	-17.9876	0.9650	-15.4259	0.9650	-14.4092
106	0	0.9611	-18.2478	0.9611	-15.6860	0.9611	-14.6693
107	2	0.9520	-21.0486	0.9520	-18.4867	0.9520	-17.4701
108	0	0.9662	-19.1877	0.9662	-16.6259	0.9662	-15.6093
109	0	0.9670	-19.6403	0.9670	-17.0785	0.9670	-16.0619
110	2	0.9730	-20.4872	0.9730	-17.9254	0.9730	-16.9087
111	2	0.9800	-18.8421	0.9800	-16.2803	0.9800	-15.2636
112	2	0.9750	-23.5864	0.9750	-21.0246	0.9750	-20.0079
113	2	0.9930	-81.6502	0.9930	-56.6135	0.9930	-48.6535
114	0	0.9601	-74.7769	0.9601	-52.3343	0.9601	-44.6475
115	0	0.9600	-74.7843	0.9600	-52.3492	0.9600	-44.6548
116	2	1.0050	-12.1222	1.0050	-8.7329	1.0050	-7.3448
117	0	0.9738	-107.8370	0.9738	-67.9411	0.9738	-61.8202

118	0	0.9465	-15.6615	0.9478	-12.9711	0.9482	-12.0038

Solution NO.		**4**		**5**		**6**	
Bus NO.	Bus Type	V (p.u.)	Angle (deg.)	V (p.u.)	Angle (deg.)	V (p.u.)	Angle (deg.)
1	2	0.9550	-75.2155	0.9550	-60.8854	0.9550	-35.8242
2	0	0.9715	-75.8685	0.9715	-61.2720	0.9714	-35.3750
3	0	0.9672	-73.8103	0.9673	-59.5987	0.9675	-34.8985
4	2	0.9980	-67.5682	0.9980	-53.9267	0.9980	-31.0006
5	0	1.0016	-66.8148	1.0016	-53.2425	1.0012	-30.5116
6	2	0.9900	-72.1614	0.9900	-57.9976	0.9900	-33.4484
7	0	0.9893	-73.6024	0.9893	-59.2152	0.9893	-33.9689
8	2	1.0150	-57.7976	1.0150	-45.1172	1.0150	-25.0459
9	0	1.0429	-50.5436	1.0429	-37.8631	1.0429	-17.7918
10	2	1.0500	-42.9627	1.0500	-30.2822	1.0500	-10.2103
11	0	0.9827	-72.8181	0.9835	-58.5731	0.9848	-33.8662
12	2	0.9900	-75.6017	0.9900	-60.8467	0.9900	-34.4525
13	0	0.9643	-71.7818	0.9659	-58.0832	0.9678	-35.6793
14	0	0.0078	-145.1318	0.9818	-58.9640	0.9839	-35.6632
15	2	0.9700	-63.7112	0.9700	-51.8838	0.9700	-37.3143
16	0	0.9724	-71.2930	0.0165	-110.1142	0.9824	-34.9031
17	0	0.9857	-59.3716	0.9365	-47.9731	0.9902	-33.4047
18	2	0.9730	-61.5598	0.9730	-50.7356	0.9730	-37.5487
19	2	0.9620	-61.8474	0.9620	-50.7599	0.9620	-39.8218
20	0	0.9484	-58.7283	0.9511	-48.1950	0.0182	-105.9121
21	0	0.9452	-55.4552	0.9491	-45.3457	0.1867	-37.8975
22	0	0.9554	-50.9578	0.9597	-41.3412	0.4567	-27.4096
23	0	0.9935	-43.0081	0.9955	-34.1566	0.9309	-22.0201
24	2	0.9920	-38.3338	0.9920	-30.6794	0.9920	-21.0883
25	2	1.0500	-39.2527	1.0500	-29.4835	1.0500	-16.5402
26	2	1.0150	-38.5703	1.0150	-28.3939	1.0150	-14.9532
27	2	0.9680	-53.0431	0.9680	-43.2502	0.9680	-30.1388
28	0	0.9614	-55.3739	0.9615	-45.4924	0.9615	-32.1117
29	0	0.9633	-57.0419	0.9633	-47.0619	0.9633	-33.3809
30	0	0.9894	-52.3069	0.9775	-41.2351	1.0029	-26.4175
31	2	0.9670	-57.1657	0.9670	-47.1505	0.9670	-33.3626
32	2	0.9630	-53.6125	0.9630	-43.8653	0.9630	-30.8622
33	0	0.9616	-58.9292	0.9646	-48.5445	0.9681	-35.7730
34	2	0.9840	-52.3673	0.9840	-43.5846	0.9840	-32.8710
35	0	0.9788	-52.7720	0.9791	-44.0003	0.9797	-33.2645
36	2	0.9800	-52.8007	0.9800	-44.0236	0.9800	-33.2878
37	0	0.9811	-51.7069	0.9826	-42.9634	0.9863	-32.2326
38	0	0.9590	-44.8502	0.9675	-36.2861	0.9888	-25.4348

39	0	0.9667	-54.5861	0.9670	-46.3701	0.9680	-36.2915
40	2	0.9700	-55.3508	0.9700	-47.4423	0.9700	-37.7498
41	0	0.9667	-55.4938	0.9668	-47.8325	0.9669	-38.4574
42	2	0.9850	-53.0687	0.9850	-46.0838	0.9850	-37.5773
43	0	0.9473	-46.5590	0.9559	-39.2896	0.9638	-30.4452
44	0	0.9388	-34.8425	0.9489	-30.0441	0.9585	-24.1373
45	0	0.9547	-29.7364	0.9613	-25.8333	0.9679	-21.0013
46	2	1.0050	-24.7638	1.0050	-21.4589	1.0050	-17.3796
47	0	1.0095	-20.3754	1.0119	-17.6286	1.0144	-14.2340
48	0	1.0143	-22.5985	1.0144	-19.4830	1.0144	-15.6219
49	2	1.0250	-21.5518	1.0250	-18.4864	1.0250	-14.6831
50	0	1.0009	-23.7053	1.0008	-20.6795	1.0008	-16.9160
51	0	0.9665	-26.4817	0.9664	-23.5070	0.9663	-19.7949
52	0	0.9564	-27.4830	0.9563	-24.5222	0.9562	-20.8240
53	0	0.9458	-28.5890	0.9457	-25.6659	0.9457	-22.0057
54	2	0.9550	-27.7736	0.9550	-24.8782	0.9550	-21.2458
55	2	0.9520	-27.8523	0.9520	-24.9653	0.9520	-21.3415
56	2	0.9540	-27.8224	0.9540	-24.9277	0.9540	-21.2960
57	0	0.9704	-26.4551	0.9703	-23.5041	0.9703	-19.8157
58	0	0.9588	-27.3474	0.9587	-24.4066	0.9587	-20.7287
59	2	0.9850	-20.7089	0.9850	-17.9540	0.9850	-14.4627
60	0	0.9931	-16.3105	0.9931	-13.5959	0.9931	-10.1449
61	2	0.9950	-15.4097	0.9950	-12.6996	0.9950	-9.2531
62	2	0.9980	-15.8398	0.9980	-13.1216	0.9980	-9.6670
63	0	0.9918	-16.8820	0.9919	-14.1711	0.9920	-10.7239
64	0	0.9979	-14.9383	0.9980	-12.2502	0.9980	-8.8258
65	2	1.0050	-11.4865	1.0050	-8.8571	1.0050	-5.4915
66	2	1.0500	-10.8915	1.0500	-8.1441	1.0500	-4.6591
67	0	1.0194	-13.9360	1.0194	-11.2016	1.0193	-7.7307
68	0	1.0120	-8.4948	1.0123	-6.7542	1.0124	-4.5313
69	3	1.0350	0	1.0350	0	1.0350	0
70	2	0.9840	-15.8948	0.9840	-13.6935	0.9840	-10.9596
71	0	0.9848	-18.1661	0.9857	-15.4718	0.9864	-12.1260
72	2	0.9800	-28.6720	0.9800	-23.4862	0.9800	-17.0495
73	2	0.9910	-18.4003	0.9910	-15.6965	0.9910	-12.3425
74	2	0.9580	-14.3002	0.9580	-12.7975	0.9580	-10.9363
75	0	0.9642	-12.1715	0.9652	-10.9111	0.9662	-9.3469
76	2	0.9430	-13.2208	0.9430	-12.0461	0.9430	-10.5826
77	2	1.0060	-8.0644	1.0060	-7.0379	1.0060	-5.7461
78	0	1.0018	-8.2998	1.0018	-7.2353	1.0018	-5.8940
79	0	1.0043	-7.8792	1.0042	-6.7413	1.0042	-5.3044

80	2	1.0400	-5.4614	1.0400	-4.1231	1.0400	-2.4209
81	0	1.0281	-7.4519	1.0282	-5.8549	1.0282	-3.8192
82	0	0.9773	-6.5259	0.9773	-5.3559	0.9774	-3.8772
83	0	0.9717	-4.2076	0.9717	-3.0279	0.9717	-1.5364
84	0	0.9747	-0.0023	0.9747	1.1932	0.9747	2.7053
85	2	0.9850	2.3368	0.9850	3.5399	0.9850	5.0617
86	0	0.9867	0.9674	0.9867	2.1704	0.9867	3.6923
87	2	1.0150	1.2266	1.0150	2.4297	1.0150	3.9515
88	0	0.9859	6.9827	0.9859	8.1993	0.9858	9.7387
89	2	1.0050	12.0783	1.0050	13.3041	1.0050	14.8556
90	2	0.9850	-0.1788	0.9850	1.0561	0.9850	2.6194
91	2	0.9800	-2.0206	0.9800	-0.7782	0.9800	0.7947
92	2	0.9900	-4.2716	0.9900	-3.0182	0.9900	-1.4309
93	0	0.9854	-6.2233	0.9854	-4.9672	0.9854	-3.3764
94	0	0.9886	-7.4596	0.9886	-6.2012	0.9887	-4.6072
95	0	0.9777	-7.8973	0.9777	-6.6444	0.9777	-5.0577
96	0	0.9878	-7.3835	0.9879	-6.1377	0.9879	-4.5602
97	0	1.0088	-6.7755	1.0088	-5.4817	1.0088	-3.8416
98	0	1.0233	-7.6668	1.0233	-6.3489	1.0233	-4.6773
99	2	1.0100	-8.6280	1.0100	-7.3322	1.0100	-5.6895
100	2	1.0170	-8.1321	1.0170	-6.8548	1.0170	-5.2361
101	0	0.9921	-7.3710	0.9921	-6.1038	0.9921	-4.4983
102	0	0.9896	-5.4098	0.9897	-4.1519	0.9897	-2.5586
103	2	1.0100	-11.8732	1.0100	-10.5958	1.0100	-8.9772
104	2	0.9710	-14.4432	0.9710	-13.1658	0.9710	-11.5471
105	2	0.9650	-15.5474	0.9650	-14.2700	0.9650	-12.6513
106	0	0.9611	-15.8076	0.9611	-14.5302	0.9611	-12.9115
107	2	0.9520	-18.6083	0.9520	-17.3309	0.9520	-15.7122
108	0	0.9662	-16.7475	0.9662	-15.4701	0.9662	-13.8514
109	0	0.9670	-17.2001	0.9670	-15.9227	0.9670	-14.3040
110	2	0.9730	-18.0470	0.9730	-16.7696	0.9730	-15.1509
111	2	0.9800	-16.4019	0.9800	-15.1245	0.9800	-13.5058
112	2	0.9750	-21.1462	0.9750	-19.8688	0.9750	-18.2501
113	2	0.9930	-58.9355	0.9930	-48.5250	0.9930	-33.2976
114	0	0.9601	-53.9359	0.9601	-44.1695	0.9601	-31.1208
115	0	0.9600	-53.9424	0.9600	-44.1727	0.9600	-31.1162
116	2	1.0050	-8.8842	1.0050	-7.1424	1.0050	-4.9189
117	0	0.9738	-77.1427	0.9738	-62.3877	0.9738	-35.9935
118	0	0.9478	-13.1243	0.9483	-11.9029	0.9488	-10.3845

Solution NO.		**7**		**8**		**9**	
Bus NO.	Bus Type	V (p.u.)	Angle (deg.)	V (p.u.)	Angle (deg.)	V (p.u.)	Angle (deg.)
1	2	0.9550	-31.6031	0.9550	-31.7435	0.9550	-50.3472
2	0	0.9714	-31.1288	0.9714	-31.2626	0.9714	-49.8800
3	0	0.9675	-30.6880	0.9675	-30.8311	0.9675	-49.4291
4	2	0.9980	-26.8394	0.9980	-26.9953	0.9980	-45.5627
5	0	1.0012	-26.3593	1.0012	-26.5177	1.0012	-45.0838
6	2	0.9900	-29.2424	0.9900	-29.3868	0.9900	-47.9822
7	0	0.9893	-29.7421	0.9893	-29.8810	0.9893	-48.4879
8	2	1.0150	-20.9944	1.0150	-21.1801	1.0150	-39.7158
9	0	1.0429	-13.7403	1.0429	-13.9260	1.0429	-32.4617
10	2	1.0500	-6.1592	1.0500	-6.3451	1.0500	-24.8808
11	0	0.9848	-29.6226	0.9848	-29.7556	0.9849	-48.3356
12	2	0.9900	-30.1914	0.9900	-30.3213	0.9900	-48.9469
13	0	0.9679	-31.3105	0.9680	-31.4015	0.9681	-49.8375
14	0	0.9840	-31.2627	0.9840	-31.3453	0.9841	-49.7931
15	2	0.9700	-32.5215	0.9700	-32.4705	0.9700	-50.4180
16	0	0.9825	-30.6078	0.9825	-30.7487	0.9821	-49.8338
17	0	0.9906	-29.0364	0.9907	-29.2013	0.9892	-49.2761
18	2	0.9730	-32.5918	0.9730	-32.5162	0.9730	-50.7495
19	2	0.9620	-34.2991	0.9620	-33.9918	0.9620	-50.3877
20	0	0.4050	-38.3925	0.5652	-37.9757	0.9562	-50.1251
21	0	0.0209	-77.6589	0.2889	-42.3680	0.9563	-48.9833
22	0	0.3417	-23.2169	0.0140	-77.7819	0.9662	-46.9260
23	0	0.9161	-18.8404	0.8718	-19.8575	0.9928	-42.7654
24	2	0.9920	-18.6076	0.9920	-20.1098	0.9920	-38.1058
25	2	1.0500	-13.0962	1.0500	-13.9766	1.0500	-37.6405
26	2	1.0150	-11.3907	1.0150	-12.0815	1.0150	-34.1951
27	2	0.9680	-26.5545	0.9680	-27.5566	0.9680	-61.2635
28	0	0.9616	-28.4328	0.9616	-29.3492	0.0101	-116.5587
29	0	0.9633	-29.5965	0.9632	-30.4173	0.7102	-64.8742
30	0	1.0047	-22.5623	1.0051	-22.8008	0.9992	-41.2595
31	2	0.9670	-29.5407	0.9670	-30.3274	0.9670	-65.1049
32	2	0.9630	-27.2898	0.9630	-28.3821	0.9630	-58.3161
33	0	0.9688	-31.6583	0.9688	-31.6547	0.9659	-47.6270
34	2	0.9840	-29.4669	0.9840	-29.5044	0.9840	-43.2720
35	0	0.9798	-29.8807	0.9798	-29.9234	0.9793	-43.6913
36	2	0.9800	-29.8978	0.9800	-29.9391	0.9800	-43.7115
37	0	0.9868	-28.8797	0.9868	-28.9290	0.9840	-42.6719
38	0	0.9924	-22.3206	0.9925	-22.4335	0.9760	-36.1890

39	0	0.9681	-33.1626	0.9681	-33.2100	0.9675	-46.0852
40	2	0.9700	-34.7520	0.9700	-34.7983	0.9700	-47.1644
41	0	0.9669	-35.5622	0.9669	-35.6077	0.9668	-47.5680
42	2	0.9850	-34.9628	0.9850	-35.0061	0.9850	-45.8562
43	0	0.9658	-27.6552	0.9658	-27.6909	0.9563	-39.0535
44	0	0.9611	-22.2913	0.9610	-22.3242	0.9494	-29.9306
45	0	0.9697	-19.5023	0.9697	-19.5341	0.9616	-25.7644
46	2	1.0050	-16.1278	1.0050	-16.1579	1.0050	-21.4167
47	0	1.0150	-13.1982	1.0150	-13.2255	1.0119	-17.6042
48	0	1.0145	-14.4431	1.0145	-14.4747	1.0144	-19.4575
49	2	1.0250	-13.5236	1.0250	-13.5556	1.0250	-18.4653
50	0	1.0008	-15.7700	1.0008	-15.8030	1.0008	-20.6659
51	0	0.9663	-18.6660	0.9663	-18.7003	0.9664	-23.5029
52	0	0.9561	-19.6999	0.9561	-19.7345	0.9563	-24.5207
53	0	0.9456	-20.8943	0.9456	-20.9299	0.9457	-25.6715
54	2	0.9550	-20.1437	0.9550	-20.1800	0.9550	-24.8890
55	2	0.9520	-20.2423	0.9520	-20.2787	0.9520	-24.9777
56	2	0.9540	-20.1942	0.9540	-20.2304	0.9540	-24.9386
57	0	0.9702	-18.6949	0.9702	-18.7297	0.9703	-23.5044
58	0	0.9586	-19.6113	0.9586	-19.6464	0.9587	-24.4089
59	2	0.9850	-13.4078	0.9850	-13.4476	0.9850	-17.9911
60	0	0.9931	-9.1035	0.9931	-9.1443	0.9931	-13.6405
61	2	0.9950	-8.2133	0.9950	-8.2542	0.9950	-12.7451
62	2	0.9980	-8.6244	0.9980	-8.6651	0.9980	-13.1656
63	0	0.9921	-9.6838	0.9921	-9.7247	0.9920	-14.2164
64	0	0.9981	-7.7934	0.9981	-7.8348	0.9980	-12.2998
65	2	1.0050	-4.4788	1.0050	-4.5217	1.0050	-8.9177
66	2	1.0500	-3.6069	1.0500	-3.6468	1.0500	-8.1824
67	0	1.0193	-6.6827	1.0193	-6.7230	1.0194	-11.2425
68	0	1.0124	-3.8649	1.0124	-3.8986	1.0123	-6.8240
69	3	1.0350	0	1.0350	0	1.0350	0
70	2	0.9840	-10.2518	0.9840	-10.6518	0.9840	-15.7022
71	0	0.9865	-11.2615	0.9865	-11.7589	0.9848	-17.9703
72	2	0.9800	-15.3932	0.9800	-16.3824	0.9800	-28.4599
73	2	0.9910	-11.4764	0.9910	-11.9747	0.9910	-18.2044
74	2	0.9580	-10.4479	0.9580	-10.6922	0.9580	-14.0279
75	0	0.9664	-8.9324	0.9663	-9.1253	0.9643	-11.8764
76	2	0.9430	-10.1839	0.9430	-10.3273	0.9430	-12.7525
77	2	1.0060	-5.3763	1.0060	-5.4465	1.0060	-7.3549
78	0	1.0018	-5.5084	1.0018	-5.5766	1.0018	-7.5391
79	0	1.0042	-4.8884	1.0042	-4.9529	1.0042	-7.0198

80	2	1.0400	-1.9187	1.0400	-1.9745	1.0400	-4.3319
81	0	1.0282	-3.2124	1.0281	-3.2534	1.0282	-5.9744
82	0	0.9774	-3.4478	0.9774	-3.5107	0.9774	-5.6232
83	0	0.9717	-1.1030	0.9717	-1.1653	0.9717	-3.2918
84	0	0.9747	3.1452	0.9747	3.0837	0.9747	0.9348
85	2	0.9850	5.5048	0.9850	5.4436	0.9850	3.2840
86	0	0.9867	4.1353	0.9867	4.0742	0.9867	1.9146
87	2	1.0150	4.3945	1.0150	4.3334	1.0150	2.1738
88	0	0.9858	10.1873	0.9858	10.1268	0.9858	7.9481
89	2	1.0050	15.3081	1.0050	15.2480	1.0050	13.0561
90	2	0.9850	3.0757	0.9850	3.0161	0.9850	0.8113
91	2	0.9800	1.2541	0.9800	1.1949	0.9800	-1.0205
92	2	0.9900	-0.9670	0.9900	-1.0257	0.9900	-3.2567
93	0	0.9854	-2.9113	0.9854	-2.9698	0.9854	-5.2048
94	0	0.9887	-4.1412	0.9887	-4.1995	0.9886	-6.4379
95	0	0.9778	-4.5939	0.9778	-4.6526	0.9777	-6.8831
96	0	0.9880	-4.0994	0.9880	-4.1584	0.9879	-6.3788
97	0	1.0088	-3.3608	1.0088	-3.4174	1.0088	-5.7062
98	0	1.0233	-4.1865	1.0233	-4.2418	1.0233	-6.5650
99	2	1.0100	-5.2080	1.0100	-5.2644	1.0100	-7.5560
100	2	1.0170	-4.7622	1.0170	-4.8196	1.0170	-7.0849
101	0	0.9921	-4.0287	0.9921	-4.0866	0.9921	-6.3375
102	0	0.9897	-2.0927	0.9897	-2.1511	0.9897	-4.3888
103	2	1.0100	-8.5033	1.0100	-8.5607	1.0100	-10.8260
104	2	0.9710	-11.0732	0.9710	-11.1306	0.9710	-13.3960
105	2	0.9650	-12.1774	0.9650	-12.2348	0.9650	-14.5002
106	0	0.9611	-12.4376	0.9611	-12.4950	0.9611	-14.7603
107	2	0.9520	-15.2383	0.9520	-15.2957	0.9520	-17.5611
108	0	0.9662	-13.3775	0.9662	-13.4349	0.9662	-15.7003
109	0	0.9670	-13.8301	0.9670	-13.8875	0.9670	-16.1529
110	2	0.9730	-14.6770	0.9730	-14.7344	0.9730	-16.9997
111	2	0.9800	-13.0319	0.9800	-13.0893	0.9800	-15.3546
112	2	0.9750	-17.7762	0.9750	-17.8336	0.9750	-20.0989
113	2	0.9930	-29.0232	0.9930	-29.3017	0.9930	-50.6650
114	0	0.9601	-27.5434	0.9601	-28.5978	0.9598	-60.1204
115	0	0.9600	-27.5379	0.9600	-28.5858	0.9597	-60.3793
116	2	1.0050	-4.2524	1.0050	-4.2862	1.0050	-7.2122
117	0	0.9738	-31.7324	0.9738	-31.8623	0.9738	-50.4879
118	0	0.9489	-9.9771	0.9489	-10.1471	0.9478	-12.7488

Solution NO.		**10**		**11**		**12**	
Bus NO.	Bus Type	V (p.u.)	Angle (deg.)	V (p.u.)	Angle (deg.)	V (p.u.)	Angle (deg.)
1	2	0.9550	-46.8041	0.9550	-29.4877	0.9550	-26.9477
2	0	0.9714	-46.4067	0.9714	-28.9657	0.9714	-26.4208
3	0	0.9675	-45.8566	0.9675	-28.5927	0.9675	-26.0548
4	2	0.9980	-41.8582	0.9980	-24.8384	0.9980	-22.3101
5	0	1.0013	-41.3492	1.0011	-24.3747	1.0011	-21.8482
6	2	0.9900	-44.3970	0.9900	-27.1558	0.9900	-24.6188
7	0	0.9893	-44.9606	0.9893	-27.6159	0.9893	-25.0748
8	2	1.0150	-35.6638	1.0150	-19.1980	1.0150	-16.6915
9	0	1.0429	-28.4097	1.0429	-11.9438	1.0429	-9.4374
10	2	1.0500	-20.8288	1.0500	-4.3630	1.0500	-1.8565
11	0	0.9846	-44.9089	0.9849	-27.4688	0.9849	-24.9238
12	2	0.9900	-45.5151	0.9900	-27.9999	0.9900	-25.4520
13	0	0.9673	-47.0765	0.9681	-28.9452	0.9681	-26.3721
14	0	0.9836	-47.1281	0.9841	-28.8378	0.9841	-26.2585
15	2	0.9700	-49.9119	0.9700	-29.4395	0.9700	-26.7714
16	0	0.9815	-45.8206	0.9823	-28.2879	0.9824	-25.7416
17	0	0.9875	-44.0024	0.9900	-26.4380	0.9903	-23.8960
18	2	0.9730	-47.1178	0.9730	-28.9785	0.9730	-26.3514
19	2	0.9620	-48.3439	0.9620	-29.6830	0.9620	-26.9777
20	0	0.9502	-45.5145	0.9552	-28.1539	0.9557	-25.6248
21	0	0.9479	-42.4656	0.9551	-26.0836	0.9559	-23.6855
22	0	0.9585	-38.2321	0.9662	-22.9776	0.9670	-20.7295
23	0	0.9957	-30.6970	0.9985	-17.1961	0.9988	-15.1824
24	2	0.9920	-27.7107	0.9920	-16.1323	0.9920	-14.4195
25	2	1.0500	-25.5434	1.0500	-11.0675	1.0500	-8.8619
26	2	1.0150	-24.2740	1.0150	-9.5353	1.0150	-7.2560
27	2	0.9680	-39.1309	0.9680	-23.8477	0.9680	-21.5799
28	0	0.9615	-41.2858	0.9616	-25.7026	0.9616	-23.4006
29	0	0.9633	-42.7578	0.9632	-26.8401	0.9632	-24.5000
30	0	0.9915	-36.5749	1.0045	-21.1202	1.0060	-18.6560
31	2	0.9670	-42.8118	0.9670	-26.7750	0.9670	-24.4213
32	2	0.9630	-39.7415	0.9630	-24.3799	0.9630	-22.1126
33	0	0.0181	-98.3286	0.9688	-31.2071	0.9692	-28.2175
34	2	0.9840	-45.2302	0.9840	-32.5459	0.9840	-28.8615
35	0	0.9719	-45.5828	0.9798	-32.7029	0.9799	-29.1631
36	2	0.9800	-45.6908	0.9800	-32.7885	0.9800	-29.2094
37	0	0.9410	-44.0600	0.9868	-31.3699	0.9872	-28.0215
38	0	0.9505	-34.9179	0.9888	-23.1243	0.9937	-20.6922

39	0	0.9515	-48.0111	0.9681	-35.5527	0.9679	-32.8101
40	2	0.9700	-49.2881	0.9700	-37.0840	0.9700	-34.6935
41	0	0.9668	-49.5896	0.9669	-37.8498	0.9669	-35.7283
42	2	0.9850	-47.5983	0.9850	-37.1290	0.9850	-35.7427
43	0	0.9539	-40.5402	0.0250	-83.1509	0.5733	-32.3876
44	0	0.9464	-30.6587	0.5594	-22.2844	0.0238	-73.9865
45	0	0.9597	-26.2165	0.7782	-20.0058	0.5102	-24.0247
46	2	1.0050	-21.7040	1.0050	-18.4196	1.0050	-23.3499
47	0	1.0118	-17.7795	1.0139	-14.7526	1.0111	-17.5217
48	0	1.0143	-19.6435	1.0143	-16.1405	1.0134	-19.0139
49	2	1.0250	-18.6245	1.0250	-15.0638	1.0250	-17.3936
50	0	1.0009	-20.7733	1.0009	-17.2226	1.0012	-19.3511
51	0	0.9665	-23.5437	0.9665	-20.0060	0.9671	-21.8751
52	0	0.9565	-24.5434	0.9564	-21.0093	0.9570	-22.8081
53	0	0.9458	-25.6449	0.9458	-22.1204	0.9461	-23.7275
54	2	0.9550	-24.8262	0.9550	-21.3088	0.9550	-22.7751
55	2	0.9520	-24.9039	0.9520	-21.3886	0.9520	-22.8116
56	2	0.9540	-24.8750	0.9540	-21.3577	0.9540	-22.8205
57	0	0.9704	-23.5143	0.9704	-19.9827	0.9707	-21.7317
58	0	0.9588	-24.4054	0.9588	-20.8764	0.9592	-22.5731
59	2	0.9850	-17.7449	0.9850	-14.2634	0.9850	-15.0108
60	0	0.9931	-13.3417	0.9931	-9.8704	0.9931	-10.4113
61	2	0.9950	-12.4403	0.9950	-8.9702	0.9950	-9.4878
62	2	0.9980	-12.8714	0.9980	-9.3993	0.9980	-9.9582
63	0	0.9918	-13.9127	0.9919	-10.4424	0.9913	-10.9642
64	0	0.9979	-11.9664	0.9979	-8.5019	0.9975	-8.9070
65	2	1.0050	-8.5077	1.0050	-5.0582	1.0050	-5.1630
66	2	1.0500	-7.9269	1.0500	-4.4470	1.0500	-5.1564
67	0	1.0194	-10.9696	1.0194	-7.4933	1.0194	-8.1344
68	0	1.0123	-6.5152	1.0124	-4.2307	1.0124	-4.2920
69	3	1.0350	0	1.0350	0	1.0350	0
70	2	0.9840	-12.8784	0.9840	-9.6270	0.9840	-9.1818
71	0	0.9859	-14.4635	0.9867	-10.4740	0.9867	-9.9178
72	2	0.9800	-21.5022	0.9800	-13.7822	0.9800	-12.6637
73	2	0.9910	-14.6852	0.9910	-10.6876	0.9910	-10.1307
74	2	0.9580	-12.2806	0.9580	-10.1055	0.9580	-9.8435
75	0	0.9655	-10.4952	0.9666	-8.6822	0.9667	-8.4801
76	2	0.9430	-11.7103	0.9430	-10.0604	0.9430	-9.9251
77	2	1.0060	-6.8242	1.0060	-5.4363	1.0060	-5.3986
78	0	1.0018	-7.0203	1.0018	-5.5847	1.0018	-5.5522
79	0	1.0042	-6.5237	1.0042	-4.9961	1.0042	-4.9738

80	2	1.0400	-3.8994	1.0400	-2.1154	1.0400	-2.1215
81	0	1.0282	-5.6210	1.0282	-3.5167	1.0282	-3.5581
82	0	0.9773	-5.1372	0.9774	-3.5692	0.9774	-3.5514
83	0	0.9717	-2.8088	0.9717	-1.2286	0.9717	-1.2121
84	0	0.9747	1.4129	0.9747	3.0129	0.9747	3.0272
85	2	0.9850	3.7598	0.9850	5.3692	0.9850	5.3825
86	0	0.9867	2.3904	0.9867	3.9998	0.9867	4.0131
87	2	1.0150	2.6496	1.0150	4.2590	1.0150	4.2723
88	0	0.9859	8.4197	0.9858	10.0460	0.9858	10.0574
89	2	1.0050	13.5249	1.0050	15.1628	1.0050	15.1729
90	2	0.9850	1.2772	0.9850	2.9265	0.9850	2.9354
91	2	0.9800	-0.5569	0.9800	1.1017	0.9800	1.1096
92	2	0.9900	-2.7966	0.9900	-1.1241	0.9900	-1.1178
93	0	0.9854	-4.7454	0.9854	-3.0695	0.9854	-3.0636
94	0	0.9886	-5.9793	0.9887	-4.3004	0.9887	-4.2948
95	0	0.9777	-6.4228	0.9777	-4.7508	0.9777	-4.7444
96	0	0.9879	-5.9163	0.9879	-4.2532	0.9879	-4.2459
97	0	1.0088	-5.2586	1.0088	-3.5352	1.0088	-3.5345
98	0	1.0233	-6.1250	1.0233	-4.3713	1.0233	-4.3739
99	2	1.0100	-7.1090	1.0100	-5.3832	1.0100	-5.3828
100	2	1.0170	-6.6322	1.0170	-4.9295	1.0170	-4.9266
101	0	0.9921	-5.8816	0.9921	-4.1917	0.9921	-4.1873
102	0	0.9897	-3.9301	0.9897	-2.2518	0.9897	-2.2461
103	2	1.0100	-10.3733	1.0100	-8.6706	1.0100	-8.6676
104	2	0.9710	-12.9433	0.9710	-11.2406	0.9710	-11.2376
105	2	0.9650	-14.0475	0.9650	-12.3448	0.9650	-12.3418
106	0	0.9611	-14.3077	0.9611	-12.6050	0.9611	-12.6020
107	2	0.9520	-17.1084	0.9520	-15.4057	0.9520	-15.4027
108	0	0.9662	-15.2476	0.9662	-13.5449	0.9662	-13.5419
109	0	0.9670	-15.7002	0.9670	-13.9975	0.9670	-13.9945
110	2	0.9730	-16.5470	0.9730	-14.8443	0.9730	-14.8414
111	2	0.9800	-14.9020	0.9800	-13.1993	0.9800	-13.1963
112	2	0.9750	-19.6463	0.9750	-17.9436	0.9750	-17.9406
113	2	0.9930	-43.7228	0.9930	-26.3945	0.9930	-23.8818
114	0	0.9601	-40.0476	0.9601	-24.7190	0.9601	-22.4515
115	0	0.9600	-40.0511	0.9600	-24.7281	0.9600	-22.4606
116	2	1.0050	-6.9033	1.0050	-4.6183	1.0050	-4.6796
117	0	0.9738	-47.0561	0.9738	-29.5409	0.9738	-26.9930
118	0	0.9484	-11.5238	0.9490	-9.7854	0.9491	-9.6142

Solution NO.		**13**		**14**		**15**	
Bus NO.	Bus Type	V (p.u.)	Angle (deg.)	V (p.u.)	Angle (deg.)	V (p.u.)	Angle (deg.)
1	2	0.9550	-41.2050	0.9550	-37.2767	0.9550	-31.1542
2	0	0.9714	-40.6799	0.9714	-36.7493	0.9714	-30.6232
3	0	0.9675	-40.3113	0.9675	-36.3838	0.9675	-30.2628
4	2	0.9980	-36.5633	0.9980	-32.6402	0.9980	-26.5261
5	0	1.0011	-36.1003	1.0011	-32.1781	1.0011	-26.0654
6	2	0.9900	-38.8750	0.9900	-34.9480	0.9900	-28.8276
7	0	0.9893	-39.3325	0.9893	-35.4036	0.9893	-29.2803
8	2	1.0150	-30.9339	1.0150	-27.0213	1.0150	-20.9239
9	0	1.0429	-23.6798	1.0429	-19.7671	1.0429	-13.6698
10	2	1.0500	-16.0987	1.0500	-12.1859	1.0500	-6.0889
11	0	0.9849	-39.1860	0.9849	-35.2548	0.9849	-29.1276
12	2	0.9900	-39.7123	0.9900	-35.7804	0.9900	-29.6522
13	0	0.9681	-40.6630	0.9681	-36.7154	0.9681	-30.5620
14	0	0.9841	-40.5523	0.9841	-36.6017	0.9841	-30.4435
15	2	0.9700	-41.1596	0.9700	-37.1565	0.9700	-30.9140
16	0	0.9821	-39.9608	0.9822	-36.0377	0.9824	-29.9237
17	0	0.9896	-38.0244	0.9899	-34.1213	0.9903	-28.0390
18	2	0.9730	-40.6042	0.9730	-36.6438	0.9730	-30.4714
19	2	0.9620	-41.3413	0.9620	-37.3291	0.9620	-31.0748
20	0	0.9532	-39.2654	0.9540	-35.4657	0.9552	-29.5487
21	0	0.9523	-36.7861	0.9534	-33.1458	0.9551	-27.4807
22	0	0.9632	-33.2102	0.9644	-29.7533	0.9662	-24.3772
23	0	0.9973	-26.6947	0.9978	-23.5240	0.9985	-18.5993
24	2	0.9920	-24.3745	0.9920	-21.6355	0.9920	-17.3920
25	2	1.0500	-21.4925	1.0500	-18.0208	1.0500	-12.6220
26	2	1.0150	-20.3514	1.0150	-16.7523	1.0150	-11.1647
27	2	0.9680	-34.4114	0.9680	-30.8742	0.9680	-25.3726
28	0	0.9615	-36.3872	0.9615	-32.8056	0.9616	-27.2336
29	0	0.9633	-37.6597	0.9633	-34.0285	0.9632	-28.3780
30	0	1.0038	-32.8735	1.0048	-28.9819	1.0064	-22.9180
31	2	0.9670	-37.6426	0.9670	-33.9937	0.9670	-28.3153
32	2	0.9630	-34.9155	0.9630	-31.3839	0.9630	-25.8916
33	0	0.9684	-43.4736	0.9687	-39.1756	0.9692	-32.4486
34	2	0.9840	-45.0763	0.9840	-40.3286	0.9840	-32.9139
35	0	0.9797	-45.3860	0.9798	-40.6894	0.9799	-33.3366
36	2	0.9800	-45.4315	0.9800	-40.7207	0.9800	-33.3505
37	0	0.9864	-44.2465	0.9867	-39.6192	0.9873	-32.3515
38	0	0.9885	-35.7179	0.9913	-31.6727	0.9958	-25.3684

39	0	0.9654	-51.3289	0.9658	-46.4506	0.9668	-38.4238
40	2	0.9700	-54.5336	0.9700	-49.5121	0.9700	-41.0498
41	0	0.9663	-56.5328	0.9664	-51.4109	0.9667	-42.6354
42	2	0.9850	-59.1827	0.9850	-53.7861	0.9850	-44.1553
43	0	0.9469	-53.3766	0.9635	-46.0286	0.9712	-35.2474
44	0	0.9392	-63.3259	0.9624	-51.8880	0.9703	-36.0944
45	0	0.9507	-66.0853	0.9717	-53.1917	0.9776	-35.5880
46	2	1.0050	-75.7309	1.0050	-56.3393	1.0050	-33.1179
47	0	0.0138	-125.5228	0.9733	-44.3538	0.9997	-29.5205
48	0	0.9994	-58.0984	0.0095	-90.1966	1.0149	-33.3607
49	2	1.0250	-53.0330	1.0250	-46.4282	1.0250	-32.9517
50	0	1.0020	-53.0558	1.0021	-46.7730	0.0105	-91.9665
51	0	0.9694	-53.0992	0.9694	-47.2287	0.9648	-39.1614
52	0	0.9599	-53.3632	0.9598	-47.6036	0.9547	-40.3124
53	0	0.9474	-52.4401	0.9474	-46.9878	0.9449	-41.8229
54	2	0.9550	-50.1219	0.9550	-44.8985	0.9550	-41.3026
55	2	0.9520	-49.7285	0.9520	-44.5782	0.9520	-41.2956
56	2	0.9540	-50.1346	0.9540	-44.9165	0.9540	-41.7614
57	0	0.9711	-51.7990	0.9714	-46.1219	0.5505	-43.2618
58	0	0.9602	-52.1431	0.9603	-46.5483	0.9576	-40.5622
59	2	0.9850	-35.0073	0.9850	-31.0668	0.9850	-26.9559
60	0	0.9928	-28.2387	0.9929	-24.6843	0.9928	-20.1029
61	2	0.9950	-27.0793	0.9950	-23.5656	0.9950	-19.0166
62	2	0.9980	-27.9413	0.9980	-24.3641	0.9980	-19.4693
63	0	0.9849	-28.6265	0.9862	-25.0963	0.9860	-20.8418
64	0	0.9923	-25.3545	0.9934	-22.0391	0.9935	-17.7119
65	2	1.0050	-18.5184	1.0050	-15.7444	1.0050	-11.5587
66	2	1.0500	-24.5228	1.0500	-20.7271	1.0500	-14.2702
67	0	1.0199	-26.8751	1.0198	-23.1783	1.0193	-17.4280
68	0	1.0108	-13.0228	1.0114	-11.2006	1.0120	-8.4573
69	3	1.0350	0	1.0350	0	1.0350	0
70	2	0.9840	-12.4983	0.9840	-11.6242	0.9840	-10.2855
71	0	0.9863	-13.8199	0.9864	-12.7804	0.9866	-11.1853
72	2	0.9800	-19.5267	0.9800	-17.6512	0.9800	-14.7607
73	2	0.9910	-14.0380	0.9910	-12.9967	0.9910	-11.3993
74	2	0.9580	-12.6634	0.9580	-11.9620	0.9580	-10.8960
75	0	0.9653	-11.1155	0.9657	-10.4762	0.9662	-9.5068
76	2	0.9430	-13.1646	0.9430	-12.4215	0.9430	-11.3009
77	2	1.0060	-9.4422	1.0060	-8.5658	1.0060	-7.2501
78	0	1.0017	-9.8452	1.0017	-8.9186	1.0018	-7.5269
79	0	1.0043	-9.7487	1.0043	-8.7247	1.0043	-7.1862

80	2	1.0400	-8.2351	1.0400	-6.9416	1.0400	-4.9944
81	0	1.0274	-11.3464	1.0278	-9.7146	1.0282	-7.2586
82	0	0.9772	-8.5375	0.9772	-7.4708	0.9773	-5.8679
83	0	0.9717	-6.2626	0.9717	-5.1829	0.9717	-3.5603
84	0	0.9747	-2.1274	0.9747	-1.0266	0.9747	0.6278
85	2	0.9850	0.1783	0.9850	1.2893	0.9850	2.9587
86	0	0.9867	-1.1911	0.9867	-0.0802	0.9867	1.5892
87	2	1.0150	-0.9319	1.0150	0.1790	1.0150	1.8484
88	0	0.9859	4.7646	0.9859	5.8934	0.9859	7.5899
89	2	1.0050	9.8194	1.0050	10.9605	1.0050	12.6754
90	2	0.9850	-2.4777	0.9850	-1.3246	0.9850	0.4084
91	2	0.9800	-4.3522	0.9800	-3.1894	0.9800	-1.4414
92	2	0.9900	-6.6518	0.9900	-5.4743	0.9900	-3.7044
93	0	0.9853	-8.6152	0.9854	-7.4345	0.9854	-5.6591
94	0	0.9885	-9.8622	0.9885	-8.6781	0.9886	-6.8980
95	0	0.9775	-10.2753	0.9775	-9.0986	0.9776	-7.3296
96	0	0.9875	-9.7299	0.9876	-8.5627	0.9878	-6.8080
97	0	1.0087	-9.3334	1.0087	-8.1027	1.0088	-6.2523
98	0	1.0233	-10.3313	1.0233	-9.0686	1.0233	-7.1700
99	2	1.0100	-11.1952	1.0100	-9.9616	1.0100	-8.1071
100	2	1.0170	-10.6181	1.0170	-9.4089	1.0170	-7.5912
101	0	0.9921	-9.8125	0.9921	-8.6167	0.9921	-6.8190
102	0	0.9896	-7.8105	0.9896	-6.6269	0.9896	-4.8478
103	2	1.0100	-14.3595	1.0100	-13.1502	1.0100	-11.3323
104	2	0.9710	-16.9296	0.9710	-15.7203	0.9710	-13.9023
105	2	0.9650	-18.0338	0.9650	-16.8245	0.9650	-15.0065
106	0	0.9611	-18.2940	0.9611	-17.0847	0.9611	-15.2666
107	2	0.9520	-21.0947	0.9520	-19.8854	0.9520	-18.0674
108	0	0.9662	-19.2339	0.9662	-18.0246	0.9662	-16.2065
109	0	0.9670	-19.6865	0.9670	-18.4772	0.9670	-16.6591
110	2	0.9730	-20.5334	0.9730	-19.3241	0.9730	-17.5060
111	2	0.9800	-18.8883	0.9800	-17.6790	0.9800	-15.8609
112	2	0.9750	-23.6326	0.9750	-22.4233	0.9750	-20.6052
113	2	0.9930	-37.8557	0.9930	-33.9946	0.9930	-27.9795
114	0	0.9601	-35.2665	0.9601	-31.7325	0.9601	-26.2363
115	0	0.9600	-35.2776	0.9600	-31.7432	0.9600	-26.2463
116	2	1.0050	-13.4185	1.0050	-11.5934	1.0050	-8.8468
117	0	0.9738	-41.2533	0.9738	-37.3214	0.9738	-31.1932
118	0	0.9482	-12.5308	0.9485	-11.8430	0.9488	-10.8031

Solution NO.		**16**		**17**		**18**	
Bus NO.	Bus Type	V (p.u.)	Angle (deg.)	V (p.u.)	Angle (deg.)	V (p.u.)	Angle (deg.)
1	2	0.9550	-26.0291	0.9550	-25.0192	0.9550	-29.2947
2	0	0.9714	-25.4966	0.9714	-24.4865	0.9714	-28.7621
3	0	0.9675	-25.1384	0.9675	-24.1286	0.9675	-28.4041
4	2	0.9980	-21.4046	0.9980	-20.3951	0.9980	-24.6708
5	0	1.0011	-20.9446	1.0011	-19.9352	1.0011	-24.2107
6	2	0.9900	-23.7035	0.9900	-22.6937	0.9900	-26.9692
7	0	0.9893	-24.1549	0.9893	-23.1449	0.9893	-27.4205
8	2	1.0150	-15.8100	1.0150	-14.8017	1.0150	-19.0765
9	0	1.0429	-8.5561	1.0429	-7.5477	1.0429	-11.8224
10	2	1.0500	-0.9752	1.0500	0.0333	1.0500	-4.2410
11	0	0.9849	-24.0000	0.9849	-22.9896	0.9849	-27.2662
12	2	0.9900	-24.5246	0.9900	-23.5143	0.9900	-27.7900
13	0	0.9681	-25.4195	0.9682	-24.4066	0.9681	-28.6892
14	0	0.9841	-25.2989	0.9841	-24.2857	0.9841	-28.5685
15	2	0.9700	-25.7213	0.9700	-24.7000	0.9700	-29.0029
16	0	0.9825	-24.8102	0.9825	-23.8027	0.9824	-28.0652
17	0	0.9906	-22.9564	0.9906	-21.9553	0.9905	-26.1889
18	2	0.9730	-25.3319	0.9730	-24.3206	0.9730	-28.5861
19	2	0.9620	-25.8837	0.9620	-24.8631	0.9620	-29.1573
20	0	0.9560	-24.6309	0.9561	-23.6639	0.9555	-27.7410
21	0	0.9563	-22.7657	0.9565	-21.8384	0.9556	-25.7545
22	0	0.9675	-19.8945	0.9677	-19.0126	0.9667	-22.7444
23	0	0.9990	-14.4801	0.9991	-13.6691	0.9987	-17.1127
24	2	0.9920	-13.8430	0.9920	-13.1447	0.9920	-16.1172
25	2	1.0500	-8.0971	1.0500	-7.2057	1.0500	-10.9906
26	2	1.0150	-6.4723	1.0150	-5.5471	1.0150	-9.4761
27	2	0.9680	-20.7717	0.9680	-19.8657	0.9680	-23.7068
28	0	0.9616	-22.5750	0.9616	-21.6577	0.9616	-25.5453
29	0	0.9632	-23.6552	0.9632	-22.7252	0.9632	-26.6647
30	0	1.0073	-17.8199	1.0074	-16.8140	1.0070	-21.0860
31	2	0.9670	-23.5695	0.9670	-22.6351	0.9670	-26.5931
32	2	0.9630	-21.3007	0.9630	-20.3968	0.9630	-24.2282
33	0	0.9694	-26.9014	0.9694	-25.8133	0.9693	-30.3534
34	2	0.9840	-26.9161	0.9840	-25.7442	0.9840	-30.5720
35	0	0.9799	-27.3618	0.9799	-26.1938	0.9799	-31.0119
36	2	0.9800	-27.3691	0.9800	-26.2001	0.9800	-31.0208
37	0	0.9876	-26.4087	0.9876	-25.2462	0.9875	-30.0509
38	0	0.9981	-20.0098	0.9985	-18.9489	0.9976	-23.4863

39	0	0.9675	-31.7735	0.9677	-30.4844	0.9673	-35.6561
40	2	0.9700	-33.9914	0.9700	-32.6292	0.9700	-38.0129
41	0	0.9668	-35.2778	0.9668	-33.8616	0.9668	-39.4019
42	2	0.9850	-35.9803	0.9850	-34.4163	0.9850	-40.3847
43	0	0.9708	-27.7278	0.9705	-26.2812	0.9711	-31.8906
44	0	0.9685	-26.3176	0.9680	-24.4615	0.9694	-31.2342
45	0	0.9756	-24.9837	0.9751	-22.9770	0.9764	-30.1773
46	2	1.0050	-22.2984	1.0050	-20.2616	1.0050	-27.5113
47	0	1.0107	-19.3274	1.0123	-17.4111	1.0060	-24.1977
48	0	1.0147	-21.6183	1.0147	-19.3974	1.0148	-27.2385
49	2	1.0250	-20.9648	1.0250	-18.6951	1.0250	-26.6928
50	0	0.9970	-24.7392	0.9968	-22.5175	0.6509	-27.9648
51	0	0.4237	-29.5485	0.7147	-26.1313	0.9514	-38.6360
52	0	0.0193	-87.3612	0.5170	-26.8883	0.9413	-40.6225
53	0	0.5331	-38.4316	0.0243	-81.2849	0.9379	-44.3575
54	2	0.9550	-34.2132	0.9550	-32.5447	0.9550	-45.4209
55	2	0.9520	-33.9359	0.9520	-31.9802	0.9520	-45.6682
56	2	0.9540	-34.2355	0.9540	-32.1740	0.9540	-46.4047
57	0	0.9661	-30.5650	0.9659	-28.4352	0.0091	-96.2568
58	0	0.6453	-33.1137	0.8127	-29.5484	0.9480	-42.2594
59	2	0.9850	-21.1127	0.9850	-19.7449	0.9850	-28.1987
60	0	0.9929	-14.6456	0.9929	-13.4418	0.9926	-20.0769
61	2	0.9950	-13.6235	0.9950	-12.4357	0.9950	-18.9618
62	2	0.9980	-13.8916	0.9980	-12.6834	0.9980	-19.0811
63	0	0.9876	-15.5103	0.9881	-14.3113	0.9836	-21.1929
64	0	0.9949	-12.6480	0.9952	-11.5367	0.9918	-17.5994
65	2	1.0050	-7.2616	1.0050	-6.3667	1.0050	-10.6951
66	2	1.0500	-7.9440	1.0500	-6.6697	1.0500	-12.2434
67	0	1.0189	-11.4405	1.0189	-10.1961	1.0185	-16.1427
68	0	1.0124	-5.6513	1.0124	-5.0679	1.0121	-7.8907
69	3	1.0350	0	1.0350	0	1.0350	0
70	2	0.9840	-9.1352	0.9840	-8.9075	0.9840	-9.9056
71	0	0.9867	-9.8248	0.9868	-9.5561	0.9867	-10.7268
72	2	0.9800	-12.3362	0.9800	-11.8593	0.9800	-13.9046
73	2	0.9910	-10.0374	0.9910	-9.7685	0.9910	-10.9403
74	2	0.9580	-9.9418	0.9580	-9.7508	0.9580	-10.6142
75	0	0.9667	-8.6229	0.9668	-8.4451	0.9664	-9.2585
76	2	0.9430	-10.2356	0.9430	-10.0189	0.9430	-11.0356
77	2	1.0060	-5.9437	1.0060	-5.6748	1.0060	-6.9649
78	0	1.0018	-6.1407	1.0018	-5.8550	1.0018	-7.2267
79	0	1.0042	-5.6458	1.0042	-5.3278	1.0043	-6.8571

80	2	1.0400	-3.0260	1.0400	-2.6182	1.0400	-4.5858
81	0	1.0283	-4.7538	1.0282	-4.2336	1.0282	-6.7484
82	0	0.9773	-4.2600	0.9774	-3.9279	0.9773	-5.5261
83	0	0.9717	-1.9318	0.9717	-1.5954	0.9717	-3.2146
84	0	0.9747	2.2895	0.9747	2.6329	0.9747	0.9797
85	2	0.9850	4.6362	0.9850	4.9829	0.9850	3.3136
86	0	0.9867	3.2668	0.9867	3.6135	0.9867	1.9441
87	2	1.0150	3.5260	1.0150	3.8727	1.0150	2.2033
88	0	0.9859	9.2958	0.9858	9.6484	0.9859	7.9501
89	2	1.0050	14.4007	1.0050	14.7574	1.0050	13.0393
90	2	0.9850	2.1528	0.9850	2.5135	0.9850	0.7759
91	2	0.9800	0.3186	0.9800	0.6825	0.9800	-1.0710
92	2	0.9900	-1.9213	0.9900	-1.5525	0.9900	-3.3297
93	0	0.9854	-3.8703	0.9854	-3.5003	0.9854	-5.2833
94	0	0.9886	-5.1042	0.9886	-4.7331	0.9886	-6.5213
95	0	0.9777	-5.5475	0.9777	-5.1789	0.9776	-6.9551
96	0	0.9879	-5.0409	0.9879	-4.6754	0.9878	-6.4363
97	0	1.0088	-4.3843	1.0088	-3.9976	1.0088	-5.8616
98	0	1.0233	-5.2512	1.0233	-4.8539	1.0233	-6.7698
99	2	1.0100	-6.2348	1.0100	-5.8473	1.0100	-7.7156
100	2	1.0170	-5.7576	1.0170	-5.3781	1.0170	-7.2070
101	0	0.9921	-5.0067	0.9921	-4.6318	0.9921	-6.4388
102	0	0.9897	-3.0549	0.9897	-2.6841	0.9896	-4.4712
103	2	1.0100	-9.4986	1.0100	-9.1192	1.0100	-10.9481
104	2	0.9710	-12.0686	0.9710	-11.6892	0.9710	-13.5180
105	2	0.9650	-13.1728	0.9650	-12.7934	0.9650	-14.6222
106	0	0.9611	-13.4330	0.9611	-13.0536	0.9611	-14.8824
107	2	0.9520	-16.2337	0.9520	-15.8543	0.9520	-17.6831
108	0	0.9662	-14.3729	0.9662	-13.9935	0.9662	-15.8223
109	0	0.9670	-14.8255	0.9670	-14.4461	0.9670	-16.2749
110	2	0.9730	-15.6724	0.9730	-15.2930	0.9730	-17.1218
111	2	0.9800	-14.0273	0.9800	-13.6479	0.9800	-15.4767
112	2	0.9750	-18.7716	0.9750	-18.3922	0.9750	-20.2210
113	2	0.9930	-22.9541	0.9930	-21.9645	0.9930	-26.1503
114	0	0.9601	-21.6412	0.9601	-20.7364	0.9601	-24.5718
115	0	0.9600	-21.6505	0.9600	-20.7456	0.9600	-24.5817
116	2	1.0050	-6.0391	1.0050	-5.4555	1.0050	-8.2797
117	0	0.9738	-26.0656	0.9738	-25.0553	0.9738	-29.3310
118	0	0.9490	-9.8347	0.9491	-9.6388	0.9489	-10.5467

Solution NO.		**19**		**20**		**21**	
Bus NO.	Bus Type	V (p.u.)	Angle (deg.)	V (p.u.)	Angle (deg.)	V (p.u.)	Angle (deg.)
1	2	0.9550	-29.8536	0.9550	-58.6664	0.9550	-27.0901
2	0	0.9714	-29.3209	0.9714	-58.1223	0.9714	-26.5552
3	0	0.9675	-28.9631	0.9675	-57.7804	0.9675	-26.2004
4	2	0.9980	-25.2299	0.9981	-54.0664	0.9980	-22.4713
5	0	1.0011	-24.7698	1.0011	-53.6124	1.0011	-22.0121
6	2	0.9900	-27.5282	0.9900	-56.3475	0.9900	-24.7659
7	0	0.9893	-27.9793	0.9893	-56.7887	0.9893	-25.2153
8	2	1.0150	-19.6358	1.0150	-48.5160	1.0150	-16.8870
9	0	1.0429	-12.3817	1.0429	-41.2660	1.0429	-9.6329
10	2	1.0500	-4.8003	1.0500	-33.6852	1.0500	-2.0520
11	0	0.9849	-27.8251	0.9849	-56.6337	0.9849	-25.0590
12	2	0.9900	-28.3487	0.9900	-57.1433	0.9900	-25.5818
13	0	0.9681	-29.2485	0.9682	-58.0374	0.9682	-26.4679
14	0	0.9841	-29.1277	0.9841	-57.9036	0.9841	-26.3443
15	2	0.9700	-29.5634	0.9700	-58.2847	0.9700	-26.7336
16	0	0.9824	-28.6221	0.9821	-57.3206	0.9825	-25.8612
17	0	0.9905	-26.7419	0.9897	-55.2295	0.9906	-23.9945
18	2	0.9730	-29.1422	0.9730	-57.6932	0.9730	-26.3483
19	2	0.9620	-29.7162	0.9620	-58.3164	0.9620	-26.8796
20	0	0.9554	-28.2725	0.9504	-55.6046	0.9559	-25.5954
21	0	0.9555	-26.2657	0.9482	-52.6436	0.9562	-23.7071
22	0	0.9666	-23.2323	0.9586	-48.5095	0.9673	-20.8093
23	0	0.9986	-17.5641	0.9950	-41.1233	0.9989	-15.3532
24	2	0.9920	-16.5078	0.9920	-37.0740	0.9920	-14.6106
25	2	1.0500	-11.4867	1.0500	-37.2680	1.0500	-9.0590
26	2	1.0150	-9.9907	1.0150	-36.7095	1.0150	-7.4746
27	2	0.9680	-24.2096	0.9680	-50.3081	0.9680	-21.7336
28	0	0.9616	-26.0541	0.9615	-52.4359	0.9616	-23.5452
29	0	0.9632	-27.1801	0.9633	-53.8772	0.9632	-24.6346
30	0	1.0069	-21.6456	1.0058	-50.6031	1.0077	-18.9158
31	2	0.9670	-27.1108	0.9670	-53.9203	0.9670	-24.5523
32	2	0.9630	-24.7297	0.9630	-50.7611	0.9630	-22.2578
33	0	0.9693	-30.9405	0.9690	-60.5807	0.9695	-27.8565
34	2	0.9840	-31.1902	0.9840	-61.7945	0.9840	-27.7699
35	0	0.9799	-31.6295	0.9799	-62.2597	0.9800	-28.2314
36	2	0.9800	-31.6386	0.9800	-62.2617	0.9800	-28.2343
37	0	0.9875	-30.6676	0.9877	-61.3331	0.9877	-27.3002
38	0	0.9975	-24.0836	1.0001	-55.1505	0.9997	-21.2616

39	0	0.9673	-36.3048	0.9672	-67.1133	0.9679	-32.3171
40	2	0.9700	-38.6800	0.9700	-69.5718	0.9700	-34.3343
41	0	0.9668	-40.0826	0.9667	-71.0373	0.9669	-35.4723
42	2	0.9850	-41.1025	0.9850	-72.2281	0.9850	-35.7689
43	0	0.9711	-32.5749	0.9713	-63.3214	0.9698	-27.7832
44	0	0.9695	-32.0165	0.9699	-62.9744	0.9669	-25.1808
45	0	0.9765	-30.9955	0.9771	-62.0315	0.9742	-23.4085
46	2	1.0050	-28.3293	1.0050	-58.8360	1.0050	-20.5081
47	0	1.0052	-24.9597	0.9593	-53.1307	1.0122	-17.5443
48	0	1.0148	-28.1148	1.0149	-59.7434	1.0146	-19.5337
49	2	1.0250	-27.5846	1.0250	-59.5104	1.0250	-18.8023
50	0	0.9895	-33.1367	0.9881	-65.3101	1.0000	-21.4649
51	0	0.3931	-38.6049	0.9464	-72.9004	0.9649	-24.8989
52	0	0.4719	-45.3715	0.9360	-75.2195	0.9547	-26.0786
53	0	0.7352	-49.0015	0.9348	-79.8395	0.9449	-27.6698
54	2	0.9550	-47.8754	0.9550	-81.5191	0.9550	-27.2092
55	2	0.9520	-47.8770	0.9520	-82.3282	0.9520	-27.3962
56	2	0.9540	-48.6161	0.9540	-81.6329	0.9540	-27.2669
57	0	0.9576	-42.4146	0.9560	-75.0781	0.9694	-25.1762
58	0	0.0087	-100.8201	0.9446	-76.9486	0.9577	-26.2012
59	2	0.9850	-29.5535	0.9850	-86.1394	0.9850	-21.9264
60	0	0.9925	-21.0889	0.0081	-169.8237	0.9932	-19.7440
61	2	0.9950	-19.9557	0.9950	-94.6950	0.9950	-18.4916
62	2	0.9980	-20.0380	0.9980	-93.3665	0.9980	-21.5827
63	0	0.9827	-22.2622	0.9324	-79.2999	0.9893	-17.8973
64	0	0.9912	-18.5193	0.9142	-75.3496	0.9944	-15.8374
65	2	1.0050	-11.3115	1.0050	-47.3557	1.0050	-9.7623
66	2	1.0500	-12.9882	1.0500	-54.9957	1.0500	-12.0099
67	0	1.0184	-16.9836	0.9633	-73.1670	0.0158	-79.0656
68	0	1.0120	-8.2931	0.9970	-32.2064	1.0122	-7.2784
69	3	1.0350	0	1.0350	0	1.0350	0
70	2	0.9840	-10.0397	0.9840	-17.5292	0.9840	-9.4622
71	0	0.9867	-10.8835	0.9853	-19.5382	0.9867	-10.1903
72	2	0.9800	-14.1751	0.9800	-28.7180	0.9800	-12.8967
73	2	0.9910	-11.0971	0.9910	-19.7671	0.9910	-10.4032
74	2	0.9580	-10.7327	0.9580	-17.6194	0.9580	-10.2903
75	0	0.9663	-9.3710	0.9615	-15.9721	0.9665	-8.9750
76	2	0.9430	-11.1783	0.9430	-19.7484	0.9430	-10.7382
77	2	1.0060	-7.1484	1.0060	-18.2819	1.0060	-6.6525
78	0	1.0018	-7.4218	1.0008	-19.2310	1.0018	-6.8984
79	0	1.0043	-7.0747	1.0036	-20.1929	1.0043	-6.4979

80	2	1.0400	-4.8656	1.0400	-21.6173	1.0400	-4.1407
81	0	1.0282	-7.1068	1.0173	-28.4211	1.0282	-6.1963
82	0	0.9773	-5.7536	0.9760	-19.4509	0.9773	-5.1534
83	0	0.9717	-3.4451	0.9712	-17.3186	0.9717	-2.8378
84	0	0.9747	0.7443	0.9747	-13.4164	0.9747	1.3631
85	2	0.9850	3.0759	0.9850	-11.2230	0.9850	3.7002
86	0	0.9867	1.7065	0.9867	-12.5925	0.9867	2.3308
87	2	1.0150	1.9657	1.0150	-12.3326	1.0150	2.5900
88	0	0.9859	7.7083	0.9862	-6.8294	0.9859	8.3424
89	2	1.0050	12.7947	1.0050	-1.9076	1.0050	13.4355
90	2	0.9850	0.5285	0.9850	-14.3371	0.9850	1.1759
91	2	0.9800	-1.3208	0.9800	-16.3184	0.9800	-0.6679
92	2	0.9900	-3.5828	0.9900	-18.7760	0.9900	-2.9220
93	0	0.9854	-5.5372	0.9850	-20.7766	0.9854	-4.8744
94	0	0.9886	-6.7759	0.9878	-22.0560	0.9886	-6.1114
95	0	0.9776	-7.2080	0.9765	-22.3878	0.9776	-6.5476
96	0	0.9878	-6.6871	0.9861	-21.7372	0.9878	-6.0318
97	0	1.0088	-6.1271	1.0081	-22.0272	1.0088	-5.4369
98	0	1.0233	-7.0427	1.0235	-23.3738	1.0233	-6.3350
99	2	1.0100	-7.9817	1.0100	-23.9246	1.0100	-7.2901
100	2	1.0170	-7.4675	1.0170	-23.0867	1.0170	-6.7891
101	0	0.9921	-6.6962	0.9920	-22.1358	0.9921	-6.0253
102	0	0.9896	-4.7257	0.9895	-20.0009	0.9896	-4.0615
103	2	1.0100	-11.2085	1.0100	-26.8279	1.0100	-10.5302
104	2	0.9710	-13.7785	0.9710	-29.3978	0.9710	-13.1002
105	2	0.9650	-14.8827	0.9650	-30.5020	0.9650	-14.2044
106	0	0.9611	-15.1429	0.9611	-30.7622	0.9611	-14.4646
107	2	0.9520	-17.9436	0.9520	-33.5629	0.9520	-17.2653
108	0	0.9662	-16.0828	0.9662	-31.7021	0.9662	-15.4045
109	0	0.9670	-16.5354	0.9670	-32.1547	0.9670	-15.8571
110	2	0.9730	-17.3823	0.9730	-33.0015	0.9730	-16.7040
111	2	0.9800	-15.7372	0.9800	-31.3565	0.9800	-15.0589
112	2	0.9750	-20.4815	0.9750	-36.1007	0.9750	-19.8032
113	2	0.9930	-26.6972	0.9930	-54.8914	0.9930	-23.9813
114	0	0.9601	-25.0739	0.9601	-51.1338	0.9601	-22.6003
115	0	0.9600	-25.0839	0.9600	-51.1486	0.9600	-22.6100
116	2	1.0050	-8.6824	1.0050	-32.6745	1.0050	-7.6670
117	0	0.9738	-29.8897	0.9738	-58.6846	0.9738	-27.1228
118	0	0.9488	-10.6733	0.9458	-18.1940	0.9489	-10.2567

Solution NO.		**22**		**23**		**24**	
Bus NO.	Bus Type	V (p.u.)	Angle (deg.)	V (p.u.)	Angle (deg.)	V (p.u.)	Angle (deg.)
1	2	0.9550	-63.8947	0.9550	-27.0225	0.9550	-27.1467
2	0	0.9714	-63.4139	0.9714	-26.4892	0.9714	-26.6127
3	0	0.9675	-62.9823	0.9675	-26.1321	0.9675	-26.2567
4	2	0.9980	-59.1437	0.9980	-22.3996	0.9980	-22.5258
5	0	1.0012	-58.6686	1.0011	-21.9400	1.0011	-22.0663
6	2	0.9900	-61.5380	0.9900	-24.6973	0.9900	-24.8220
7	0	0.9893	-62.0323	0.9893	-25.1481	0.9893	-25.2721
8	2	1.0150	-53.3485	1.0150	-16.8095	1.0150	-16.9387
9	0	1.0429	-46.0944	1.0429	-9.5554	1.0429	-9.6845
10	2	1.0500	-38.5135	1.0500	-1.9745	1.0500	-2.1037
11	0	0.9849	-61.8807	0.9849	-24.9912	0.9849	-25.1152
12	2	0.9900	-62.4727	0.9900	-25.5168	0.9900	-25.6398
13	0	0.9681	-63.3727	0.9682	-26.3988	0.9682	-26.5214
14	0	0.9841	-63.3126	0.9841	-26.2770	0.9841	-26.3987
15	2	0.9700	-63.9198	0.9700	-26.6599	0.9700	-26.7780
16	0	0.9821	-63.2179	0.9825	-25.8195	0.9825	-25.9360
17	0	0.9891	-62.3538	0.9908	-24.0035	0.9908	-24.1058
18	2	0.9730	-64.4157	0.9730	-26.3261	0.9730	-26.4324
19	2	0.9620	-64.6350	0.9620	-26.8299	0.9620	-26.9395
20	0	0.9508	-69.2990	0.9568	-25.8818	0.9566	-25.9058
21	0	0.9500	-71.7618	0.9575	-24.2420	0.9572	-24.2027
22	0	0.9597	-73.7733	0.9687	-21.6281	0.9684	-21.5166
23	0	0.9843	-76.0321	0.9994	-16.6166	0.9993	-16.3920
24	2	0.9920	-88.5924	0.9920	-16.6263	0.9920	-16.2049
25	2	1.0500	-59.7630	1.0500	-9.7686	1.0500	-9.6908
26	2	1.0150	-53.8259	1.0151	-7.9463	1.0150	-7.9336
27	2	0.9680	-71.4463	0.9680	-22.3634	0.9680	-22.3045
28	0	0.9613	-71.9906	0.9616	-24.1021	0.9616	-24.0619
29	0	0.9627	-71.6659	0.9632	-25.1102	0.9632	-25.0910
30	0	0.9956	-54.9714	1.0081	-18.8292	1.0080	-18.9635
31	2	0.9670	-71.0804	0.9670	-24.9989	0.9670	-24.9871
32	2	0.9630	-72.4055	0.9630	-22.9055	0.9630	-22.8414
33	0	0.9629	-59.8857	0.9695	-27.4769	0.9695	-27.6598
34	2	0.9840	-54.1927	0.9840	-27.0390	0.9840	-27.2908
35	0	0.9788	-54.5875	0.9800	-27.5048	0.9800	-27.7580
36	2	0.9800	-54.6188	0.9800	-27.5065	0.9800	-27.7593
37	0	0.9811	-53.5101	0.9877	-26.5790	0.9878	-26.8343
38	0	0.9590	-46.8313	0.9998	-20.6839	1.0000	-20.9608

39	0	0.9667	-56.3011	0.9681	-31.3100	0.9681	-31.5797
40	2	0.9700	-57.0151	0.9700	-33.1616	0.9700	-33.4398
41	0	0.9667	-57.1187	0.9669	-34.1754	0.9669	-34.4600
42	2	0.9850	-54.5857	0.9850	-34.1326	0.9850	-34.4350
43	0	0.9457	-48.1305	0.9686	-26.3918	0.9687	-26.6767
44	0	0.9368	-35.9893	0.9650	-22.7965	0.9651	-23.1313
45	0	0.9534	-30.7307	0.9727	-20.6586	0.9728	-21.0117
46	2	1.0050	-25.6492	1.0050	-17.6270	1.0050	-17.9798
47	0	1.0088	-21.1394	1.0141	-14.7841	1.0139	-15.1136
48	0	1.0143	-23.4694	1.0146	-16.3196	1.0146	-16.7021
49	2	1.0250	-22.4189	1.0250	-15.5000	1.0250	-15.8904
50	0	1.0009	-24.5789	1.0004	-17.9464	1.0004	-18.3562
51	0	0.9665	-27.3637	0.9656	-21.1006	0.9656	-21.5357
52	0	0.9564	-28.3674	0.9555	-22.2045	0.9554	-22.6464
53	0	0.9458	-29.4796	0.9453	-23.5895	0.9453	-24.0500
54	2	0.9550	-28.6688	0.9550	-22.9784	0.9550	-23.4524
55	2	0.9520	-28.7488	0.9520	-23.1196	0.9520	-23.5978
56	2	0.9540	-28.7177	0.9540	-23.0323	0.9540	-23.5067
57	0	0.9704	-27.3411	0.9699	-21.2488	0.9698	-21.6955
58	0	0.9588	-28.2351	0.9582	-22.2174	0.9582	-22.6692
59	2	0.9850	-21.6273	0.9850	-16.9449	0.9850	-17.4871
60	0	0.9931	-17.2355	0.9931	-12.8411	0.9931	-13.4026
61	2	0.9950	-16.3354	0.9950	-11.9736	0.9950	-12.5374
62	2	0.9980	-16.7642	0.9980	-12.3437	0.9980	-12.9035
63	0	0.9919	-17.8076	0.9925	-13.4406	0.9926	-14.0040
64	0	0.9979	-15.8677	0.9984	-11.6636	0.9985	-12.2379
65	2	1.0050	-12.4256	1.0050	-8.6416	1.0050	-9.2443
66	2	1.0500	-11.8112	1.0500	-7.1768	1.0500	-7.7220
67	0	1.0194	-14.8578	1.0193	-10.3201	1.0193	-10.8719
68	0	1.0119	-9.3053	1.0106	-9.3453	1.0102	-10.0391
69	3	1.0350	0	1.0350	0	1.0350	0
70	2	0.9840	-28.6683	0.9840	-14.6053	0.9840	-13.3702
71	0	0.7899	-31.9504	0.9868	-15.0611	0.9868	-13.8967
72	2	0.9800	149.9971	0.9800	-16.3868	0.9800	-15.5808
73	2	0.9910	-34.9562	0.9910	-15.2727	0.9910	-14.1085
74	2	0.9580	-22.3179	0.9580	-18.8925	0.9580	-16.8168
75	0	0.9562	-18.4671	0.9559	-18.4505	0.9596	-16.1837
76	2	0.9430	-17.9275	0.9430	-26.4298	0.9430	-22.6761
77	2	1.0060	-10.2891	1.0060	-30.2880	1.0060	-24.7508
78	0	1.0018	-10.4493	0.6607	-29.7470	1.0018	-25.0128
79	0	1.0042	-9.8834	0.0126	-63.8862	1.0043	-24.6436

80	2	1.0400	-7.0666	1.0400	-20.2960	1.0400	-22.3734
81	0	1.0279	-8.5470	1.0182	-13.3308	1.0163	-14.5214
82	0	0.9774	-8.4665	0.9766	-25.3966	0.0227	-83.9209
83	0	0.9717	-6.1289	0.9706	-22.8509	0.2924	-63.6289
84	0	0.9747	-1.8923	0.9741	-18.2828	0.7523	-62.1445
85	2	0.9850	0.4617	0.9850	-15.7726	0.9850	-61.4989
86	0	0.9867	-0.9077	0.9867	-17.1421	0.9867	-62.8684
87	2	1.0150	-0.6485	1.0150	-16.8828	1.0150	-62.6091
88	0	0.9858	5.1343	0.9855	-10.8110	0.9773	-51.8947
89	2	1.0050	10.2482	1.0050	-5.4986	1.0050	-43.3936
90	2	0.9850	-1.9908	0.9850	-17.5427	0.9850	-52.3557
91	2	0.9800	-3.8179	0.9800	-19.2105	0.9800	-51.4549
92	2	0.9900	-6.0472	0.9900	-21.2034	0.9900	-49.5672
93	0	0.9854	-7.9935	0.9855	-23.0879	0.8818	-48.0986
94	0	0.9887	-9.2251	0.9888	-24.2660	0.7968	-45.9030
95	0	0.9777	-9.6738	0.9779	-24.8316	0.6685	-44.8354
96	0	0.9879	-9.1740	0.9881	-24.4800	0.5443	-39.9244
97	0	1.0088	-8.4709	1.0084	-22.7407	0.7708	-29.1842
98	0	1.0233	-9.3144	1.0229	-23.0669	1.0046	-32.0051
99	2	1.0100	-10.3195	1.0100	-24.5561	1.0100	-40.0639
100	2	1.0170	-9.8601	1.0170	-24.4967	1.0170	-45.0472
101	0	0.9921	-9.1191	0.9923	-23.9749	0.9919	-47.8256
102	0	0.9897	-7.1763	0.9898	-22.2324	0.9898	-49.0915
103	2	1.0100	-13.6012	1.0100	-28.2378	1.0100	-48.7883
104	2	0.9710	-16.1711	0.9710	-30.8078	0.9710	-51.3583
105	2	0.9650	-17.2753	0.9650	-31.9120	0.9650	-52.4625
106	0	0.9611	-17.5355	0.9611	-32.1722	0.9611	-52.7226
107	2	0.9520	-20.3362	0.9520	-34.9729	0.9520	-55.5234
108	0	0.9662	-18.4754	0.9662	-33.1121	0.9662	-53.6626
109	0	0.9670	-18.9280	0.9670	-33.5647	0.9670	-54.1152
110	2	0.9730	-19.7749	0.9730	-34.4116	0.9730	-54.9620
111	2	0.9800	-18.1298	0.9800	-32.7665	0.9800	-53.3169
112	2	0.9750	-22.8741	0.9750	-37.5108	0.9750	-58.0612
113	2	0.9930	-63.8757	0.9930	-24.0673	0.9930	-24.1492
114	0	0.9601	-72.5649	0.9601	-23.2405	0.9601	-23.1785
115	0	0.9600	-72.5433	0.9600	-23.2489	0.9600	-23.1873
116	2	1.0050	-9.6953	1.0050	-9.7421	1.0050	-10.4380
117	0	0.9738	-64.0137	0.9738	-27.0578	0.9738	-27.1808
118	0	0.9435	-18.6861	0.9411	-22.6402	0.9438	-19.6720

Solution NO.		**25**		**26**		**27**	
Bus NO.	Bus Type	V (p.u.)	Angle (deg.)	V (p.u.)	Angle (deg.)	V (p.u.)	Angle (deg.)
1	2	0.9550	-26.1411	0.9550	-23.7433	0.9550	-25.5089
2	0	0.9714	-25.6072	0.9714	-23.2100	0.9714	-24.9751
3	0	0.9675	-25.2510	0.9675	-22.8530	0.9675	-24.6188
4	2	0.9980	-21.5198	0.9980	-19.1207	0.9980	-20.8877
5	0	1.0011	-21.0603	1.0011	-18.6611	1.0011	-20.4282
6	2	0.9900	-23.8163	0.9900	-21.4182	0.9900	-23.1842
7	0	0.9893	-24.2665	0.9893	-21.8689	0.9893	-23.6344
8	2	1.0150	-15.9321	1.0150	-13.5307	1.0150	-15.2999
9	0	1.0429	-8.6778	1.0429	-6.2766	1.0429	-8.0458
10	2	1.0500	-1.0969	1.0500	1.3044	1.0500	-0.4649
11	0	0.9849	-24.1097	0.9849	-21.7123	0.9849	-23.4776
12	2	0.9900	-24.6343	0.9900	-22.2375	0.9900	-24.0022
13	0	0.9682	-25.5166	0.9682	-23.1212	0.9682	-24.8848
14	0	0.9841	-25.3940	0.9841	-22.9994	0.9841	-24.7622
15	2	0.9700	-25.7753	0.9700	-23.3869	0.9700	-25.1445
16	0	0.9825	-24.9307	0.9825	-22.5365	0.9825	-24.2980
17	0	0.9908	-23.1008	0.9908	-20.7122	0.9908	-22.4669
18	2	0.9730	-25.4291	0.9730	-23.0429	0.9730	-24.7966
19	2	0.9620	-25.9377	0.9620	-23.5540	0.9620	-25.3066
20	0	0.9565	-24.9030	0.9566	-22.5455	0.9565	-24.2624
21	0	0.9572	-23.1991	0.9572	-20.8610	0.9571	-22.5516
22	0	0.9684	-20.5122	0.9685	-18.1961	0.9684	-19.8567
23	0	0.9993	-15.3863	0.9993	-13.1048	0.9993	-14.7184
24	2	0.9920	-15.1990	0.9920	-12.9831	0.9920	-14.5109
25	2	1.0500	-8.6842	1.0500	-6.3519	1.0500	-8.0319
26	2	1.0150	-6.9275	1.0150	-4.5724	1.0151	-6.2770
27	2	0.9680	-21.2988	0.9680	-18.9623	0.9680	-20.6479
28	0	0.9616	-23.0564	0.9616	-20.7139	0.9616	-22.4075
29	0	0.9632	-24.0856	0.9632	-21.7364	0.9632	-23.4389
30	0	1.0080	-17.9559	1.0080	-15.5501	1.0080	-17.3235
31	2	0.9670	-23.9818	0.9670	-21.6303	0.9670	-23.3360
32	2	0.9630	-21.8359	0.9630	-19.5014	0.9630	-21.1846
33	0	0.9695	-26.6633	0.9695	-24.2677	0.9695	-26.0430
34	2	0.9840	-26.3038	0.9840	-23.9078	0.9840	-25.6967
35	0	0.9800	-26.7698	0.9800	-24.3706	0.9800	-26.1621
36	2	0.9800	-26.7715	0.9800	-24.3732	0.9800	-26.1639
37	0	0.9878	-25.8446	0.9877	-23.4411	0.9878	-25.2362
38	0	0.9999	-19.9479	0.9996	-17.4820	0.9999	-19.3267

39	0	0.9681	-30.6119	0.9680	-28.2555	0.9681	-30.0190
40	2	0.9700	-32.4845	0.9700	-30.1553	0.9700	-31.9006
41	0	0.9669	-33.5142	0.9669	-31.2053	0.9669	-32.9371
42	2	0.9850	-33.5149	0.9850	-31.2614	0.9850	-32.9562
43	0	0.9688	-25.7514	0.9691	-23.4911	0.9689	-25.1875
44	0	0.9653	-22.2990	0.9656	-20.2428	0.9654	-21.8001
45	0	0.9729	-20.2136	0.9731	-18.2325	0.9730	-19.7386
46	2	1.0050	-17.2270	1.0050	-15.3537	1.0050	-16.7812
47	0	1.0143	-14.4343	1.0154	-12.7404	1.0146	-14.0332
48	0	1.0146	-15.9178	1.0145	-13.9599	1.0146	-15.4548
49	2	1.0250	-15.0978	1.0250	-13.1175	1.0250	-14.6302
50	0	1.0004	-17.5369	1.0005	-15.4865	1.0004	-17.0540
51	0	0.9657	-20.6817	0.9659	-18.5408	0.9657	-20.1791
52	0	0.9555	-21.7830	0.9557	-19.6175	0.9556	-21.2750
53	0	0.9453	-23.1611	0.9454	-20.9288	0.9453	-22.6386
54	2	0.9550	-22.5449	0.9550	-20.2638	0.9550	-22.0117
55	2	0.9520	-22.6846	0.9520	-20.3885	0.9520	-22.1481
56	2	0.9540	-22.5987	0.9540	-20.3164	0.9540	-22.0653
57	0	0.9699	-20.8256	0.9700	-18.6428	0.9699	-20.3138
58	0	0.9582	-21.7922	0.9584	-19.5912	0.9583	-21.2765
59	2	0.9850	-16.4861	0.9850	-13.9595	0.9850	-15.8995
60	0	0.9931	-12.3750	0.9931	-9.7785	0.9931	-11.7732
61	2	0.9950	-11.5067	0.9950	-8.9023	0.9950	-10.9032
62	2	0.9980	-11.8783	0.9980	-9.2883	0.9980	-11.2779
63	0	0.9925	-12.9738	0.9924	-10.3706	0.9925	-12.3706
64	0	0.9984	-11.1927	0.9983	-8.5499	0.9984	-10.5808
65	2	1.0050	-8.1601	1.0050	-5.4152	1.0050	-7.5261
66	2	1.0500	-6.7168	1.0500	-4.1792	1.0500	-6.1278
67	0	1.0193	-9.8576	1.0193	-7.2963	1.0193	-9.2635
68	0	1.0108	-8.8898	1.0119	-5.9579	1.0111	-8.2230
69	3	1.0350	0	1.0350	0	1.0350	0
70	2	0.9840	-12.3637	0.9840	-10.4188	0.9840	-11.5918
71	0	0.9868	-12.8902	0.9868	-10.9218	0.9868	-12.1256
72	2	0.9800	-14.5746	0.9800	-12.4867	0.9800	-13.8469
73	2	0.9910	-13.1021	0.9910	-11.1336	0.9910	-12.3375
74	2	0.9580	-15.3294	0.9580	-12.5303	0.9580	-14.1601
75	0	0.9617	-14.5869	0.9648	-11.5815	0.9631	-13.3219
76	2	0.9430	-20.1162	0.9430	-15.3278	0.9430	-18.0729
77	2	1.0060	-20.9992	1.0060	-13.9232	1.0060	-17.9696
78	0	1.0017	-21.3346	1.0018	-14.1394	1.0016	-18.4525
79	0	1.0043	-21.1071	1.0043	-13.6818	1.0043	-18.5104

80	2	1.0400	-19.2308	1.0400	-11.1658	1.0400	-17.4271
81	0	1.0190	-12.6563	1.0244	-7.8795	1.0204	-11.5810
82	0	0.4202	-30.3817	0.9709	-22.3644	0.8943	-26.5558
83	0	0.0110	-95.5252	0.9692	-26.0703	0.9173	-27.6370
84	0	0.6591	-73.0127	0.9733	-31.4149	0.9581	-28.8073
85	2	0.9850	-72.4005	0.9850	-33.6352	0.9850	-29.0020
86	0	0.9867	-73.7699	0.9867	-35.0046	0.9867	-30.3714
87	2	1.0150	-73.5107	1.0150	-34.7454	1.0150	-30.1122
88	0	0.9682	-59.2996	0.0213	-92.2157	0.9889	-28.0515
89	2	1.0050	-48.4015	1.0050	-21.0956	1.0050	-25.4918
90	2	0.9850	-55.1052	0.9850	-29.4366	0.9850	-40.2734
91	2	0.9800	-52.2612	0.9800	-28.0066	0.9800	-44.1429
92	2	0.9900	-47.3432	0.9900	-25.3020	0.9900	-49.3618
93	0	0.9223	-44.2572	0.9847	-24.3948	0.0069	-86.9537
94	0	0.8739	-40.6963	0.9870	-23.1574	0.6921	-38.4224
95	0	0.7948	-38.6249	0.9750	-22.6179	0.7344	-34.8473
96	0	0.7285	-33.6572	0.9845	-20.8601	0.8260	-29.4060
97	0	0.8679	-25.8224	1.0036	-16.3637	0.9202	-23.3037
98	0	1.0073	-28.2576	1.0187	-16.6666	1.0024	-27.5520
99	2	1.0100	-35.7155	1.0100	-20.7145	1.0100	-36.1046
100	2	1.0170	-40.2714	1.0170	-22.7105	1.0170	-41.4336
101	0	0.9907	-44.1288	0.9924	-24.6737	0.9902	-45.6532
102	0	0.9892	-46.3776	0.9901	-25.1974	0.9889	-48.2321
103	2	1.0100	-44.0125	1.0100	-26.4516	1.0100	-45.1747
104	2	0.9710	-46.5825	0.9710	-29.0216	0.9710	-47.7447
105	2	0.9650	-47.6867	0.9650	-30.1258	0.9650	-48.8489
106	0	0.9611	-47.9468	0.9611	-30.3859	0.9611	-49.1090
107	2	0.9520	-50.7476	0.9520	-33.1867	0.9520	-51.9098
108	0	0.9662	-48.8868	0.9662	-31.3259	0.9662	-50.0489
109	0	0.9670	-49.3394	0.9670	-31.7785	0.9670	-50.5015
110	2	0.9730	-50.1862	0.9730	-32.6253	0.9730	-51.3484
111	2	0.9800	-48.5411	0.9800	-30.9802	0.9800	-49.7033
112	2	0.9750	-53.2854	0.9750	-35.7245	0.9750	-54.4476
113	2	0.9930	-23.1443	0.9930	-20.7625	0.9930	-22.5083
114	0	0.9601	-22.1729	0.9601	-19.8376	0.9601	-21.5218
115	0	0.9600	-22.1817	0.9600	-19.8462	0.9600	-21.5306
116	2	1.0050	-9.2857	1.0050	-6.3483	1.0050	-8.6173
117	0	0.9738	-26.1753	0.9738	-23.7785	0.9738	-25.5432
118	0	0.9453	-17.6230	0.9476	-13.7845	0.9464	-15.9938

Solution NO.		**28**		**29**		**30**	
Bus NO.	Bus Type	V (p.u.)	Angle (deg.)	V (p.u.)	Angle (deg.)	V (p.u.)	Angle (deg.)
1	2	0.9550	-25.3490	0.9550	-27.5041	0.9550	-23.4966
2	0	0.9714	-24.8152	0.9714	-26.9699	0.9714	-22.9632
3	0	0.9675	-24.4589	0.9675	-26.6142	0.9675	-22.6063
4	2	0.9980	-20.7276	0.9980	-22.8838	0.9980	-18.8741
5	0	1.0011	-20.2681	1.0011	-22.4245	1.0011	-18.4145
6	2	0.9900	-23.0242	0.9900	-25.1796	0.9900	-21.1715
7	0	0.9893	-23.4745	0.9893	-25.6295	0.9893	-21.6221
8	2	1.0150	-15.1397	1.0150	-17.2978	1.0150	-13.2844
9	0	1.0429	-7.8855	1.0429	-10.0436	1.0429	-6.0303
10	2	1.0500	-0.3047	1.0500	-2.4627	1.0500	1.5507
11	0	0.9849	-23.3177	0.9849	-25.4725	0.9849	-21.4655
12	2	0.9900	-23.8424	0.9900	-25.9968	0.9900	-21.9906
13	0	0.9682	-24.7251	0.9682	-26.8781	0.9682	-22.8744
14	0	0.9841	-24.6026	0.9841	-26.7551	0.9841	-22.7525
15	2	0.9700	-24.9854	0.9700	-27.1326	0.9700	-23.1400
16	0	0.9825	-24.1386	0.9825	-26.2910	0.9825	-22.2887
17	0	0.9908	-22.3082	0.9908	-24.4566	0.9908	-20.4624
18	2	0.9730	-24.6380	0.9730	-26.7839	0.9730	-22.7941
19	2	0.9620	-25.1480	0.9620	-27.2916	0.9620	-23.3061
20	0	0.9565	-24.1077	0.9565	-26.2333	0.9566	-22.2847
21	0	0.9571	-22.3998	0.9571	-24.5121	0.9572	-20.5907
22	0	0.9684	-19.7082	0.9683	-21.8053	0.9685	-17.9151
23	0	0.9993	-14.5750	0.9993	-16.6483	0.9993	-12.8068
24	2	0.9920	-14.3769	0.9920	-16.4041	0.9920	-12.6561
25	2	1.0500	-7.8808	1.0500	-9.9886	1.0500	-6.0762
26	2	1.0151	-6.1246	1.0152	-8.2441	1.0150	-4.3057
27	2	0.9680	-20.4967	0.9680	-22.6088	0.9680	-18.6886
28	0	0.9616	-22.2555	0.9616	-24.3717	0.9616	-20.4430
29	0	0.9632	-23.2859	0.9632	-25.4067	0.9632	-21.4686
30	0	1.0080	-17.1628	1.0080	-19.3244	1.0079	-15.3043
31	2	0.9670	-23.1826	0.9670	-25.3051	0.9670	-21.3636
32	2	0.9630	-21.0336	0.9630	-23.1442	0.9630	-19.2270
33	0	0.9695	-25.8818	0.9695	-28.0313	0.9695	-24.0320
34	2	0.9840	-25.5336	0.9840	-27.6793	0.9840	-23.6847
35	0	0.9800	-25.9988	0.9800	-28.1472	0.9800	-24.1475
36	2	0.9800	-26.0007	0.9800	-28.1483	0.9800	-24.1501
37	0	0.9878	-25.0725	0.9878	-27.2246	0.9877	-23.2179
38	0	0.9999	-19.1585	1.0001	-21.3647	0.9996	-17.2557

39	0	0.9681	-29.8580	0.9681	-31.9673	0.9680	-28.0402
40	2	0.9700	-31.7412	0.9700	-33.8258	0.9700	-29.9447
41	0	0.9669	-32.7788	0.9669	-34.8449	0.9669	-30.9982
42	2	0.9850	-32.8011	0.9850	-34.8168	0.9850	-31.0637
43	0	0.9689	-25.0324	0.9687	-27.0551	0.9691	-23.2895
44	0	0.9654	-21.6570	0.9651	-23.4946	0.9657	-20.0733
45	0	0.9730	-19.6000	0.9728	-21.3695	0.9732	-18.0748
46	2	1.0050	-16.6496	1.0050	-18.3231	1.0050	-15.2081
47	0	1.0147	-13.9139	1.0137	-15.4266	1.0154	-12.6108
48	0	1.0146	-15.3169	1.0146	-17.0640	1.0145	-13.8103
49	2	1.0250	-14.4906	1.0250	-16.2572	1.0250	-12.9668
50	0	1.0004	-16.9094	1.0003	-18.7372	1.0005	-15.3315
51	0	0.9657	-20.0280	0.9655	-21.9349	0.9659	-18.3803
52	0	0.9556	-21.1221	0.9554	-23.0506	0.9558	-19.4555
53	0	0.9453	-22.4808	0.9452	-24.4677	0.9454	-20.7627
54	2	0.9550	-21.8505	0.9550	-23.8799	0.9550	-20.0946
55	2	0.9520	-21.9858	0.9520	-24.0283	0.9520	-20.2185
56	2	0.9540	-21.9039	0.9540	-23.9345	0.9540	-20.1472
57	0	0.9699	-20.1597	0.9698	-22.1032	0.9700	-18.4797
58	0	0.9583	-21.1210	0.9582	-23.0805	0.9584	-19.4270
59	2	0.9850	-15.7205	0.9850	-17.9639	0.9850	-13.7753
60	0	0.9931	-11.5892	0.9931	-13.8935	0.9931	-9.5900
61	2	0.9950	-10.7186	0.9950	-13.0298	0.9950	-8.7133
62	2	0.9980	-11.0944	0.9980	-13.3931	0.9980	-9.1001
63	0	0.9925	-12.1861	0.9926	-14.4963	0.9924	-10.1817
64	0	0.9984	-10.3935	0.9985	-12.7381	0.9983	-8.3585
65	2	1.0050	-7.3313	1.0050	-9.7650	1.0050	-5.2174
66	2	1.0500	-5.9481	1.0500	-8.2009	1.0500	-3.9943
67	0	1.0193	-9.0821	1.0193	-11.3556	1.0193	-7.1099
68	0	1.0112	-8.0137	1.0099	-10.6067	1.0119	-5.7560
69	3	1.0350	0	1.0350	0	1.0350	0
70	2	0.9840	-11.4964	0.9840	-13.3330	0.9840	-9.9720
71	0	0.9868	-12.0269	0.9868	-13.8800	0.9868	-10.4853
72	2	0.9800	-13.7311	0.9800	-15.6683	0.9800	-12.1031
73	2	0.9910	-12.2387	0.9910	-14.0919	0.9910	-10.6971
74	2	0.9580	-14.0308	0.9580	-16.6875	0.9580	-11.8279
75	0	0.9633	-13.1848	0.9598	-16.0306	0.9654	-10.8115
76	2	0.9430	-17.8584	0.9430	-22.3949	0.9430	-14.0701
77	2	1.0060	-17.6562	1.0060	-24.3113	1.0060	-12.0199
78	0	1.0016	-18.1071	1.0015	-24.8196	1.0017	-12.4021
79	0	1.0043	-18.1029	1.0043	-24.9266	1.0043	-12.2651

80	2	1.0400	-16.8472	1.0400	-23.9797	1.0400	-10.6404
81	0	1.0208	-11.2386	1.0148	-15.4617	1.0247	-7.5612
82	0	0.7500	-24.2828	0.4718	-37.1888	0.8279	-12.9171
83	0	0.8151	-24.9352	0.6161	-42.7165	0.8681	-11.2324
84	0	0.9245	-25.4793	0.8582	-47.4274	0.9415	-8.5148
85	2	0.9850	-25.3503	0.9850	-48.4789	0.9850	-7.0125
86	0	0.9867	-26.7197	0.9867	-49.8483	0.9867	-8.3820
87	2	1.0150	-26.4605	1.0150	-49.5891	1.0150	-8.1227
88	0	0.9879	-22.6980	0.9874	-45.2403	0.9863	-2.7045
89	2	1.0050	-18.9712	1.0050	-41.1110	1.0050	2.1591
90	2	0.9850	-32.5831	0.9850	-54.3228	0.9850	-10.3264
91	2	0.9800	-35.5211	0.9800	-56.9388	0.9800	-12.3542
92	2	0.9900	-39.3855	0.9900	-60.3317	0.9900	-14.8806
93	0	0.7543	-39.7354	0.7541	-61.2999	0.9159	-16.1545
94	0	0.5601	-39.2472	0.5598	-61.7550	0.8593	-16.8665
95	0	0.0252	-69.1076	0.2784	-67.6497	0.7689	-16.7749
96	0	0.5340	-27.5429	0.0140	-94.5992	0.6860	-14.6218
97	0	0.7708	-21.1860	0.4979	-26.1079	0.0095	-59.7639
98	0	1.0028	-26.8746	0.9797	-37.9925	1.0215	-14.6436
99	2	1.0100	-35.3293	1.0100	-50.5869	1.0100	-17.2810
100	2	1.0170	-40.5902	1.0170	-58.5475	1.0170	-18.1568
101	0	0.9926	-40.9498	0.9925	-60.1696	0.9923	-17.6422
102	0	0.9901	-40.0121	0.9901	-60.3825	0.9898	-15.9064
103	2	1.0100	-44.3313	1.0100	-62.2886	1.0100	-21.8979
104	2	0.9710	-46.9013	0.9710	-64.8586	0.9710	-24.4679
105	2	0.9650	-48.0055	0.9650	-65.9628	0.9650	-25.5721
106	0	0.9611	-48.2656	0.9611	-66.2230	0.9611	-25.8323
107	2	0.9520	-51.0664	0.9520	-69.0237	0.9520	-28.6330
108	0	0.9662	-49.2056	0.9662	-67.1629	0.9662	-26.7722
109	0	0.9670	-49.6582	0.9670	-67.6155	0.9670	-27.2248
110	2	0.9730	-50.5050	0.9730	-68.4624	0.9730	-28.0716
111	2	0.9800	-48.8599	0.9800	-66.8173	0.9800	-26.4266
112	2	0.9750	-53.6042	0.9750	-71.5616	0.9750	-31.1709
113	2	0.9930	-22.3506	0.9930	-24.4942	0.9930	-20.5097
114	0	0.9601	-21.3708	0.9601	-23.4820	0.9601	-19.5635
115	0	0.9600	-21.3795	0.9600	-23.4909	0.9600	-19.5721
116	2	1.0050	-8.4077	1.0050	-11.0073	1.0050	-6.1461
117	0	0.9738	-25.3834	0.9738	-27.5378	0.9738	-23.5316
118	0	0.9465	-15.8205	0.9440	-19.4588	0.9481	-12.7875

Solution NO.		**31**		**32**		**33**	
Bus NO.	Bus Type	V (p.u.)	Angle (deg.)	V (p.u.)	Angle (deg.)	V (p.u.)	Angle (deg.)
1	2	0.9550	-23.1245	0.9550	-22.8139	0.9550	-24.3056
2	0	0.9714	-22.5912	0.9714	-22.2807	0.9714	-23.7721
3	0	0.9675	-22.2342	0.9675	-21.9235	0.9675	-23.4154
4	2	0.9980	-18.5020	0.9980	-18.1910	0.9980	-19.6836
5	0	1.0011	-18.0423	1.0011	-17.7313	1.0011	-19.2241
6	2	0.9900	-20.7994	0.9900	-20.4887	0.9900	-21.9807
7	0	0.9893	-21.2501	0.9893	-20.9395	0.9893	-22.4312
8	2	1.0150	-12.9120	1.0150	-12.6004	1.0150	-14.0946
9	0	1.0429	-5.6579	1.0429	-5.3463	1.0429	-6.8406
10	2	1.0500	1.9230	1.0500	2.2346	1.0500	0.7404
11	0	0.9849	-21.0935	0.9849	-20.7830	0.9849	-22.2745
12	2	0.9900	-21.6187	0.9900	-21.3083	0.9900	-22.7994
13	0	0.9682	-22.5027	0.9682	-22.1925	0.9682	-23.6827
14	0	0.9841	-22.3808	0.9841	-22.0708	0.9841	-23.5606
15	2	0.9700	-22.7691	0.9700	-22.4603	0.9700	-23.9460
16	0	0.9825	-21.9167	0.9825	-21.6074	0.9825	-23.0967
17	0	0.9908	-20.0905	0.9908	-19.7834	0.9908	-21.2687
18	2	0.9730	-22.4229	0.9730	-22.1156	0.9730	-23.5996
19	2	0.9620	-22.9355	0.9620	-22.6281	0.9620	-24.1107
20	0	0.9566	-21.9134	0.9566	-21.6182	0.9566	-23.0817
21	0	0.9572	-20.2189	0.9572	-19.9327	0.9572	-21.3822
22	0	0.9685	-17.5427	0.9685	-17.2667	0.9684	-18.7002
23	0	0.9993	-12.4335	0.9993	-12.1735	0.9993	-13.5820
24	2	0.9920	-12.2821	0.9920	-12.0507	0.9920	-13.4122
25	2	1.0500	-5.7018	1.0500	-5.4219	1.0500	-6.8655
26	2	1.0150	-3.9328	1.0152	-3.6324	1.0151	-5.1007
27	2	0.9680	-18.3159	0.9680	-18.0319	0.9680	-19.4798
28	0	0.9616	-20.0704	0.9616	-19.7837	0.9616	-21.2360
29	0	0.9632	-21.0962	0.9632	-20.8065	0.9632	-22.2635
30	0	1.0079	-14.9315	1.0079	-14.6188	1.0080	-16.1159
31	2	0.9670	-20.9912	0.9670	-20.7004	0.9670	-22.1592
32	2	0.9630	-18.8543	0.9630	-18.5711	0.9630	-20.0176
33	0	0.9695	-23.6636	0.9695	-23.3473	0.9695	-24.8394
34	2	0.9840	-23.3202	0.9840	-22.9967	0.9840	-24.4911
35	0	0.9800	-23.7826	0.9799	-23.4585	0.9800	-24.9549
36	2	0.9800	-23.7852	0.9800	-23.4613	0.9800	-24.9572
37	0	0.9877	-22.8523	0.9877	-22.5275	0.9877	-24.0267
38	0	0.9996	-16.8814	0.9995	-16.5464	0.9997	-18.0855

39	0	0.9680	-27.6831	0.9680	-27.3627	0.9680	-28.8328
40	2	0.9700	-29.5924	0.9700	-29.2746	0.9700	-30.7278
41	0	0.9669	-30.6495	0.9669	-30.3336	0.9669	-31.7743
42	2	0.9850	-30.7249	0.9850	-30.4142	0.9850	-31.8207
43	0	0.9691	-22.9485	0.9692	-22.6388	0.9690	-24.0490
44	0	0.9657	-19.7678	0.9658	-19.4788	0.9656	-20.7625
45	0	0.9732	-17.7823	0.9732	-17.5009	0.9731	-18.7382
46	2	1.0050	-14.9328	1.0050	-14.6650	1.0050	-15.8347
47	0	1.0156	-12.3624	1.0157	-12.1192	1.0151	-13.1771
48	0	1.0145	-13.5232	1.0145	-13.2417	1.0145	-14.4652
49	2	1.0250	-12.6765	1.0250	-12.3914	1.0250	-13.6292
50	0	1.0006	-15.0311	1.0006	-14.7351	1.0005	-16.0175
51	0	0.9659	-18.0669	0.9660	-17.7568	0.9658	-19.0967
52	0	0.9558	-19.1386	0.9558	-18.8247	0.9557	-20.1801
53	0	0.9455	-20.4361	0.9455	-20.1119	0.9454	-21.5098
54	2	0.9550	-19.7611	0.9550	-19.4293	0.9550	-20.8581
55	2	0.9520	-19.8827	0.9520	-19.5486	0.9520	-20.9870
56	2	0.9540	-19.8134	0.9540	-19.4814	0.9540	-20.9111
57	0	0.9700	-18.1603	0.9701	-17.8438	0.9700	-19.2102
58	0	0.9584	-19.1049	0.9584	-18.7855	0.9584	-20.1635
59	2	0.9850	-13.4064	0.9850	-13.0364	0.9850	-14.6214
60	0	0.9931	-9.2109	0.9931	-8.8301	0.9931	-10.4597
61	2	0.9950	-8.3331	0.9950	-7.9510	0.9950	-9.5856
62	2	0.9980	-8.7220	0.9980	-8.3421	0.9980	-9.9676
63	0	0.9923	-9.8017	0.9923	-9.4197	0.9924	-11.0536
64	0	0.9983	-7.9728	0.9982	-7.5847	0.9983	-9.2438
65	2	1.0050	-4.8170	1.0050	-4.4131	1.0050	-6.1372
66	2	1.0500	-3.6237	1.0500	-3.2518	1.0500	-4.8441
67	0	1.0193	-6.7359	1.0193	-6.3605	1.0193	-7.9678
68	0	1.0120	-5.3305	1.0121	-4.8931	1.0116	-6.7382
69	3	1.0350	0	1.0350	0	1.0350	0
70	2	0.9840	-9.5950	0.9840	-9.4819	0.9840	-10.6491
71	0	0.9868	-10.1086	0.9868	-9.9852	0.9868	-11.1694
72	2	0.9800	-11.7277	0.9800	-11.5522	0.9800	-12.8219
73	2	0.9910	-10.3204	0.9910	-10.1970	0.9910	-11.3812
74	2	0.9580	-11.2656	0.9580	-11.1342	0.9580	-12.8101
75	0	0.9658	-10.1999	0.9659	-10.0645	0.9645	-11.8721
76	2	0.9430	-13.0838	0.9430	-12.8832	0.9430	-15.7657
77	2	1.0060	-10.5330	1.0060	-10.2452	1.0060	-14.5533
78	0	1.0016	-10.9545	1.0017	-10.5543	1.0017	-14.9554
79	0	1.0043	-10.8933	1.0043	-10.2761	1.0043	-14.8569

80	2	1.0400	-9.4794	1.0400	-8.2590	1.0400	-13.3391
81	0	1.0252	-6.8713	1.0258	-6.1521	1.0232	-9.1607
82	0	0.9772	-11.8462	0.9772	-12.8419	0.9725	-21.1048
83	0	0.9727	-9.9815	0.9736	-11.4671	0.9720	-21.0255
84	0	0.9754	-6.5038	0.9761	-8.7723	0.9761	-20.3960
85	2	0.9850	-4.5110	0.9850	-7.1531	0.9850	-19.7675
86	0	0.9867	-5.8804	0.9867	-8.5226	0.9867	-21.1369
87	2	1.0150	-5.6212	1.0150	-8.2634	1.0150	-20.8777
88	0	0.9866	-0.4867	0.9872	-3.7915	0.9885	-18.0815
89	2	1.0050	4.1820	1.0050	0.4223	1.0050	-15.0175
90	2	0.9850	-8.4957	0.9850	-12.7056	0.9850	-29.2921
91	2	0.9800	-10.6797	0.9800	-15.2540	0.9800	-32.7595
92	2	0.9900	-13.4369	0.9900	-18.5476	0.9900	-37.3956
93	0	0.9850	-15.1843	0.9850	-18.8789	0.9797	-33.8184
94	0	0.9876	-16.2450	0.9871	-18.7142	0.9809	-30.2446
95	0	0.9766	-15.6563	0.9756	-17.5225	0.9679	-27.8951
96	0	0.9873	-13.8430	0.9866	-14.9445	0.9797	-23.8335
97	0	1.0079	-12.0134	1.0066	-11.9548	1.0005	-18.9262
98	0	0.0237	-76.3001	1.0169	-14.4685	1.0119	-21.1706
99	2	1.0100	-17.9051	1.0100	-19.1907	1.0100	-27.4561
100	2	1.0170	-19.4716	1.0170	-21.7101	1.0170	-31.1569
101	0	0.9913	-17.7939	0.0199	-63.0210	0.4533	-34.2504
102	0	0.9891	-14.9936	0.6633	-19.1600	0.0028	-83.3003
103	2	1.0100	-23.2127	1.0100	-25.4512	1.0100	-34.8980
104	2	0.9710	-25.7827	0.9710	-28.0212	0.9710	-37.4680
105	2	0.9650	-26.8869	0.9650	-29.1254	0.9650	-38.5722
106	0	0.9611	-27.1471	0.9611	-29.3855	0.9611	-38.8323
107	2	0.9520	-29.9478	0.9520	-32.1863	0.9520	-41.6331
108	0	0.9662	-28.0870	0.9662	-30.3255	0.9662	-39.7722
109	0	0.9670	-28.5396	0.9670	-30.7781	0.9670	-40.2248
110	2	0.9730	-29.3864	0.9730	-31.6249	0.9730	-41.0717
111	2	0.9800	-27.7414	0.9800	-29.9798	0.9800	-39.4266
112	2	0.9750	-32.4857	0.9750	-34.7241	0.9750	-44.1709
113	2	0.9930	-20.1378	0.9930	-19.8335	0.9930	-21.3140
114	0	0.9601	-19.1908	0.9601	-18.9073	0.9601	-20.3544
115	0	0.9600	-19.1995	0.9600	-18.9159	0.9600	-20.3631
116	2	1.0050	-5.7202	1.0050	-5.2822	1.0050	-7.1298
117	0	0.9738	-23.1597	0.9738	-22.8493	0.9738	-24.3404
118	0	0.9484	-12.0016	0.9484	-11.8359	0.9474	-14.1438

Solution NO.		**34**		**35**		**36**	
Bus NO.	Bus Type	V (p.u.)	Angle (deg.)	V (p.u.)	Angle (deg.)	V (p.u.)	Angle (deg.)
1	2	0.9550	-61.4890	0.9550	-59.9020	0.9550	-35.6155
2	0	0.9714	-61.0336	0.9714	-59.4430	0.9714	-35.4648
3	0	0.9675	-60.5658	0.9675	-58.9803	0.9675	-34.5627
4	2	0.9980	-56.6752	0.9980	-55.0970	0.9980	-30.0275
5	0	1.0012	-56.1930	1.0012	-54.6158	1.0014	-29.4782
6	2	0.9900	-59.1168	0.9900	-57.5320	0.9900	-33.0584
7	0	0.9893	-59.6323	0.9893	-58.0445	0.9894	-33.8273
8	2	1.0150	-50.7831	1.0150	-49.2189	1.0150	-23.1251
9	0	1.0429	-43.5290	1.0429	-41.9648	1.0429	-15.8710
10	2	1.0500	-35.9481	1.0500	-34.3839	1.0500	-8.2901
11	0	0.9848	-59.4797	0.9848	-57.8914	0.9846	-33.4584
12	2	0.9900	-60.1075	0.9900	-58.5148	0.9900	-34.7199
13	0	0.9680	-60.9913	0.9681	-59.3968	0.9679	-34.0069
14	0	0.9841	-60.9606	0.9841	-59.3618	0.9838	-34.2977
15	2	0.9700	-61.6048	0.9700	-59.9890	0.9700	-31.3493
16	0	0.9819	-61.1125	0.9819	-59.4915	0.9811	-33.5105
17	0	0.9886	-60.8091	0.9888	-59.1271	0.9902	-28.4214
18	2	0.9730	-62.1289	0.9730	-60.4813	0.9730	-30.6395
19	2	0.9620	-61.6052	0.9620	-59.9957	0.9620	-31.0307
20	0	0.9554	-62.1414	0.9556	-60.4842	0.9552	-29.5118
21	0	0.9547	-61.5810	0.9551	-59.8894	0.9551	-27.4490
22	0	0.9633	-60.1767	0.9640	-58.4471	0.9662	-24.3514
23	0	0.9862	-57.0290	0.9873	-55.2419	0.9984	-18.5825
24	2	0.9920	-50.5374	0.9920	-48.9718	0.9920	-17.3053
25	2	1.0500	-51.8650	1.0500	-50.1532	1.0500	-12.6147
26	2	1.0150	-47.4551	1.0150	-45.7952	1.0150	-11.1341
27	2	0.9680	-79.8575	0.9680	-78.0748	0.9680	-25.4955
28	0	0.9600	-78.7368	0.9598	-76.8211	0.9615	-27.3923
29	0	0.9615	-76.5482	0.9614	-74.4832	0.9633	-28.5766
30	0	0.9942	-52.2301	0.9952	-50.6943	1.0056	-22.8338
31	2	0.9670	-75.3026	0.9670	-73.1850	0.9670	-28.5281
32	2	0.9630	-78.0143	0.9630	-75.4929	0.9630	-26.0349
33	0	0.9632	-57.6228	0.9636	-56.1865	0.9689	-30.7600
34	2	0.9840	-51.9711	0.9840	-50.7301	0.9840	-28.7944
35	0	0.9789	-52.3732	0.9790	-51.1351	0.9798	-29.2434
36	2	0.9800	-52.4019	0.9800	-51.1624	0.9800	-29.2511
37	0	0.9816	-51.3091	0.9819	-50.0784	0.9868	-28.2880
38	0	0.9615	-44.6435	0.9639	-43.4477	0.9934	-22.1119

39	0	0.9668	-54.2146	0.9670	-53.0544	0.9680	-32.6164
40	2	0.9700	-54.9954	0.9700	-53.8766	0.9700	-34.2322
41	0	0.9667	-55.1535	0.9667	-54.0693	0.9669	-35.0626
42	2	0.9850	-52.7698	0.9850	-51.7803	0.9850	-34.5184
43	0	0.9479	-46.2519	0.9492	-45.2243	0.9662	-27.1217
44	0	0.9394	-34.6836	0.9410	-34.0099	0.9616	-21.9703
45	0	0.9551	-29.6311	0.9561	-29.0849	0.9701	-19.2594
46	2	1.0050	-24.6899	1.0050	-24.2274	1.0050	-15.9378
47	0	1.0095	-20.3242	1.0099	-19.9403	1.0151	-13.0494
48	0	1.0143	-22.5427	1.0143	-22.1077	1.0145	-14.2753
49	2	1.0250	-21.5008	1.0250	-21.0732	1.0250	-13.3617
50	0	1.0009	-23.6621	1.0009	-23.2406	1.0007	-15.6141
51	0	0.9665	-26.4485	0.9665	-26.0350	0.9662	-18.5180
52	0	0.9564	-27.4526	0.9564	-27.0412	0.9561	-19.5540
53	0	0.9458	-28.5660	0.9458	-28.1605	0.9456	-20.7542
54	2	0.9550	-27.7560	0.9550	-27.3548	0.9550	-20.0078
55	2	0.9520	-27.8363	0.9520	-27.4365	0.9520	-20.1077
56	2	0.9540	-27.8050	0.9540	-27.4039	0.9540	-20.0584
57	0	0.9704	-26.4266	0.9704	-26.0167	0.9702	-18.5505
58	0	0.9588	-27.3209	0.9588	-26.9127	0.9586	-19.4685
59	2	0.9850	-20.7189	0.9850	-20.3397	0.9850	-13.2934
60	0	0.9931	-16.3284	0.9931	-15.9555	0.9931	-8.9952
61	2	0.9950	-15.4284	0.9950	-15.0562	0.9950	-8.1057
62	2	0.9980	-15.8570	0.9980	-15.4835	0.9980	-8.5155
63	0	0.9919	-16.9005	0.9919	-16.5283	0.9921	-9.5761
64	0	0.9979	-14.9614	0.9979	-14.5926	0.9981	-7.6891
65	2	1.0050	-11.5211	1.0050	-11.1615	1.0050	-4.3834
66	2	1.0500	-10.9028	1.0500	-10.5249	1.0500	-3.4935
67	0	1.0194	-13.9500	1.0194	-13.5740	1.0193	-6.5713
68	0	1.0120	-8.5682	1.0121	-8.3277	1.0124	-3.7979
69	3	1.0350	0	1.0350	0	1.0350	0
70	2	0.9840	-19.2140	0.9840	-18.7692	0.9840	-9.9029
71	0	0.9830	-22.2990	0.9832	-21.7509	0.9866	-10.8287
72	2	0.9800	-36.9332	0.9800	-35.8593	0.9800	-14.5357
73	2	0.9910	-22.5545	0.9910	-22.0033	0.9910	-11.0429
74	2	0.9580	-16.3441	0.9580	-16.0478	0.9580	-10.2316
75	0	0.9625	-13.7719	0.9628	-13.5286	0.9665	-8.7599
76	2	0.9430	-14.3897	0.9430	-14.1767	0.9430	-10.0500
77	2	1.0060	-8.5767	1.0060	-8.4134	1.0060	-5.3000
78	0	1.0018	-8.7888	1.0018	-8.6214	1.0018	-5.4326
79	0	1.0043	-8.3231	1.0042	-8.1477	1.0042	-4.8136

80	2	1.0400	-5.7844	1.0400	-5.5869	1.0400	-1.8483
81	0	1.0281	-7.6136	1.0281	-7.3887	1.0282	-3.1435
82	0	0.9773	-6.9500	0.9773	-6.7712	0.9774	-3.3734
83	0	0.9717	-4.6257	0.9717	-4.4459	0.9717	-1.0287
84	0	0.9747	-0.4107	0.9747	-0.2291	0.9747	3.2193
85	2	0.9850	1.9331	0.9850	2.1155	0.9850	5.5788
86	0	0.9867	0.5637	0.9867	0.7460	0.9867	4.2093
87	2	1.0150	0.8227	1.0150	1.0052	1.0150	4.4685
88	0	0.9859	6.5872	0.9859	6.7711	0.9858	10.2611
89	2	1.0050	11.6885	1.0050	11.8734	1.0050	15.3817
90	2	0.9850	-0.5629	0.9850	-0.3771	0.9850	3.1492
91	2	0.9800	-2.4002	0.9800	-2.2135	0.9800	1.3275
92	2	0.9900	-4.6445	0.9900	-4.4566	0.9900	-0.8937
93	0	0.9854	-6.5945	0.9854	-6.4063	0.9854	-2.8380
94	0	0.9886	-7.8293	0.9886	-7.6410	0.9887	-4.0679
95	0	0.9777	-8.2704	0.9777	-8.0827	0.9778	-4.5206
96	0	0.9879	-7.7610	0.9879	-7.5740	0.9880	-4.0260
97	0	1.0088	-7.1235	1.0088	-6.9313	1.0088	-3.2880
98	0	1.0233	-8.0000	1.0233	-7.8052	1.0233	-4.1140
99	2	1.0100	-8.9748	1.0100	-8.7824	1.0100	-5.1352
100	2	1.0170	-8.4901	1.0170	-8.2997	1.0170	-4.6892
101	0	0.9921	-7.7353	0.9921	-7.5460	0.9921	-3.9555
102	0	0.9897	-5.7800	0.9897	-5.5915	0.9897	-2.0195
103	2	1.0100	-12.2313	1.0100	-12.0409	1.0100	-8.4303
104	2	0.9710	-14.8013	0.9710	-14.6109	0.9710	-11.0002
105	2	0.9650	-15.9055	0.9650	-15.7151	0.9650	-12.1044
106	0	0.9611	-16.1657	0.9611	-15.9752	0.9611	-12.3646
107	2	0.9520	-18.9664	0.9520	-18.7760	0.9520	-15.1653
108	0	0.9662	-17.1056	0.9662	-16.9152	0.9662	-13.3045
109	0	0.9670	-17.5582	0.9670	-17.3678	0.9670	-13.7571
110	2	0.9730	-18.4050	0.9730	-18.2146	0.9730	-14.6040
111	2	0.9800	-16.7600	0.9800	-16.5695	0.9800	-12.9589
112	2	0.9750	-21.5043	0.9750	-21.3138	0.9750	-17.7032
113	2	0.9930	-63.2842	0.9930	-61.4863	0.9930	-28.3332
114	0	0.0034	-138.7763	0.1407	-80.0878	0.9601	-26.3710
115	0	0.1096	-89.1579	0.0091	-137.1197	0.9600	-26.3796
116	2	1.0050	-8.9576	1.0050	-8.7170	1.0050	-4.1855
117	0	0.9738	-61.6485	0.9738	-60.0558	0.0319	-88.1868
118	0	0.9469	-14.5257	0.9470	-14.2963	0.9490	-9.8224